
FINAL REPORT

U.F. Project No. 00059678

RPWO#: 67

Contract No: BD545

**MODULUS OF ELASTICITY, CREEP AND
SHRINKAGE OF CONCRETE – PHASE II**

PART 1 – CREEP STUDY

**Mang Tia
YanJun Liu
Boris Haranki
Yu-Min Su**

October 2009

**Department of Civil & Coastal Engineering
College of Engineering
University of Florida
Gainesville, Florida 32611-6580**

DISCLAIMER

“The opinions, findings, and conclusions expressed in this publication are those of the authors and not necessarily those of the State of Florida Department of Transportation or the U.S. Department of Transportation.

Prepared in cooperation with the State of Florida Department of Transportation and the U.S. Department of Transportation.”

SI (MODERN METRIC) CONVERSION FACTORS (from FHWA)

APPROXIMATE CONVERSIONS TO SI UNITS

SYMBOL	WHEN YOU KNOW	MULTIPLY BY	TO FIND	SYMBOL
LENGTH				
in	inches	25.4	millimeters	mm
ft	feet	0.305	meters	m
yd	yards	0.914	meters	m
mi	miles	1.61	kilometers	km

SYMBOL	WHEN YOU KNOW	MULTIPLY BY	TO FIND	SYMBOL
AREA				
in ²	squareinches	645.2	square millimeters	mm ²
ft ²	squarefeet	0.093	square meters	m ²
yd ²	square yard	0.836	square meters	m ²
ac	acres	0.405	hectares	ha
mi ²	square miles	2.59	square kilometers	km ²

SYMBOL	WHEN YOU KNOW	MULTIPLY BY	TO FIND	SYMBOL
VOLUME				
fl oz	fluid ounces	29.57	milliliters	mL
gal	gallons	3.785	liters	L
ft ³	cubic feet	0.028	cubic meters	m ³
yd ³	cubic yards	0.765	cubic meters	m ³
NOTE: volumes greater than 1000 L shall be shown in m ³				

SYMBOL	WHEN YOU KNOW	MULTIPLY BY	TO FIND	SYMBOL
MASS				
oz	ounces	28.35	grams	g
lb	pounds	0.454	kilograms	kg
T	short tons (2000 lb)	0.907	megagrams (or "metric ton")	Mg (or "t")

SYMBOL	WHEN YOU KNOW	MULTIPLY BY	TO FIND	SYMBOL
TEMPERATURE (exact degrees)				
°F	Fahrenheit	5 (F-32)/9 or (F-32)/1.8	Celsius	°C

SYMBOL	WHEN YOU KNOW	MULTIPLY BY	TO FIND	SYMBOL
ILLUMINATION				
fc	foot-candles	10.76	lux	lx
fl	foot-Lamberts	3.426	candela/m ²	cd/m ²

SYMBOL	WHEN YOU KNOW	MULTIPLY BY	TO FIND	SYMBOL
FORCE and PRESSURE or STRESS				
lbf	poundforce	4.45	newtons	N
lbf/in ²	poundforce per square inch	6.89	kilopascals	kPa

APPROXIMATE CONVERSIONS TO SI UNITS

SYMBOL	WHEN YOU KNOW	MULTIPLY BY	TO FIND	SYMBOL
LENGTH				
mm	millimeters	0.039	inches	in
m	meters	3.28	feet	ft
m	meters	1.09	yards	yd
km	kilometers	0.621	miles	mi

SYMBOL	WHEN YOU KNOW	MULTIPLY BY	TO FIND	SYMBOL
AREA				
mm ²	square millimeters	0.0016	square inches	in ²
m ²	square meters	10.764	square feet	ft ²
m ²	square meters	1.195	square yards	yd ²
ha	hectares	2.47	acres	ac
km ²	square kilometers	0.386	square miles	mi ²

SYMBOL	WHEN YOU KNOW	MULTIPLY BY	TO FIND	SYMBOL
VOLUME				
mL	milliliters	0.034	fluid ounces	fl oz
L	liters	0.264	gallons	gal
m ³	cubic meters	35.314	cubic feet	ft ³
m ³	cubic meters	1.307	cubic yards	yd ³

SYMBOL	WHEN YOU KNOW	MULTIPLY BY	TO FIND	SYMBOL
MASS				
g	grams	0.035	ounces	oz
kg	kilograms	2.202	pounds	lb
Mg (or "t")	megagrams (or "metric ton")	1.103	short tons (2000 lb)	T

SYMBOL	WHEN YOU KNOW	MULTIPLY BY	TO FIND	SYMBOL
TEMPERATURE (exact degrees)				
°C	Celsius	1.8C+32	Fahrenheit	°F

SYMBOL	WHEN YOU KNOW	MULTIPLY BY	TO FIND	SYMBOL
ILLUMINATION				
lx	lux	0.0929	foot-candles	fc
cd/m ²	candela/m ²	0.2919	foot-Lamberts	fl

SYMBOL	WHEN YOU KNOW	MULTIPLY BY	TO FIND	SYMBOL
FORCE and PRESSURE or STRESS				
N	newtons	0.225	poundforce	lbf
kPa	kilopascals	0.145	poundforce per square inch	lbf/in ²

*SI is the symbol for International System of Units. Appropriate rounding should be made to comply with Section 4 of ASTM E380.
(Revised March 2003)

TECHNICAL REPORT DOCUMENTATION PAGE

1. Report No. 00059678	2. Government Accession No.	3. Recipient's Catalog No.	
4. Title and Subtitle Modulus of Elasticity, Creep and Shrinkage of Concrete – PHASE II: Part 1– Creep Study		5. Report Date October 2009	
		6. Performing Organization Code	
7. Author(s) Mang Tia, Yanjun Liu, Boris Haranki, and Yu-Min Su		8. Performing Organization Report No. 00059678	
9. Performing Organization Name and Address Department of Civil and Coastal Engineering 365 Weil Hall – P.O. Box 116580 University of Florida Gainesville, FL 32611-6580		10. Work Unit No. (TRAIS)	
		11. Contract or Grant No. BD-545 #67	
12. Sponsoring Agency Name and Address Florida Department of Transportation 605 Suwannee Street, MS 30 Tallahassee, FL 32399		13. Type of Report and Period Covered Final Report 02/10/06 - 10/31/09	
		14. Sponsoring Agency Code	
15. Supplementary Notes Prepared in cooperation with the U.S. Department of Transportation and the Federal Highway Administration			
16. Abstract <p>A laboratory testing program was performed to evaluate the physical and mechanical properties of typical Class II, IV, V and VI concrete mixtures made with a Miami Oolite limestone, a Georgia granite, and a lightweight aggregate Stalite, including compressive strength, indirect tensile strength, modulus of elasticity, creep, and shrinkage. A total of 18 different concrete mixes, with water-to-cement (w/c) ratio varying from 0.24 to 0.44, were evaluated. Fly ash and ground blast-furnace slag were also incorporated as mineral additives in these mixes.</p> <p>Creep apparatuses were designed and built for this study. The creep apparatuses and testing procedures used were found to work satisfactorily. The creep apparatus was capable of applying and maintaining a load up to 145,000 lb on the test specimens with an error of less than 2%. Curing condition had a significant effect on the creep behavior of concrete evaluated in this study. The concretes which had been moist-cured for 14 days had substantially lower creep coefficients than those which had been moist-cured for only 7 days.</p> <p>Using the test results from the concretes investigated, relationships were developed between various mechanical properties, including compressive strength, splitting tensile strength, and elastic modulus. Relationships were also established between compressive strength of the concrete and the creep coefficient of the concretes. The predicted ultimate shrinkage strains and ultimate creep coefficients were determined for the concretes evaluated. The predicted ultimate creep coefficients of most of the concrete tested appeared to exceed 2.0.</p>			
17. Key Words Creep Test, Shrinkage, Compressive Strength, Elastic Modulus, Splitting Tensile Strength, Creep Coefficient, Miami Oolite, Georgia Granite, Lightweight Aggregate		18. Distribution Statement No restrictions.	
19. Security Classif. (of this report) Unclassified	20. Security Classif. (of this page) Unclassified	21. No. of Pages 224	22. Price

ACKNOWLEDGMENTS

The Florida Department of Transportation (FDOT) is gratefully acknowledged for providing the financial support for this study. The FDOT Materials Office provided the additional testing equipment materials and personnel needed for this investigation. Sincere thanks go to the project manager, Mr. Michael Bergin, for providing his technical coordination and advice throughout the project. Sincere gratitude is extended to the FDOT Materials Office personnel, particularly to Messrs. Charles Ishee, Richard DeLorenzo, Craig Roberts, and Luke Goolsby for their invaluable help on this project. Special thanks are given to the Florida Rock Industries Company for donating the ground blast-furnace slag; the Boral Materials Company for donating the fly ash; the W. R. Grace and Company for donating the chemical admixtures; and the Carolina Stalite Company for donating the lightweight aggregate for this study. Sincere thanks also go to the support of the staff at the Department of Civil and Coastal Engineering at the University of Florida, particularly to Messrs. Danny Brown, George Lopp, and Chuck Broward for their technical support in the lab, and to Ms. Candace Leggett for her expert editing of this report.

EXECUTIVE SUMMARY

Research Objectives

The values of the modulus of elasticity, ultimate shrinkage strain, and ultimate creep coefficient of concrete, which are used in structural design in Florida, are either based on the arbitrary available literature or on the limited research of the locally available material. There is a great need for comprehensive testing and evaluation of locally available concrete mixes to determine these physical properties of Florida normal-weight, as well as lightweight, concretes especially for the concretes used in pre-stressed concrete structures, so that correct values for these properties can be used in structural design. To address this need, a prior FDOT research project “Modulus of Elasticity, Creep and Shrinkage of Concrete,” was conducted to evaluate ten typical Florida normal-weight and lightweight concretes used in prestressed structures for their modulus of elasticity, creep, and shrinkage properties. Creep properties up to 90 days of loading were evaluated in that study. While these data were very valuable, they were limited in scope due to the constraint of time and budget. Due to the time constraint, no replicate batch of the concrete mixes in the testing program was tested. There was a need to test the replicates of these concrete mixes to establish reliability of the findings and to evaluate the variability of the test results. There was also a need to extend this study to evaluate the effects of other aggregate types and to use a longer creep testing period of one year for better prediction of the ultimate creep coefficients of these concretes.

This research had the following major objectives:

- 1) To design and recommend an effective and reliable laboratory testing set-up and procedure for performing creep tests on concrete.
- 2) To evaluate the effects of aggregate, mineral additives, and water-to-cementitious (w/c) materials ratio on strength, elastic modulus, shrinkage and creep behavior of concrete.

- 3) To determine the strength, elastic modulus, shrinkage, and creep behavior of the typical concretes used in Florida.
- 4) To determine the relationship among compressive strength, splitting tensile strength, and modulus of elasticity of concretes made with typical Florida aggregate.
- 5) To develop prediction equations or models for estimation of shrinkage and creep characteristics of typical Florida concretes.

Performance of Creep Apparatus

Creep apparatuses were designed and built for this study. The creep apparatuses and testing procedures were found to work very well. The creep apparatus was capable of applying and maintaining a load up to 145,000 lb on the test specimens with an error of less than 2%. Three specimens could be stacked for simultaneous loading.

Scope of Laboratory Testing Program

A laboratory testing program was performed to evaluate the physical and mechanical properties of typical Class II, IV, V, and VI concrete mixtures made with a Miami Oolite limestone, a Georgia granite, and a lightweight aggregate (Stalite) including compressive strength, indirect tensile strength, modulus of elasticity, creep behavior, and shrinkage behavior. A total of 18 different concrete mixes, with w/c varying from 0.24 to 0.44, were evaluated. Fly ash and ground blast-furnace slag were also used as mineral additives in these mixes.

Strength and Elastic Modulus of Concretes Investigated

The splitting tensile strength of the concrete mixtures using granite aggregate was significantly lower than that of mixtures using Miami Oolite limestone aggregate. The compressive strength of concretes with granite aggregate was comparable to or lower than that of concretes with Miami Oolite limestone aggregate. The concrete with granite aggregate had higher elastic modulus than that with Miami Oolite limestone aggregate, while the lightweight aggregate concretes had lower elastic modulus than the normal weight concretes.

Fly ash concretes developed compressive strength and splitting tensile strength at a slower rate than the slag concretes. Fly ash concrete showed significant strength gain after 28 days, while this was not seen in the slag concrete mixtures.

A relationship between compressive strength (f'_c) and splitting tensile strength (f_{ct}) was established for the concrete mixtures investigated in this study. The Carino and Lew model, given as follows,

$$f_{ct} = 1.15(f'_c)^{0.71}$$

was modified to the following equation:

$$f_{ct} = 2.4(f'_c)^{0.62}$$

where f'_c and f_{ct} are in units of psi.

The relationship between compressive strength and modulus of elasticity was refined in this study using least square of curve-fitting technique. The ACI 318-89 equation, which is

$$E_c = 57000\sqrt{f'_c}$$

was modified to the following equation:

$$E_c = \alpha\sqrt{f'_c}$$

where α is equal to 55,824 for Miami Oolite limestone aggregate; 63,351 for Georgia granite aggregate; and 43,777 for Stalite lightweight aggregate, and f'_c and E_c are in units of psi.

For all three aggregate types investigated in this study, a modified ACI 318-95 prediction equation was developed:

$$E = 31.92 \cdot w^{1.5} \cdot \sqrt{f'_c} + 345300$$

where w is the density of concrete in pound per cubic foot, and f'_c and E_c are in units of psi.

Shrinkage Characteristics of Concretes Investigated

Fly ash concrete mixtures had slightly higher shrinkage strain at 91 days than slag concretes. This is probably due to the slow hydration rate of fly ash in comparison with that of slag. As a result of a slower rate of hydration, there is more free water evaporating from the interior of the concrete, which may cause the concrete to shrink more. Thus, it is recommended that using a longer wet-curing time would be helpful to reduce shrinkage of fly ash concrete.

Water content had a significant effect on drying shrinkage strain of concrete. The higher the water content, the more the concrete tended to shrink. However, no clear trend can be seen on the effects of the w/c materials ratio on shrinkage of concrete.

The predicted ultimate shrinkage strain of concrete made with Georgia granite was slightly lower than that of the corresponding concrete made with Miami Oolite limestone aggregate. Lightweight aggregate concrete shrank more than the normal weight aggregate concrete. This might be explained by their difference in elastic modulus. The concrete with higher elastic modulus had a stronger resistance to the movement caused by shrinkage of the cement paste.

There appeared to be a relationship between the compressive strength (f'_c) at the age when the shrinkage test was started and the shrinkage strain (ϵ_{sh}) at 91 days as follows:

$$\epsilon_{sh} = 0.000414 \cdot e^{-0.0000745 \cdot f'_c}$$

where f'_c is in unit of psi.

There appeared to be a relationship between elastic modulus (E_c) at the age when the shrinkage test was started and the shrinkage strain (ϵ_{sh}) at 91 days as follows:

$$\epsilon_{sh} = 0.000562 \cdot e^{-1.92 \times 10^{-7} \cdot E_c}$$

where E_c is in unit of psi.

For the concrete investigated in this study, the ultimate shrinkage strain ranged from 1.37×10^{-4} to 3.14×10^{-4} for the concrete with Georgia granite aggregate; from 2.02×10^{-4} to 3.34×10^{-4} for the concrete with Miami Oolite limestone aggregate; and from 3.49×10^{-4} to 4.22×10^{-4} for the concrete with Stalite lightweight aggregate concrete.

Creep Characteristics of Concretes Investigated

Curing condition had a significant effect on the creep behavior of concrete evaluated in this study. The concretes which had been moist-cured for 14 days had substantially lower creep coefficients than those which had been moist-cured for only 7 days.

For the stress levels used (40% and 50% of compressive strength), the measured creep strain was linearly proportional to the stress applied. Thus, the computed creep coefficients were not affected by the stress level in this study.

The creep coefficient of the concrete using Georgia granite was much higher than that of the concrete using Miami Oolite limestone aggregate.

A linear relationship was found between creep coefficient at 365 days and compressive strength (f'_c). The regression equation which related compressive strength at loading age to creep coefficient at 360 days (φ_c) is given as follows:

$$\varphi_c = \alpha \cdot f'_c + \beta$$

where α is equal to -3.39×10^{-4} ; β equal to 4.302, and f'_c is in unit of psi.

Ultimate creep coefficient of the concretes investigated was predicted from the creep test results up to 365 days. The predicted ultimate creep coefficients of the concrete investigated are listed in Table 7-4. The predicted ultimate creep coefficients of most of the concrete tested appeared to exceed 2.0.

TABLE OF CONTENTS

	<u>page</u>
ACKNOWLEDGMENTS	vi
EXECUTIVE SUMMARY	vii
LIST OF TABLES	xvi
LIST OF FIGURES	xviii
CHAPTER	
1 INTRODUCTION	1
1.1 Background and Research Needs.....	1
1.2 Objectives of Study.....	3
1.3 Scope of Study	4
1.4 Research Approach	4
2 LITERATURE REVIEW	5
2.1 Introduction.....	5
2.2 Strength of Concrete	5
2.2.1 Significance of Studying Strength of Concrete	5
2.2.2 Effect of Coarse Aggregate on Strength of Concrete	6
2.2.3 Prediction of Strength of Concrete	8
2.3 Elastic Modulus of Concrete.....	9
2.3.1 Definition and Determination of Elastic Modulus of Concrete	9
2.3.2 Significance of Studying Elastic Modulus of Concrete.....	9
2.3.3 Effect of Coarse Aggregate on Elastic Modulus of Concrete.....	11
2.3.4 Models for Predicting Elastic Modulus of Concrete.....	14
2.3.4.1 Model recommended by Florida LRFD guidelines [FDOT, 2002]	15
2.3.4.2 Prediction equations recommended by ACI 209	15
2.3.4.3 CEB-FIP Model [CEB-FIP, 1990].....	16
2.4 Shrinkage Behavior of Concrete.....	17
2.4.1 Origin of Shrinkage of Concrete.....	17
2.4.2 Significance of Studying Shrinkage of Concrete.....	18
2.4.3 Effect of Raw Materials on Shrinkage of Concrete	19
2.4.3.1 Effect of aggregate content on shrinkage behavior of concrete.....	19
2.4.3.2 Effects of coarse aggregate type on concrete shrinkage	21
2.4.3.3 Effects of size and shape of coarse aggregate on concrete shrinkage.....	21

2.4.3.4	Effect of other factors on shrinkage behaviors of concrete	22
2.4.4	Models to Predict Concrete Shrinkage	24
2.4.4.1	CEB-FIP model for shrinkage strain prediction	25
2.4.4.2	Prediction model recommended by ACI 209 Report	27
2.5	Creep of Concrete	28
2.5.1	Rheology of Materials and Definition of Creep of Concrete	28
2.5.2	Significance of Studying Creep Behavior of Concrete	30
2.5.3	Effect of Aggregate on Creep of Hardened Concrete	31
2.5.4	Prediction Models and Their Limitations of Concrete Creep	33
2.5.4.1	CEB-FIP model code	35
2.5.4.2	ACI 209 model	37
3	MATERIALS AND EXPERIMENTAL PROGRAMS	39
3.1	Introduction	39
3.2	Concrete Mixtures Evaluated	39
3.2.1	Mix Proportion of Concrete	39
3.2.2	Mix Ingredients	41
3.3	Fabrication of Concrete Specimens	45
3.3.1	The Procedure for Mixing Concrete	45
3.3.2	The Procedure for Fabricating Specimens	46
3.4	Curing Conditions for Concrete Specimens	47
3.5	Tests on Fresh Concrete	48
3.6	Tests on Hardened Concrete	49
3.6.1	Compressive Strength Test	50
3.6.2	Splitting Tensile Strength Test (or Brazilian Test)	51
3.6.3	Elastic Modulus Test	53
3.6.4	Shrinkage Test	54
4	CREEP TEST APPARATUS DESIGN AND TESTING PROCEDURE	56
4.1	Introduction	56
4.2	Creep Test Apparatus	56
4.2.1	Design Requirements of Creep Test Apparatus	56
4.2.2	Design of the Creep Apparatus	57
4.2.2.1	Determination of the maximum capacity of the creep apparatus	57
4.2.2.2	Design of the springs	57
4.2.2.3	Design of the header plate	59
4.2.2.4	Determination of the size of steel rod	61
4.2.2.5	Stress relaxation due to deflection of the header plate and creep of concrete	61
4.3	Design of the Gage-Point Positioning Guide	62
4.4	Design of the Alignment Frame	65
4.5	Mechanical Strain Gage	65
4.6	Other Details on Creep Apparatus	65
4.7	Creep Testing Procedure	68

4.8	Summary on the Performance of the Creep Apparatus	74
5	ANALYSIS OF STRENGTH TEST	76
5.1	Introduction.....	76
5.2	Results and Analysis of Compressive Strength Tests.....	76
5.2.1	Effects of Water-to-Cement Ratio on Compressive Strength.....	76
5.2.2	Effects of Aggregate Types on Compressive Strength.....	79
5.2.3	Effects of Fly Ash and Slag on Compressive Strength of Concrete.....	84
5.3	Analysis of Splitting Tensile Strength Test Results	85
5.3.1	Effects of Water-to-Cement Ratio on Splitting Tensile Strength	85
5.3.2	Effects of Coarse Aggregate Type on Splitting Tensile Strength.....	88
5.3.3	Effects of Fly Ash and Slag on Splitting Tensile Strength of Concrete.....	88
5.4	Relationship Between Compressive Strength and Splitting Tensile Strength	93
5.5	Analysis of Elastic Modulus Test Results	95
5.6	Relationship Between Compressive Strength and Elastic Modulus	101
5.7	Summary of Findings.....	105
6	ANALYSIS OF SHRINKAGE TEST	107
6.1	Introduction.....	107
6.2	Results and Analysis of Shrinkage Tests.....	107
6.2.1	Effects of Curing Conditions on Shrinkage Behavior of Concrete.....	107
6.2.2	Effects of Mineral Additives on Shrinkage Behavior.....	111
6.2.3	Effects of Water Content on Shrinkage Behaviors.....	112
6.2.4	Effects of Aggregate Types on Shrinkage Behavior.....	113
6.2.5	Relationship Between Compressive Strength and Shrinkage Strain.....	113
6.2.6	Relationship Between Elastic Modulus and Shrinkage Strain.....	115
6.3	Evaluation on Shrinkage Prediction Models.....	117
6.3.1	ACI 209 Model	117
6.3.2	CEB-FIP Model	118
6.4	Prediction of Ultimate Shrinkage Strain	120
6.5	Summary of Findings.....	123
7	ANALYSIS OF CREEP TEST.....	125
7.1	Introduction.....	125
7.2	Analysis of Creep Coefficients	125
7.2.1	Effects of Stress Level on Creep Coefficient.....	126
7.2.2	Effects of Curing Conditions on Creep Coefficient.....	128
7.2.3	Effects of Water Content on Creep Coefficient.....	130
7.2.4	Effects of Compressive Strength at Loading Age on Creep Coefficient.....	130
7.2.5	Effects of Coarse Aggregate Type on Creep Coefficient	134

7.3	Prediction of Ultimate Creep Strain.....	135
7.4	Evaluation on Creep Prediction Models	138
7.4.1	Burgers Model	138
7.4.2	CEB-FIP Model (1990).....	141
7.4.3	ACI-209R Model	146
7.5	Summary of Findings.....	149
8	CONCLUSIONS AND RECOMMENDATIONS	150
8.1	Design of Creep Apparatus.....	150
8.2	Findings from This Study	150
8.2.1	Strength and Elastic Modulus	150
8.2.2	Shrinkage Characteristics of Concretes Investigated.....	151
8.2.3	Creep Characteristics of Concretes Investigated	153
8.3	Recommendations.....	153
	REFERENCES	155
	APPENDIX	
A	MEASUREMENTS FROM STRENGTH TESTS.....	160
B	MEASURED AND CALCULATED RESULTS FROM CREEP TESTS	166

LIST OF TABLES

<u>Table</u>	<u>page</u>
3-1	Mix Proportions of the 18 Concrete Mixtures Used in this Study40
3-2	Physical Properties of Type I Cement.....41
3-3	Chemical Ingredients of Type I Cement41
3-4	Physical and Chemical Properties of Fly Ash.....42
3-5	Physical and Chemical Properties of Slag.....42
3-6	Physical Properties of Fine Aggregate.....42
3-7	Physical Properties of Coarse Aggregates.....43
3-8	The Testing Programs on Fresh Concrete48
3-9	Properties of Fresh Concrete49
3-10	The Testing Program on Hardened Concrete.....49
5-1	Compressive Strength of the Concrete Mixtures Evaluated (psi)77
5-2	Splitting Tensile Strengths of the Concrete Mixtures Evaluated (psi).....86
5-3	Results of Regression Analysis for Relating Compressive Strength to Splitting Tensile Strength.....95
5-4	Elastic Modulus of the Concrete Mixtures Evaluated ($\times 10^6$ psi).....96
5-5	Results of Regression Analysis for Prediction of Elastic Modulus Using the Equation Recommended by ACI 318-89.....103
5-6	Results of Regression Analysis for Prediction of Elastic Modulus Using ACI 318-95 Equation.....104
6-1	Shrinkage Strains of the Concrete Mixtures Evaluated at Various Curing Ages.....108
6-2	Results of Regression Analysis on Relationship of Compressive Strength to Shrinkage Strain.....115
6-3	Results of Regression Analysis on Relationship of Elastic Modulus to Shrinkage Strain117
6-4	Correction Factors for the ACI 209 Model on Shrinkage Prediction.....118
6-5	Results of Regression Analysis for Prediction of Shrinkage Strain.....122
7-1	Regression Analysis on Relationship of Compressive Strength to Creep Coefficient at 91 Days133
7-2	Regression Analysis on Relationship of Compressive Strength to Creep Coefficient at 360 Days134

7-3	Predicted Ultimate Creep Strain and Creep Coefficient Based on Creep Measurements up to 91 Days.....	137
7-4	Predicted Ultimate Creep Strain and Creep Coefficient Based on Creep Measurements up to at 360 Days.....	137
7-5	Regression Analysis on Relation of Creep Coefficient to f_c / E	145
7-6	Correction Factors for the ACI 209 Model	148
A-1	Results of Compressive Strength Tests (psi).....	161
A-2	Normalized Compressive Strength Development Characteristics of the Concrete Mixtures Evaluated	162
A-3	Results of Splitting Tensile Strength Tests (psi).....	163
A-4	Normalized Splitting Tensile Strength Development Characteristics of the Concrete Mixtures Evaluated	164
A-5	Results of Elastic Modulus Tests ($\times 10^6$ psi)	165
B-1	Measured and Calculated Results from Creep Tests.....	167

LIST OF FIGURES

<u>Figure</u>	<u>page</u>
2-1 Representation of the stress-strain relation for concrete	10
2-2 Stress-strain relations for cement paste, aggregate, and concrete	12
2-3 Effect of coarse aggregate content on the shrinkage of concrete: a) Lean concrete; and b) Rich concrete	19
2-4 Creep diagram of concrete material	29
2-5 Strain-time plot of concrete under a sustained load and after release of load	30
3-1 Gradation of fine aggregate (Goldhead sand)	42
3-2 Gradation of coarse aggregate (Miami Oolite limestone)	43
3-3 Gradation of coarse aggregate (Georgia granite)	44
3-4 Gradation of lightweight aggregate (Stalite)	44
3-5 Compulsive pan mixer.....	45
3-6 Typical failure modes of concrete cylinders in compression test	50
3-7 Loading configuration for splitting tensile test	52
3-8 MTS system used for elastic modulus and compressive strength tests	53
3-9 Cylindrical specimen with gage points installed	55
4-1 Creep test apparatus.....	58
4-2 Boundary conditions used for finite element analysis.....	59
4-3 Finite element mesh used in the header plate analysis	60
4-4 Contour plot of deflection of header plate.....	60
4-5 Design of gage-point positioning guide	63
4-6 Gage-point position guide	64
4-7 Plastic cylindrical mold inside the gage-point position guide.....	64
4-8 Schematic of alignment frame design	66
4-9 Mechanical gage.....	67
4-10 Positioning springs on the bottom plate	68
4-11 Cracking around gage insert.....	69
4-12 Concrete cylinder with both end surfaces ground	70
4-13 Centering the specimens into a creep frame.....	70
4-14 Centering the hydraulic jack cylinder	71
4-15 Leveling the plate on the top of load cell	72

5-1	Effects of water-to-cementitious materials ratio on compressive strength at 28 days of mixes using Miami Oolite limestone and Georgia granite aggregate	78
5-2	Effects of water-to-cementitious materials ratio on compressive strength at 91 days of mixes using Miami Oolite limestone and Georgia granite aggregate	78
5-3	Effects of coarse aggregate type on compressive strength of Mixes 1F and 1GF	79
5-4	Effects of coarse aggregate type on compressive strength of Mixes 2F and 2GF	80
5-5	Effects of coarse aggregate type on compressive strength of Mixes 3F and 3GF	80
5-6	Effects of coarse aggregate type on compressive strength of Mixes 4F and 4GF	81
5-7	Effects of coarse aggregate type on compressive strength of Mixes 5S and 5GS	81
5-8	Effects of coarse aggregate type on compressive strength of Mixes 6S and 6GS	82
5-9	Effects of coarse aggregate type on compressive strength of Mixes 7S and 7GS	82
5-10	Effects of coarse aggregate type on compressive strength of Mixes 8S and 8GS	83
5-11	Effects of fly ash and slag on compressive strength of concrete.....	85
5-12	Effects of w/c materials ratio on splitting tensile strength at 28 days	87
5-13	Effects of w/c materials ratio on splitting tensile strength at 91 days	87
5-14	Effects of aggregate type on splitting tensile strength of Mixes 1F and 1GF	88
5-15	Effects of aggregate type on splitting tensile strength of Mixes 2F and 2GF	89
5-16	Effects of aggregate type on splitting tensile strength of Mixes 3F and 3GF	89
5-17	Effects of aggregate type on splitting tensile strength of Mixes 4F and 4GF	90
5-18	Effects of aggregate type on splitting tensile strength of Mixes 5S and 5GS	90
5-19	Effects of aggregate type on splitting tensile strength of Mixes 6S and 6GS	91
5-20	Effects of aggregate type on splitting tensile strength of Mixes 7S and 7GS	91
5-21	Effects of aggregate type on splitting tensile strength of Mixes 8S and 8GS	92
5-22	Effects of fly ash and slag on splitting tensile strength of concrete using Miami Oolite.....	93
5-23	Relationship between compressive strength and splitting tensile strength	94

5-24	Effects of aggregate type on modulus of elasticity of Mixes 1F and 1GF	97
5-25	Effects of aggregate type on modulus of elasticity of Mixes 2F and 2GF	98
5-26	Effects of aggregate type on modulus of elasticity of Mixes 3F and 3GF	98
5-27	Effects of aggregate type on modulus of elasticity of Mixes 4F and 4GF	99
5-28	Effects of aggregate type on modulus of elasticity of Mixes 5S and 5GS	99
5-29	Effects of aggregate type on modulus of elasticity of Mixes 6S and 6GS	100
5-30	Effects of aggregate type on modulus of elasticity of Mixes 7S and 7GS	100
5-31	Effects of aggregate type on modulus of elasticity of Mixes 8S and 8GS	101
5-32	Relationship between compressive strength and elastic modulus based on ACI Code	103
5-33	Plot of elastic modulus against $w^{1.5} \cdot \sqrt{f'_c}$ for all curing conditions	105
6-1	Effects of curing condition on shrinkage strain of concrete mixtures containing Miami Oolite limestone aggregate at 91 days	109
6-2	Effects of curing condition on shrinkage strain of concrete mixtures containing Georgia granite aggregate at 91 days	110
6-3	Effects of curing condition on shrinkage strain of concrete mixtures containing lightweight aggregate at 91 days	111
6-4	Effects of water content on shrinkage strain at 91 days	112
6-5	Effects of coarse aggregate type on shrinkage behavior of concrete	113
6-6	Relationship between compressive strength and shrinkage strain at 91 days	114
6-7	Relationship between shrinkage strain at 91 days and modulus of elasticity	116
6-8	Comparison between the shrinkage strain at 91 days and the shrinkage strain calculated by the ACI 209 model and the CEB-FIP model.....	121
6-9	Predicted ultimate shrinkage strains of limestone and granite concretes	123
7-1	Effects of stress level on creep coefficient at 91 days of concrete moist-cured for 7 days	127
7-2	Effects of stress level on creep coefficient at 91 days of concrete moist-cured for 14 days	127
7-3	Effects of stress level on creep coefficient at 360 days of concrete moist-cured for 14 days	128
7-4	Effects of curing condition on creep coefficient of concrete at 91 days	129
7-5	Effects of curing condition on creep coefficient of concrete at 360 days	129
7-6	Effects of water content on creep coefficient at 91 days	130
7-7	Relationship between compressive strength and creep coefficient at 91 days for specimens loaded at 14 days	131

7-8	Relationship between compressive strength and creep coefficient at 91 days for specimens loaded at 28 days.....	131
7-9	Relationship between compressive strength at loading age and corresponding creep coefficient at 91 days	132
7-10	Relationship between compressive strength at loading age and corresponding creep coefficient at 360 days	134
7-11	Effects of coarse aggregate type on creep coefficient at 91 days.....	135
7-12	Behavior of a Burgers model.....	138
7-13	Evaluation on Burgers model	141
7-14	Comparison on the effectiveness of the CEB-FIP model and ACI model	143
7-15	Comparison between the creep strain at 91 days from experimental data and the predicted creep strain using the CEB-FIP model.....	144
7-16	Relationship between creep strain and mechanical properties at loading age.....	145
7-17	Comparison between the ultimate creep strain calculated by CEB-FIP model and that by curve-fitting	146
7-18	Evaluation on ACI-209 model and CEB-FIP model.....	148

CHAPTER 1 INTRODUCTION

1.1 Background and Research Needs

Prestressed concrete structures, such as prestressed girders for long-span bridges, are widely used in the U.S. as well as other countries in the world. This is attributed mainly to the advantages of prestressed concrete structures, which include: 1) eliminating or considerably reducing the net tensile stresses caused by load; 2) increasing the capacity of the structure; and 3) decreasing the self-weight of concrete members. Also, prestressed concrete elements are slimmer than reinforced concrete and more pleasing aesthetically.

In the application of prestressed concrete, there are concerns about severe prestress loss caused mainly by elastic shortening, shrinkage and creep of concrete. Consequently, the design capacity of the prestressed concrete structure could be extremely reduced, or the structure could even fail prematurely. Hence, the values of elastic modulus, ultimate shrinkage strain, and ultimate creep coefficient of concrete must be estimated reasonably and accurately at the production stage in order to avoid loss of structural capacity, or even unexpected structural failure caused by prestress loss.

For the sake of avoiding unexpected prestress loss, the strict requirements on shrinkage and creep properties of the concrete used for prestressed concrete structures have been specified by American Concrete Institute (ACI) Code as well as other specifications. For example, the *AASHTO LRFD Bridge Construction Specifications-2001 Interim Revisions* [American Association of State Highway Transportation Officials (AASHTO), 2001] specifies that, for the design of continuous prestressed concrete I-girder superstructures, the ultimate creep coefficient should be 2.0 and the ultimate shrinkage strain will take the value of 0.0004, in accordance with the

recommendation of ACI 209. The specification also states that, when specific data are not available, estimates of shrinkage and creep may be made using the provisions of the Comité Euro-International du Béton-Federation Internationale de la Precontrainte (CEB-FIP) model or the ACI 209 model.

Over the past decades, many attempts have been made to develop general constitutive equations for the description of time-dependent behavior of concrete. However, most of them are empirical in nature and are limited to the scopes of the experiments. There are great uncertainties in extrapolation to later times and to the conditions not covered in the laboratory. AASHTO LRFD Specifications state the following: “Without results from tests on the specific concretes or prior experience with the materials, the use of the creep and shrinkage values referenced in these Specifications can not be expected to yield results with errors less than $\pm 50\%$.”

The values of the modulus of elasticity, ultimate shrinkage strain, and ultimate creep coefficient of concrete, which are used in structural design in Florida, are either based on the arbitrary available literature or on the limited research of the locally available material. Particularly, since very limited creep testing has been performed on Florida concretes, the knowledge of creep characteristics of Florida concrete is still a blank page. Moreover, the susceptibility of the elastic modulus, shrinkage and creep of concrete to the variation of concrete mix ingredients, such as particular aggregates in Florida, water content and mineral additives, puts more uncertainties in using these values.

There is a great need for comprehensive testing and evaluation of locally available concrete mixes to determine these physical properties of Florida normal-weight, as well as

lightweight, concretes especially for the concretes used in pre-stressed concrete structures, so that correct values for these properties can be used in structural design.

To address this need, a prior FDOT research project “Modulus of Elasticity, Creep and Shrinkage of Concrete,” was conducted to evaluate ten typical Florida normal-weight and lightweight concretes used in prestressed structures for their modulus of elasticity, creep, and shrinkage properties. Creep properties up to 90 days of loading were evaluated in that study. While these data were very valuable, they were limited in scope due to the constraint of time and budget. Due to the time constraint, no replicate batch of the concrete mixes in the testing program was tested. There was a need to test the replicates of these concrete mixes to establish reliability of the findings and to evaluate the variability of the test results. There was also a need to extend this study to evaluate the effects of other aggregate types, and to use a longer creep testing period of one year for better prediction of the ultimate creep coefficients of these concretes.

1.2 Objectives of Study

This research had the following major objectives:

- 1) To design and recommend an effective and reliable laboratory testing set-up and procedure for performing creep tests on concrete.
- 2) To evaluate the effects of aggregate, mineral additives and water-to-cementitious-materials ratio on strength, elastic modulus, shrinkage and creep behavior of concrete.
- 3) To determine the strength, elastic modulus, shrinkage and creep behavior of the typical concretes used in Florida.
- 4) To determine the relationship among compressive strength, splitting tensile strength, and modulus of elasticity of concretes made with typical Florida aggregate.
- 5) To develop prediction equations or models for estimation of shrinkage and creep characteristics of typical Florida concretes.

1.3 Scope of Study

The scope of this research covered the following major tasks:

- 1) To review the literature about previous and current study on elastic modulus, shrinkage, and creep of concrete.
- 2) To design, construct, and evaluate the effectiveness of creep test set-up and procedures.
- 3) To perform a comprehensive laboratory study on the physical and mechanical properties of typical Class II, IV, V and VI concrete mixtures made with normal weight aggregate and lightweight aggregate, including compressive strength, indirect tensile strength, modulus of elasticity, creep behavior, and shrinkage behavior. A total of 18 different concrete mixes were evaluated.
- 4) To analyze the experimental data; to determine the relationships among different properties; and to develop prediction equations for estimation of shrinkage and creep behaviors of concrete.

1.4 Research Approach

Objectives of this study were realized with the following research approaches:

- 1) To conduct laboratory testing programs to determine the various properties of concrete. ASTM standard test methods were used for a compressive strength test, splitting tensile test, elastic modulus test and shrinkage test. A creep test set-up was designed, evaluated and refined to be used for this purpose.
- 2) To perform statistical analysis to determine relationships and trends among the fundamental properties of the concretes evaluated in this study.
- 3) To evaluate existing prediction models for creep and shrinkage, and to develop improved models for estimation of shrinkage and creep behaviors of concrete.

CHAPTER 2 LITERATURE REVIEW

2.1 Introduction

This chapter presents a literature review on the susceptibility of strength, elastic modulus, shrinkage and creep properties of concrete to various factors, and on the existing models for predicting the strength, elastic modulus, and shrinkage and creep properties of concrete.

2.2 Strength of Concrete

2.2.1 Significance of Studying Strength of Concrete

Strength is commonly considered as the most valuable property of concrete, and it gives an overall picture of the quality of concrete because of its direct relation to the micro-structure of the hydrated cement paste. Moreover, the strength of concrete is almost invariably a vital element of structural design and is specified for compliance purposes. Also, knowing strength development characteristics of concrete is very critical in decision-making about when to remove formworks, when to continue the next construction step, or when to open a structure for use. It would be advantageous for an economic analyzer to know the aforementioned information in order to optimize the budget of a project.

With the broad development and application of new concrete techniques characterized by high strength concrete and high performance concrete over the past decades, durable concrete structures and complex structural design have become realizable. For example, high-rise buildings have enabled humankind to make full use of the limited living space on this planet in a plausible way; and long-span bridges are comparably more cost-effective and resource-saving, as well as quite pleasing aesthetically.

However, even though a large amount of information has been accumulated about concrete strength design, engineers are still far from knowing well the strength properties of concrete. To design a concrete mixture with pre-assigned properties is still an engineer's dream. The causes are attributed to the volatility of concrete strength induced by the variation of raw materials and their proportions. Thus, the properties of concrete materials are still worthy of study.

2.2.2 Effect of Coarse Aggregate on Strength of Concrete

The investigation on the effect of raw materials and their proportions on strength development has been the focus of efforts by many engineers.

For example, Aitcin and Mehta [1990] studied the effect of coarse aggregate characteristics on mechanical properties of high-strength concrete. The experiment was carried out using four coarse aggregate types available in Northern California and similar mix proportions. The results showed that using diabase and limestone aggregates produced concretes with significantly higher strength and elastic modulus than those using granite and river gravel. They concluded that the mineralogical differences in the aggregate types were responsible for this behavior.

Sarkar and Aitcin [1990] carried out research on the importance of petrological, petrographical, and mineralogical characteristics of aggregate in very high-strength concrete. They pointed out that the intrinsic strength of aggregate, particularly that of coarse aggregates, receives scant attention from concrete technologists and researchers as long as the water-to-cement (w/c) ratio falls within the 0.50 to 0.70 range, primarily due to the fact that the cement-aggregate bond or the hydrated cement paste fails long before aggregates do. This, however, does not hold true for very high-strength concretes with very low w/c ratios of 0.20 to 0.30. Compressive strength testing of very high-strength concrete has indicated that aggregates can assume the weaker role, exhibited in the form of transgranular fractures on the surface of failure, as has already been observed in some lightweight concretes. The authors have carried out

detailed petrological, petrographical, and mineralogical characterization of twelve different coarse aggregates that have performed with variable success in very high-strength concrete in Canada and the United States. Suitability for such an application has been linked to a special set of lithological characteristics: the minerals must be strong, unaltered, and fine grained. Intra- and intergranular fissures, partially decomposed coarse-grained minerals, and the presence of cleavages and lamination planes tend to weaken the aggregate, and therefore the ultimate strength of the concrete.

Ezeldin and Aitcin [1991] studied the effect of four coarse aggregates with different characteristics on the compressive strength, flexural strength, and flexural strength/compressive strength ratio of normal- and high-strength concretes. The study investigated the possibility of obtaining a relatively high flexural strength/compressive strength ratio at high compressive strength by using different aggregate types.

The study by Alexander and Addis [1992] showed that aggregates play an important role in governing mechanical properties of high-strength concrete. Generally, andesite and dolomite aggregates give superior results. Tests were also done on “artificial” interfaces between paste and these two rock types in order to characterize the interfacial bond properties. Results show that andesite achieves higher interfacial fracture energy values than dolomite, which helps to confirm the macroscopic engineering properties measured on concretes.

Giaccio et al. [1992] pointed out that concrete is a heterogeneous material whose properties depend on the properties of its component phases and the interactions between them. They studied the effects of granitic, basaltic, and calcareous aggregates on the mechanical properties of high-strength concrete, including compressive strength, flexural strength, modulus of

elasticity, and stress-strain behavior of concrete. The results indicated that the effect of coarse aggregate characteristics on the mechanical properties of high-strength concretes is substantial.

The impact of aggregate strength on concrete compressive strength was evaluated by Lindgard, and Smeplass [1993] as well. The significance of the aggregate strength has been compared with the effect of the cement type and the use of silica fume. According to the obtained results, the impact of the aggregate strength on the strength of high-strength concrete is limited, compared with the impact of the binder type, while the differences in elastic modulus between the different aggregate types is fully reflected in the concrete elastic modulus. This contradiction is explained by a hypothesis based on stress concentrations due to the difference in rigidity between the binder and the aggregates.

2.2.3 Prediction of Strength of Concrete

If there is no specific testing data available, it is a good alternative to have a reliable equation that gives an effective prediction of the strength of concrete at a desired age. An accurate approximation of the strength of concrete at specific ages is of great importance to know in order to decide when to remove formwork, when to continue with the next construction step, and when to open the structure for use.

In analyzing the characteristics of development of compressive strength with time, an empirical equation has been provided by ACI 209R Code as follows:

$$f'_c(t) = \frac{t}{\alpha + \beta \cdot t} \cdot f'_{c28} \quad (2-1)$$

Where α (in days) and β are constants, f'_{c28} is compressive strength of concrete at 28 days, and t is the age of concrete (in days). For tests using 6" \times 12" cylinders, type I cement, and moist curing conditions, the two constants α and β are equal to 4.0 and 0.85, respectively.

Because of the substantial effect of coarse aggregate types on the properties of concrete, and because of the absence of such mineral additives as fly ash and slag, which have substantial effects on the development of concrete strength, when the aforementioned formula was developed, caution must be taken when it is used. If possible, further investigation should be made to calibrate the above equation.

2.3 Elastic Modulus of Concrete

2.3.1 Definition and Determination of Elastic Modulus of Concrete

The modulus of elasticity or “Young’s Modulus,” a very important mechanical property reflecting the capability of concrete to deform elastically, is defined as the slope of the stress-strain curve within the proportional limit of a material.

For a concrete material, usually the most commonly used value in structure design is the secant modulus, which is defined as the slope of the straight line drawn from the origin of axes to the stress-strain curve at some percentage of the ultimate strength. Since no portion of the stress-strain curve is a straight line, the usual method of determining the modulus of elasticity is to measure the tangent modulus, which is defined as the slope of the tangent to the stress-strain curve at some percentage of the ultimate strength of the concrete as determined by compression tests on 6" × 12" cylinders. Figure 2-1 illustrates the stress-strain plot of concrete as it is loaded and unloaded. From this figure, we can see that the secant modulus is almost identical to the tangent modulus obtained at some lower percentage of the ultimate strength.

2.3.2 Significance of Studying Elastic Modulus of Concrete

Concrete, as a building material, is utilized in the elastic range. Thus, it is very important to know the relationship between stress and strain for a given concrete before it can be used for buildings, bridges, pavement and so forth. The relationship between stress and strain for a

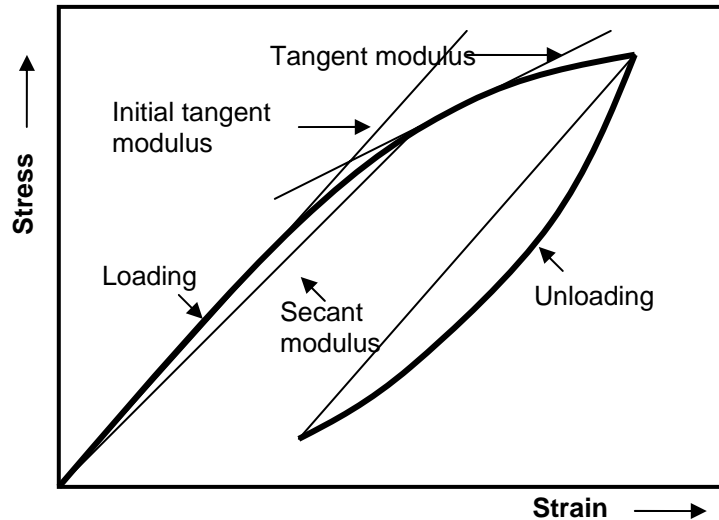


Figure 2-1. Representation of the stress-strain relation for concrete.

concrete material can be characterized by its elastic modulus, which is the property of concrete materials.

For reinforced concrete structures, the knowledge of the elastic property of a specific concrete mix will not only make the deformation of the concrete members well-controlled, but also decrease the extra stress transfer to other concrete elements, which can cause the concrete to crack or fail prematurely.

For prestressed concrete structures, elastic shortening is blamed for causing prestress loss. The prestress loss, on one hand, will decrease the capacity of a concrete structure, and even lead to unexpected collapse of the structure; and on the another hand, it will result in the increased volume of tendon for satisfying the design requirement because of over-estimation on elastic shortening, which can result in possible waste of materials and increased cost.

In addition, in order to make full use of the compressive strength potential, the structures using high-strength concrete tend to be slimmer and require a higher elastic modulus to maintain its stiffness. Therefore, the knowledge of the elastic modulus of high-strength concrete is very

important in avoiding excessive deformation, providing satisfactory serviceability, and achieving the most cost-effective designs.

Lastly, for concrete pavement, high elastic modulus concrete is not desirable because it increases the pavement cracking probability. Thus, high strength but low modulus concrete is preferable. As to how to obtain the concrete material with the properties desired, one way to approach this goal is to change the properties of individual concrete components and their proportions. And most importantly, the significant effects of different types of coarse aggregate on elastic modulus of concrete must be investigated.

2.3.3 Effect of Coarse Aggregate on Elastic Modulus of Concrete

Since concrete is a multiphase material, modulus of elasticity is very susceptible to the variation of coarse aggregate content and coarse aggregate type. In a study by Stock et al. [1979], it was reported that for concretes with a fixed w/c of 0.5, as the volume of coarse aggregate varied from 20% to 60%, the compressive strength of concrete remained almost same. This result is very consistent with the “w/c law” established by Duff Abrams in 1919. That is to say, for a given mix proportion, the compressive strength of concrete will be determined by its water-to-cement ratio. This is especially true for normal concrete with compressive strength less than 60 MPa. However, the elastic modulus of the concrete was substantially influenced by the changes in its coarse aggregate content. As shown in Figure 2-2 [Neville, 1996], we can see that the elastic modulus of concrete is remarkably different from that of hardened cement paste. Also, Neville [1996] pointed out that, for a concrete of a given strength, because normal weight aggregate has a higher elastic modulus than hydrated cement paste, a higher aggregate content results in a higher modulus of elasticity of the concrete.

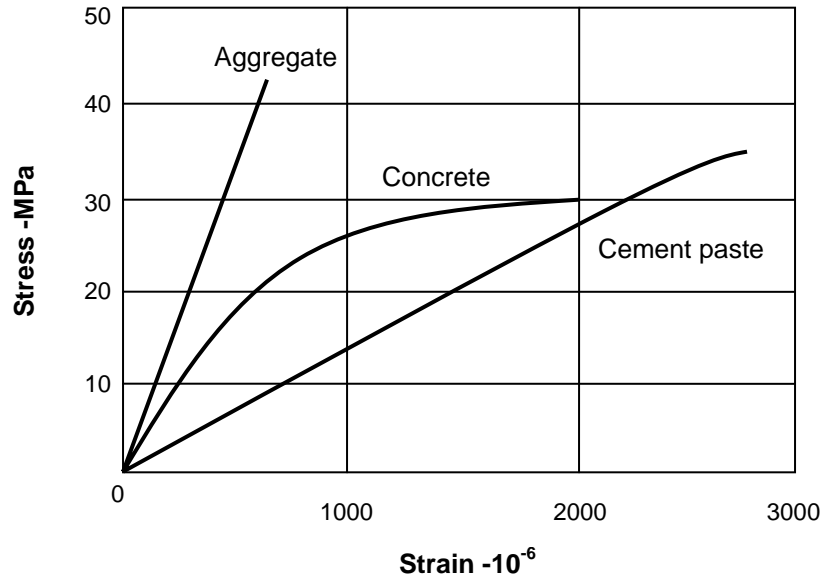


Figure 2-2. Stress-strain relations for cement paste, aggregate, and concrete.

In a study by Persson [2001], it was reported that the elastic modulus of self-compacting concrete was the same as that for normal concrete as long as their compressive strengths were the same. However, in a study by Schlumpf [2004], the elastic modulus of self-compacting concrete was reported to be 20% lower than that of normal concrete with a similar strength. In addition, the findings from the study by Chi et al. [2003] also indicated that the aggregate fraction in concrete had a considerable effect on the elastic modulus of concrete.

Coarse aggregate type is another very important factor affecting the elastic modulus of hardened concrete. Different types of aggregate can have quite distinct effects on elastic modulus. Even different coarse aggregates of the same type but from different locations can have substantially different properties. The reported findings by Zhou et al. [1995] show that the coarse aggregate type has a considerable influence on the elastic modulus of concrete. In that study, the effects of expanded clay, sintered fly ash, limestone, gravel, glass, and steel aggregates on the elastic modulus of concrete were investigated. In addition, the study by Shideler [1957]

on concrete mixtures using gravel and expanded clay as aggregate also indicate the same conclusion as reported by Zhou et al. [1995].

Aitcin and Mehta [1990] also investigated the effect of coarse aggregate characteristics on mechanical properties of high-strength concrete. In their study, the influence of four coarse-aggregate types available in Northern California on the compressive strength and elastic behavior of a very high-strength concrete mixture was studied using identical materials and similar mix proportions. The results indicated that the diabase and limestone aggregates were found to produce concretes with significantly higher strength and elastic modulus than did the granite and river gravel. The mineralogical differences in the aggregate types are considered to be responsible for this behavior.

The study by Alexander [1996] on the influence of 23 different aggregate types on the properties of hardened concrete showed that aggregates exert a profound and important influence on the elastic property of concrete.

Later, Aykut and Carrasquillo [1998] carried out an investigation on the effects of four coarse aggregate types locally available in central Texas on the mechanical properties of high-performance concrete. Test results showed that the mineralogical characteristics of coarse aggregate, as well as the aggregate shape, surface texture, and hardness appeared to be responsible for the differences in the performance of high performance concretes. Also, it was observed that there appeared to be no one single equation for high-performance concrete mixtures with different coarse aggregates that could estimate the elastic modulus with sufficient accuracy, as in the case of normal strength concretes. Wu et al. [2001] carried out a study on the effects of coarse aggregate type, including crushed quartzite, crushed granite, limestone, and marble coarse aggregate, on the compressive strength, splitting tensile strength, fracture energy,

characteristic length, and elastic modulus of concrete. The results indicated that the stiffness of concrete depends on the type of aggregate, especially for high-strength concrete.

Beshr et al. [2003], Rashid et al. [2002], and Huo et al. [2001] reported that different types of coarse aggregate have pronounced effects on elastic modulus of concrete.

2.3.4 Models for Predicting Elastic Modulus of Concrete

As mentioned in the literature about the factors affecting elastic modulus of concrete for a given type of aggregate, although the modulus of elasticity of concrete will increase with the strength of concrete, the factors that affect the modulus of elasticity of concrete do not always have a corresponding effect on the strength of concrete. Thus, there is no universal equation that can possibly be applied to relate compressive strength to elastic modulus of concrete. Thus, both the ACI model and CEB-FIP model, may need to be modified in order to be applied to a structure to achieve full function and serviceability in its entire life span. The above hypothesis can be easily confirmed by an extensive testing program to investigate the effects of coarse aggregate types on elastic modulus of concrete.

The study by Shih et al. [1989] suggested that Young's modulus of high-strength concrete has a somewhat higher value than that of normal-strength concrete. Pauw's equation for modulus of elasticity of concrete, which is based on experimental normal-strength concrete, needs to be reexamined.

Baalbaki et al. [1991] studied the influence of different types of crushed rocks on elastic properties of high-performance concrete. Testing results pointed to the important role played by coarse aggregates through the elastic properties of the parent rock. They also recommended that the present formulas relating the prediction of elastic modulus of concrete recommended by some codes be reviewed.

Nilsen and Aitcin [1992] investigated the properties of high-strength concrete containing lightweight, normal weight and heavyweight aggregates. In this study, a comparison of the values of elastic modulus determined experimentally with those calculated according to the formula recommended by the ACI Building Code, the British Standard Code, and the Norwegian Standard Code, showed that all codes overestimated the elastic modulus of high-strength heavyweight concrete.

In the following section, the formulas used to predict the elastic modulus of concrete by Florida LRFD guidelines, the ACI model, and the CEB-FIP model are given.

2.3.4.1 Model recommended by Florida LRFD guidelines [FDOT, 2002]

According to this guideline, in the absence of more precise data, the modulus of elasticity for concretes with unit weights between 0.090 and 0.155 kcf, can be estimated from the following formula [FDOT, 2002]:

$$E_c = \alpha \cdot w_c^\beta \cdot \sqrt{f'_c} \quad (2-2)$$

where E_c = elastic modulus in ksi;

w_c = unit weight of concrete (kcf);

f'_c = compressive strength of concrete (ksi);

α = constant, $\alpha = 33000$ is recommended by Florida LRFD guidelines; and

β = constant, $\beta = 1.5$ is recommended by Florida LRFD guidelines.

2.3.4.2 Prediction equations recommended by ACI 209

The prediction equations recommended by ACI for estimating the elastic modulus of concrete are given as follows:

$$E_c = A\sqrt{f'_c} \quad (2-3)$$

where E_c = elastic modulus (psi);

f'_c = compressive strength of concrete (psi); and

A = constant, $A = 57000$ is recommended by ACI 318.

The following equation recommended by ACI 318-89 (revised 1992) for structural calculation is applicable to normal weight concrete:

$$E_c = \alpha \sqrt{f'_c} + \beta \quad (2-4)$$

where E_c = elastic modulus (GPa);

f'_c = compressive strength of concrete (MPa);

α = constant, $\alpha = 3.32$ is recommended by ACI 318; and

β = constant, $\beta = 6.9$ is recommended by ACI 318.

The next equation given by ACI 363R-92 [ACI 363, 1992]] is applicable for predicting elastic modulus of concretes with compressive strength up to 83 MPa (12000 psi)

$$E_c = 3.65 \sqrt{f'_c} \quad (2-5)$$

where E_c = elastic modulus (GPa); and

f'_c = compressive strength of concrete (MPa).

2.3.4.3 CEB-FIP Model [CEB-FIP, 1990]

The CEB-FIP Model (Comité Euro-International du Béton-Federation Internationale de la Precontrainte) Code [CEB-FIP, 1990] also offers the following model for prediction of time-dependent modulus of elasticity. The equation is given as follows:

$$E_{ci}(t) = \left(\exp \left(s \cdot \left(1 - \left(\frac{28}{t/t_1} \right)^{0.5} \right) \right) \right)^{0.5} \cdot E_{ci} \quad (2-6)$$

where s = a coefficient depending on the type of cement ($s = 0.20$ for rapid hardening high strength cements; 0.25 for normal and rapid hardening cements; and 0.38 for slow hardening cements);

t = age of concrete (days);

t_1 = age of one (1) day; and

E_{ci} = modulus of elasticity of concrete at age of 28 days.

2.4 Shrinkage Behavior of Concrete

2.4.1 Origin of Shrinkage of Concrete

According to the mechanisms of concrete shrinkage, shrinkage of concrete consists of plastic shrinkage, autogenous shrinkage (a process known as self-desiccation), drying shrinkage, and carbonation shrinkage.

Autogenous shrinkage is the consequence of withdrawal of water from the capillary pores by the anhydrous cement particles. Most of the autogenous shrinkage will take place at the early age of hydration of cement. However, for concrete mixtures with a very low w/c ratio, this procedure may last longer if moisture is available from the ambient environment.

Plastic shrinkage and drying shrinkage are caused by withdrawal of water from concrete under the condition of humidity gradient between the interior of concrete and air. Plastic shrinkage may lead to the interconnection among capillary pores, the main factor contributing to cracking of concrete at an early age, as well as increasing permeability of concrete.

Carbonation shrinkage is caused by carbonation of calcium hydroxide in the concrete. Thus, carbonation shrinkage normally takes place on the surface of concrete elements. But, if there are penetrated cracks in concrete, carbonation shrinkage may take place in the interior of concrete. Carbonation of concrete will decrease the PH-value inside concrete so that steel reinforcement can be easily corroded.

2.4.2 Significance of Studying Shrinkage of Concrete

Shrinkage of concrete, one of the main factors in determination of the endurance of concrete structure, is a very important property of concrete to be evaluated. Excessive shrinkage is blamed for leading concrete to crack, even fail. During the early aging process of concrete, the low strength of the concrete cannot resist the stresses induced by drying shrinkage so that shrinkage-induced cracking can subsequently lead to premature failure of the concrete structure. Cracks in concrete increase the permeability of concrete and affect the corrosion initiation time and corrosion rate of steel reinforcement in the concrete structure. Shrinkage-induced cracks become a severe problem for marine concrete structures or concrete structures close to the coastal region. The penetration of aggressive ions through cracks into the interior of concrete is a very critical factor in causing the corrosion of steel reinforcement. For prestressed concrete elements, not only does the shrinkage-induced cracking speed up the corrosion of reinforcement, the shrinkage deformation, which accounts for up to 15% of total prestress loss, is also one of the main factors contributing to prestress loss.

The shrinkage behavior of concrete is greatly affected by coarse aggregate content, coarse aggregate type, cementitious material content, and water content. For instance, an increase in volume of aggregate in concrete will usually lead to a decrease in cement content, which would lead to reduced shrinkage of the concrete. However, a reduction in cement content does not necessarily cause a reduction in the strength of the concrete. Thus, through optimizing mix proportions of a concrete mixture, it is possible to design a concrete with low cement content and low shrinkage without sacrificing strength.

2.4.3 Effect of Raw Materials on Shrinkage of Concrete

2.4.3.1 Effect of aggregate content on shrinkage behavior of concrete

The contribution of coarse aggregate to decreased shrinkage of concrete is attributed to the decrease of cement paste volume in the concrete mix. In the 1950's, Pichett [1956] reported that shrinkage ratio increases significantly as aggregate content decreases. The possible reason to explain the effects of coarse aggregate content on shrinkage strain of concrete is shown in Figure 2-3. For the lean concrete mixture with a high coarse aggregate content, the coarse aggregate particles will have point-to-point contacts or even face-to-face contacts with each other. A concrete mixture with such a stiff aggregate skeleton will be very effective in resisting stresses caused by cement paste shrinkage because aggregate particles cannot be pushed more closely under the action of interior stress cause by shrinkage. Thus, shrinkage strain is dramatically reduced. But, for rich concrete, the situation is otherwise.

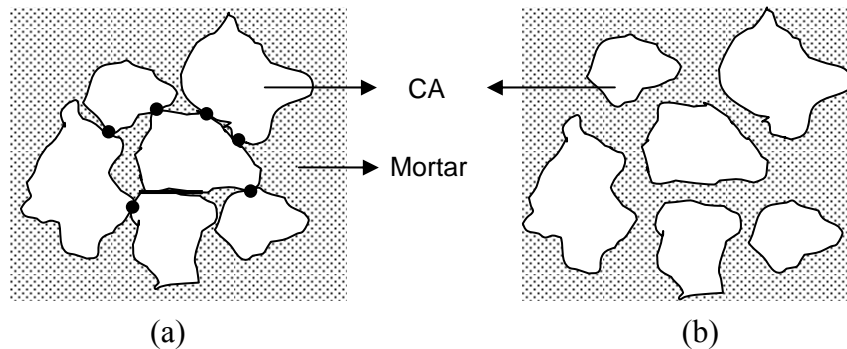


**Figure 2-3. Effect of coarse aggregate content on the shrinkage of concrete:
a) Lean concrete; and b) Rich concrete.**

Similarly, Hermite [1960] carried out a study of the effects of cement content on shrinkage behavior of concrete. The tests were performed at a curing temperature of 68° F, 50% relative humidity and wind velocity of 2.25 miles per hour (mph). The results indicated that, at the early age of concrete, the shrinkage strain of the concrete with a cement content of 850 lb/yd³ (typical

cement content for flowable concrete) is almost three times higher than that of concrete mixtures with a cement content of 340 lb/yd³.

Leming [1990] investigated the mechanical properties of high-strength concrete with different raw materials. These materials represent those used in structures built under North Carolina Department of Transportation control. The data from shrinkage tests showed that shrinkage strain of concrete varies significantly depending on the specific raw materials used and the strength levels attained.

Later, research was carried out by Alfes [1992] on how shrinkage was affected by the aggregate content, the aggregate modulus of elasticity, and the silica fume content. The experiment was conducted using a w/c ratio in the range of 0.25 to 0.3 with 20% silica fume by weight of cement; varying the amounts and type of aggregates (basalt, LD-slag, and iron granulate); and the compressive strength of concrete at 28 days was in the range of 102 to 182 MPa (14,600 to 26,000 psi). The test results showed that there is a direct and linear relationship between the shrinkage value and the modulus of elasticity of the concrete.

The next year Zia et al. [1993a, 1993b, 1993c] evaluated the shrinkage behavior of VES, HES, VHS concretes with different aggregates (crushed granite, marine marl, rounded gravel, and dense limestone). Shrinkage measurements were made for three to nine months in different cases. The observed behavior followed the general trend of conventional concrete except for the two cases of VES concrete using special blended cement (Pyrament) with marine marl and rounded gravel as aggregates. In these two cases, the specimens exhibited an expansion of approximately 140 microstrains, rather than shrinkage for the entire period of 90 days. The expansion was attributed to the lack of evaporable water in the concrete because of its very low w/c ratio (0.17 for marine marl, and 0.22 for rounded gravel).

2.4.3.2 Effects of coarse aggregate type on concrete shrinkage

The skeleton of coarse aggregate in a concrete mixture can restrain the shrinkage of the cement matrix. The extent to which the coarse aggregate skeleton can resist the stress caused by shrinkage-induced stress from cement matrix depends on the stiffness of the coarse aggregate. That is to say, the elastic modulus of the aggregate determines the extent of restraining action to the shrinkage of concrete. For example, the shrinkage of a concrete mixture made with a steel aggregate will be lower than the one made with a normal aggregate. Similarly, the shrinkage of a concrete mixture made with expanded shale aggregate will be higher than the one made with a normal aggregate.

The above hypothesis was verified by the many studies performed in the past decades. Troxell et al. [1958] performed tests to study the effects of coarse aggregate of different types on shrinkage behavior of concrete. The tests were carried out on the concrete mixtures with a fixed mix proportion. The results showed that there was a considerable variation in the shrinkage strain of the resulting concrete batched with coarse aggregate of different types, and it was concluded that this phenomenon was due very likely to the difference in modulus of elasticity among aggregates of different types. Generally speaking, the elastic property of aggregate determines the degree of restraint to the cement matrix.

Reichard [1964] agreed that the coarse aggregate has a significant effect on the shrinkage behavior of concrete. A normal natural aggregate is usually not subject to shrinkage. However, rocks exist that can shrink up to the same magnitude as the shrinkage of concrete made with non-shrinking aggregate.

2.4.3.3 Effects of size and shape of coarse aggregate on concrete shrinkage

Aggregate size and shape also affect the shrinkage of hardened concrete. The experimental study conducted by Collins [1989] on shrinkage of five high-strength concrete mixtures with

varied paste content and aggregate size, showed that shrinkage deformations were somewhat less for concrete mixtures with lower paste contents and larger aggregate size.

A study by Bisschop and Van Mier [2000] indicated that the total length and the depth of micro-cracking caused by shrinkage of concrete will increase with larger aggregate size.

McQueen et al. [2002] performed laboratory shrinkage tests in accordance with ASTM C 157 on a matrix of 16 concrete mixes to evaluate the effects of coarse aggregate size on shrinkage of concrete. The tests were conducted on mixes with ASTM C 33, No. 57 (38-mm maximum aggregate size) and No. 467 (64-mm maximum aggregate size) coarse aggregates. The results of the laboratory shrinkage tests revealed that the maximum size of the coarse aggregate (No. 57 or 467) did not influence the shrinkage.

A study on evaluation of high-performance concrete pavement carried out by Ozyildirim [2000] showed that concrete using smaller coarse aggregate commonly exhibits greater shrinkage and increases potential for slab cracking because of increased paste requirements. Larger maximum coarse aggregate sizes on the other hand, require less paste, less cementitious material, and less water, thereby resulting in reduced shrinkage; they also provide increased mechanical interlock at joints and cracks.

Thus, there is still some controversy about how coarse aggregate size will affect the shrinkage behavior of concrete. Test data from the specific concrete are necessary to control concrete quality.

2.4.3.4 Effect of other factors on shrinkage behaviors of concrete

Shrinkage behavior of concrete is affected not only by coarse aggregate, but also by other factors, such as water content, specimen size, ambient conditions, admixtures as well as mineral additives.

Water content is the most important factor influencing shrinkage behavior of concrete. Normally, the higher the w/c ratio is, the higher the shrinkage. This occurs due to two interrelated effects. As the w/c ratio increases, paste strength and stiffness decrease; and as water content increases, shrinkage potential increases.

The specimen size affects the diffusion rate of free water from the interior to exterior of concrete. Thus, both the rate and the total magnitude of shrinkage decrease with an increase in the volume of the concrete member because, for larger members, more time is needed for shrinkage effects to reach the interior regions. For instance, the study by El-Hindy et al. [1994] showed that dry shrinkage of small specimens measured by the conventional laboratory test was found to over-estimate shrinkage of the concrete in the real structure.

Ambient conditions, such as relative humidity and temperature, greatly affect the magnitude of shrinkage. These are blamed for affecting shrinkage behavior because they create the relative humidity gradient and relative temperature gradient between the interior and exterior of concrete, which is a driving force to concrete shrinkage. The higher the relative humidity is, the lower the rate of shrinkage. The lower the temperature gradient is, the lower the shrinkage rate. Thus, the investigation conducted on shrinkage behavior of concrete has to simulate the real environmental conditions in order to not overestimate shrinkage strain. For example, Aitcin and Mehta [1990] reported that under field conditions, the surface shrinkage strains were considerably lower than those measured under laboratory conditions.

The effect of mineral additives on shrinkage behavior varies according to the type of mineral additive. Any material which substantially changes the pore structure of the paste will affect the shrinkage characteristics of the concrete. In general, as pore refinement is enhanced, shrinkage is increased. Pozzolans typically increase the drying shrinkage, due to several factors.

With adequate curing, pozzolans generally increase pore refinement. Use of a pozzolan results in an increase in the relative paste volume due to the following two mechanisms:

- 1) In practice, slowly reacting pozzolans (such as Class F fly ash) are frequently added to replace cement by weight rather than by volume according to conventional concrete mix design methods. This will increase paste volume since pozzolans have a lower specific gravity than Portland cement.
- 2) Additionally, since pozzolans such as fly ash and slag do not contribute significantly to early strength, concrete containing pozzolans generally has a lower stiffness at earlier ages as well, making them more susceptible to increased shrinkage under standard testing conditions.

2.4.4 Models to Predict Concrete Shrinkage

Misprediction of shrinkage usually does not cause structural collapse, but puts the structure out of service, i.e., the structure does not live as long as the projected life span. The widespread occurrence of such lack of long-term serviceability inflicts a tremendous economic damage on many nations. The direct signs of damage that puts a structure out of service are typically cracks, which may cause major fractures.

Even though the mechanisms of shrinkage, such as micromechanics mechanism and diffusion mechanism, have been studied extensively, their correlations with macroscopic behaviors have been intuitive and non-quantitative. As pointed out by Bazant and Carol [1993], such studies generally have not borne much fruit. Since the uncertainty in the prediction of shrinkage behavior with the variations of concrete compositions and random environmental conditions is enormous, the models established at present rely on purely empirical relations without micromechanics models involved. In addition, substantial effort has been paid in stochastic phenomena and probabilistic models, but similar to the preceding topic, nothing is being introduced into practice.

At present, the empirical formula given by the ACI Committee 209 [ACI 209, 1992] is widely used to predict shrinkage strain. But, it should be noted that the ACI 209 equation could well be in error unless broad corrections are applied, for instance, correcting for curing and size effects, and accounting for humidity and composition effects. As pointed out by El-Hindy et al. [1994], the ACI 209 predictive equation was found to be valid for the high-performance concretes only if new values for the parameters were introduced.

Thus, owing to many uncertainties in current models, it is very necessary to perform tests on the specific concrete mixtures designed using local available materials to guarantee the safety of structures. Then, based on the accumulated data, constitutive parameters characterizing the shrinkage behaviors of concretes designed based on local available materials can be obtained.

In the following sections, the shrinkage prediction models offered by CEB-FIP model code (1990) and ACI 209 (1992) are reviewed briefly.

2.4.4.1 CEB-FIP model for shrinkage strain prediction

In this model, the effects of cement type, ambient relative humidity, compressive strength of concrete, and size effect of specimen on shrinkage strain of concrete are taken into consideration. The total shrinkage strain may be estimated by the following equation:

$$\varepsilon_{cs}(t, t_s) = \varepsilon_{cs0} \cdot \beta_s(t - t_s) \quad (2-7)$$

where $\varepsilon_{cs}(t, t_s)$ = time-dependent total shrinkage strain;

ε_{cs0} = notational shrinkage coefficient; and

$\beta_s(t - t_s)$ = coefficient to describe the development of shrinkage with time.

Coefficient ε_{cs0} can be estimated by the following equation:

$$\varepsilon_{cs0} = \left(160 + 10\beta_{sc} \left(9 - \left(\frac{f_{cm}}{f_{cm0}} \right) \right) \right) \times 10^{-6} \cdot \beta_{RH} \quad (2-8)$$

where β_{sc} = A coefficient which depends on the type of cement ($\beta_{sc} = 4$ for slowly hardening cements; 5 for normal or rapid hardening cements; 8 for rapid hardening high strength cements);

f_{cm} = mean compressive strength of concrete at the age of 28 days;

$f_{cm0} = 1$ MPa;

$\beta_{RH} = -1.55 \beta_{sRH}$ for $40\% \leq RH < 99\%$; $\beta_{RH} = 0.25$ for $RH \geq 99\%$

$$\text{where} \quad B_{sRH} = 1 - \left(\frac{RH}{RH_0} \right)^3 \quad (2-9)$$

RH = the relative humidity of the ambient environment (%); and

$RH_0 = 100\%$.

Coefficient $\beta_s(t - t_s)$ can be estimated by the following equation:

$$\beta_s(t - t_s) = \left(\frac{\frac{(t - t_s)}{t_1}}{350 \cdot \left(\frac{h}{h_0} \right)^2 + \frac{t - t_s}{t_1}} \right)^{0.5} \quad (2-10)$$

where $h = 2A_c/u$ = the notational size of member (in mm), where A_c is the cross-sectional area (mm^2) and u is the perimeter (mm) of the member in contact with the atmosphere;

$h_0 = 100$ mm; and

$t_1 = \text{one (1) day}$.

2.4.4.2 Prediction model recommended by ACI 209 Report [1992]

The concrete shrinkage prediction model recommended by ACI 209 [1992] is shown by the following equation:

$$(\varepsilon_{sh})_t = \frac{t}{35+t}(\varepsilon_{sh})_u \quad (2-11)$$

where $(\varepsilon_{sh})_t$ = time-dependent shrinkage strain;

$(\varepsilon_{sh})_u$ = ultimate shrinkage strain; and

t = time in days.

If there is no available shrinkage data from the concrete to be evaluated, the ultimate shrinkage strain, $(\varepsilon_{sh})_u$, can be assumed to be the following:

$$(\varepsilon_{sh})_u = 780 \times 10^{-6} \times \gamma_{sh} \quad (2-12)$$

where γ_{sh} = a product of all the applicable correction factors for the testing conditions other than the standard condition; $\gamma_{sh} = 1$ under standard testing condition, and is obtained by multiplying the ultimate shrinkage strain under the standard condition by the appropriate correction factors as described in the following.

- Correction factors for the effect of initial moist curing. The correction factor is equal to 1.0 for concrete cylinders moist-cured for 7 days, and 0.93 for that moist-cured for 14 days.
- Correction factor for the effect of ambient relative humidity. The following formulas are given for use in obtaining the correction factor for shrinkage test performed under the condition of ambient relative humidity greater than 40%.

$$\gamma_\lambda = 1.40 - 0.0102\lambda, \text{ for } 40 \leq \lambda \leq 80 \quad (2-13)$$

$$\gamma_\lambda = 3.00 - 0.030\lambda, \text{ for } 80 \leq \lambda \leq 100 \quad (2-14)$$

where γ_λ = correction factor for the effect of relative humidity; and

λ = relative humidity.

- Correction factor for the effects of specimen size. The correction factor in consideration of the specimen size effect (γ_{vs}) is given by the following equation:

$$\gamma_{vs} = 1.2 \exp\left(-0.12 \cdot \frac{v}{s}\right) \quad (2-15)$$

where γ_{vs} = correction factor for the effects of specimen size; and

$\frac{v}{s}$ = volume-surface area ratio of the specimen in inches.

- Correction factor for concrete composition. Various equations for calculating the correction factors for the effects of the slump of the fresh concrete, aggregate content, cement content and air content of the concrete have also been given in this model.

2.5 Creep of Concrete

2.5.1 Rheology of Materials and Definition of Creep of Concrete

The philosophical origin of rheology is owed to Heraclitus. As exemplified in his famous aphorism *panta rhei* (or *panta rei*), “everything flows and nothing stands still.”

Inspired by this expression, the term “rheology” was coined in 1920 by Eugene Bingham, a professor at Lehigh University, and defined as the study of the deformation and flow of matter under the influence of an applied stress. One of the tasks of rheology is to empirically establish the relationships between deformations and stresses by adequate measurements. Such relationships are then amenable to mathematical treatment by the established methods of continuum mechanics.

The rheological phenomenon of concrete materials, also termed as creep, is one of very important rheological properties of concrete. Since creep behavior of concrete is characterized by time-dependence, it generates substantial effects on the structural stability during its service

life. Thus, it is of great importance to know the creep behavior of specific concrete before it can be used for structure design.

Creep of concrete can be defined as the time-dependent deformation of concrete materials under a sustained stress. As shown in Figure 2-4, load-induced creep consists of three stages, namely primary (or transient) creep stage, steady-state creep (or secondary creep) stage and tertiary creep stage. The primary (transient) creep is characterized by a monotonic decrease in the rate of creep. During the secondary (steady-state) creep stage, the material shows a constant creep rate. Lastly, in tertiary creep stage, the creep rate increases until the material fails.

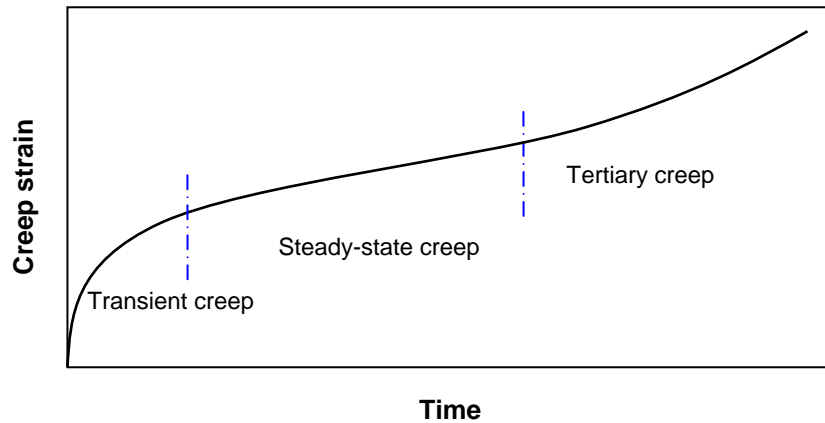


Figure 2-4. Creep diagram of concrete material.

Figure 2-5 shows a plot of strain versus time for a concrete that was loaded for some time and then unloaded. The permanent strain that remains after the load has been released is called the creep strain. For concrete materials, creep strain consists of two main components. The first component is the true or basic creep, which occurs under the conditions of no moisture movement to or from the ambient medium. This is the case for concrete elements functioning in underground foundations or in water. The second component is the drying creep, which takes place while concrete is subjected to ambient conditions. Normally, the creep strain that is considered in structural design is the sum of basic creep strain and drying creep strain.

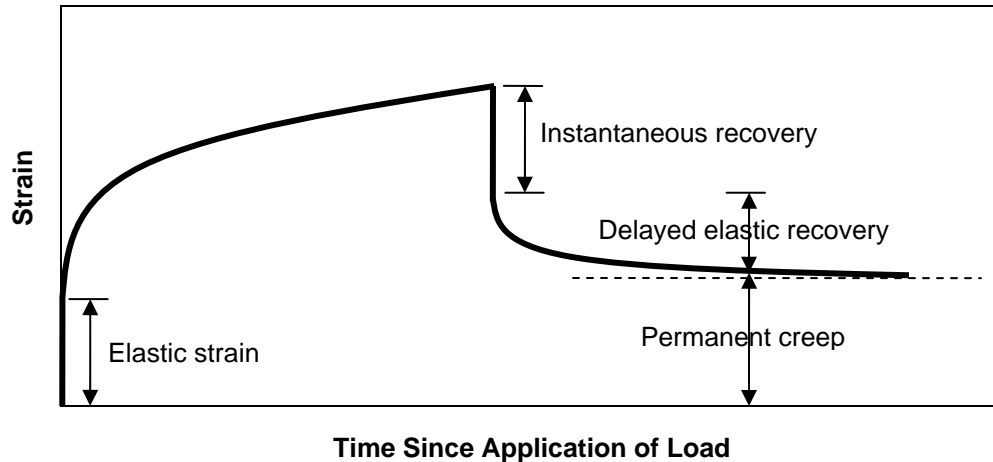


Figure 2-5. Strain-time plot of concrete under a sustained load and after release of load.

The total creep strain usually includes both the delayed elastic deformation and permanent creep deformation due to the difficulty of differentiating delayed elastic strain from creep strain and the convenience of building a numerical model that simulates a time-creep strain curve with the delayed elastic deformation included. Also, the abovementioned approach is usually taken since the delayed elastic strain is usually very small compared to the total creep strain.

The creep behavior of concrete materials plays a great role in the stability of concrete structures. Also, the creep behavior of concrete is subjected to severe volatility caused by the variation of raw materials for concrete mixtures and their proportions. Therefore, over the past decades, the study of creep behavior in concrete has been one of the focuses of engineers.

2.5.2 Significance of Studying Creep Behavior of Concrete

Creep in concrete can have both positive as well as negative effects on the performance of concrete structures. On the positive side, creep can relieve stress concentrations induced by shrinkage, temperature changes, or the movement of supports. For example, in an indeterminate beam with two fixed ends, creep deformation would be very helpful in reducing tensile stress caused by shrinkage and temperature variation.

On the other hand, in some concrete structures creep can do harm to the safety of the structures. For instance, creep deformation can lead to an excessive deflection of structural members, creep buckling or other serviceability problems especially in high-rise buildings, eccentrically loaded columns and long bridges. In mass concrete, creep may be a cause of cracking when a restrained concrete mass undergoes a cycle of temperature change due to the development of heat of hydration and subsequent cooling. For prestressed concrete structures, such as composite bridges, pre-stressed shells, or continuous girders, the desirable creep of concrete would be as low as possible. Heavily pre-stressed members and long members are particularly susceptible to large volume changes. If a pre-stressed member is restrained in position prior to the majority of the volume change taking place, the pre-stressed members will exert excessive forces on its connections and supporting structures that could cause a structural failure. Also, another very important issue caused by creep deformation is prestress loss, accounting for more than 25% of total pre-stress loss.

2.5.3 Effect of Aggregate on Creep of Hardened Concrete

Aggregates play an important role in creep of concrete. Coarse aggregate reduces creep deformation by reducing the cement paste content and restraining the cement paste against contraction. Generally, concretes made with an aggregate that is hard and dense and have low absorption and high modulus of elasticity, are desirable when low creep strain is needed.

The study by Troxell et al. [1958] indicated that the creep strains of the concrete mixtures with different types of aggregate will behave differently. The highest creep value is obtained from the concrete made with sandstone aggregate, and the lowest creep value is obtained from the concrete made with limestone.

Rüsch et al. [1963] found an even greater difference between the creep strains of concretes made with different aggregates. After 18 months under load at a relative humidity of 65%, the maximum creep strain of the concrete made with sandstone was five times higher than the minimum creep strain of the concrete made with basalt.

Alexander et al. [1980] studied the influence of 23 aggregate types on creep deformation of concrete. Creep tests were conducted in a controlled environment at 23° C and 60% relative humidity. Creep tests were conducted for six months after a 28-day water cured period in lime-saturated water to allow for minimal effects of hydration. Strains were measured using longitudinal gages on two opposite faces of the prism with a gage length of 100 mm (4"). The conclusion was that aggregates with a lower absorption will produce concrete with a lower creep deformation. It was further determined that the aggregate with a high elastic modulus will produce low creep values.

Collins [1989] examined the creep property of high-strength concrete. Creep tests were conducted according to ASTM C 512. The results demonstrated that a concrete with a larger aggregate size and lower paste content would provide a lower creep strain.

Creep tests done by Hua et al. [1995] on pure hardened cement pastes and on a reference concrete (made with the same paste) also show that creep is reduced by the presence of aggregate.

In addition, the conclusion on the effect of coarse aggregate content on creep of concrete is also confirmed by the tests on lightweight aggregate concrete. The study by Gesoğlu et al. [2004] showed that concretes containing higher lightweight coarse aggregate content had a lower creep strain at all w/c ratios.

2.5.4 Prediction Models and Their Limitations of Concrete Creep

With the exception of creep buckling, overestimation or underestimation of creep usually does not lead to structural collapse, but merely shortens the structural service life. But, misprediction of creep could lead to tremendous economic loss.

Thus, accurate prediction of the ultimate creep strain of concrete is of great importance. In order to obtain an accurate prediction, the following mechanisms possibly resulting in creep of concrete have been studied, including micromechanics mechanisms, diffusion phenomena, thermodynamics mechanisms, and other mechanisms coupled with damage and fracture.

Micromechanics mechanisms in creep behavior have been studied extensively for decades through the study of the microstructure of cement and concrete. However, the macroscopic constitutive relations based on the intuitively and non-quantitatively observed phenomena, or postulated on the microstructure or even molecular level, generally are not promising. The uncertainty in the prediction of long-term creep associated with the variations of concrete composition is enormous, actually much larger than any uncertainty except that due to the randomness of environment. Thus, even though the attempts at the mathematical micro-mechanical modeling of some phenomena have already begun, there is still a lot to do to make them practical.

Diffusion phenomena can be considered another very important mechanism for creep behavior of concrete because creep of concrete is always associated with the moisture and heat transport between the interior concrete and outside environment. Therefore, in concrete structures exposed to the environment or subjected to variable temperatures, there is no hope of obtaining realistic stresses without actually solving the associated problems of moisture and heat transport, at least in an approximate manner. It has been shown that creep and shrinkage analysis

based on diffusion analysis of a box girder bridge segment yields enormous stresses which are routinely neglected in practice.

The models based on statistics have been studied extensively. Although the statistical variability of concrete creep under controlled laboratory conditions is quite small, very large statistical fluctuations are caused by the environment as well as the uncertainties in the effect of concrete composition. In most practical situations, sophisticated deterministic mathematical analysis makes in fact little sense, because the uncertainties of stochastic origin are much larger than the errors of simple effective modulus solutions compared with sophisticated deterministic analytical solutions of differential or integral equations.

Due to complex influences coming from raw materials and the ambient environment, the common problem with current models is that they are only feasible to be used for the creep prediction of similar concretes, which means concretes from the same geographical region. The concretes used in the Florida region are generally quite similar and, instead of repeating measurements for each new major structure, one can greatly improve predictions on the basis of previously obtained data for a similar concrete from the same region. Equally important will be application of the existing fundamental research results in practice. Since each of these models is applicable under specific conditions for a certain class of materials, the proper utilization of these models depends essentially on the practical experience of the researcher. The accumulation of this experience is the purpose of most experimental work on creep. This is due mainly to the fact that, 1) more than one microscopic mechanism is involved in inducing creep of concrete; and 2) some empirical models can only be used for certain types of concretes without the variation of concrete components, proportions and applied environmental conditions. If the

empirical model obtained from the concretes used in a given region is applied to predict creep strain of the concretes in another region, the results could be very scary.

Over the years, many equations have been developed for the description of steady-state and transient creep. But, most of them are either too complicated theoretically to bring them into practical use, or they have an empirical character and were determined on the basis of a fit to the experiments, which causes great uncertainties in the extrapolation to long time intervals and to conditions not covered in the laboratory.

In the following sections, two creep prediction models, namely the CEB-FIP model and the ACI 209 model will be reviewed.

2.5.4.1 CEB-FIP model code

In this model, the creep strain can be predicted by the following equation:

$$\varepsilon_{cr}(t, t_0) = \frac{\sigma_c(t_0)}{E_{ci}} \cdot \phi_{28}(t, t_0) \quad (2-16)$$

where $\varepsilon_{cr}(t, t_0)$ = creep strain at time t;

$\sigma_c(t_0)$ = applied stress;

$\phi_{28}(t, t_0)$ = creep coefficient; and

E_{ci} = modulus of elasticity at the age of 28 days.

The modulus of elasticity can be estimated by the following equation:

$$E_{ci} = \alpha_E \cdot 10^4 \cdot \left(\frac{f_{ck} + \Delta f}{f_{cmo}} \right)^{\frac{1}{3}} \quad (2-17)$$

where f_{ck} = characteristic strength of concrete (in MPa);

Δf = 8 MPa;

f_{cmo} = 10 MPa; and

α_E = 2.15×10^4 MPa.

The creep coefficient $\phi_{28}(t, t_0)$ can be calculated as follows:

$$\phi_{28}(t, t_0) = \phi_0 \cdot \beta_c(t - t_0) \quad (2-18)$$

where ϕ_0 = notational creep coefficient;

β_c = coefficient to describe the development of creep with time after loading;

t = age of concrete in days; and

t_0 = age of concrete when loaded in days.

The notational creep coefficient can be estimated as follows:

$$\begin{aligned} \phi_0 &= \phi_{RH} \cdot \beta(f_{cm}) \cdot \beta(t_0) \\ \phi_{RH} &= 1 + \frac{1 - RH / RH_0}{0.46 \cdot (h / h_0)^{1/3}} \\ \beta(f_{cm}) &= \frac{5.3}{\sqrt{f_{cm} / f_{cm0}}} \\ \beta(t_0) &= \frac{1}{0.1 + (t_0 / t_1)^{0.2}} \end{aligned} \quad (2-19)$$

where $f_{cm} = f_{ck} + \Delta f$;

h = notational size of the member (in mm) = $2A_c / u$;

A_c = cross-sectional area (in mm²);

u = perimeter of the member in contact with the atmosphere (in mm);

h_0 = 100 mm;

RH = relative humidity of the ambient environment (in %);

RH_0 = 100%; and

t_1 = one (1) day.

$$\beta(t-t_0) = \left[\frac{(t-t_0)/t_1}{\beta_H + (t-t_0)/t_1} \right]^{0.3} \quad (2-20)$$

$$\beta_H = 150 \cdot \left[1 + \left(1.2 \cdot \frac{RH}{RH_0} \right)^{18} \right] \cdot \frac{h}{h_0} + 250 \leq 1500$$

2.5.4.2 ACI 209 model

In the ACI 209 (1992) model, the creep coefficient is estimated as follows:

$$\phi_{28}(t, t_0) = \phi_{\infty}(t_0) \cdot \frac{(t-t_0)^{0.6}}{10 + (t-t_0)^{0.6}} \quad (2-21)$$

where $\phi_{28}(t, t_0)$ = creep coefficient at time t ;

$\phi_{\infty}(t_0)$ = ultimate creep coefficient; and

t_0 = time of loading.

The ultimate creep coefficient can be expressed as:

$$\phi_{\infty}(t_0) = \gamma_c \cdot \phi_{\infty} \quad (2-22)$$

The constant $\phi_{\infty} = 2.35$ is recommended. The correction factors γ_c consist of the following terms:

$$\gamma_c = \gamma_{la} \cdot \gamma_{RH} \cdot \gamma_{at} \cdot \gamma_s \cdot \gamma_{\rho} \cdot \gamma_a \quad (2-23)$$

where γ_{la} = correction factor for loading age (for loading ages later than 7 days and moist cured concrete, $\gamma_{la} = 1.25 \cdot (t_0)^{-0.118}$; for loading ages later than 1-3 days and steam cured concrete, $\gamma_{la} = 1.13 \cdot (t_0)^{-0.094}$);

γ_{RH} = correction factor ambient relative humidity (for ambient relative humidity greater than 40%, $\gamma_{RH} = 1.27 - 0.0067 \cdot RH$ (RH is the ambient relative humidity in %));

γ_s = correction factor for slump of fresh concrete, $\gamma_s = 0.82 + 0.00264 \cdot S_l$ (S_l in mm);

γ_{ρ} = correction factor for fine-to-total aggregate ratio, $\gamma_{\rho} = 0.88 + 0.0024 \cdot \rho_a$ (ρ_a is fine-to-total aggregate ratio);

γ_a = correction factor for air content, $\gamma_a = 0.46 + 0.09 \cdot a_a$ (a_a is air content); and

γ_{at} = correction factor for thickness of member. When the average thickness or volume to surface ratio of a structural member differs from 150 mm or 38 mm, respectively, two methods are offered for estimating the factor of member size γ_{at} :

- *Average-thickness method.* For an average thickness of a member smaller than 150 mm, the factors are given by the ACI 209 Report. For an average thickness of a member larger than 150 mm and up to about 300 to 380 mm, the correction factor for thickness is given as:

$$\gamma_{at} = 1.14 - 0.00092 \cdot h_a \quad (\text{during the first year after loading})$$

$$\gamma_{at} = 1.10 - 0.00067 \cdot h_a \quad (\text{for ultimate values})$$

where h_a = average thickness of a member in mm.

- *Volume-surface ratio method.*

$$\gamma_{at} = \frac{2}{3} \cdot \left[1 + 1.13 \cdot e^{-0.0213 \cdot (v/s)} \right] \quad (2-24)$$

where v/s = volume-to-surface ratio in mm.

CHAPTER 3 MATERIALS AND EXPERIMENTAL PROGRAMS

3.1 Introduction

This chapter describes the mix proportions and ingredients of typical concrete mixtures used in this research, the method of preparation of the concrete mixtures, fabrication procedure of the test specimens and routine ASTM testing methods and procedures used in this study.

3.2 Concrete Mixtures Evaluated

3.2.1 Mix Proportion of Concrete

The concrete mixtures were randomly selected from typical Class II, IV, V, and VI concretes made with normal-weight and lightweight aggregates. They are representative concrete mixes broadly used in Florida. The range of designed compressive strength of concretes varied from 4,000 to 11,000 psi at the age of 28 days. Class F fly ash and ground blast-furnace slag were used as additives in these mixes. Water reducing and air entraining admixtures were used throughout all the mixtures.

Water-to-cementitious materials (w/c) ratio for all the mixtures was determined according to the design strength of specified concrete. Workability of fresh concrete in terms of slump value was controlled by the dosage of water reducer, super plasticizer, and air entraining agents. Since strength of concrete is very sensitive to the variation of air content and water content, to meet the target slump value the dosages of water reducer and super plasticizer were adjusted rather than the dosages of air entraining agent and water. In addition, another reason to add air entraining agent to concrete is to improve the durability of the concrete.

A total of 18 different concrete mixtures were evaluated. The detailed mix proportions for mixtures are presented in Table 3-1. Miami Oolite limestone was used as a coarse aggregate

Table 3-1. Mix Proportions of the 18 Concrete Mixtures Used in this Study

Coarse Aggregate	No. of Mix	W/C	Cement (lbs/yd ³)	Fly Ash (lbs/yd ³)	Slag (lbs/yd ³)	Water (lbs/yd ³)	FA (lbs/yd ³)	CA (lbs/yd ³)	Admixture	
									AE	WRDA/ADVA
Miami Oolite	Mix 1F	0.24	800	200	---	236.0	931	1679	7.5 OZ	(WRDA60)-30OZ (ADVA120)-60OZ
	Mix 2F	0.33	656	144	---	265.6	905	1740	12.0 OZ	(WRDA60)-30OZ
	Mix 3F	0.41	494	123	---	254.0	1175	1747	0.5 OZ	(WRDA60)-33.4OZ
	Mix 4F	0.37	600	152	---	278.0	1000	1774	2.0 OZ	(WRDA60)-56OZ
	Mix 5S	0.33	400	---	400	262.0	1062	1750	6.0 OZ	(WRDA60)-24OZ (ADVA120)-48OZ
	Mix 6S	0.36	380	---	380	270.0	1049	1736	1.9 OZ	(ADVA120)-38OZ
	Mix 7S	0.41	197	---	461	267.0	1121	1750	4.6 OZ	(WRDA60)-32.9OZ
	Mix 8S	0.44	306	---	306	269.0	1206	1710	3.1 OZ	(WRDA60)-30.6OZ
Stalite lightweight	Mix 9LF	0.31	602	150	---	235.3	952	1239	9.6 OZ	(WRDA64)-30OZ
	Mix 10LS	0.39	282	---	423	275.0	853	1300	8.8 OZ	(WRDA64)-31.7OZ
Georgia granite	Mix 1GF	0.24	800	200	---	236.0	960	1948	7.5 OZ	(WRDA60)-30OZ (ADVA120)-160OZ
	Mix 2GF	0.33	656	144	---	265.6	909	1981	12.0 OZ	(WRDA60)-30OZ
	Mix 3GF	0.41	494	123	---	254.0	1176	2027	0.5 OZ	(WRDA60)-33.4OZ
	Mix 4GF	0.37	600	152	---	278.0	1000	2056	2.0 OZ	(WRDA60)-56OZ
	Mix 5GS	0.33	400	---	400	262.0	1066	2045	6.0 OZ	(WRDA60)-24OZ (ADVA120)-48OZ
	Mix 6GS	0.36	380	---	380	270.0	1049	2075	1.9 OZ	(ADVA120)-38OZ
	Mix 7GS	0.41	197	---	461	267.0	1125	2045	4.6 OZ	(WRDA60)-32.9OZ
	Mix 8GS	0.44	306	---	306	269.0	1125	2044	3.1 OZ	(WRDA60)-30.6OZ

for Mixes 1F, 2F, 3F, 4F, 5S, 6S, 7S, and 8S. Stalite lightweight aggregate was used for Mix 9LF and Mix 10LS. Fly ash was used in Mixes 1F, 2F, 3F, 4F, and 9LF, and slag was used in Mixes 5S, 6S, 7S, 8S, and 10LS. Mixes 1GF, 2GF, 3GF, 4GF, 5GS, 6GS, 7GS, and 8GS had similar mix proportions to Mixes 1F, 2F, 3F, 4F, 5S, 6S, 7S, and 8S with the exception that the coarse aggregate was replaced by granite aggregate by volume. Two replicate batches for each mix design were produced and tested. However, it must be pointed out that the first replicate batch of the eight concrete mixes using Miami Oolite and the two concrete mixes using Stalite lightweight aggregate were tested in the first phase of this study, therefore, only one replicate batch of these ten mixes was produced and tested in this phase of the study.

3.2.2 Mix Ingredients

The mix ingredients used in producing the concrete mixtures are described as follows:

- *Water* – Potable water was used as mixing water for production of the concrete mixtures. The water temperature was around 64° F.
- *Cement* – Type-I Portland cement from CEMEX Company was used. The physical and chemical properties of the cement as provided by the Florida State Materials Office are shown in Tables 3-2 and 3-3.

Table 3-2. Physical Properties of Type I Cement

Loss on Ignition	Insoluble Residue	Setting Time	Fineness	Compressive Strength at 3 Days	Compressive Strength at 7 Days
(%)	(%)	(min)	(m ² /kg)	(psi)	(psi)
1.5	0.48	125/205	402.00	2400	2930

Table 3-3. Chemical Ingredients of Type I Cement

	Ingredients										
	SiO ₂	Al ₂ O ₃	CaO	SO ₃	Na ₂ O-K ₂ O	MgO	Fe ₂ O ₃	C ₃ A	C ₃ S	C ₂ S	C ₄ AF+C ₂ F
Percent (%)	20.3	4.8	63.9	3.1	0.51	2.0	3.3	7	59	13.8	15.8

- *Fly ash* – The fly ash used in this study was provided by the Boral Company. Its physical and chemical properties as provided by the Florida State Materials Office are presented in Table 3-4.

Table 3-4. Physical and Chemical Properties of Fly Ash

SO ₃ (%)	Oxide of Si, Fe, Al (%)	Fineness (ASTM C430) (%)	Strength (7d) (ASTM C109) (%)	Strength (28d) (ASTM C109) (%)	Loss on Ignition (ASTM C311) (%)	% of Water (ASTM C-618) (%)
0.3	84	32	N/A	78	4.3	102

- *Slag* – The slag used in this study was provided by the Lafarge Company. See Table 3-5 for its physical and chemical properties as provided by the Florida State Materials Office.

Table 3-5. Physical and Chemical Properties of Slag

SO ₃ (%)	Oxide of Si, Fe, Al (%)	Fineness (ASTM C430) (%)	Strength (7d) (ASTM C109) (%)	Strength (28d) (ASTM C109) (%)	Loss on Ignition (ASTM C311) (%)	% of Water (ASTM C-618) (%)
1.7%	N/A	4	92	129	N/A	N/A

- *Fine aggregate* – The fine aggregate used was a silica sand from Goldhead of Florida. The physical properties of the fine aggregate as determined by the Florida State Materials Office are shown in Table 3-6. The gradation of the fine aggregate is shown in Figure 3-1. The fine aggregate was oven-dried before it was mixed with the other mix ingredients in the production of the concrete mixtures.

Table 3-6. Physical Properties of Fine Aggregate

Fineness Modulus	SSD Specific Gravity	Apparent Specific Gravity	Bulk Specific Gravity	Absorption (%)
2.30	2.644	2.664	2.631	0.5

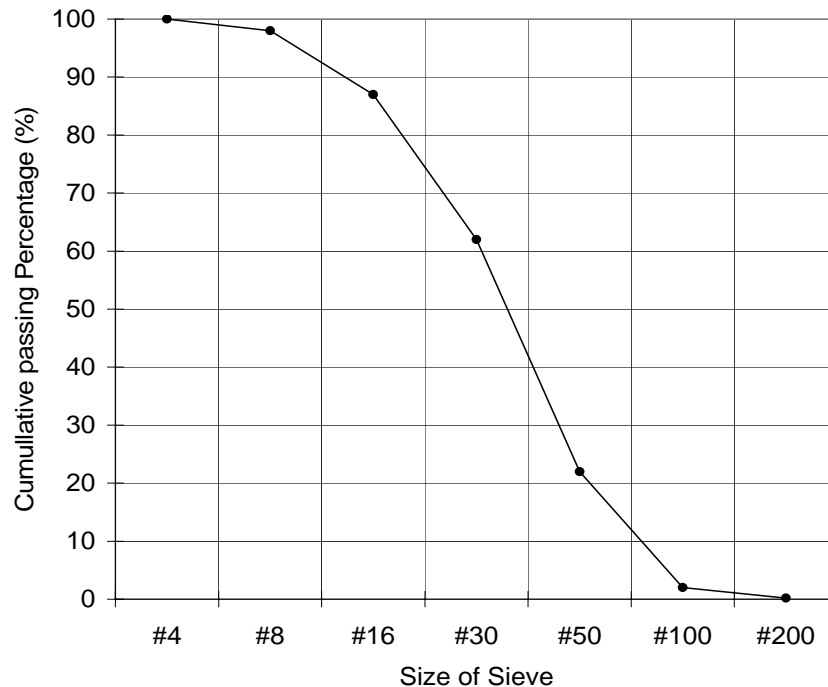


Figure 3-1. Gradation of fine aggregate (Goldhead sand).

- *Air-entraining admixture* – The air-entraining admixture used was Darex AEA from W.R. Grace and Company. Darex AEA is a liquid admixture for use as an air-entraining agent, providing freeze thaw durability. It contains a catalyst for more rapid and complete hydration of Portland cement. As it imparts workability into the mix, Darex AEA is particularly effective with slag, lightweight, or manufactured aggregates which tend to produce harsh concrete.
- *Coarse aggregates* – Three different types of coarse aggregates were used in this study: the first was a normal weight Miami Oolite limestone; the second was Georgia granite aggregate; and the third was a lightweight aggregate from South Carolina called “Stalite”. The physical properties of these three coarse aggregates are displayed in Table 3-7. The gradation of the Miami Oolite is shown in Figure 3-2; the gradation of the Georgia granite aggregate is plotted in Figure 3-3; and the gradation of Stalite aggregate is presented in Figure 3-4. In order to have a good control on the moisture content of coarse aggregates, the coarse aggregates were soaked in water for at least 48 hours and the free water on the surface of aggregate was drained off before being mixed with the other mix ingredients to produce the concrete mixtures.

Table 3-7. Physical Properties of Coarse Aggregates

Aggregate	SSD Specific Gravity	Apparent Specific Gravity	Bulk Specific Gravity	Absorption (%)
Miami Oolite	2.431	2.541	2.360	3.03
Stalite	1.55	-	-	6.60
Georgia granite	2.82	2.85	2.80	0.58

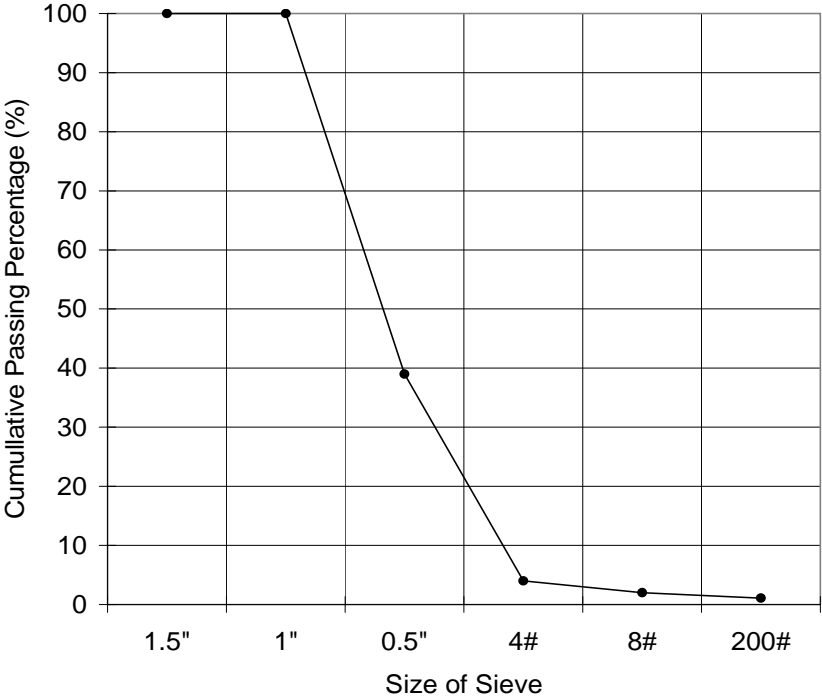


Figure 3-2. Gradation of coarse aggregate (Miami Oolite limestone).

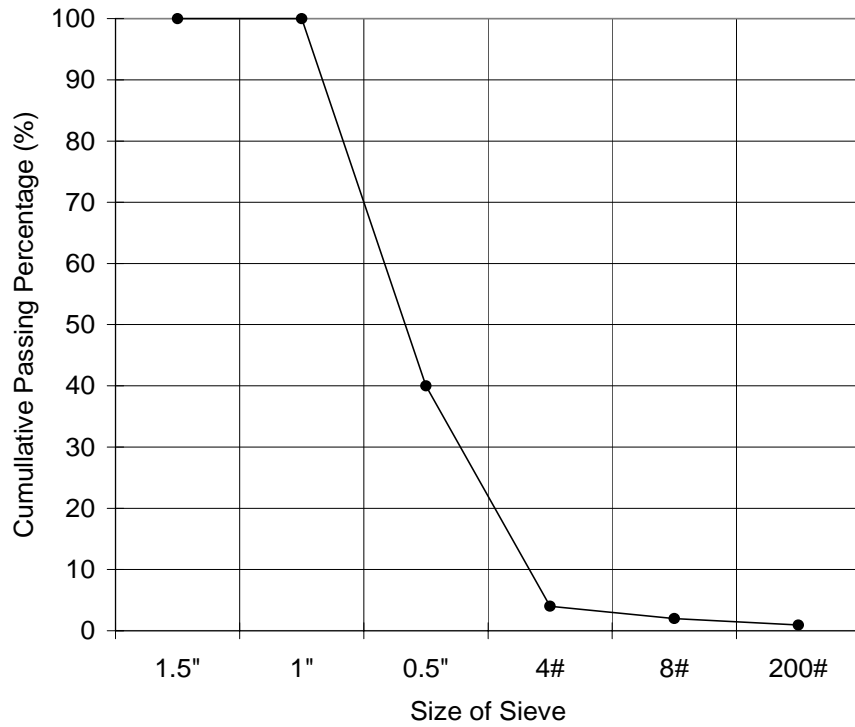


Figure 3-3. Gradation of coarse aggregate (Georgia granite).

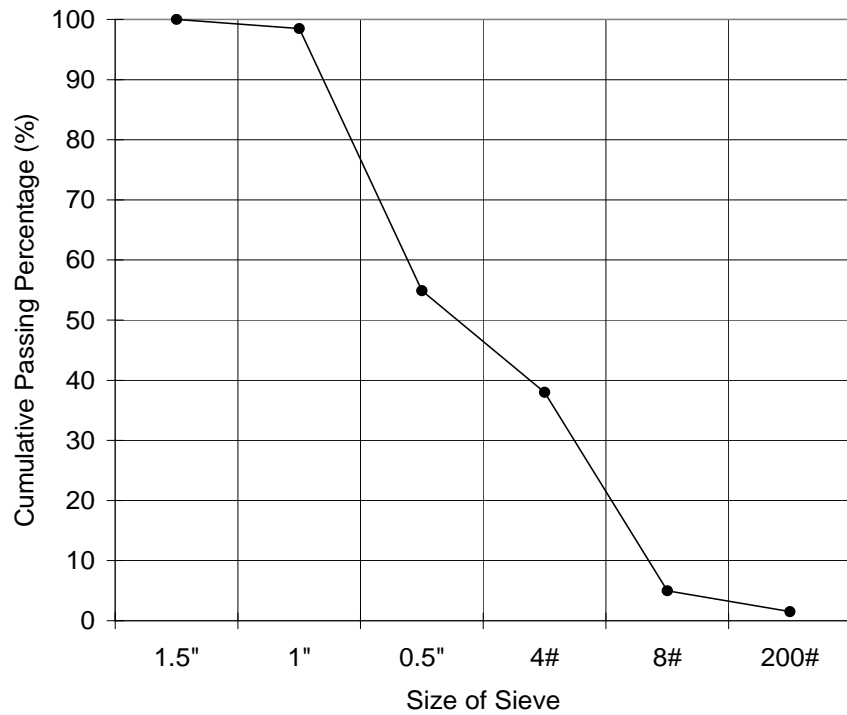


Figure 3-4. Gradation of lightweight aggregate (Stalite).

- *Water-reducing admixture* – The water-reducing admixtures used included WRDA60, WRDA64, and ADVA120 from W. R. Grace and Company. WRDA60 is a polymer-based aqueous solution of complex organic compounds producing a concrete with lower water content (typically 8-10% reduction), improved workability, and higher strengths. It can be used in ready mix, job site, and concrete paver plants for normal and lightweight concrete. It also can be used in block, precast, and prestress work. In addition, it offers significant advantages over single component water reducers and performs especially well in warm and hot weather climates to maintain slump and workability in high ambient temperatures. WRDA64 is a polymer-based aqueous solution of complex organic compounds producing a concrete with lower water content (typically 8-10% reduction), greater plasticity, and higher strength. ADVA120, a super plasticizer, is a polymer-based liquid organic compounds increasing plasticity of concrete.

3.3 Fabrication of Concrete Specimens

3.3.1 The Procedure for Mixing Concrete

The concrete mixtures investigated in this study were produced in the laboratory using a compulsive pan mixer with a capacity of 17 cubic feet (ft³), as shown in Figure 3-5. For each mixture, 13 ft³ of fresh concrete was produced to fabricate sixty (60) 6" × 12" cylindrical specimens.



Figure 3-5. Compulsive pan mixer.

The procedures for fabricating the cylindrical specimens were as follows:

- According to mix proportion design, the coarse aggregate, fine aggregate, cement, mineral admixtures, water, high range water reducer, and air entraining agent were measured out.
- Coarse aggregate and fine aggregate were placed into the pan mixer and mixed for about 30 seconds.
- Two-thirds of the water was placed together with the air-entraining admixture into the mixer and mixed for 1 minute.
- Cement, mineral additives, such as slag or fly ash, as well as a certain amount of high-range water reducer were placed into the pan mixer and mixed for 3 minutes, followed by a 2-minute rest, then, mixed for another 3 minutes.
- A slump test (according to ASTM C143) was performed to determine whether or not the target slump has been reached.
- If the target slump was not satisfactory, some more water-reducing admixture (instead of water) was added to adjust the slump of the fresh concrete. In doing so, it was assured that the design strength of the concrete would not be affected by adding extra water, which would change the water-to-cementitious material ratio.
- The fresh concrete was re-mixed for two more minutes. Then, another slump test was performed to check if the target slump had been reached. This procedure was repeated as necessary until the target slump was achieved.

3.3.2 Procedure for Fabricating Specimens

After the mixing procedure was completed, the fresh concrete was placed into 6" × 12" plastic cylinder molds. Then, two different procedures were used to consolidate the fresh concrete inside the plastic cylinder molds.

The first procedure was used when the slump of the fresh concrete was less than 7". In this case, each cylinder mold was filled to one-third of its height, and the mold placed on a vibrating table for 45 seconds. Then, the mold was filled to another one-third of its height, and placed on the vibrating table for another 45 seconds. Then the mold was filled fully, and placed on the vibrating table for another 45 seconds. In addition for the mixtures without any slump

value, the vibrating time to consolidate the concrete was increased or the vibrating intensity was adjusted.

The second procedure was used when the slump of the concrete was more than 7". Each cylinder mold was filled in three layers with each layer being rodded manually 25 times, as specified in ASTM C31.

Using these procedures assured that the mixtures with low slump value could be well-compacted, while the mixtures with very high slump value would not be segregated due to over-consolidation.

After consolidation, the surface of each concrete specimen was finished using a trowel and the top of the cylinder covered with a plastic lid to keep moisture from evaporating. Then, the concrete was allowed to cure in the cylinder molds for 24 hours before demolding. But, for concretes with very low compressive strength after 24 hours, another 24 hours of curing was allowed in the mold before demolding.

Lastly, the demolded concrete specimens were set in the standard moist curing room for the specified curing time until testing.

3.4 Curing Conditions for Concrete Specimens

The concrete specimens for compressive strength test, split tensile strength test, and elastic modulus test were cured in the standard moist room until the desired curing age for testing. Two different curing conditions were applied to the concrete specimens of Mix 1F to Mix 10LS for shrinkage and creep tests. The first condition was curing the concrete specimens for 7 days in the moist room, followed by another 7 days under room condition. The second was curing the concrete specimens for 14 days in the moist room, followed by another 14 days under room condition.

Only the latter curing condition was applied for Mixes 2GF, 3GF, 5GS and 7GS, i.e., 14 days in the moist room, followed by another 14 days under room condition.

3.5 Tests on Fresh Concrete

In order to obtain concrete mixtures with uniform quality, ASTM standard tests, as shown in Table 3-8 on fresh concrete, were performed and described in detail as follows:

Table 3-8. The Testing Programs on Fresh Concrete

Test	Slump	Air Content	Unit Weight	Setting Time	Temperature
Test Standard	ASTM C143	ASTM C 173	ASTM C138	ASTM C403/C 403M	ASTM C 1064

- *Slump test* – Slump test was performed in accordance with ASTM C143 standard. The slump value was used to evaluate the consistency of fresh concrete.
- *Air content test* – Air content test was carried out in accordance with ASTM C 173 standard. The volumetric method was employed for this test.
- *Unit weight test* – The procedures of ASTM C138 standard was followed in running the unit weight test. This test was carried out to verify the density of concrete mixtures for quality control.
- *Setting time test* – ASTM C403/C 403M standard was followed to perform the setting time test. The mortar specimen for the setting time test was obtained by wet-sieving the selected portion of fresh concrete through a 4.75mm sieve. The proctor penetration probe was employed for running this test. In this test, the initial setting time is determined when the penetration resistance equals 500 psi, and the final setting time is determined when the penetration resistance reaches 4000 psi.
- *Temperature test* – Temperature of the fresh concrete was determined in accordance with ASTM C 1064 standard. This test was used to ensure that the temperature of the fresh concrete was within the normal range, and that there was no unexpected condition in the fresh concrete. A digital thermometer was used to monitor the temperature of concrete.

The properties of the fresh concrete for each of the ten mixtures are presented in Table 3-9. The concrete mixes evaluated in the creep test for one year are designated as (1y) following their mix numbers, while those tested for three months were designated as (3m).

Table 3-9. Properties of Fresh Concrete

Mix	Slump (inches)	Air Content (%)	Unit Weight (pcf)	Theoretical Unit Weight (pcf)	Temperature (° F)
1F (1y)	7.75 (9.75)*	1.50 (1.25)*	143.1 (145.5)*	142.4	80 (81)*
2F (1y)	7.50 (4.25)*	7.30 (4.50)*	133.4 (137.7)*	137.4	79 (73)*
3F (1y)	1.50 (2.00)*	1.60 (2.50)*	145.7 (143.9)*	140.5	79 (76)*
4F (1y)	3.00 (3.00)*	1.30 (2.00)*	142.6 (143.8)*	140.9	74 (74)*
5S (1y)	8.25	7.30	133.3	143.5	75
5S (3m)	7.25 (9.00)*	6.80 (3.75)*	136.9 (141.6)*	143.5	81 (78)*
6S (1y)	1.50	3.80	139.3	141.3	76
6S (3m)	3.50 (5.50)*	3.40 (2.25)*	143.4 (140.4)*	141.3	79 (81)*
7S (1y)	4.50	8.60	129.8	140.6	76
7S (3m)	4.00 (5.75)*	5.50 (5.50)*	138.8 (138.1)*	140.6	77 (79)*
8S (1y)	6.50	6.80	135.1	140.6	78
8S (3m)	2.75 (3.00)*	5.30 (3.75)*	138.9 (140.4)*	140.6	80 (76)*
9LF (1y)	3.75 (2.50)*	5.20 (3.00)*	116.9 (117.7)*	117.7	79 (80)*
10LS (1y)	3.50 (2.75)*	5.50 (5.25)*	111.6 (109.2)*	116.0	77 (78)*
1GF (1y)	2.00	2.70	150.8	152.4	81
1GF (3m)	1.00	2.90	147.0	153.5	85
2GF (1y)	7.50	3.40	144.9	146.5	78
2GF (3m)	3.50	6.00	144.1	146.5	79
3GF (1y)	7.50	1.50	150.1	150.9	79
3GF (3m)	3.25	3.00	150.5	150.9	83
4GF (1y)	8.50	3.00	147.0	151.3	81
4GF (3m)	2.50	1.90	150.7	151.3	85
5GS (1y)	6.50	5.50	145.8	154.6	76
5GS (3m)	7.25	8.50	138.8	154.6	80
6GS (1y)	4.25	1.70	150.5	153.9	77
6GS (3m)	2.50	2.60	151.0	153.9	77
7GS (1y)	2.25	3.80	147.3	151.7	74
7GS (3m)	5.75	3.50	146.6	151.7	80
8GS (1y)	6.50	2.90	147.6	150.0	78
8GS (3m)	6.00	6.90	144.1	150.0	75

* the values in () were those obtained from the replicate mixes from the previous phase of this study.

3.6 Tests on Hardened Concrete

Routine ASTM standard tests on the hardened concrete specimens are given in Table 3-10.

Table 3-10. The Testing Program on Hardened Concrete

Test	Compressive Strength	Splitting Tensile Strength	Elastic Modulus	Shrinkage	Creep
Test Standard	ASTM C 39	ASTM C 496	ASTM C 469	Described in this chapter	Described in this chapter

3.6.1 Compressive Strength Test

Compressive strength tests were performed on all the concrete mixtures investigated in this study. Through the compressive strength test, the strength development characteristics of the concretes typically used in Florida could be obtained. Furthermore, the results from compressive strength tests could be used to calibrate the prediction equation given by ACI 209R Code so that a reliable prediction equation could be obtained.

The test procedure of ASTM C39 standard was followed for compressive strength tests. For each concrete mixture, three replicate 6" × 12" cylindrical specimens were tested for their compressive strength at the age of 3, 7, 14, 28, 56, and 91 days, with a total of 18 specimens tested. Before testing, both ends of the concrete cylinders were ground in order to support the load uniformly. The loading rate was controlled at 1000 foot-pounds (lbf) per second. Two typical failure modes in the compression test were column failure and shear failure. These two failure modes are illustrated in Figure 3-6.



Figure 3-6. Typical failure modes of concrete cylinders in compression test.

The compressive strength of the test specimen was calculated by dividing the maximum load attained from the test by the cross-sectional area of the specimen, as shown by the following equation:

$$f_i = \frac{P_i}{\pi \cdot r^2} = \frac{4P_i}{\pi \cdot D^2} \quad (3-1)$$

where f_i = ultimate compressive strength of cylinder i in psi;

P_i = ultimate compressive axial load applied to cylinder i in lbs; and

D = diameter of cylinder specimen in inches.

The average value of compressive strength from the three cylinders was taken as the compressive strength of the concrete.

3.6.2 Splitting Tensile Strength Test (or Brazilian Test)

The splitting tensile strength test is simpler to perform than other tensile tests, such as the flexural strength test and the direct tensile test. The strength determined from the splitting tensile test is believed to be close to the direct tensile strength of the concrete. In this study, the testing procedure of ASTM C 496 standard was followed in running the splitting tensile strength test. A 6" × 12" cylindrical specimen identical to that used for compressive strength test was marked with four lines on the sides to delineate the edges of the loaded plane to help align the test specimen before load was applied. The specimen was then placed with its axial horizontally aligned between the platens of a testing machine.

Figure 3-7 shows the loading configuration for this test. As shown in Figure 3-7 two 3 mm-thick and 25 mm-wide strips of plywood used as packing material were interposed between the cylinder and the platens so that the force applied to the cylinder could be uniformly distributed. Then, the load was applied and increased until failure took place by indirect tension in the form of splitting along the vertical diameter.

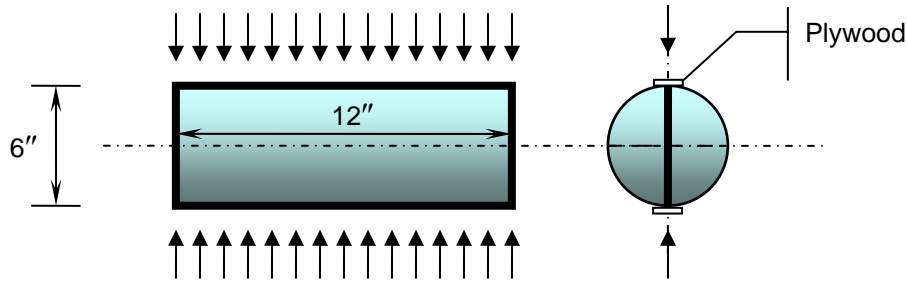


Figure 3-7. Loading configuration for splitting tensile test.

The splitting tensile strength of a cylinder specimen can be calculated by the following equation:

$$T_i = \frac{2p_i}{\pi \cdot l \cdot D} \quad (3-2)$$

where T = splitting tensile strength of cylinder in psi;

p_i = maximum applied load to break cylinder in lbf;

l = length of cylinder in inches; and

D = diameter of cylinder in inches.

The splitting tensile strength of the concrete takes the average value of the splitting tensile strengths of three cylinders.

Due to the sensitivity and susceptibility of the splitting tensile strength to the effects of internal flaws, such as voids, the results of some splitting tensile strength tests may be unusually low and may need to be discarded. For this reason, five extra concrete cylinders were prepared for use in repeating this test, if needed.

At last, the same curing conditions as those for the compressive strength test were used for the splitting tensile strength test. Three replicate specimens were tested at each of the curing times, which were 3, 7, 14, 28, 56, and 91 days. A total of 18 specimens per concrete mixture were tested for splitting tensile strength.

3.6.3 Elastic Modulus Test

The testing procedure of ASTM C 469 standard was followed to determine the elastic modulus of the concrete specimens. In this method, the chord modulus of elasticity of concrete cylinders was determined when a compressive load was applied on a concrete cylinder in the longitudinal direction.

A strain gage was attached on the concrete cylinder to measure the deformation of the concrete cylinder during the compression test. The load and deformation data were recorded by means of a computer data acquisition system. A MTS machine, as shown in Figure 3-8, controlled the loading rate by controlling displacement automatically.



Figure 3-8. MTS system used for elastic modulus and compressive strength tests.

Prior to the test for modulus of elasticity, one of the three concrete cylinders was broken first to determine the compressive strength of concrete in accordance with ASTM C39 standard. Then, 40% of the ultimate compressive strength of concrete specimen was applied on the other

two concrete cylinders to perform the elastic modulus test. The cylinders for the modulus of elasticity test were loaded and unloaded three times. Then, the data from the first load cycle were disregarded. The average value from the last two load cycles was recorded as the elastic modulus of the concrete. Since the elastic modulus of concrete will vary with age of the concrete, the elastic modulus of concrete at the ages of 3, 7, 14, 28, 56, and 91 days were evaluated. Throughout the test, the ambient temperature and relative humidity were maintained at 73° F and 100%, respectively.

3.6.4 Shrinkage Test

For the concrete mixtures with either Miami Oolite limestone aggregate or Stalite lightweight aggregate, six 6" × 12" concrete cylinders were made to evaluate their shrinkage behavior under two distinct curing conditions. Three cylinders were cured for 7 days in a moist room, followed by curing for another 7 days under room condition. Another three cylinders were cured for 14 days in a moist room, then for another 14 days cured under room condition.

For concrete mixtures with Georgia granite aggregate, their shrinkage behaviors were investigated under just one curing condition, i.e., 14 days under moist curing followed by 14 days under room condition.

Three pairs of gage points, which were spaced 10" apart, were placed on each of the concrete cylinders. A gage-point guide was used to position the gage points on the plastic cylinder mold before the concrete was cast. Figure 3-9 shows a picture of the concrete with the gage points attached on them after the molds have been removed. A digital mechanical gage was used to measure the change in the distance between the gage points as the concrete cylinder shrank. The digital mechanical gage had a resolution of 0.0001".



Figure 3-9. Cylindrical specimen with gage points installed.

Three sets of measurements were taken from each specimen. A total of nine sets of measurements were taken from the three replicate specimens for each concrete mixture.

Measurements were taken every day in the first two weeks, and then once a week up to three months. The initial distance between the gage points was measured immediately after the required curing time was fulfilled. Then, the shrinkage test was run under conditions of a temperature of 73° F and a relative humidity of 50%. The shrinkage strain was taken as the average of the nine readings from the three replicate cylinders, and can be expressed as follows:

$$\varepsilon_{sh} = \frac{1}{9} \sum_{i=1}^9 \frac{(l_i - l_o)}{l_o} \quad (3-3)$$

where l_i = measured distance between i^{th} pair of gage points; and

l_o = original distance between i^{th} pair of gage points measured immediately after de-molding.

CHAPTER 4 CREEP TEST APPARATUS DESIGN AND TESTING PROCEDURE

4.1 Introduction

This chapter describes the design of the creep test apparatus and its auxiliary tools, which include a gage-point positioning guide for positioning gage points on a creep test specimen, and an alignment frame for aligning the specimens in a vertical direction. The creep testing procedures are also described in detail in this chapter.

4.2 Creep Test Apparatus

4.2.1 Design Requirements of Creep Test Apparatus

In order to carry out the creep test program, a simple creep test apparatus was designed to satisfy the following design requirements:

- Creep test apparatus should be capable of applying and maintaining the required load on specimen, despite any change in the dimension of the specimen.
- The bearing surfaces of the header plates shall not depart from a plane by more than 0.001" to ensure even pressure distribution on the concrete test specimens.
- Several specimens can be stacked for simultaneous loading so that more measurements can be made, and the reliability of test results will be increased by taking an average of all the measurements.
- The height between two header plates shall not exceed 70". If the height between two header plates is over 70", the apparatus will not be easily operated manually. Also, if the total height of the stacked test specimens is very high, the specimens may buckle easily under load.
- The applied load should be controlled so that it will vary by less than 2% of the target applied load.
- Means shall be provided to make sure that concrete specimens are centered properly and vertical.

The designed creep test apparatus, which is a spring-supported system, is shown in Figure 4-1. The detailed design of creep apparatus used in this study is presented as follows.

4.2.2 Design of the Creep Apparatus

4.2.2.1 Determination of the maximum capacity of the creep apparatus

In this study, the maximum design capacity of creep apparatus was determined according to the maximum compressive strength (10 ksi) of concrete mixtures commonly used in Florida. The creep test was run under the loading condition of 50% of compressive strength of concrete on 6" × 12" cylindrical concrete specimens. Thus, the maximum load applied to the creep frame can be computed as:

$$P_{\max} = 0.5 \times 10000 \times \pi \times 3^2 = 141300 \text{ lbf}$$

If a 4" × 8" cylindrical concrete specimen was used, the creep test could be run on the concrete with a compressive strength as high as 22 ksi.

4.2.2.2 Design of the springs

The spring constant of the larger spring (k_1) was selected as 9822 foot pounds per inch (lbf/in), while the spring constant of the smaller spring (k_2) was selected as 3314 lbf/in. The maximum travel distance (Δ) for both springs was 1.625". If nine sets of springs were used, the maximum load (P_{spring}) that the springs could hold would be calculated to be:

$$P_{spring} = 9 \times (k_1 + k_2) \times \Delta = 1.92 \times 10^5 \text{ lbf} > P_{\max} \text{ ---OK}$$

Thus, the spring capacity was judged as o.k.

It is of importance to mention that in order to maintain the load on the specimen constant and keep the frame stable, the maximum travel distance of spring design could not be more than the maximum travel capacity of the springs.

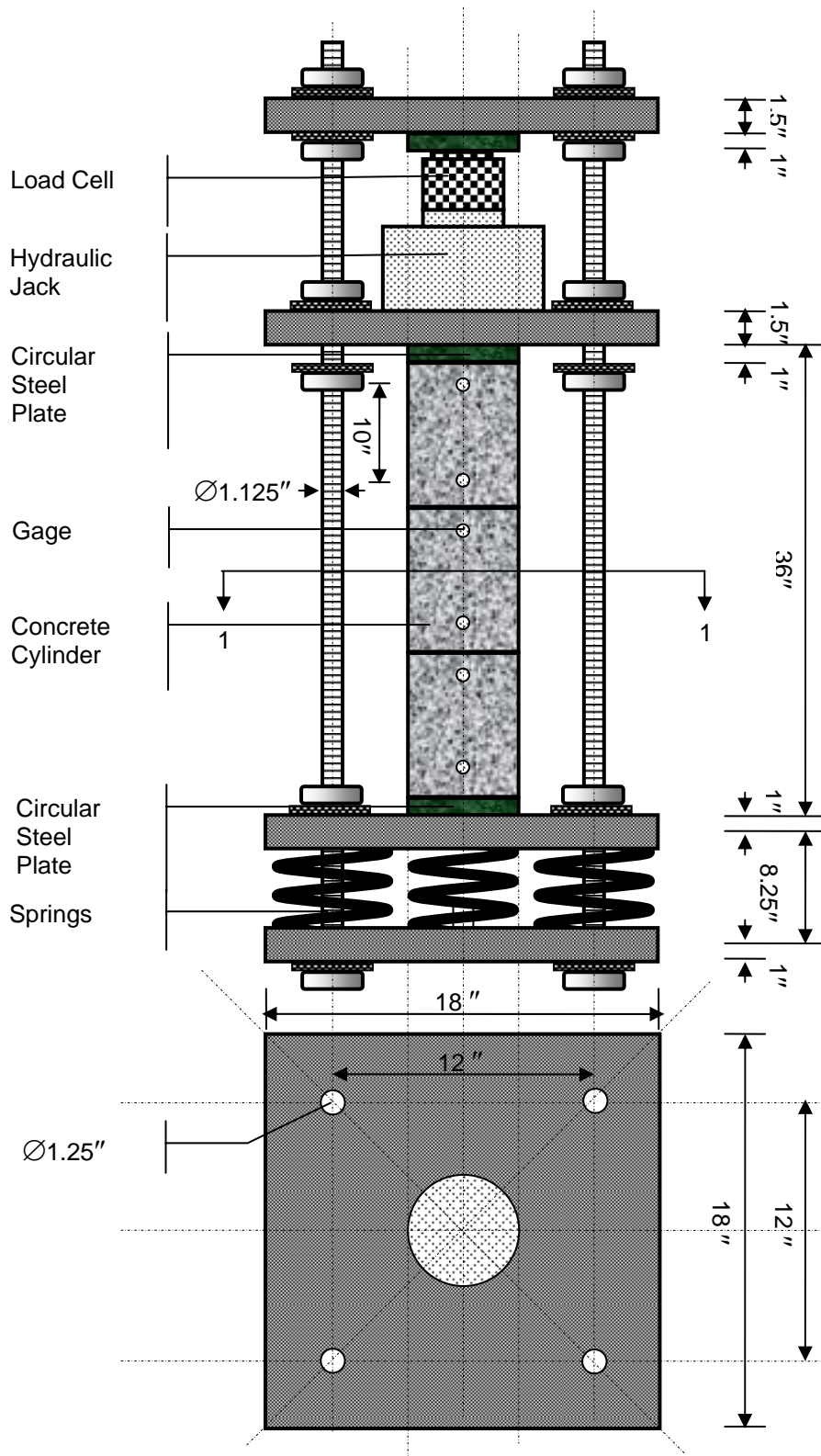


Figure 4-1. Creep test apparatus.

4.2.2.3 Design of the header plate

In order to apply load uniformly to the test specimens, the deflection of the header plate should not deviate too much for a plane surface when the specimens are loaded. The required thickness of the header plates was determined using a finite element analysis. The steel plate was modeled as an isotropic elastic material with an elastic modulus of 29,000 ksi and Poisson's ratio of 0.30, which are typical properties of steel. The plate was modeled as fixed from rotation about the x, y and z axis along the four boundary lines along the four holes on the steel plate as shown in Figure 4-2.

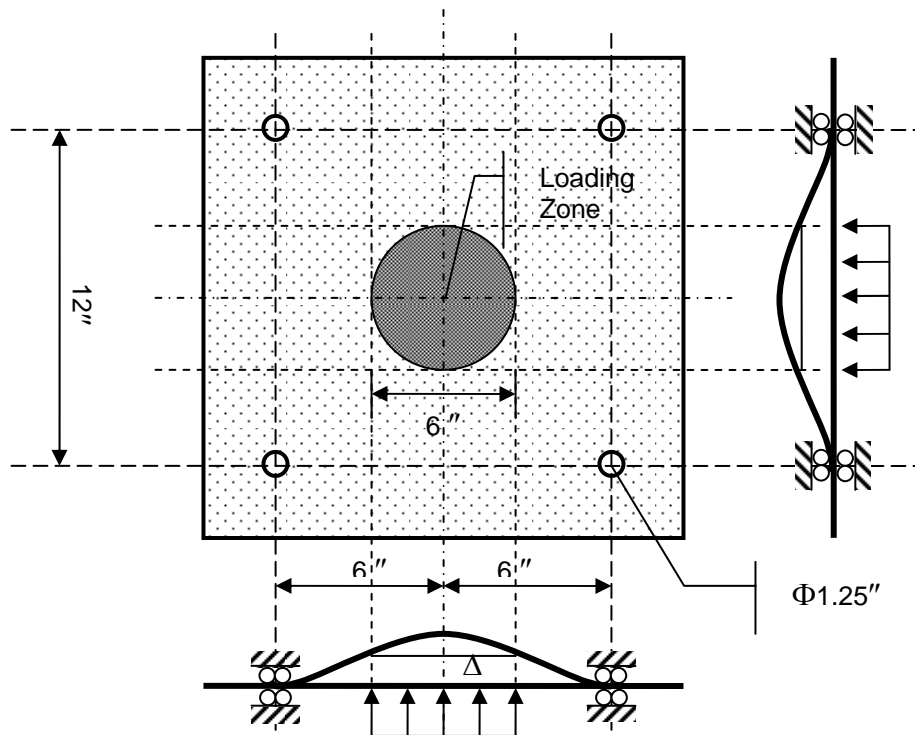


Figure 4-2. Boundary conditions used for finite element analysis.

The loading zone was modeled as a circular area identical to the cross sectional area of a 6"-diameter concrete cylinder. The maximum load used in the analysis had a pressure of 5000 psi, which is 50% of the maximum compressive strength of concrete investigated in this study.

The finite element mesh used in the analysis consisted of triangle elements and rectangular elements as shown in Figure 4-3. The header plate with a thickness of 1.5" was analyzed. The deflection contour plot is shown in Figure 4-4, and as can be seen, the deflection from the center of the header plate to a position 3" away from the center changes from 0.00408" to 0.0033". In other words, if the test specimens are loaded to a maximum pressure of 5,000 psi, the deflection of the steel plate will differ by less than 0.00078", which is less than 0.001". Thus, a header steel plate with a thickness of 1.5" was determined to be adequate and was selected for use.

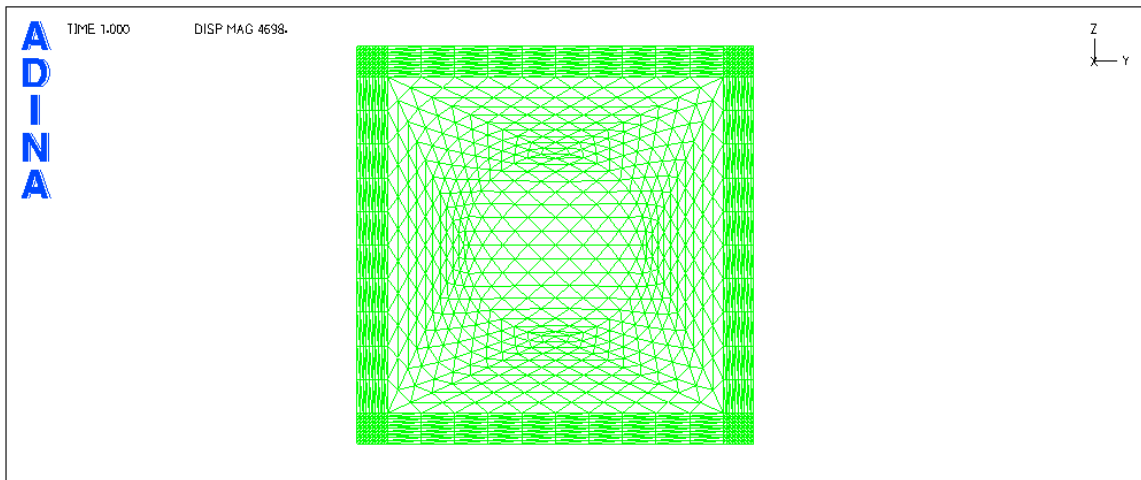


Figure 4-3. Finite element mesh used in the header plate analysis.

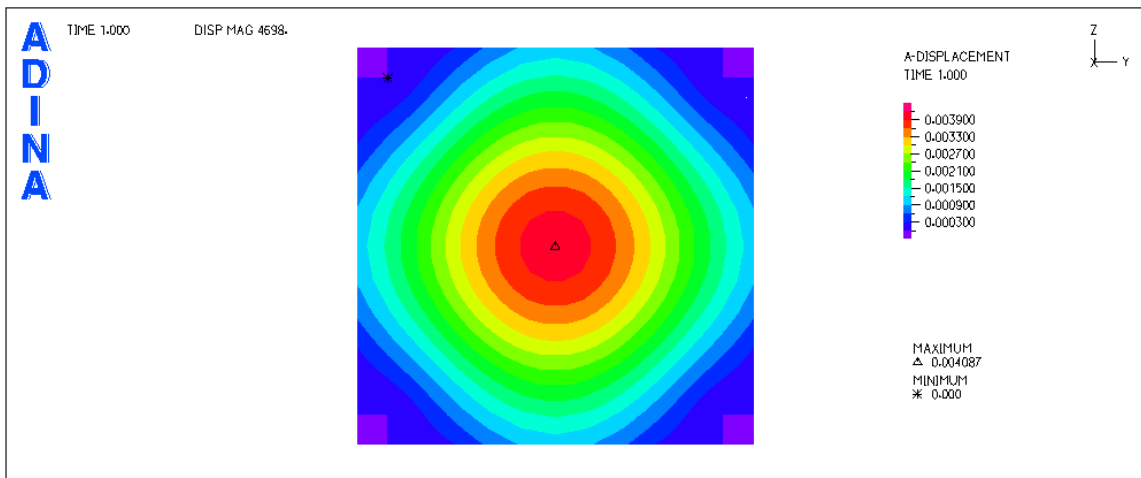


Figure 4-4. Contour plot of deflection of header plate.

4.2.2.4 Determination of the size of the steel rod

When the concrete specimens are loaded in the creep frame, each of the four steel rods will carry one-quarter of the total load. The steel rods are 1.125" in diameter and are made of high-strength alloy steel with a yield strength of 105,000 psi. If the concrete specimens are loaded up to the maximum capacity of the creep apparatus of 141,300 lbf, the maximum stress on the steel rods would be equal to:

$$\frac{141300}{4 \cdot 0.5625^2 \cdot \pi} = 35556 \text{ psi.}$$

This maximum possible stress in the steel rods is less than half of the yield strength of the steel rod, which is 105,000 psi. Thus, the selected steel rod meets design requirements.

4.2.2.5 Stress relaxation due to deflection of the header plate and creep of concrete

When the full capacity of creep frame is used, the total stress released due to plate deflection can be approximated as follows:

$$P_{relaxed} = \Delta_{deflection} \times k_{total} = 0.0041 \times 13136 \times 9 \approx 485 \text{ lb}$$

where $\Delta_{deflection}$ = maximum deflection of the header plate; and

k_{spring} = elastic constant of the spring.

According to the design requirement, the allowable load relaxation is

$$141300 \times 0.02 = 2826 \text{ lb.}$$

In addition, since partial load will be relaxed due to the creep of concrete, the applied load on the concrete specimen should be adjusted in order to keep the load the same as the initially applied one. To have an error of less than 2,826 lbf in the applied load, the following inequality must be satisfied:

$$36 \cdot \epsilon_{cr} \cdot k_{total} + 485 \text{ lbf} \leq 2826 \text{ lbf.}$$

Solving the above inequality, we obtain that

$$\varepsilon_{cr} \leq 0.0006.$$

This means that the applied load should be adjusted at every 0.0006 increment of creep strain. Otherwise, the load relaxed would be more than 2826 lbf, the allowable maximum load relaxation.

4.3 Design of the Gage-Point Positioning Guide

Three pairs of gage points with a gage distance of 10" were to be placed in each test concrete specimen. A gage-point positioning guide, as shown in Figure 4-5, was designed for use in positioning the gage points on the plastic cylinder mold. By inserting a 6" × 12" cylinder mold into the gage-point position guide and tightening the six screws on the guide, the precise locations for the three pairs of gage points, with a gage distance of 10", could be conveniently marked on the mold. Three lines of gage points are uniformly distributed with a 120° angle along the periphery of the specimen. The use of the gage-point positioning guide is of great importance because the maximum travel distance of the mechanical strain gage is 0.4". The mechanical strain gage cannot be used to measure a distance of more than 10.4". Thus, it was very important that the two gage points be placed at an exact distance of 10" from one another. Figure 4-6 shows a picture of the gage-point position guide, and Figure 4-7 shows a plastic cylinder inside the gage-point position guide.

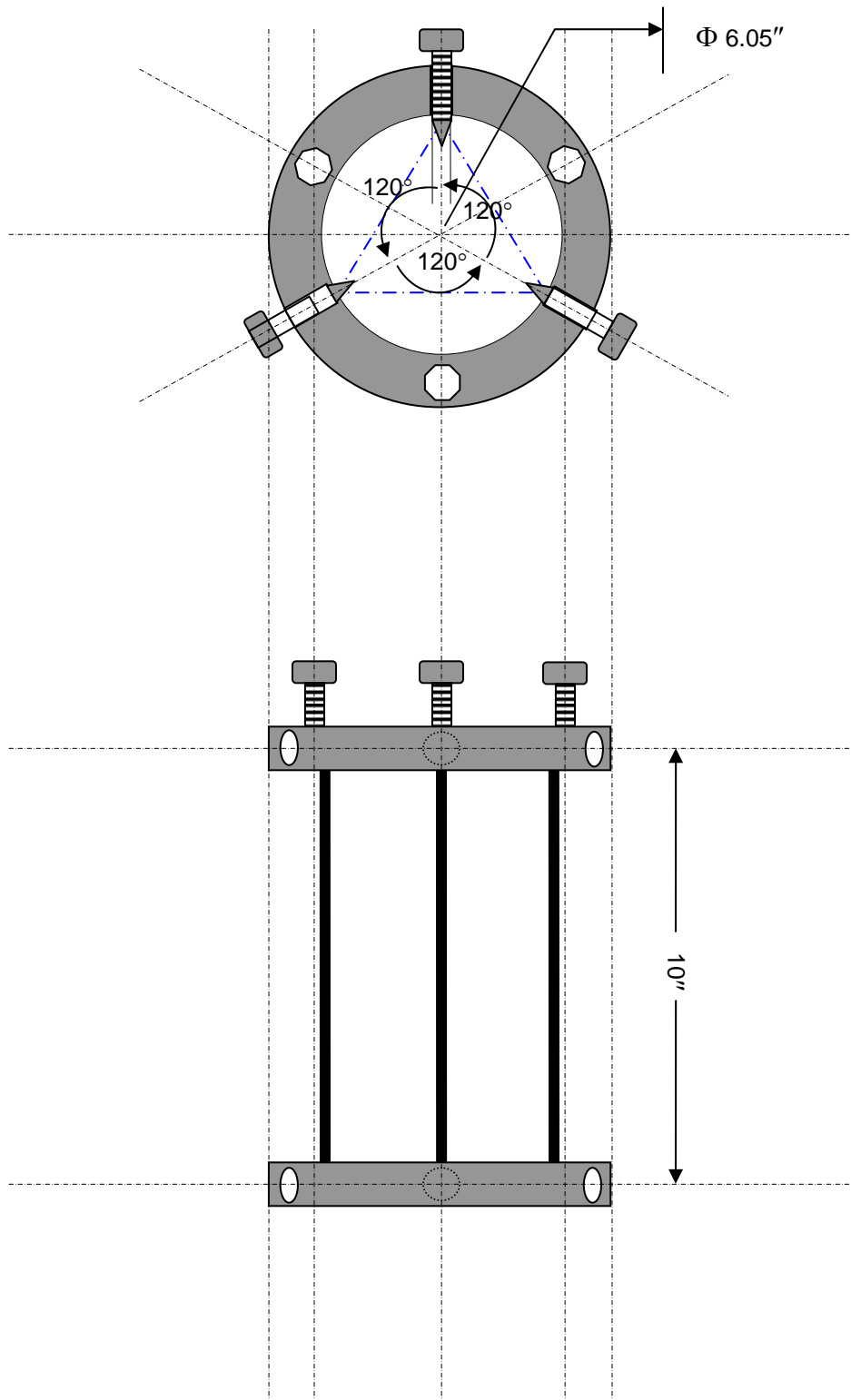


Figure 4-5. Design of gage-point positioning guide.



Figure 4-6. Gage-point position guide.



Figure 4-7. Plastic cylindrical mold inside the gage-point position guide.

4.4 Design of the Alignment Frame

An alignment frame was designed and constructed to be used to align the concrete specimens in a vertical direction when they were placed in the test frame. Figure 4-8 shows the design of the alignment frame. The alignment frame consists of one piece of angle steel and one piece of channel steel with three pieces of $0.5'' \times 2'' \times 10''$ steel plates welded on them, respectively. They are connected together using six steel rods. The use of the alignment frame is described in Section 4.7 concerning the creep testing procedure.

4.5 Mechanical Strain Gage

A mechanical strain gage, as shown in Figure 4-9, was used to measure the distance change between two gage points. The instrument frame was made of aluminum alloy and had five master settings of 2'', 4'', 6'', 8'', and 10'' easily set for gaging. The digital indicator had a minimum graduation of 0.0001''. In this study, the master setting of 10'' was selected so that the mechanical strain gage was suitable for the measurement of longitudinal strain to the nearest 10 millionths. In addition, the effective range of displacement measurement was 0.3''.

4.6 Other Details on Creep Apparatus

For each test frame, three $6'' \times 12''$ cylindrical specimens were placed on top of one another and tested under the same load. The load was applied by means of an electronic hydraulic jack (with a maximum capacity of 200,000 lbs) and monitored by a load cell with a digital readout indicating the load applied. The load cell had a capacity of 200 kips, and a minimum readable digit of 10 lb. When the desired load was reached, the nuts on the threaded rods were tightened so that they snugly pressed against the plate underneath the hydraulic jack so as to hold the plate in that position, and thus hold the applied load. After the nuts were positioned properly to hold

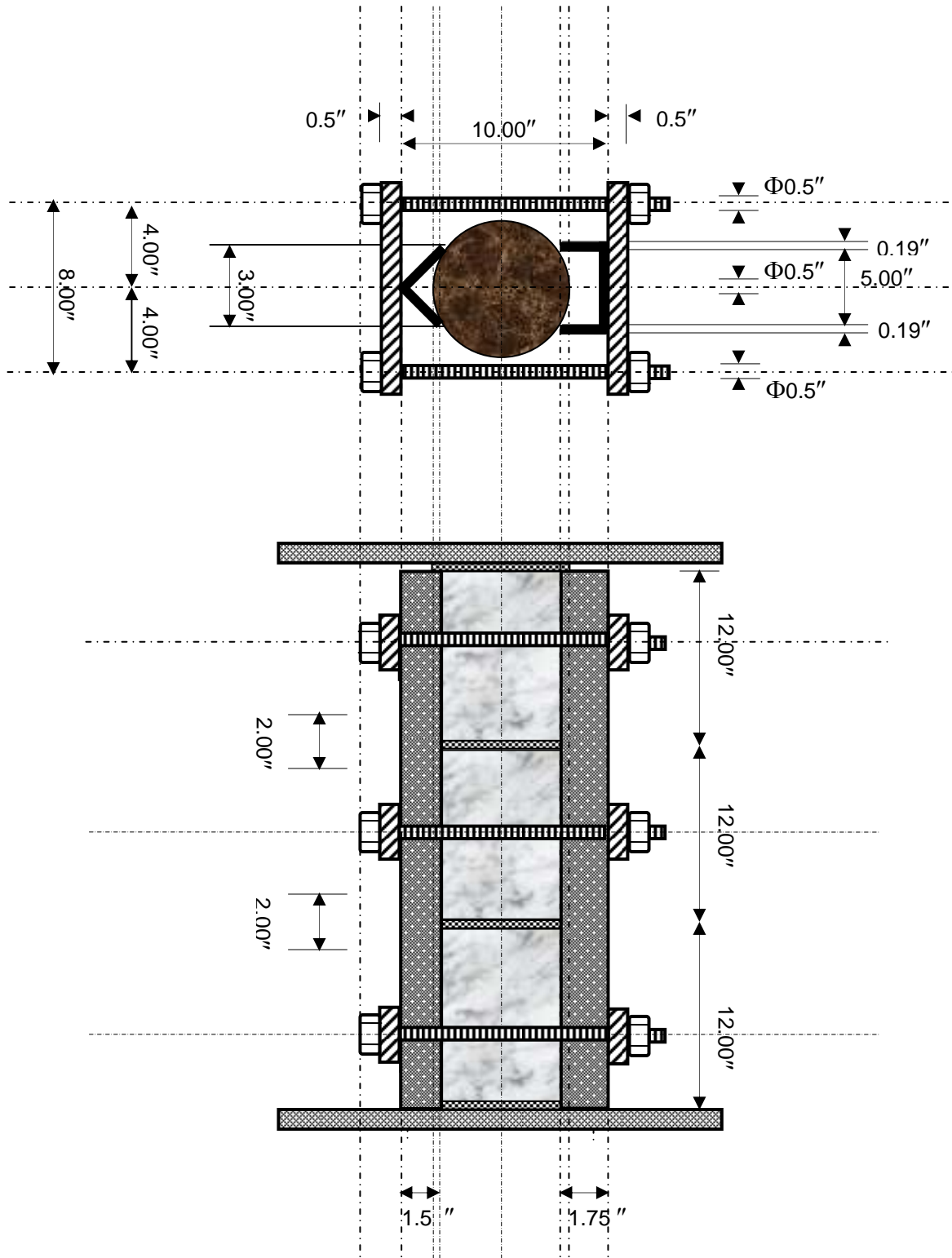


Figure 4-8. Schematic of alignment frame design.



Figure 4-9. Mechanical gage.

the applied load, the jack and the load cell could be removed from the test frame and used to load another test frame. The springs at the bottom of the creep frame helped to maintain the balance of the creep frame as well as a constant load on the specimens despite any change in its length, as the creep process of the concrete specimens took place under load. Up to nine sets of springs could be used in this test frame. Figure 4-10 shows the positions of the springs in the test frame. Each set of springs consisted of a smaller spring sitting inside a larger spring. In addition, the springs must be manufactured so that both ends of the spring can be flattened, and nine sets of springs should have the same height, and positioned symmetrically to keep load distribution even. In doing so, no spherical bearing device was needed to guarantee that the load be evenly transferred to the specimens.

As the concrete specimens were loaded in the creep frame, the rectangular steel plates, which were at the top and bottom of the test specimens, were deflected slightly. To keep the loading surfaces flat and the test specimens vertical when the load was applied, two 1"-thick

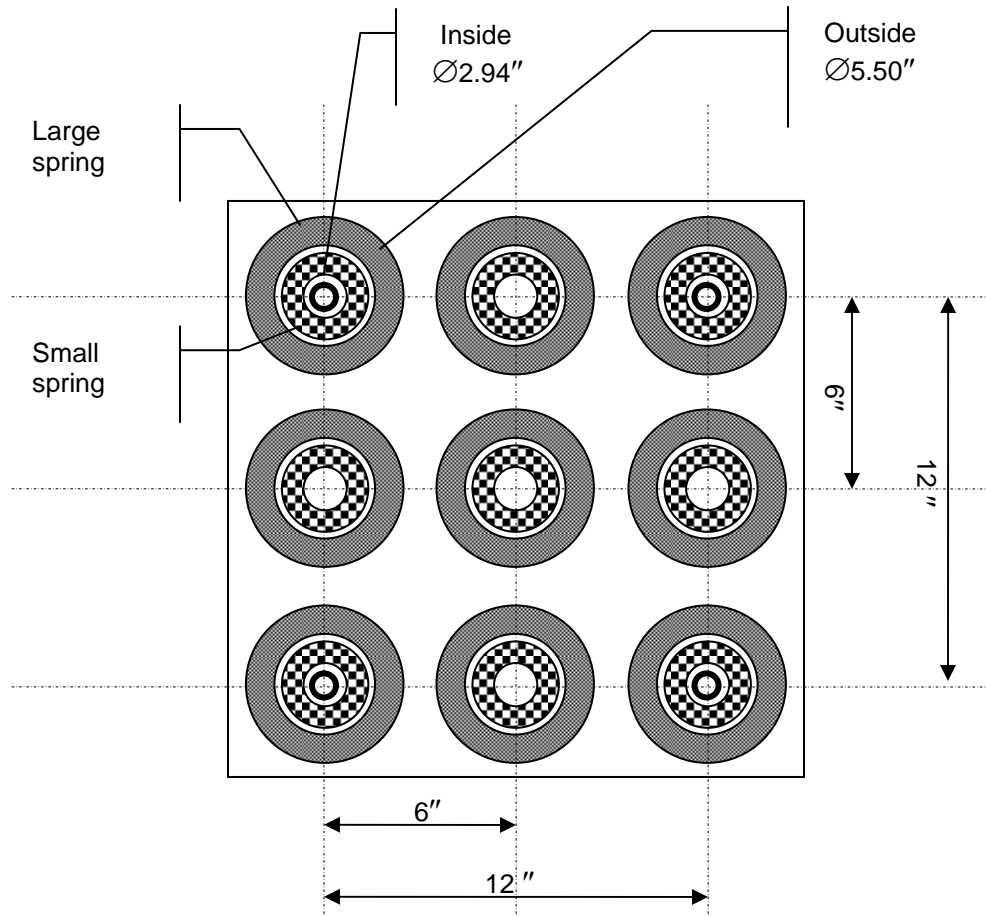


Figure 4-10. Positioning springs on the bottom plate.

circular steel plates with a diameter of 6" were placed on the top and bottom of the stack of concrete test specimens, as shown in Figure 4-1. Both surfaces of the circular plate should be polished to avoid any uneven pressure on the concrete cylinder.

4.7 Creep Testing Procedure

- 1) Gage points were installed on plastic cylindrical molds using the gage-point position guide. Each creep test specimen contained three pairs of gage points installed on the concrete cylinder using the gage position guide, which were placed 10" apart from each other.
- 2) Fresh concrete was placed into the plastic cylinder molds in three layers. Each layer was consolidated with 45 seconds of vibration on a vibrating table. After consolidation, the top

surface of the concrete was gently finished. This was a very important detail in making the specimen in order to avoid cracking around the gage insert as shown in Figure 4-11. If too much pressure was applied to finish the surface, gage inserts could be pushed downward because the plastic cylinder was not very stiff and could not prevent the gage inserts from being pushed downward. Once pressure was released, the gage insert returned to its original position, while the concrete could not since plastic deformation cannot be recovered. Thus, some space between the gage insert and the concrete was created and this affected the measurement.

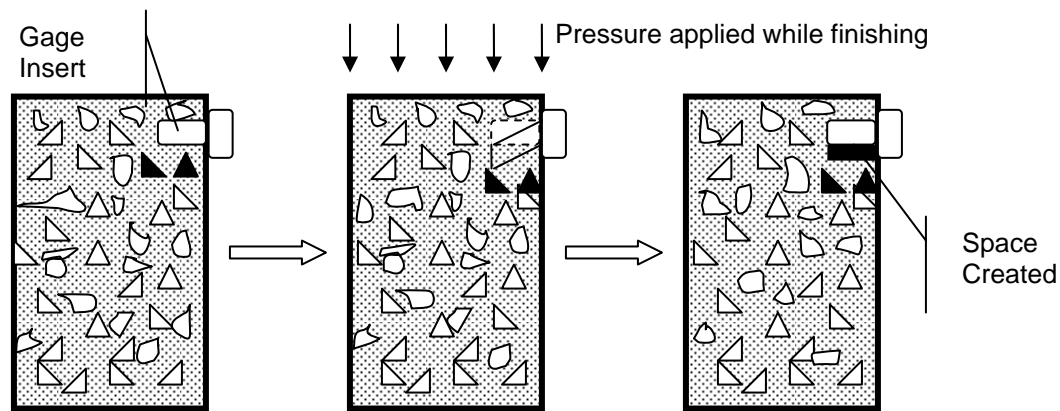


Figure 4-11. Cracking around gage insert.

- 3) The concrete specimens were demolded after 24 hours of curing, and the specimens were placed in a moist room to cure for the required time.
- 4) Both end surfaces of each concrete cylinder was ground in order to make them even, as shown in Figure 4-12.
- 5) Both ends of each cylinder were capped using sulfur mortar to make end surfaces smooth and even.
- 6) Three replicate specimens were stacked vertically on top of one another using the alignment frame designed for this study.
- 7) Circular plates were put on the top and bottom of each concrete cylinder.
- 8) The creep frame and concrete specimens were adjusted to make sure the specimens were centered and vertical. The creep frame was adjusted through moving the header plate back and forth with the nuts on the top of the plate. As shown in Figure 4-13, the centers of header plate and the plate on the top of springs were marked. On each plate was also marked

a 3" diameter with eight mark points along the boundary of the circle. If the concrete column consisting of three cylinders was placed so that it lined up with the circles on the header and the bottom plates, then the concrete cylinders were deemed centered and vertical.



Figure 4-12. Concrete cylinder with both end surfaces ground.

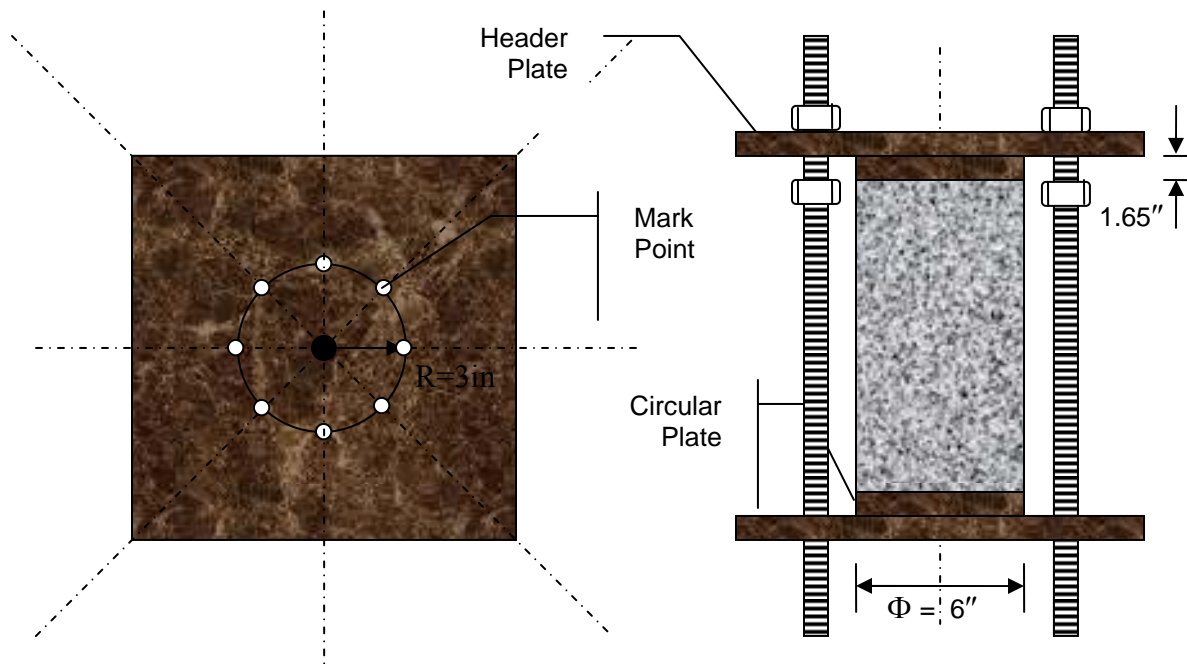


Figure 4-13. Centering the specimens into a creep frame.

- 9) After the concrete specimens were centered, the nuts supporting the header plate were turned downward at least 1.65" away from the bottom of the header plate to avoid the header plate making contact with the nuts once load was applied. Then, the four nuts on the top of the header plate were tightened slightly to hold the centered concrete specimens.
- 10) A hydraulic jack and load cell were set up in the creep frame, and the position of hydraulic jack was checked to make sure that it was co-axial with the concrete specimens in order to avoid loading the concrete specimens eccentrically. As shown in Figure 4-14, in order to make the hydraulic jack co-axial with the concrete specimens, the center of the header plate was also marked on the top side. A circle with diameter identical to the diameter of jack cylinder was also drawn on top of the header plate, with four marks hammered along the boundary of the circle.

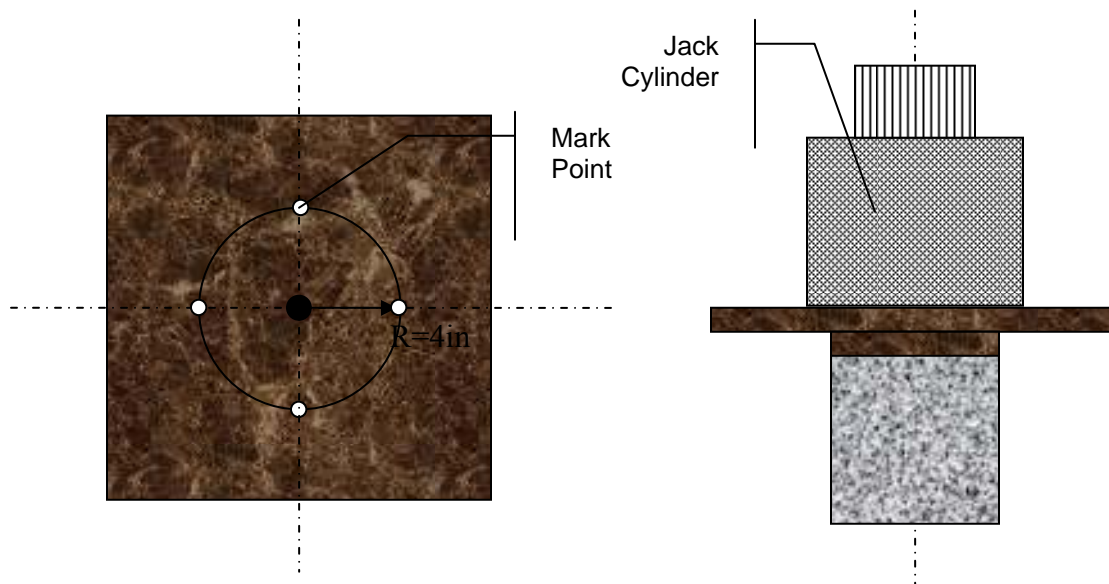


Figure 4-14. Centering the hydraulic jack cylinder.

- 11) As shown in Figure 4-15, the plate on the top of load cell was checked to make sure that the plate was level. Then, the four steel nuts holding the top plate were tightened slightly.
- 12) The frame was preloaded up to 500 lbf to properly seat the concrete test specimens in the creep frame.
- 13) The initial measurements were taken, which is the initial distance between two gage points.

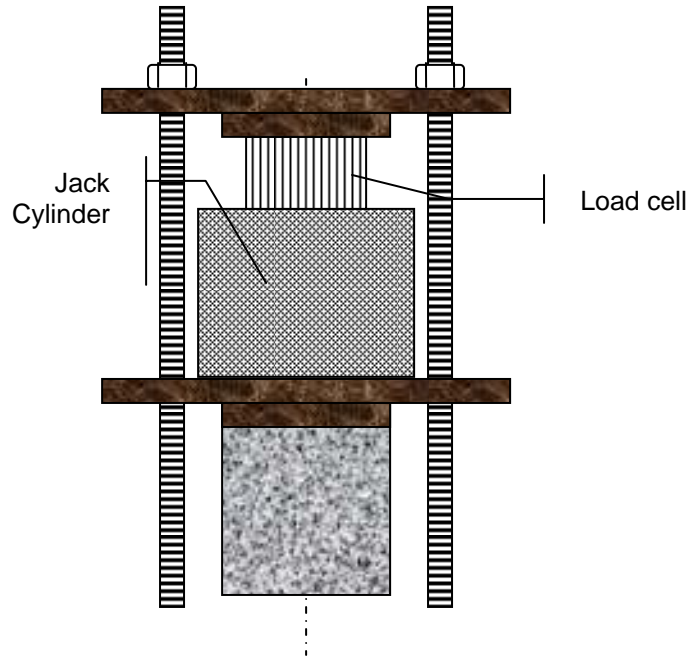


Figure 4-15. Leveling the plate on the top of load cell.

- 14) The load was applied through the electronic hydraulic jack up to the target load. Use of an electronic hydraulic jack is strongly recommended due to several advantages. Firstly, the load could be applied to the loading frame continuously. Secondly, since the electronic hydraulic jack applied load on the cylinder within one minute, instantaneous measurements were available to be taken within seconds immediately after the loading procedure was completed. Thus, the instantaneous measurement taken in this way was very close to true elastic deformation. Thirdly, the dynamic effect that can cause the cylinders to break easily, can be avoided. In addition, less effort was needed to load the frames compared with a manual hydraulic jack, which can take hundreds of pushes to reach the desired load level.
- 15) Immediately after the target load was reached, the four nuts on the top of the header plate were tightened to hold the load on the specimens.
- 16) Instantaneous measurements were taken using the digital mechanical gage immediately after loading, followed by measurements taken at one hour, three hours and six hours. After that, measurements were taken every day during the first two weeks, and then once a week until ninety-one days, followed by once a month if the testing period was to continue.
- 17) The load was adjusted at every 0.0008 increment of creep strain to keep the load loss due to creep relaxation at less than 2% of the total load applied at the beginning.

The importance of taking the first set of readings as quickly as possible in order to obtain a more accurate instantaneous deformation of the concrete deserves to be emphasized again. Otherwise, substantial early creep deformation may take place before the initial readings can be taken. The first set of readings can be taken within three minutes.

The creep strain was calculated by subtracting the shrinkage strain from the total strain as follows:

$$\varepsilon_C = \varepsilon_T - \varepsilon_S = \frac{1}{9} \left(\sum_{i=1}^9 \frac{l_i^T - l_{0(i)}^T}{l_{0(i)}^T} - \sum_{i=1}^9 \frac{l_i^S - l_{0(i)}^S}{l_{0(i)}^S} \right) \quad (4-1)$$

where ε_C = creep strain of concrete;

ε_T = sum of creep strain and shrinkage strain;

ε_S = shrinkage strain of concrete;

l_i^T = measurement taken from the i^{th} pair of gage points for creep test;

$l_{0(i)}^T$ = initial length of the i^{th} pair of gage points for creep test;

l_i^S = measurement taken from the i^{th} pair of gage points for shrinkage test;

$l_{0(i)}^S$ = initial length of the i^{th} pair of gage points for shrinkage test; and

i = number of pairs of gage points from 1 to 9.

The creep coefficient, which is used in concrete structure design, was calculated by taking the ratio of creep strain of the concrete at the testing age to elastic strain of concrete at the same curing age. It can be expressed as follows:

$$C_{cr} = \frac{\varepsilon_C}{\varepsilon_E} \quad (4-2)$$

where C_{cr} = creep coefficient;

ε_C = creep strain of concrete; and

ε_E = elastic strain of concrete.

Creep modulus, E_C , is computed dividing the applied stress by the total strain without including shrinkage strain, as shown in Equation 4-3.

$$E_C = \frac{\sigma}{\varepsilon_E + \varepsilon_C} \quad (4-3)$$

4.8 Summary on the Performance of the Creep Apparatus

The creep apparatus designed in this study was capable of applying and maintaining the required load on the test specimens. Three specimens were stacked for simultaneous loading. The unevenness of the deflection of bearing surface of the header plates was less than 0.001" and the pressure distribution on the concrete specimens varied by less than 0.026%, or 1.5 psi. Load was applied to a precision of 10 lbs, as a load cell with resolution of 10 lbs was used to control the applied load. The mechanical gage used was able to measure longitudinal strain to a precision of 0.00001. Strains were measured on three gage lines spaced uniformly around the periphery of the specimen. An electronic hydraulic pump system was used to apply load to the creep frame. This enabled the loading process to be done in seconds, and instantaneous strains were measured from the creep test within a short time after loading.

The gage-point position guide that was designed to position gage points on a plastic cylindrical mold was very effective and was an important auxiliary tool in the preparation of test specimens. It enabled the placement of gage points at accurate locations on the test specimen so that the maximum travel distance of the mechanical gage was not exceeded, which resulted in reduced measurement errors.

The alignment frame that was designed to align concrete specimens vertically in the creep frame made the job of stacking three concrete specimens together for testing possible.

Experimental results indicate that the creep apparatus designed for this study was effective, reliable and practical. It can be used to run creep tests on concrete with a maximum compressive strength of up to 10,000 psi, if 6" × 12" cylinder specimens are used. If 4" × 8" cylinder specimens are used, the maximum compressive strength of the concrete could be as high as 22,000 psi.

CHAPTER 5 ANALYSIS OF STRENGTH TEST

5.1 Introduction

This chapter presents the results from compressive strength, splitting tensile strength and elastic modulus tests on the 18 concrete mixes evaluated in this study. The effects of various factors on strength are discussed. The prediction equations establishing inter-relationship between compressive strength and splitting tensile strength are given. The prediction equations relating compressive strength to elastic modulus are also presented.

5.2 Results and Analysis of Compressive Strength Tests

The average compressive strengths at various curing times for the 18 concrete mixes that were evaluated are presented in Table 5-1. The individual compressive strength values are shown in Table A-1 in Appendix A.

5.2.1 Effects of Water-to-Cement Ratio on Compressive Strength

As a general rule, the strength of comparable concretes is inversely proportional to the water-to-cement (w/c) ratio. Higher w/c ratios will produce relatively weaker concretes and lower w/c ratios will produce stronger concretes. The compressive strength data in this study generally follow this rule. Figure 5-1 shows the plot of compressive strength at 28 days of the concrete mixtures using Miami Oolite and Georgia granite versus w/c ratio. Figure 5-2 shows similar plots for the compressive strengths at 91 days. Compressive strength tends to decrease as water-to-cementitious materials ratio increases. It can also be observed that the concretes using Miami Oolite had relatively higher strengths than those using Georgia granite at the same water-to-cementitious materials ratio.

Table 5-1. Compressive Strength of the Concrete Mixtures Evaluated (psi)

Mix Number	W/C	Fly Ash (%)	Slag (%)	Age of Testing					
				3 days (psi)	7 days (psi)	14 days (psi)	28 days (psi)	56 days (psi)	91 days (psi)
1F (1y)	0.24	20	---	8077	8572	8993	9536	10771	11267
2F (1y)	0.33	20	---	4077	4658	6028	6506	6838	7607
3F (1y)	0.41	20	---	5289	6470	7567	8241	8449	9426
4F (1y)	0.37	20	---	5712	6919	7114	7236	8996	9271
5S (1y)	0.33	---	50	4382	5270	5899	5574	6131	6459
5S (3m)	0.33	---	50	5554	7235	8248	8832	9139	9456
6S (1y)	0.36	---	50	5253(6)*	5816	5915	6039(30)*	---	7019(94)*
6S (3m)	0.36	---	50	6375	7699	8587	9111	9529	9661
7S (1y)	0.41	---	70	3642(6)*	3868	4260	5299(30)*	4622	4097
7S (3m)	0.41	---	70	4324	5374	5927	6392	6794	6917
8S (1y)	0.44	---	50	3101	3955	4517	4793	4880	4548
8S (3m)	0.44	---	50	4795	6114	6939	7525	8119	8208
9LF (1y)	0.31	20	---	3039	3941	5136	5929	6690	6961
10LS (1y)	0.39	---	60	1467	2191	2937	3744	4312	4727
1GF (1y)	0.24	20	---	6941	7334	7246	8379	8466(89)*	---
1GF (3m)	0.24	20	---	6552	7519	6686	7954	8609	8697
2GF (1y)	0.33	20	---	3885	4952	5807	6469	6952	7201
2GF (3m)	0.33	20	---	3855	4422	4918	5654	6289	6595
3GF (1y)	0.41	20	---	2975	4692	5692	7008	7854	7961
3GF (3m)	0.41	20	---	3922	4523	5175	5748	6395	6805
4GF (1y)	0.37	20	---	4889	4987	5640	6446	7528(89)*	---
4GF (3m)	0.37	20	---	4244	4810	5605	6219	6991	7405
5GS (1y)	0.33	---	50	3818	5151	6137	7262	7782	8041
5GS (3m)	0.33	---	50	2713	4262(10)*	4502	5163	5898	5130
6GS (1y)	0.36	---	50	2654	3571	5113(16)*	5628	6984	6543(92)*
6GS (3m)	0.36	---	50	---	5045	6047	6951	6769	7253
7GS (1y)	0.41	---	70	2267	4303	5222	6612	6741	7233
7GS (3m)	0.41	---	70	2277	3568(10)*	4036	5088	5207(54)*	5806(100)*
8GS (1y)	0.44	---	50	2123	---	3949(16)*	4994	6258	6157(92)*
8GS (3m)	0.44	---	50	---	3545	3899	4789	5304	5181

* number in parenthesis () indicates actual age in days of samples when tested.

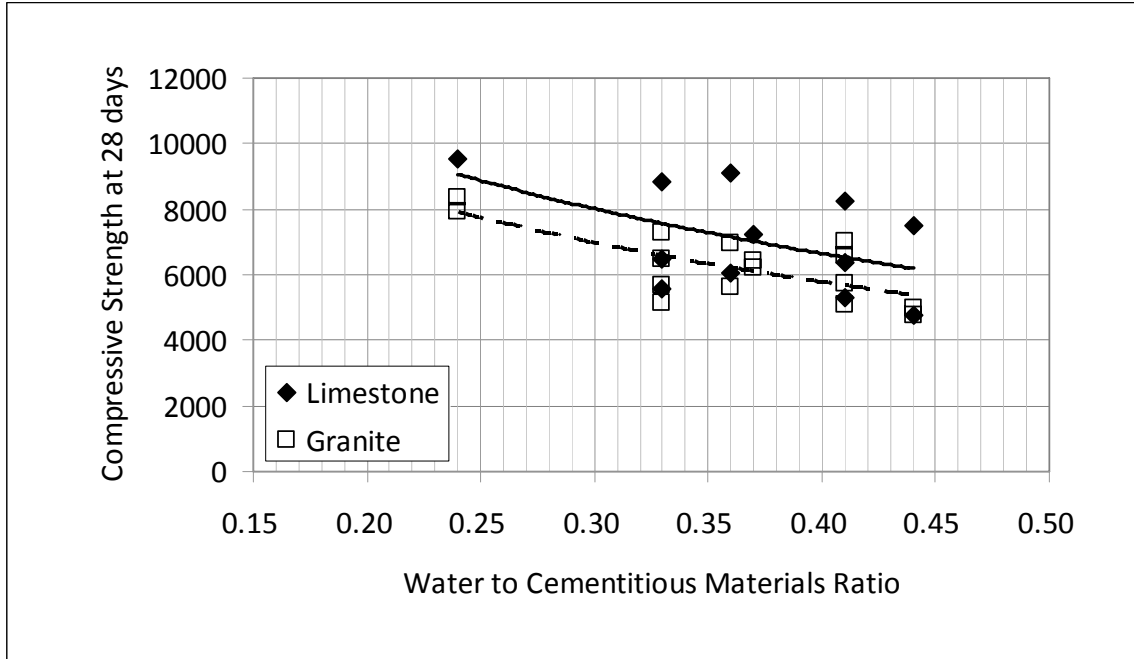


Figure 5-1. Effects of water-to-cementitious materials ratio on compressive strength at 28 days of mixes using Miami Oolite limestone and Georgia granite aggregate.

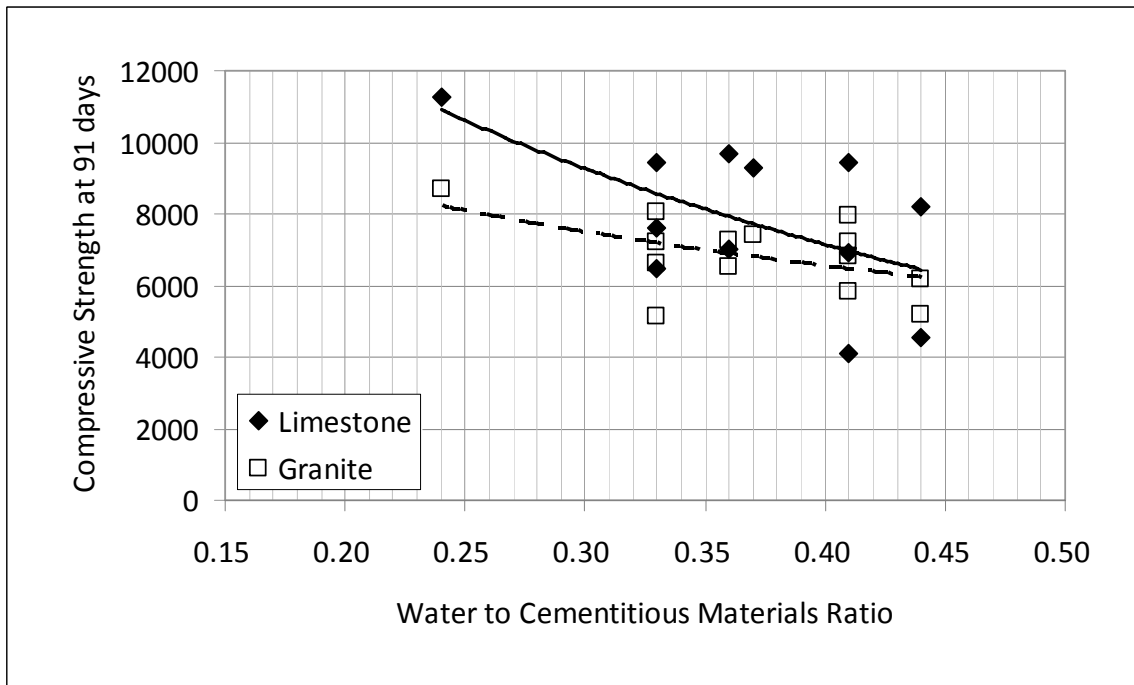


Figure 5-2. Effects of water-to-cementitious materials ratio on compressive strength at 91 days of mixes using Miami Oolite limestone and Georgia granite aggregate.

5.2.2 Effects of Aggregate Types on Compressive Strength

Figures 5-3 to 5-10 show the comparison of the strengths of concretes using Miami Oolite with those of comparable mixes using Georgia granite. The two mixes in each comparison have the same curing time and the same mix design with the exception of the coarse aggregate used. The mixes containing the letter “G” are the mixes containing Georgia granite as coarse aggregate. For example, Figure 5-3 shows the compressive strength development of Mix 1F made with Miami Oolite, and that of Mix 1GF made with Georgia granite.

Overall, comparable mixes containing Miami Oolite limestone aggregate are stronger than mixes containing Georgia granite aggregate. The difference appears to be more pronounced for concretes with a low w/c ratio. For example, in the comparison between Mix 1F and Mix 1GF with a w/c ratio of 0.24 (Figure 5-3), it can be seen that Mix 1F continues to gain strength with time, while the strength of Mix 1GF appears to level off after it reaches about 8000 psi.

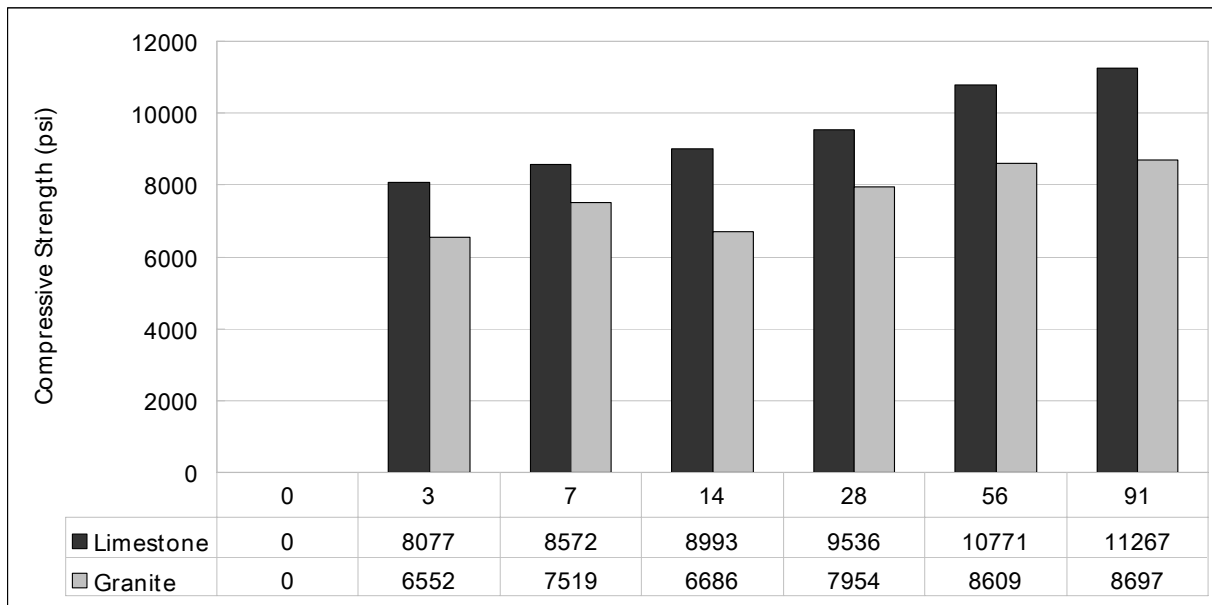


Figure 5-3. Effects of coarse aggregate type on compressive strength of Mixes 1F and 1GF.

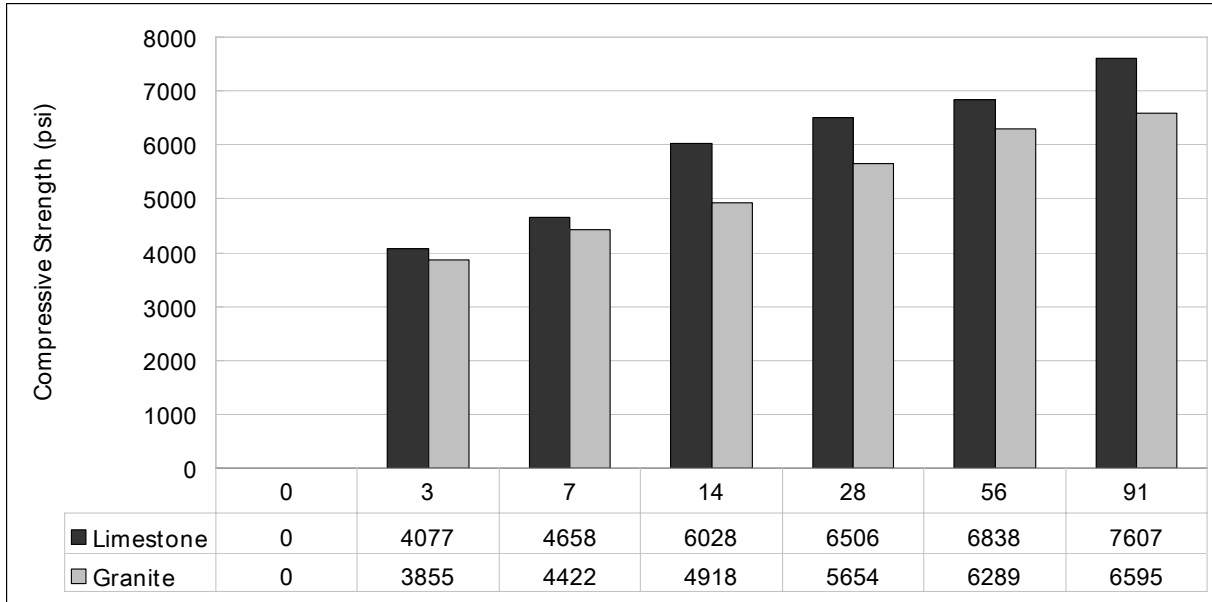


Figure 5-4. Effects of coarse aggregate type on compressive strength of Mixes 2F and 2GF.

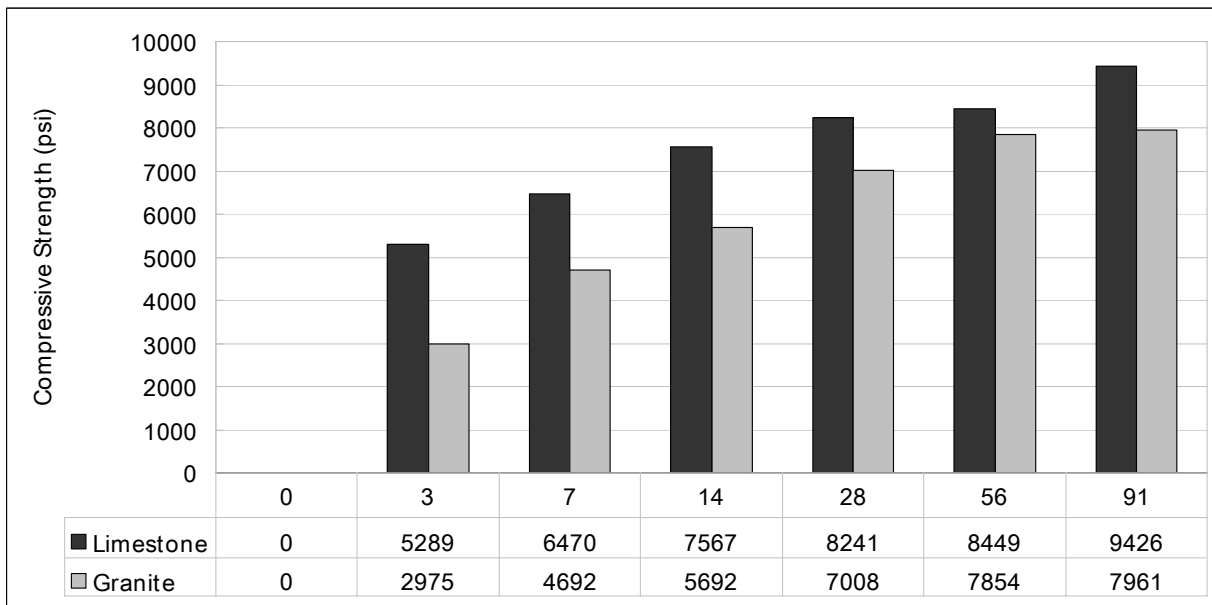


Figure 5-5. Effects of coarse aggregate type on compressive strength of Mixes 3F and 3GF.

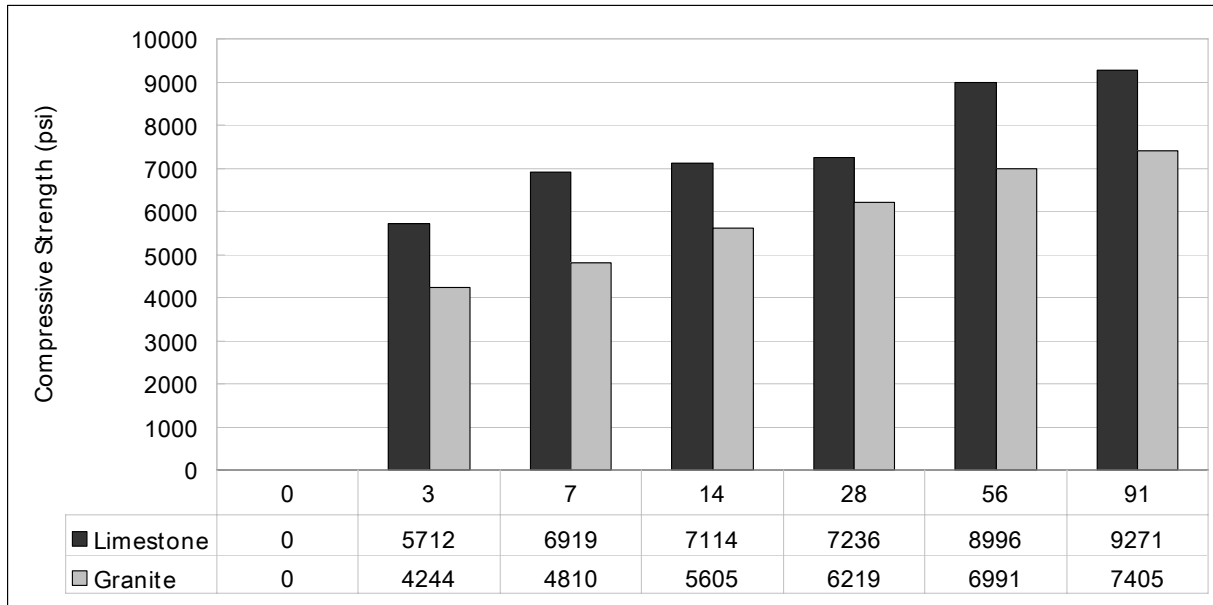


Figure 5-6. Effects of coarse aggregate type on compressive strength of Mixes 4F and 4GF.

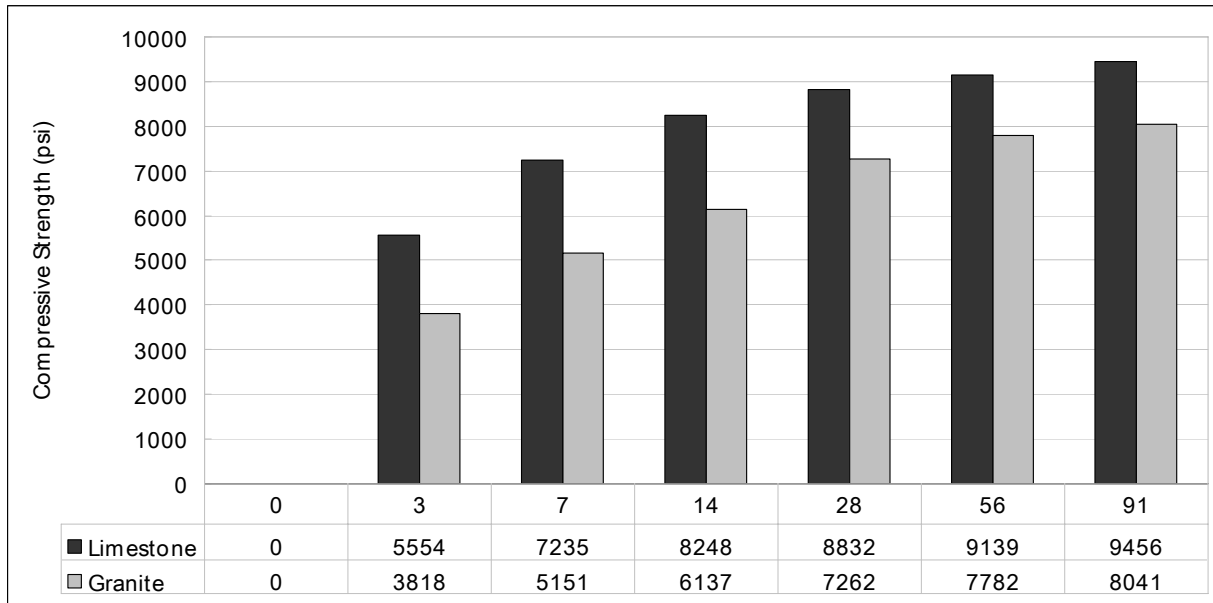


Figure 5-7. Effects of coarse aggregate type on compressive strength of Mixes 5S and 5GS.

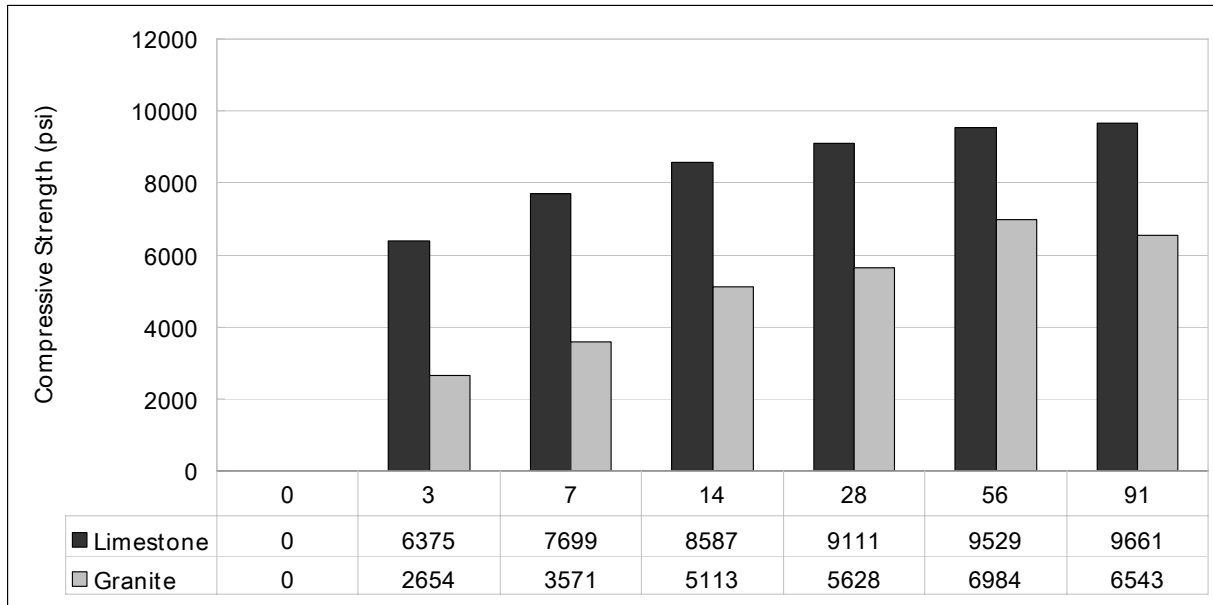


Figure 5-8. Effects of coarse aggregate type on compressive strength of Mixes 6S and 6GS.

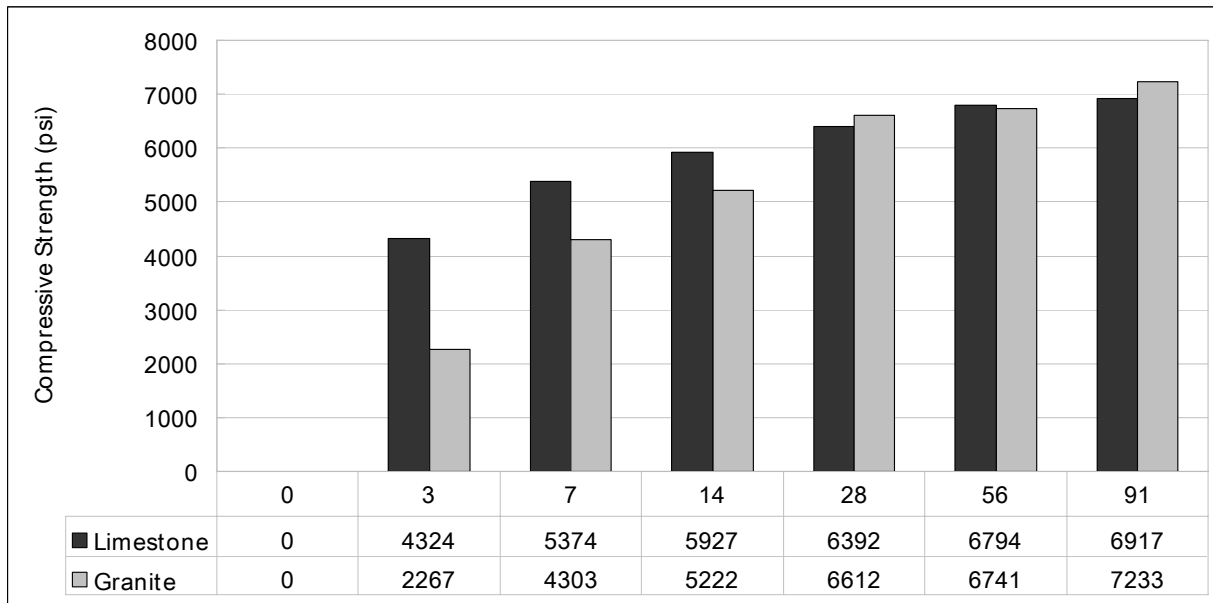


Figure 5-9. Effects of coarse aggregate type on compressive strength of Mixes 7S and 7GS.

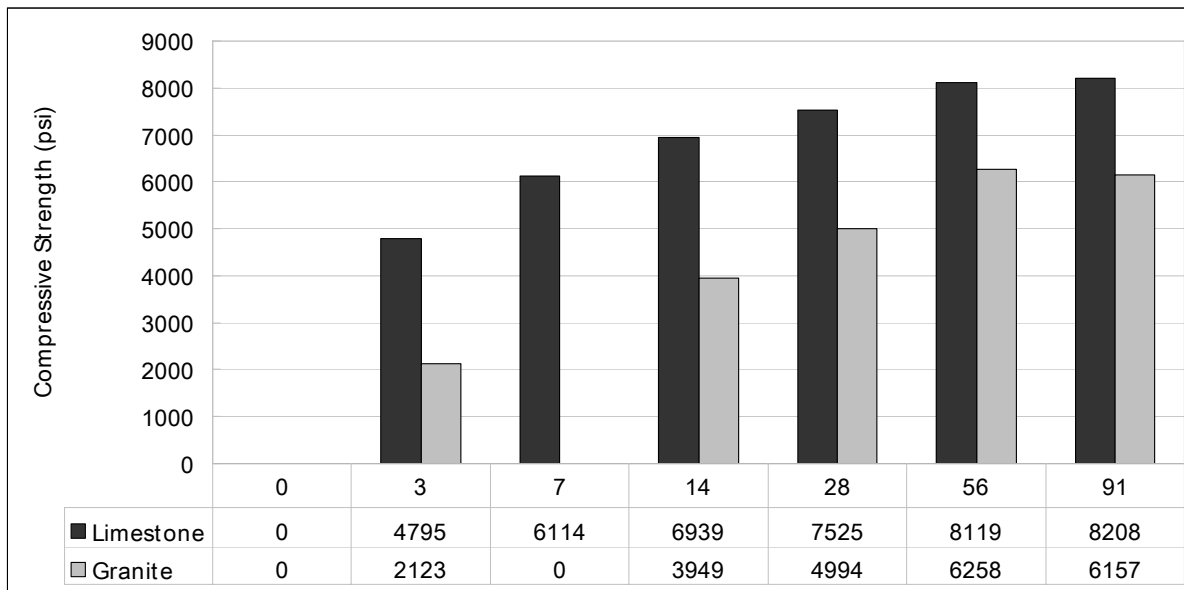


Figure 5-10. Effects of coarse aggregate type on compressive strength of Mixes 8S and 8GS.

The cause for the difference can probably be attributed to the shape of the aggregate, surface characteristics, and other physical properties such as water absorption. Most of the aggregate particles of Georgia granite have an elongated and flaky shape, which is not desirable to be used for high-strength concrete because flaky particles tend to be oriented in one plane, with bleeding water and air voids forming underneath. Thus, the interfacial transition zone between aggregate and hardened mortar may be weaker, causing the compressive strength of concrete to be lower. Most of the aggregate particles of Miami Oolite limestone have a spherical shape, which is preferred for a durable concrete mix because the spherical aggregate particles have a lower surface-to-volume ratio, and they will pack better in a mortar matrix.

The surface texture of Georgia granite aggregate is very dense and smooth, which may have a disadvantage in developing tight interlocks between the aggregate and mortar matrix. Miami Oolite limestone has a very rough texture and appreciable voids on the surface, and thus strong interlocks can be formed since the cement slurry can penetrate into those voids.

The water inside the limestone aggregate can migrate outward as cement hydration proceeds since the relative humidity gradient will be generated between the internal aggregate and the mortar. This water may possibly provide the water needed for hydration of the cement as moisture is lost through evaporation to the environment.

5.2.3 Effects of Fly Ash and Slag on Compressive Strength of Concrete

Fly ash and slag are used mandatorily in Florida mainly for the purpose of concrete durability. The investigation on their effects on the development of the compressive strength of a concrete mixture is of great importance because of the significance of their use in concrete. In this study, fly ash was used as a cement substitute in an amount of 20% of total cementitious materials by mass, and slag was in an amount of 50% ~ 70% of total cementitious materials by mass. The strength development characteristics of fly ash concrete and slag concrete with time were normalized as the ratio of compressive strength at various curing ages to the compressive strength at 91 days, and the normalized values are presented in Table A-2 in Appendix A.

The strength development characteristics of four fly ash concretes and four slag concretes using Miami Oolite are illustrated in Figure 5-11. As can be seen in Figure 5-11, the fly ash concretes had significant strength gain from 28 days to 91 days, while the slag concretes had already achieved more than 90% of their 91-day strength at 28 days.

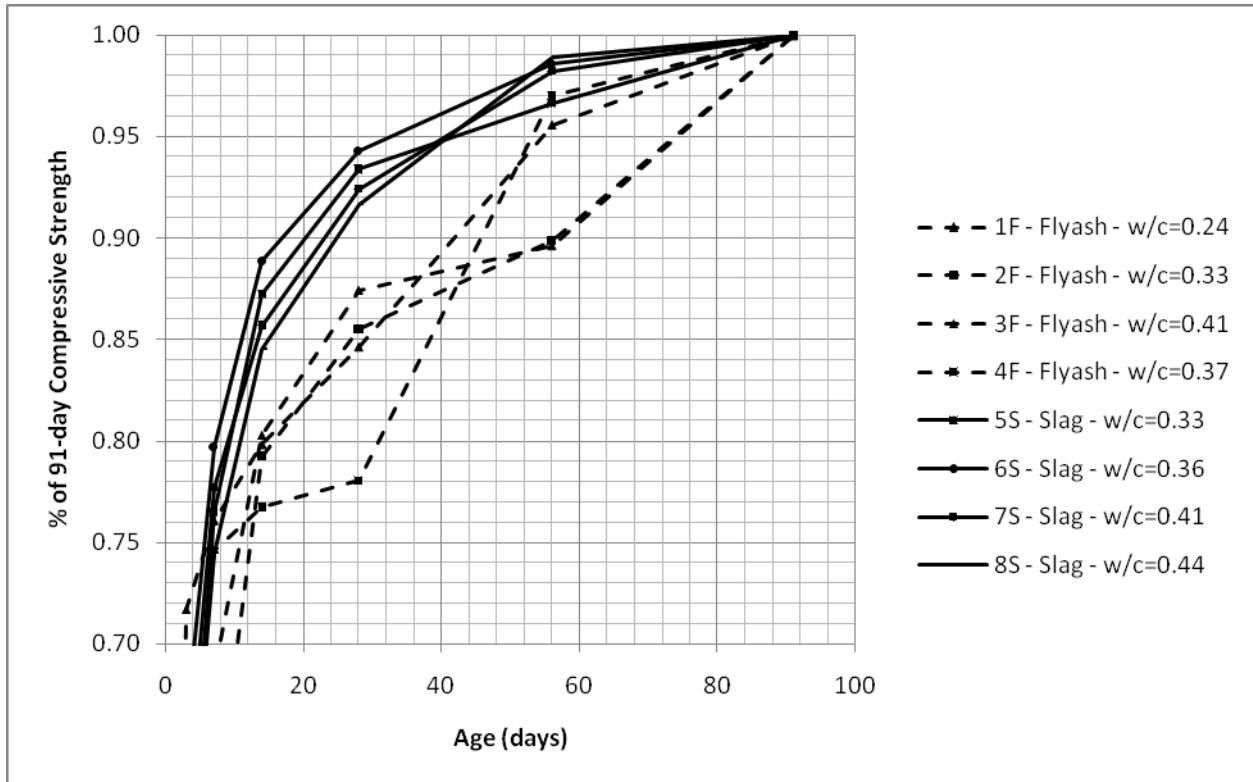


Figure 5-11. Effects of fly ash and slag on compressive strength of concrete.

5.3 Analysis of Splitting Tensile Strength Test Results

The average splitting tensile strengths at various curing times of the 18 concrete mixes evaluated are displayed in Table 5-2. The individual splitting tensile strength values are shown in Table A-3 in Appendix A.

5.3.1 Effects of Water-to-Cement Ratio on Splitting Tensile Strength

Water-to-cementitious (w/c) materials ratio has a significant effect not only on compressive strength, but also on the splitting tensile strength of concrete.

Figures 5-12 and 5-13 show the effect of the w/c materials ratio on the splitting tensile strength of concrete at 28 days and at 91 days, respectively. They indicate that splitting tensile strength decreases as the w/c materials ratio increases.

Table 5-2. Splitting Tensile Strengths of the Concrete Mixtures Evaluated (psi)

Mix Number	W/C	Fly Ash (%)	Slag (%)	Age of Testing					
				3 days (psi)	7 days (psi)	14 days (psi)	28 days (psi)	56 days (psi)	91 days (psi)
1F (1y)	0.24	20		592	628	715	795	834	849
2F (1y)	0.33	20		408	484	528	542	621	659
3F (1y)	0.41	20		513	539	562	624	674	731
4F (1y)	0.37	20		457	520	566	670	759	770
5S (1y)	0.33		50	454	476	621	614(27)*	646	664(105)*
5S (3m)	0.33		50	442	574	634	689	711	738
6S (1y)	0.36		50	668(6)*	562	605	641(30)*	624(69)*	530(94)*
6S (3m)	0.36		50	570	602	648	672	690	718
7S (1y)	0.41		70	367(6)*	431	455	444	490(69)*	496(94)*
7S (3m)	0.41		70	426	473	518	548	590	596
8S (1y)	0.44		50	399	389	536	496	480(57)*	465(106)*
8S (3m)	0.44		50	372	499	550	633	693	703
9LF (1y)	0.31	20		350	404	448	490	551	577
10LS (1y)	0.39		60	212	288	364	405	418	430
1GF (1y)	0.24	20		628(5)*	676	666	693	786(89)*	808
1GF (3m)	0.24	20		485	560	622	655	688	744
2GF (1y)	0.33	20		352	421	489	544	549	595
2GF (3m)	0.33	20		416	463	498	528	606	623
3GF (1y)	0.41	20		282	420	462	525	591	649
3GF (3m)	0.41	20		391	421	459	513	559	607
4GF (1y)	0.37	20		449(5)*	447	535	562	654(90)*	751
4GF (3m)	0.37	20		429	455	486	612	620	649
5GS (1y)	0.33		50	382	409	503	560	600	651
5GS (3m)	0.33		50	293	464(10)*	362	518	479	535
6GS (1y)	0.36		50	273	378	440	514	464	500(92)*
6GS (3m)	0.36		50	---	454	555	593	634	572
7GS (1y)	0.41		70	245	362	430	504	554	577
7GS (3m)	0.41		70	261	366(10)*	417	392	471(54)*	432
8GS (1y)	0.44		50	217	312(8)*	401(16)*	475	432	432(92)*
8GS (3m)	0.44		50	---	350	441	454	486	478

* number in parenthesis () indicates actual age in days of samples when tested.

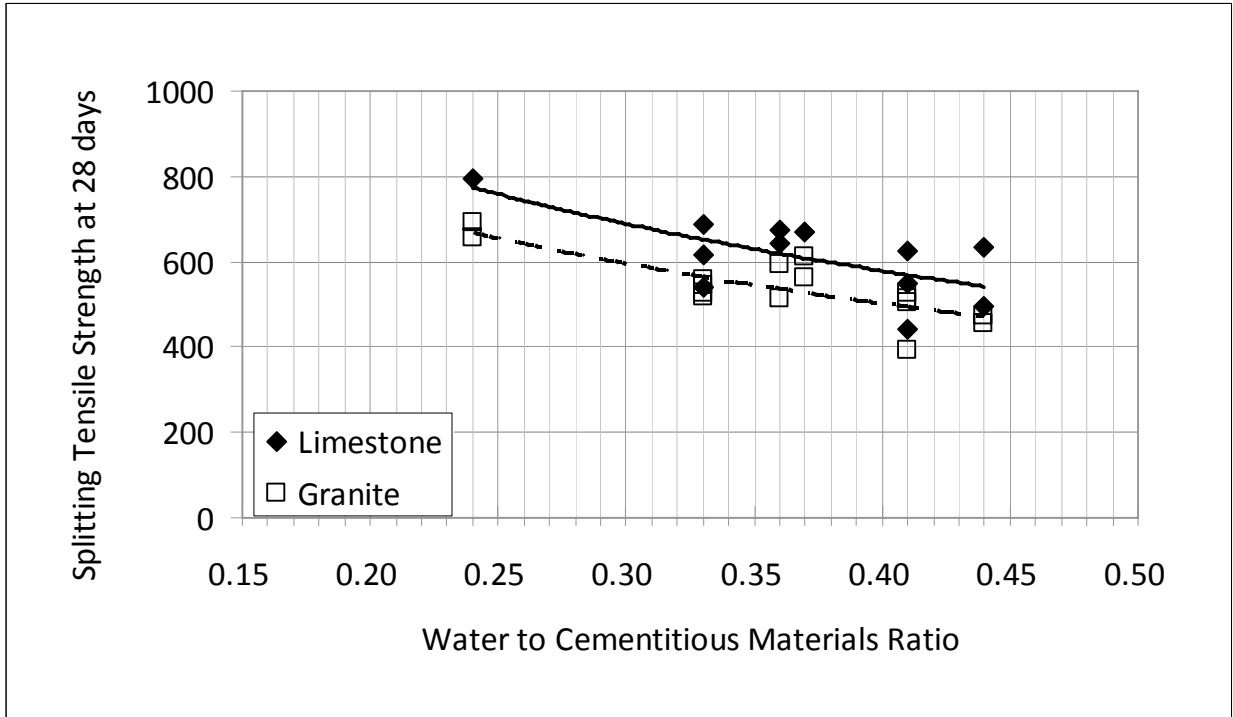


Figure 5-12. Effects of w/c materials ratio on splitting tensile strength at 28 days.

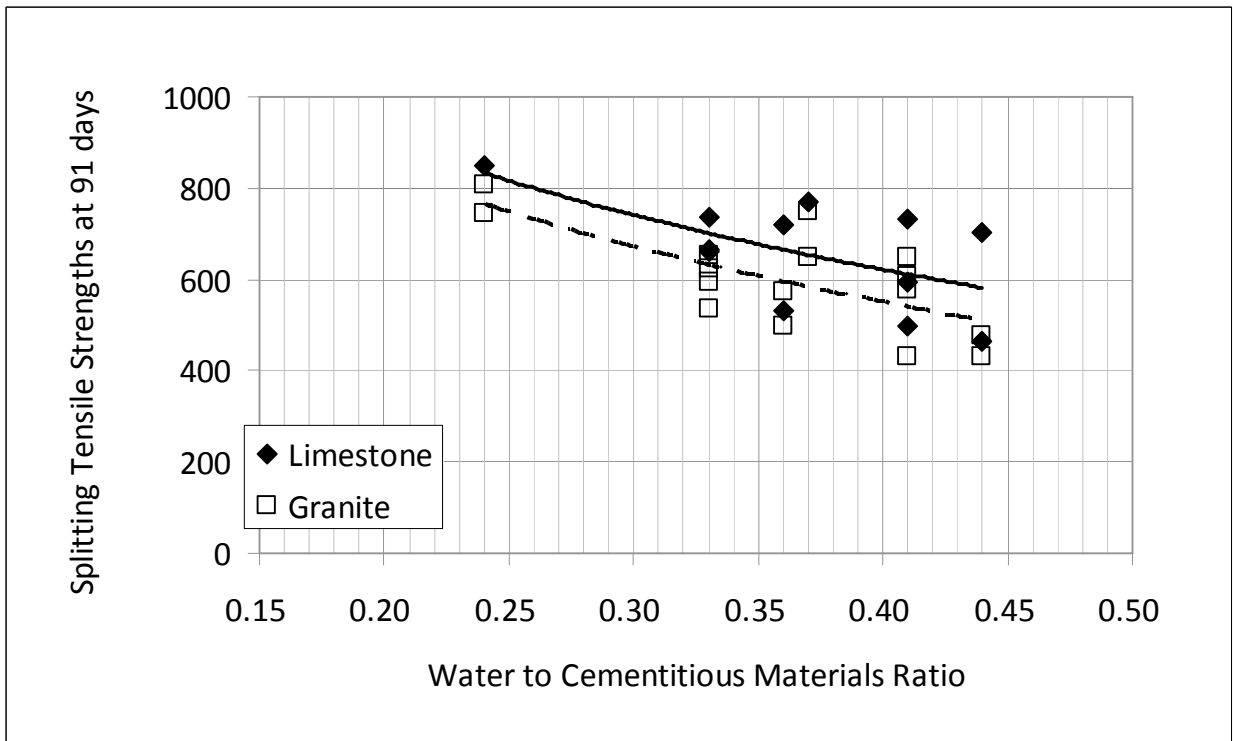


Figure 5-13. Effects of w/c materials ratio on splitting tensile strength at 91 days.

5.3.2 Effects of Coarse Aggregate Type on Splitting Tensile Strength

Figures 5-14 through 5-21 show the comparison of the splitting tensile strengths of concretes using Miami Oolite with those of comparable mixes using Georgia granite. In general, the splitting tensile strengths of mixes containing Georgia granite are lower as compared with those of the mixes containing Miami Oolite limestone. For example, at 91 days, Mix 2F has a splitting tensile strength of 659 psi versus 595 psi for Mix 2GF, and Mix 3F has a splitting tensile strength of 731 psi versus 561 psi for Mix 3GF.

5.3.3 Effects of Fly Ash and Slag on Splitting Tensile Strength of Concrete

Fly ash and slag have a significant effect on splitting tensile strength. In order to see the effects of fly ash and slag on splitting tensile strength, the strength development characteristics of splitting tensile strength were normalized as the ratio of splitting tensile strength at various curing ages to the splitting tensile strength at 91 days and the normalized values are listed in Table A-4 in Appendix A. As can be seen in Table A-2, the splitting tensile strengths of fly ash concrete mixtures increase slowly in 28 days after demolding, and the 28-day splitting tensile

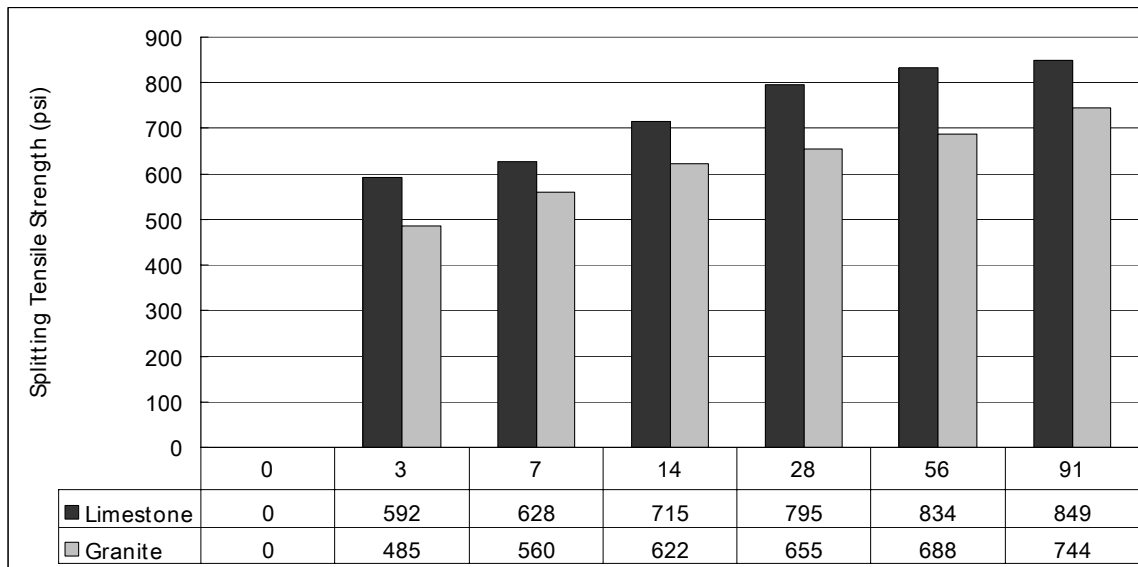


Figure 5-14. Effects of aggregate type on splitting tensile strength of Mixes 1F and 1GF.

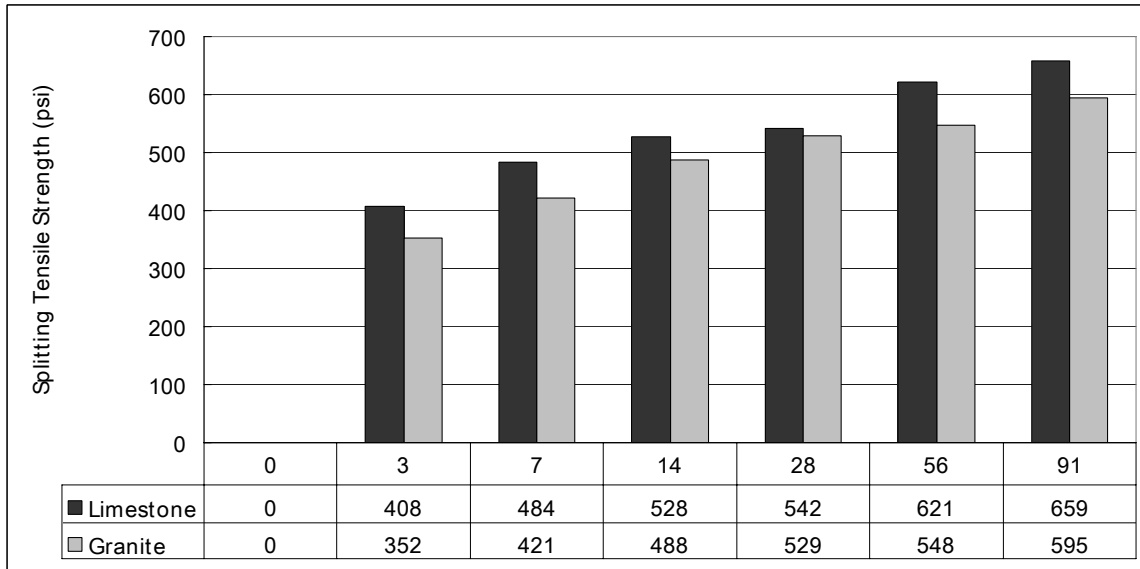


Figure 5-15. Effects of aggregate type on splitting tensile strength of Mixes 2F and 2GF.

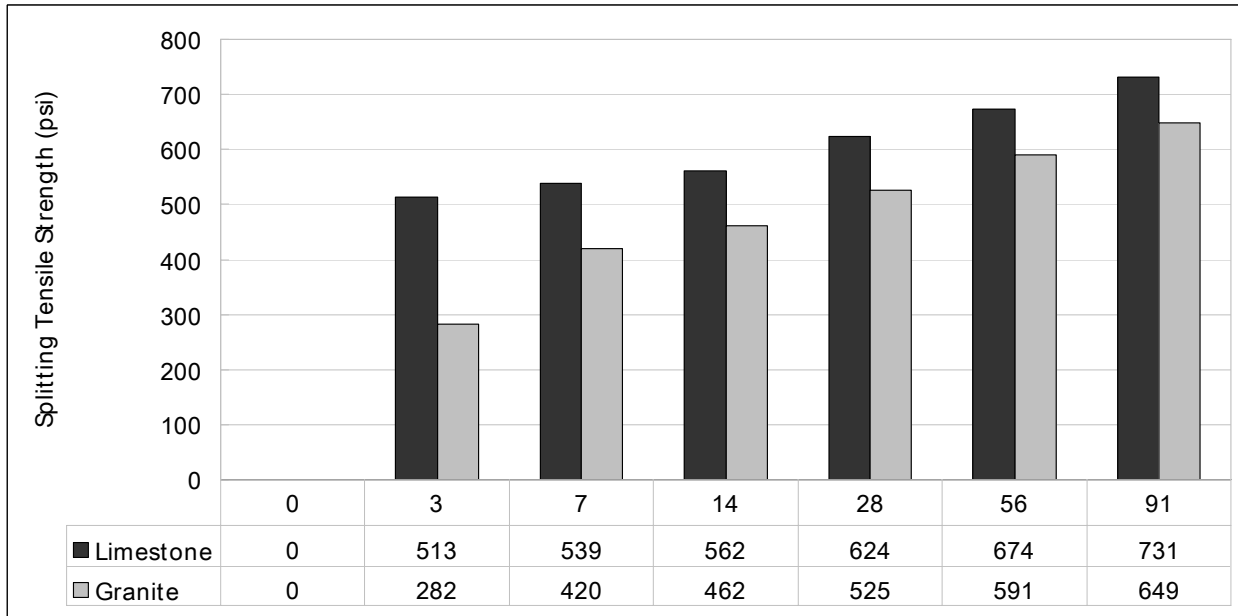


Figure 5-16. Effects of aggregate type on splitting tensile strength of Mixes 3F and 3GF.

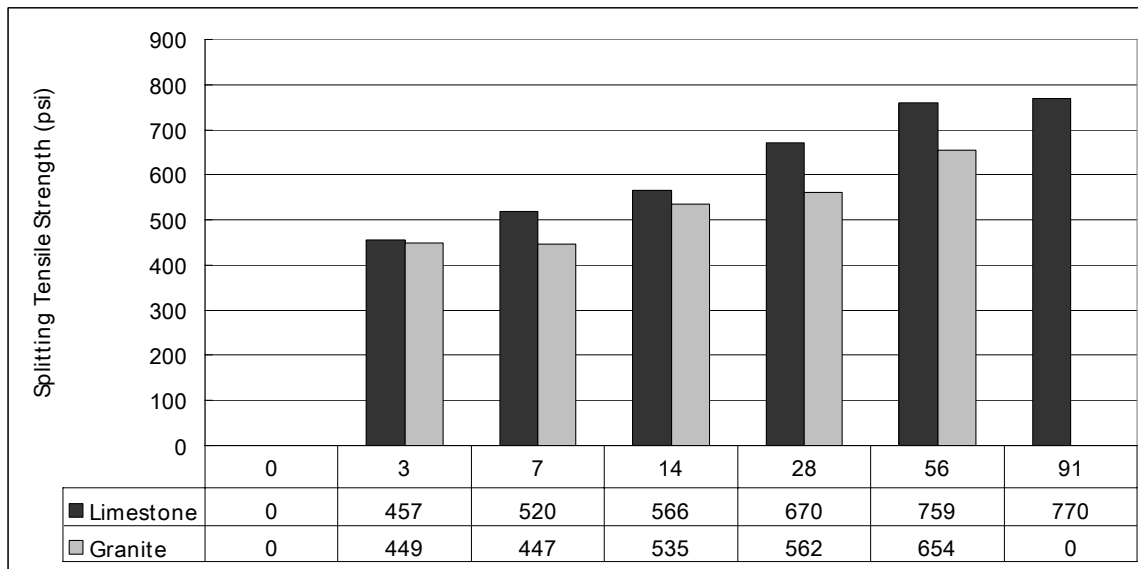


Figure 5-17. Effects of aggregate type on splitting tensile strength of Mixes 4F and 4GF.

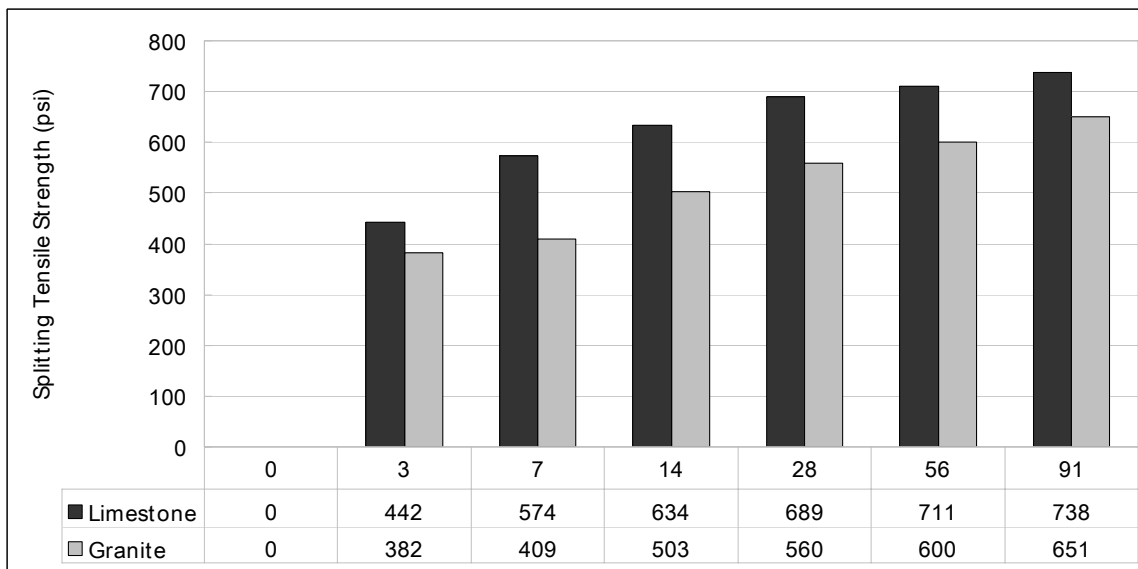


Figure 5-18. Effects of aggregate type on splitting tensile strength of Mixes 5S and 5GS.

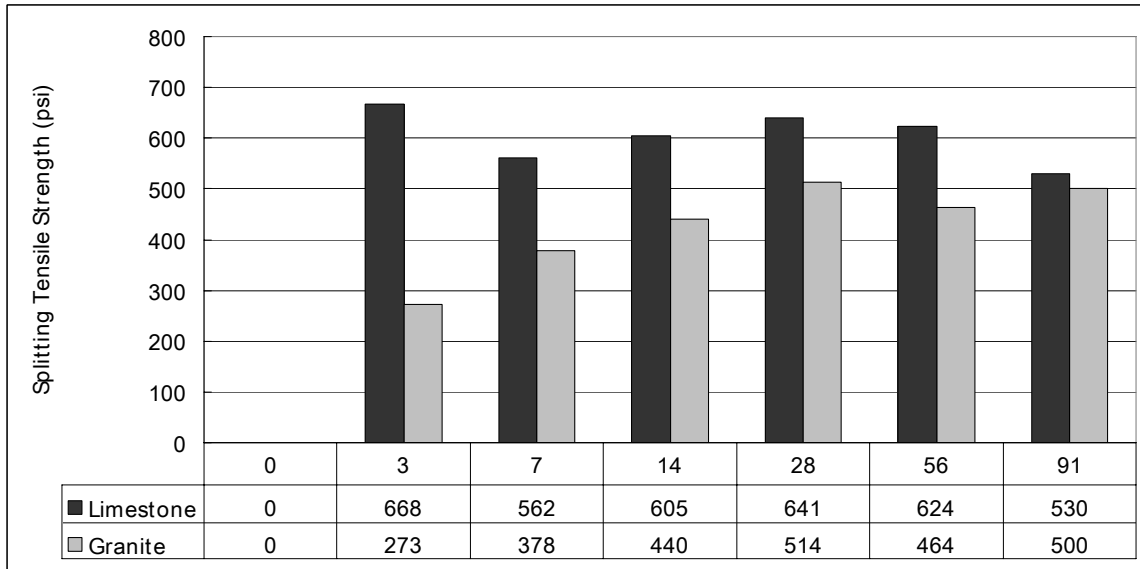


Figure 5-19. Effects of aggregate type on splitting tensile strength of Mixes 6S and 6GS.

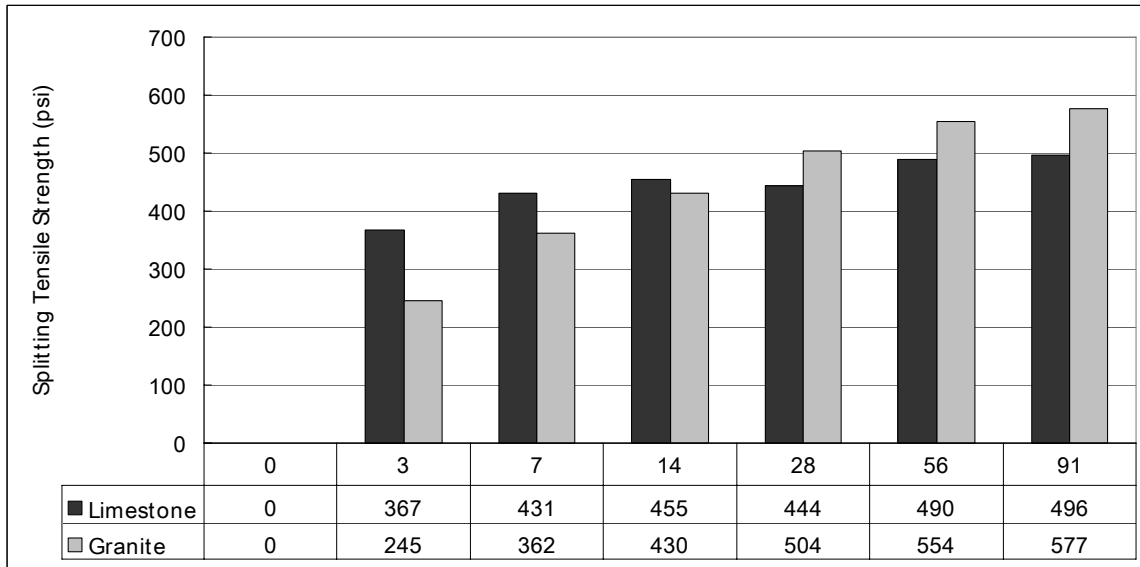


Figure 5-20. Effects of aggregate type on splitting tensile strength of Mixes 7S and 7GS.

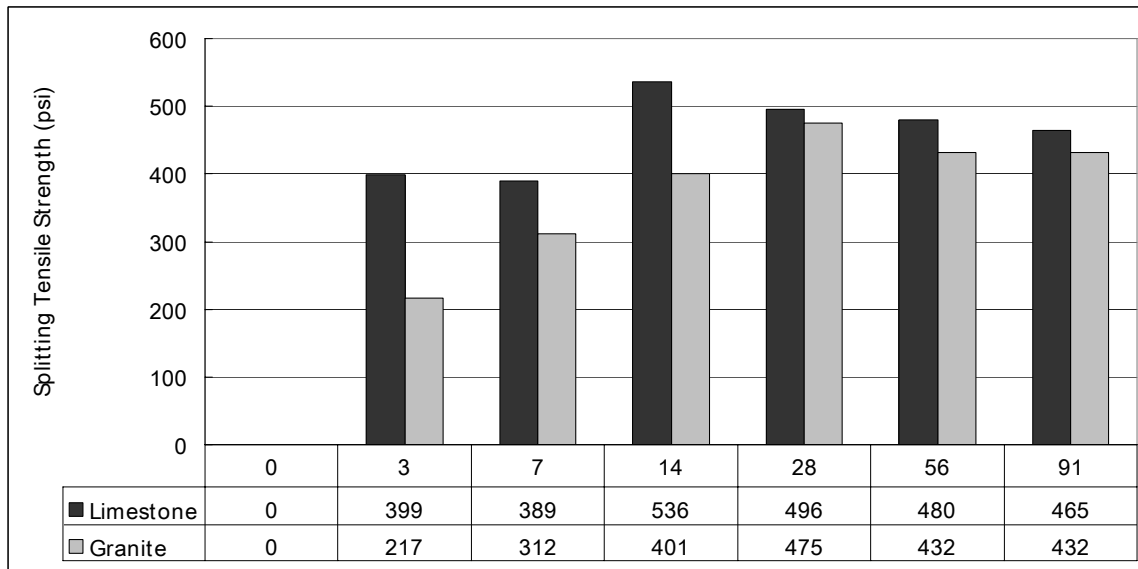


Figure 5-21. Effects of aggregate type on splitting tensile strength of Mixes 8S and 8GS.

strength is around 85% of splitting tensile strength at 91 days, while the splitting tensile strength of slag concrete increased very rapidly in 28 days after demolding, up to 94% of splitting tensile strength at 91 days.

For example, the splitting tensile strength of Mix 2F at 91 days is 659 psi, increasing 21.6% in comparison with that at 28 days. Mix 3F has a splitting tensile strength of 731 psi at 91 days, increasing 17.1% in comparison with that at 28 days. But, for the concrete mixtures with slag and limestone coarse aggregate, there is no appreciable increase in splitting tensile strength after 28 days curing. For example, Mixes 5S, 6S, 7S, and 8S increase in splitting tensile strength by less than 10% at 91 days as compared with that at 28 days. For the concrete mixtures with Georgia granite aggregate, a substantial increase in splitting tensile strength after 28 days also occurred in the mixtures with fly ash, while no significant increase was found in concrete mixtures with slag. For two lightweight aggregate concrete mixtures, similar trends can be observed as well.

The splitting tensile strength development characteristics of the four fly ash concretes and four slag concretes using Miami Oolite are shown in Figure 5-22.

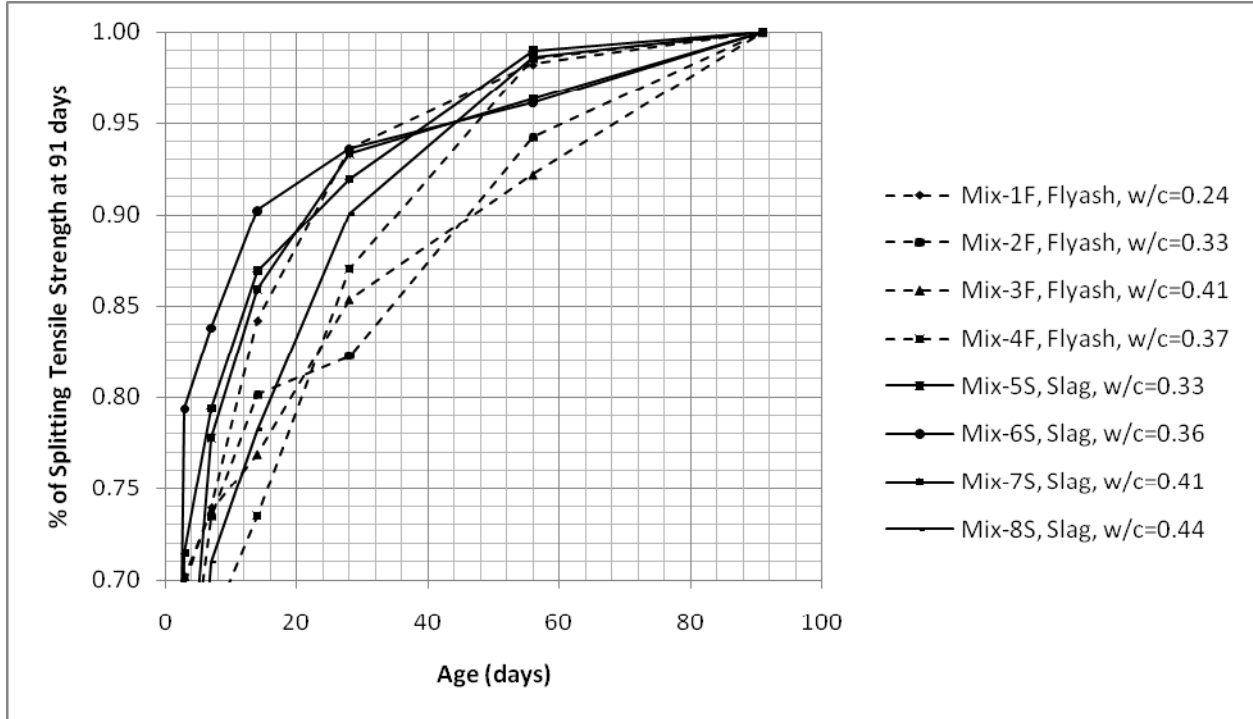


Figure 5-22. Effects of fly ash and slag on splitting tensile strength of concrete using Miami Oolite.

5.4 Relationship Between Compressive Strength and Splitting Tensile Strength

The compressive strengths of the concretes (as tabulated in Table A-1) were plotted against the corresponding splitting tensile strengths (as tabulated in Table A-2) for all curing conditions in Figure 5-23. Regression analyses were performed to establish an empirical relationship between compressive strength and splitting tensile strengths using the following equations:

$$f_{ct} = A \cdot \sqrt{f'_c} \quad (5-3)$$

$$f_{ct} = A \cdot (f'_c)^B \quad (5-4)$$

where f_{ct} = splitting tensile strength (psi);
 f'_c = compressive strength (psi); and
 A, B = coefficients.

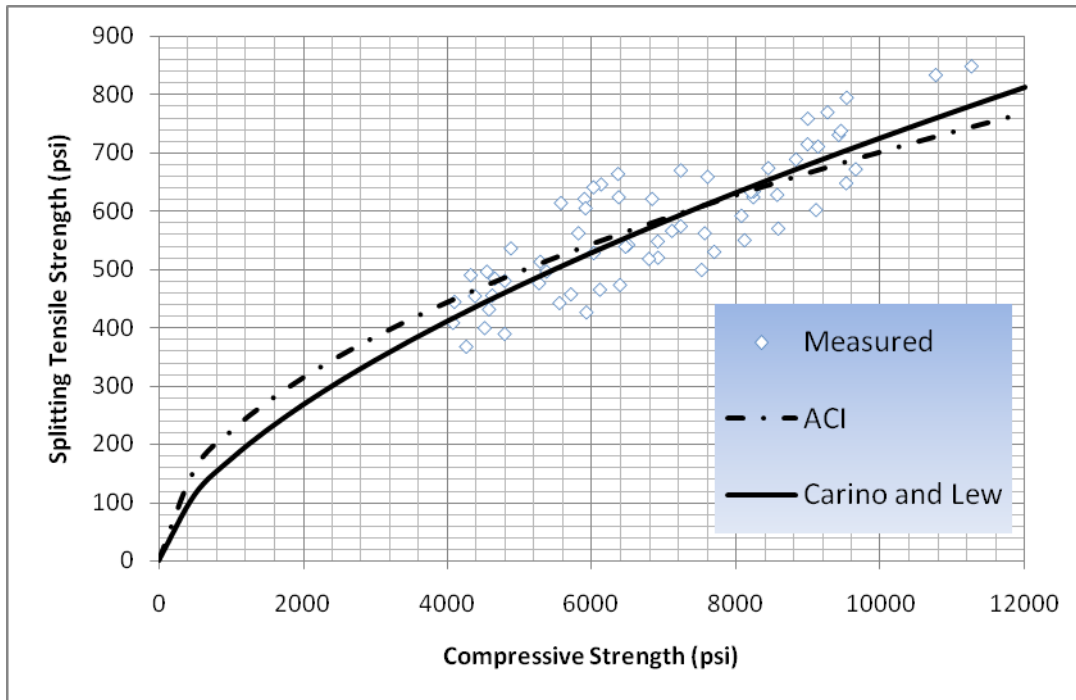


Figure 5-23. Relationship between compressive strength and splitting tensile strength.

The ACI Code 318 uses Equation 5-3 for estimation of splitting tensile strength of lightweight concrete, where the coefficient A is equal to 6.7 [ACI 318, 1983]. The investigation by Carino and Lew [1982] determined that the coefficient A was approximately 6.49. They suggested that Equation 5-4 was better than Equation 5-3 in the estimation of splitting tensile strength from compressive strength. The coefficient A was determined to be 1.15 and B was determined to be 0.71 in their investigation.

Results from the regression analysis are shown in Table 5-3. For the ACI model, the coefficient A was found to be 7.02 which is slightly higher than the value of 6.7 by ACI. For the Carino and Lew model, A was found to be 2.40 which is higher than the value of 1.15, and B was

found to be 0.70, which is slightly lower than the value of 0.71. Figure 5-23 shows the measured values and both modified models plotted. It seems that the Carino and Lew model gives a slightly better fit, especially at low compressive strengths. It also seems that the ACI model underestimates the splitting tensile strength values, especially at high compressive strengths.

Table 5-3. Results of Regression Analysis for Relating Compressive Strength to Splitting Tensile Strength

Equation	Curing Condition	Coefficient <i>A</i> or <i>B</i>	Standard Error	Standard Error of the Estimate
ACI Code				
$f_{ct} = A\sqrt{f'_c}$	Moist curing	$A = 7.02$	0.09529	63.3
Carino and Lew model				
$f_{ct} = A(f'_c)^B$	Moist curing	$A = 2.40$ $B = 0.62$	1.0926	61.1

5.5 Analysis of Elastic Modulus Test Results

The average elastic modulus values at various curing ages of the 18 concrete mixes evaluated are displayed in Table 5-4. The individual elastic modulus values are shown in Table A-3 in Appendix A.

It can be seen in Table 5-4 that the elastic modulus of mixes containing Miami Oolite limestone range from 3.10×10^6 to 5.70×10^6 psi; mixes containing lightweight aggregate range in values from 1.75×10^6 to 3.50×10^6 psi; and mixes containing Georgia granite have the widest range with values from 2.43×10^6 to 5.96×10^6 psi.

Table 5-4. Elastic Modulus of the Concrete Mixtures Evaluated ($\times 10^6$ psi)

Mix Number	W/C	Fly Ash (%)	Slag (%)	Age of Testing					
				3 days (psi)	7 days (psi)	14 days (psi)	28 days (psi)	56 days (psi)	91 days (psi)
1F (1y)	0.24	20		4.74	4.93	5.23	5.40	5.54	5.58
2F (1y)	0.33	20		3.43	3.77	4.08	4.31	4.43	4.67
3F (1y)	0.41	20		4.40	4.85	5.05	5.14	5.28	5.70
4F (1y)	0.37	20		4.49	4.61	4.88	5.01	5.15	5.29
5S (1y)	0.33		50	3.63	3.93	4.03	4.45(27)*	4.36	4.35
5S (3m)	0.33		50	4.11	4.66	4.88	5.09	5.23	5.23
6S (1y)	0.36		50	4.06(6)*	4.20	4.29	4.44(30)*	---	---
6S (3m)	0.36		50	4.27	4.92	5.18	5.45	5.62	5.66
7S (1y)	0.41		70	3.18(6)*	3.43	3.55	3.46(30)*	3.68(56)*	4.15(94)*
7S (3m)	0.41		70	3.90	4.30	4.52	4.60	4.73	4.76
8S (1y)	0.44		50	3.10	3.30	3.60	3.86	4.10(57)*	4.05
8S (3m)	0.44		50	3.96	4.39	4.84	5.00	5.13	5.16
9LF (1y)	0.31	20		2.76	2.92	3.13	3.27	3.40	3.50
10LS (1y)	0.39		60	1.75	1.88	2.36	2.69	3.01	3.04
1GF (1y)	0.24	20		5.20	5.29	5.46	5.74	5.78(89)*	---
1GF (3m)	0.24	20		5.04	5.41	5.61	5.50	5.60	5.74
2GF (1y)	0.33	20		3.80	4.22	4.61	4.96	5.06	5.19
2GF (3m)	0.33	20		4.06	4.39	4.50	4.99	5.06	5.53
3GF (1y)	0.41	20		4.15	4.62	5.52	5.61	5.93	5.96
3GF (3m)	0.41	20		4.24	4.55	4.85	5.10	5.55	5.66
4GF (1y)	0.37	20		4.30	4.41	4.64	4.93	5.34(89)*	---
4GF (3m)	0.37	20		4.49	4.10	4.85	5.10	5.36	5.71
5GS (1y)	0.33		50	3.15	3.82	4.65	5.17	5.37	5.56
5GS (3m)	0.33		50	2.85	3.91(10)*	4.20	4.16	4.41	4.10
6GS (1y)	0.36		50	2.80	3.49	4.15(16)*	4.78	5.35	5.65(92)*
6GS (3m)	0.36		50	---	4.35	5.03	5.41	5.63	5.73
7GS (1y)	0.41		70	2.69	3.38	4.10	5.25	5.60	5.73
7GS (3m)	0.41		70	2.43	3.35(10)*	3.76	4.46	4.90(54)*	4.73(100)*
8GS (1y)	0.44		50	2.66	---	3.89(16)*	4.15	4.85	5.20(92)*
8GS (3m)	0.44		50	---	3.55	4.35	4.88	5.00	4.88

* number in parenthesis () indicates actual age in days of samples when tested.

Figures 5-24 through 5-31 show the comparison of the elastic modulus of concretes using Miami Oolite with those of comparable mixes using Georgia granite. In general, the elastic moduli of mixes containing Georgia granite are higher than those of the mixes containing Miami Oolite limestone. For example, by comparing the elastic moduli at 91 days of Mixes 2F and

2GF, it can be seen that the elastic modulus of Mix 2F is 4.67×10^6 psi versus 5.19×10^6 psi for Mix 2GF. This is also the case for the 91-day elastic moduli for Mixes 3F and 3GF: 5.70×10^6 psi versus 5.96×10^6 psi, respectively. Figure 5-28 shows 91-day elastic moduli of 5.23×10^6 psi versus 5.56×10^6 psi for Mixes 5S and 5GS, respectively. Figure 5-30 shows 91-day elastic moduli of 4.76×10^6 psi versus 5.73×10^6 psi for Mixes 7S and 7GS, respectively. Figure 5-31 shows 91-day elastic moduli of 5.16×10^6 psi versus 5.20×10^6 psi for Mixes 8S and 8GS, respectively.

It is interesting to note that high-strength but low-elastic modulus concrete can be obtained through using lightweight aggregate. For example Mix 9LF, a lightweight aggregate concrete, has similar compressive strength and splitting tensile strength to Mix 7S with Miami Oolite limestone aggregate, while the elastic modulus of Mix 9LF at 91 days is only about 3.50×10^6 psi, which is about 36% lower than that of Mix 7S. Thus, to achieve high-strength but low-elastic modulus concrete, which is desirable for concrete pavement, a lightweight aggregate may be used.

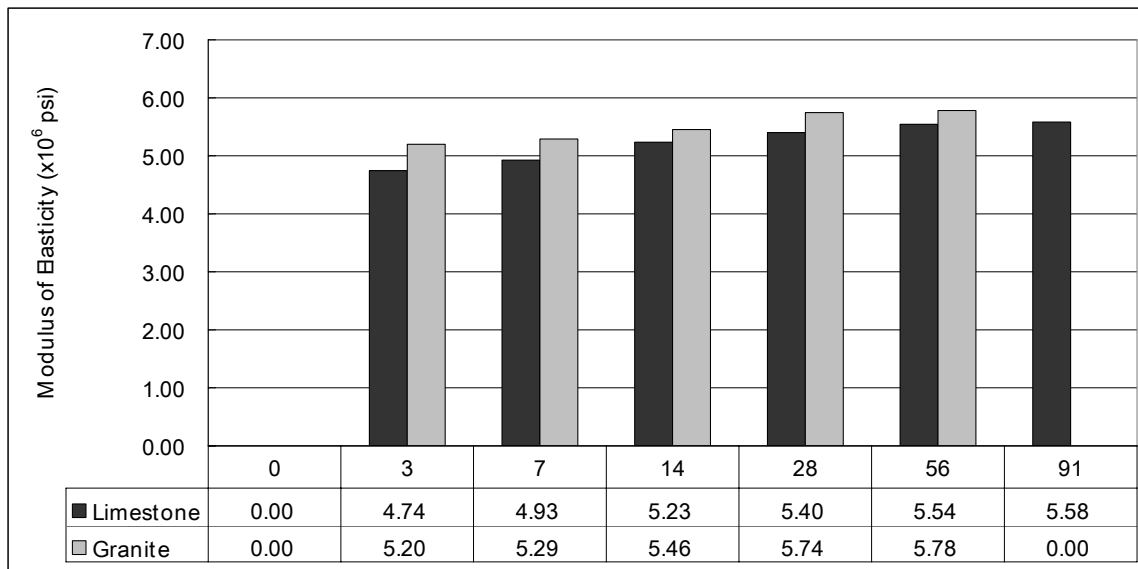


Figure 5-24. Effects of aggregate type on modulus of elasticity of Mixes 1F and 1GF.

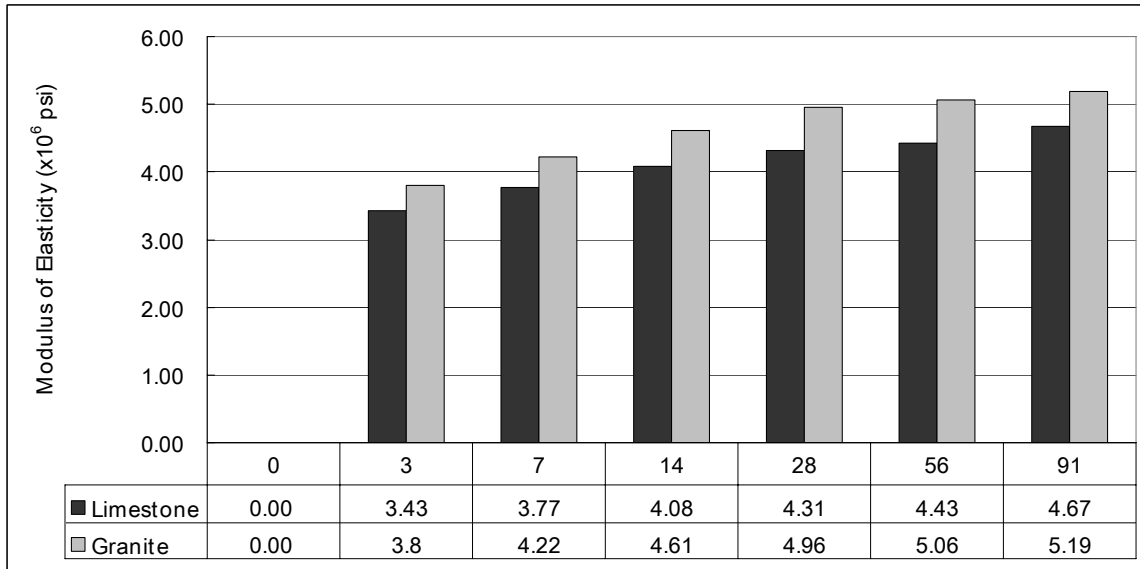


Figure 5-25. Effects of aggregate type on modulus of elasticity of Mixes 2F and 2GF.

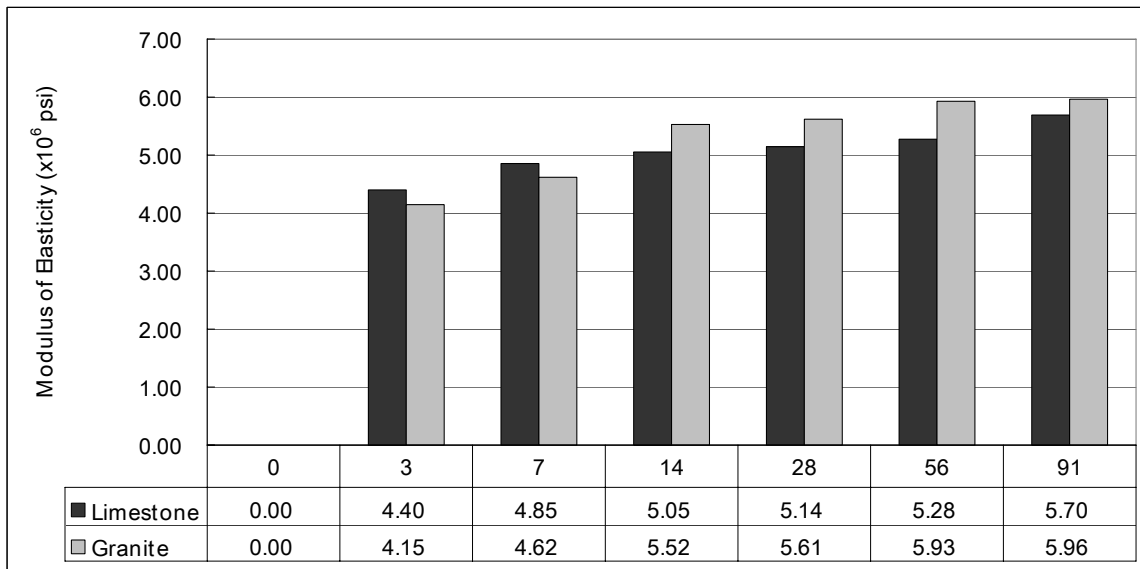


Figure 5-26. Effects of aggregate type on modulus of elasticity of Mixes 3F and 3GF.

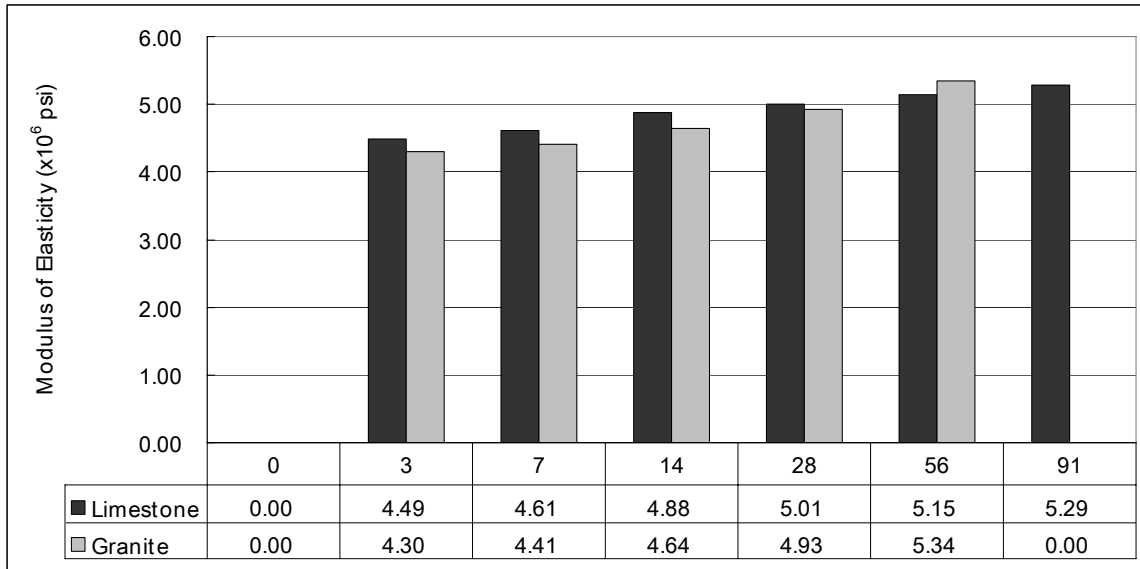


Figure 5-27. Effects of aggregate type on modulus of elasticity of Mixes 4F and 4GF.

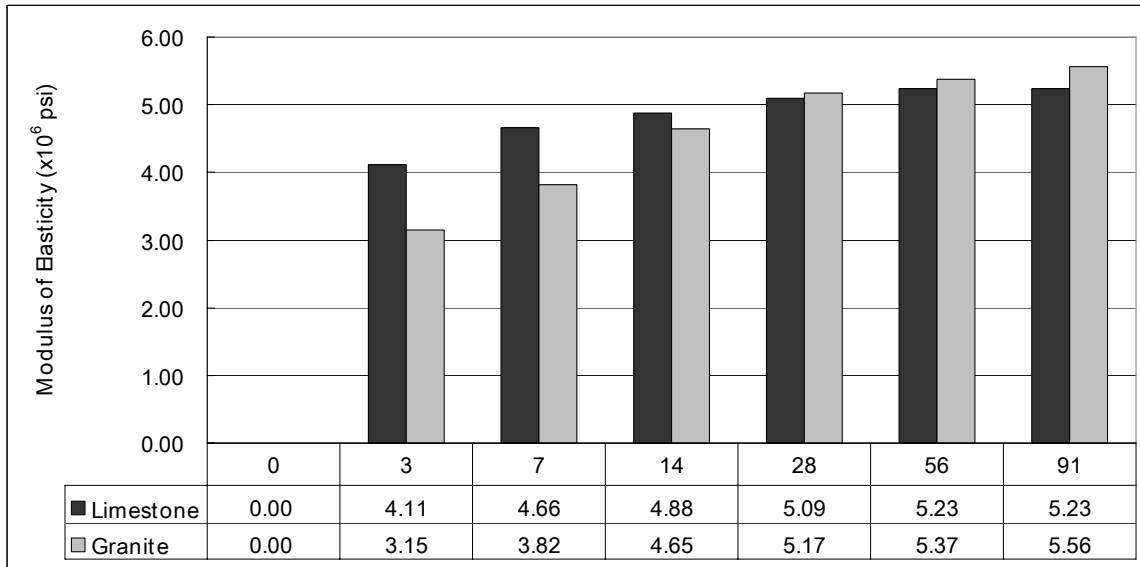


Figure 5-28. Effects of aggregate type on modulus of elasticity of Mixes 5S and 5GS.

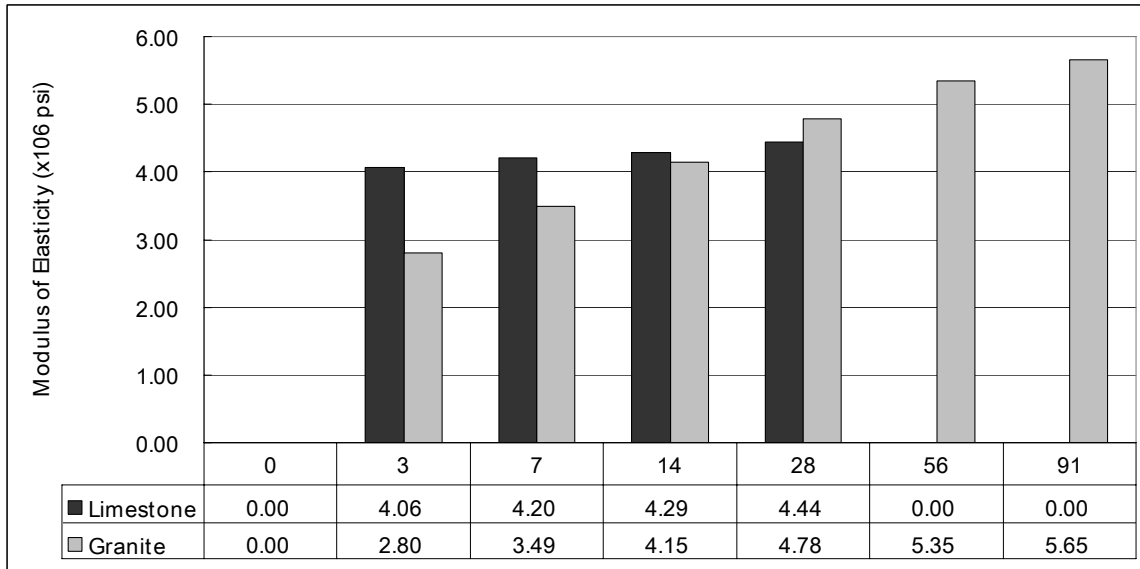


Figure 5-29. Effects of aggregate type on modulus of elasticity of Mixes 6S and 6GS.

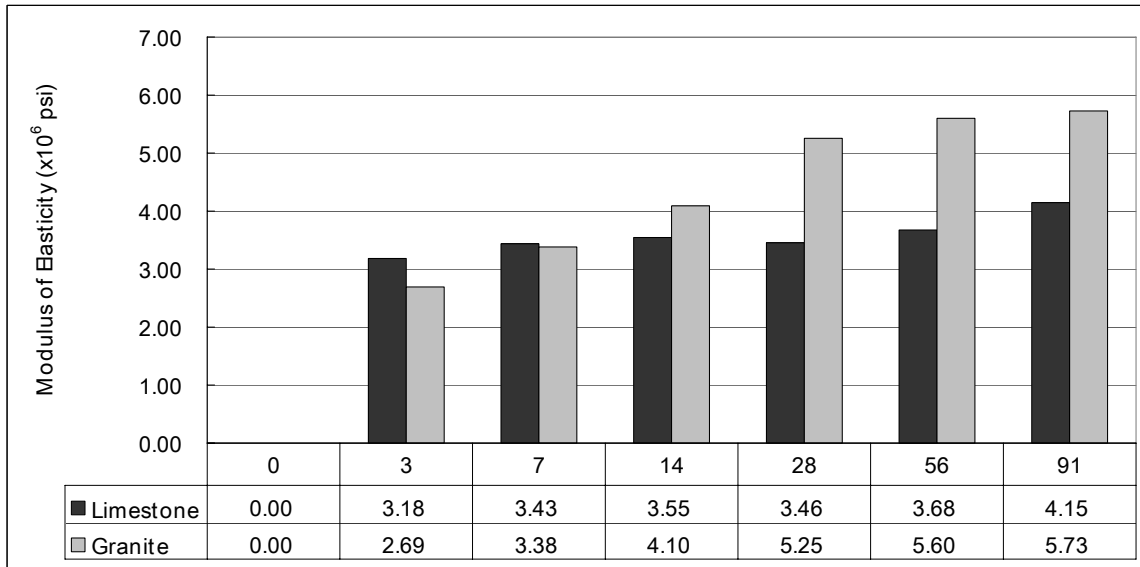


Figure 5-30. Effects of aggregate type on modulus of elasticity of Mixes 7S and 7GS.

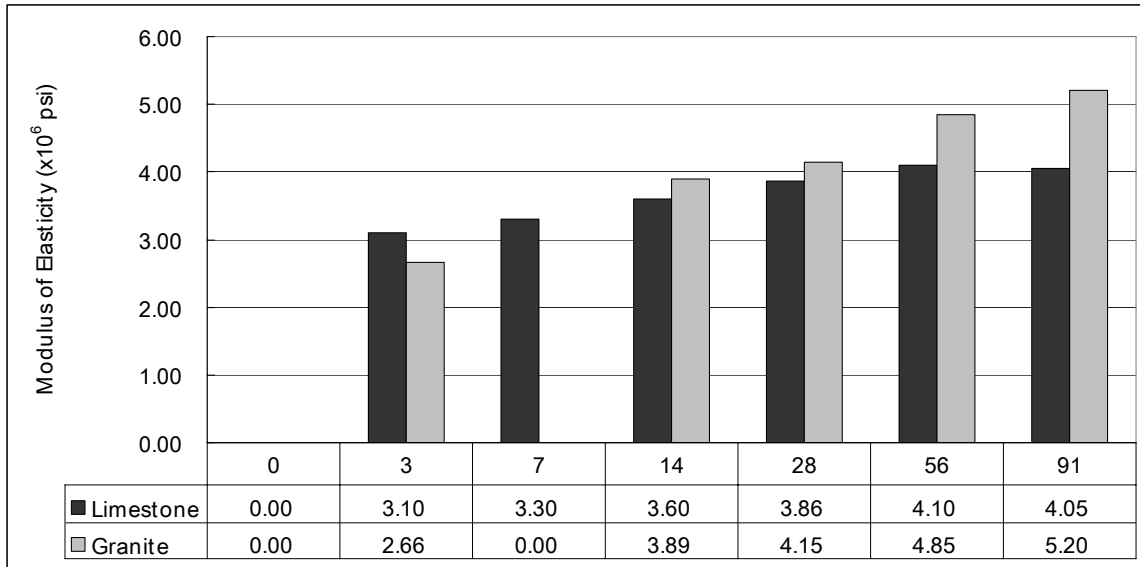


Figure 5-31. Effects of aggregate type on modulus of elasticity of Mixes 8S and 8GS.

5.6 Relationship Between Compressive Strength and Elastic Modulus

The elastic modulus of concrete is affected by the modulus of elasticity of the aggregate and by the volumetric proportion of aggregate in the concrete. Thus, there is no surprise that there is no agreement on the precise form of the relationship between compressive strength and elastic modulus.

In this study, modification was made on the expression recommended by ACI 318-89, given as follows:

$$E_c = \alpha \cdot \sqrt{f'_c} \quad (5-5)$$

In Equation 5-5, α is a parameter to be determined through curve-fitting regression analysis. Its value recommended by ACI is 57,000.

The regression analysis was carried out on the expression recommended by ACI 318-95, given as follows, to fit the experimental data. In this formula, the unit weight of concrete was also used.

$$E = A \cdot w^{1.5} \cdot \sqrt{f'_c} \quad (5-6)$$

where E = elastic modulus in psi;

f'_c = compressive strength in psi;

w = unit weight of concrete in pcf; and

A = coefficient to be determined through regression analysis.

The recommended value by ACI 318-95 is 33.0.

The compressive strengths of the 18 concrete mixtures were plotted against their elastic modulus at corresponding curing ages, as shown in Figure 5-32. It can be clearly seen that the aggregate type has significant effects on the elastic modulus of concrete. Concretes containing Georgia granite will exhibit higher elastic modulus for the same compressive strength as compared to concretes made with Miami Oolite limestone or lightweight aggregate. Concretes made with Miami Oolite limestone will display higher elastic modulus as compared to concretes made with lightweight aggregate.

Regression analyses using the equation recommended by ACI 318-89 (Equation 5-5) were performed, and the results are presented in Table 5-5. It can be seen that the value of 57,000 recommended by ACI for normal weight concrete is close to the regression analysis on concretes containing Miami Oolite limestone, which yields a value for α of 55,824. But, it is well below the value obtained for concretes containing Georgia granite ($\alpha = 63,351$) and well above the values obtained for concretes made with lightweight aggregate ($\alpha = 43,777$).

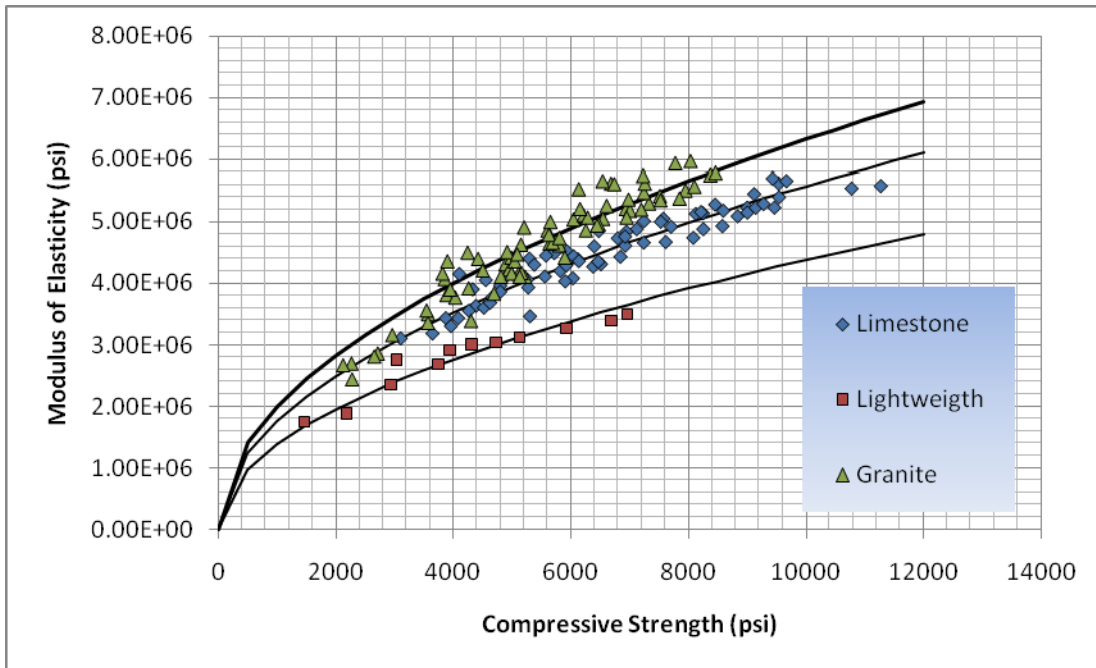


Figure 5-32. Relationship between compressive strength and elastic modulus based on ACI Code.

Table 5-5. Results of Regression Analysis for Prediction of Elastic Modulus Using the Equation Recommended by ACI 318-89

Aggregate Type	Granite	Lightweight	Limestone
Results			
α (Best-fit values)	63351	43777	55824
α (Standard error)	811.3	692.3	292.5
α (95% confidence intervals)	62540 to 64162	42253 to 45301	55240 to 56407
Degrees of Freedom	91	11	69
R^2	0.9067	0.922	0.9088
Absolute sum of squares	7.863E+12	2.693E+11	2.77E+12
Sy.x	293944	156461	200295
Number of points analyzed	92	12	70

Regression analyses using the equation recommended by ACI 318-95 (Equation 5-6) were performed for concretes with unit weight ranging from 90 to 155 lb/ft³. The results of these regression analyses are presented in Table 5-6. Plots of elastic modulus versus $w^{1.5} \cdot \sqrt{f'_c}$ are shown in Figure 5-33. The value obtained for coefficient A of 33.6 is almost the same as the

Table 5-6. Results of Regression Analysis for Prediction of Elastic Modulus Using ACI 318-95 Equation

Best-fit values	With Equation Going Through the Origin	Without Forcing the Equation to go Through the Origin
Slope	33.64 ± 0.1625	31.92 ± 0.7781
Y-intercept when X = 0.0	0.0000	345328 ± 101545
X-intercept when Y = 0.0	0.0000	-16048
1/slope	0.02973	0.03313
95% Confidence Intervals		
Slope	34.19 to 34.83	30.38 to 33.45
Sy.x	264919	256327

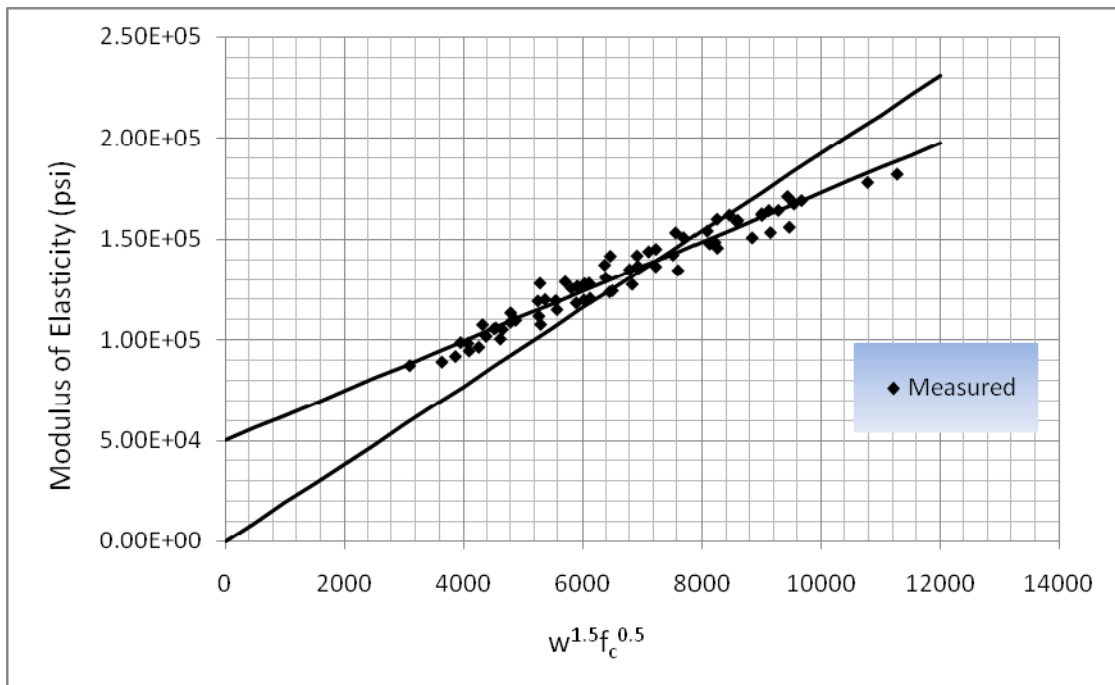


Figure 5-33. Plot of elastic modulus against $w^{1.5} \cdot \sqrt{f'_c}$ for all curing conditions.

value recommended by ACI 318-95, which is equal to 33.0. But by plotting the model on the measured data, it is obvious that a constant must be added for a better approximation of the model. The modified ACI equation then has the form:

$$E = A \cdot w^{1.5} \cdot \sqrt{f'_c} + C \quad (5-7)$$

where E = elastic modulus in psi;

A = a coefficient to be determined through regression analysis;

w = unit weight of concrete in lb/ft³;

f'_c = compressive strength of concrete in psi; and

C = constant determined through regression analysis.

Regression analysis was performed using this modified model, and the results are also presented in Table 5-6. The constant for A is determined to be equal to 31.92. This value is slightly lower than the value recommended by ACI318-95, which is equal to 33.0, but because of the added constant, this model gives a much better approximation of the data. The modified equation is presented below; this equation can be used to predict the elastic modulus of the concretes investigated in this study:

$$E = 31.92 \cdot w^{1.5} \cdot \sqrt{f'_c} + 345,300 \quad (5-8)$$

5.7 Summary of Findings

This chapter presents the testing results from the strength tests in this study. The major findings are given as follows:

- 1) Splitting tensile strengths of the concrete mixtures using granite aggregate were significantly lower than those using Miami Oolite limestone aggregate. This is due probably to the poor bonding condition between hardened cement paste and granite aggregate.
- 2) Compressive strengths of concretes with granite aggregate were comparable to or lower than those of concretes with Miami Oolite limestone aggregate.
- 3) The concrete with granite aggregate had higher elastic modulus than that with Miami Oolite limestone aggregate, while the lightweight aggregate concretes had lower elastic modulus than the normal weight concretes.

- 4) Fly ash concretes develop compressive strength and splitting tensile strength at a slower rate than the slag concretes. Fly ash concrete shows significant strength gain after 28 days, while this was not observed with the slag concrete mixtures.
- 5) The relationship between compressive strength (f'_c) and splitting tensile strength (f_{ct}) is established for the concrete mixtures investigated in this study. The Carino and Lew model, given as follows,

$$f_{ct} = 1.15 \cdot (f'_c)^{0.71}$$

was modified to the following equation:

$$f_{ct} = 2.40 \cdot (f'_c)^{0.62}$$

where f'_c and f_{ct} are in units of psi.

- 6) The relationship between compressive strength and modulus of elasticity was refined in this study using Least Square of Curve-fitting Technique. The ACI 318-89 Equation, which is

$$E_c = 57000 \sqrt{f'_c}$$

was modified to the following equation:

$$E_c = \alpha \sqrt{f'_c}$$

where α is equal to 55,824 for Miami Oolite limestone aggregate; 63,351 for Georgia granite aggregate; and 43,777 for Stalite lightweight aggregate. Values for f'_c and E_c are in units of psi.

- 7) For all three aggregate types investigated in this study, a modified ACI 318-95 prediction equation was developed:

$$E = 31.92 \cdot w^{1.5} \cdot \sqrt{f'_c} + 345,300$$

where w is the density of concrete in pound per cubic foot. Values for f'_c and E are in units of psi.

CHAPTER 6 ANALYSIS OF SHRINKAGE TEST

6.1 Introduction

This chapter presents the results from shrinkage tests on the concrete mixes evaluated in this study. The effects of various factors on shrinkage behavior of concrete were discussed. Regression analysis was performed to establish the relationship between compressive strength at the age when the shrinkage test was started and shrinkage strain at 91 days and to establish the relationship between elastic modulus and shrinkage of concrete. Empirical equations relating compressive strength and elastic modulus to shrinkage of concrete are given. Also, the evaluation was made on ACI 209 model and CEB-FIP model for their effectiveness in shrinkage prediction. At last, ultimate shrinkage strain of the concretes investigated in this study was approximated using an asymptotic equation with three unknown parameters to fit experimental data.

6.2 Results and Analysis of Shrinkage Tests

Table 6-1 presents the measured shrinkage strains at ages up to 91 days for the 18 concrete mixes evaluated in this study. One group of concrete specimens was moist-cured for 7 days and then air-dried in the laboratory for the rest of the time; another group of specimens were moist-cured for 14 days and then air-dried for the remainder of the time.

6.2.1 Effects of Curing Conditions on Shrinkage Behavior of Concrete

Figure 6-1 shows the comparison of shrinkage strains at 91 days for the 7-day and 14-day curing conditions for the concrete mixes containing Miami Oolite limestone as aggregate. It can be seen that the shrinkage strains for the concrete after moist curing for 7 days are significantly higher than those after moist curing for 14 days. For the mixes containing fly ash, the percent

Table 6-1. Shrinkage Strains of the Concrete Mixtures Evaluated at Various Curing Ages

Mix Number	Moist Curing Time	Age of Testing						Predicted Ultimate Shrinkage Strain
		3 days	7 days	14 days	28 days	56 days	91 days	
1F (1y)	7-day	2.00E-05	4.40E-05	7.50E-05	1.18E-04	1.63E-04	2.02E-04	2.66E-04
	14-day	1.40E-05	3.50E-05	6.10E-05	1.00E-04	1.36E-04	1.67E-04	2.27E-04
2F (1y)	7-day	5.10E-05	9.70E-05	1.54E-04	2.10E-04	2.61E-04	2.86E-04	3.39E-04
	14-day	3.10E-05	6.90E-05	1.12E-04	1.73E-04	2.33E-04	2.58E-04	3.20E-04
3F (1y)	7-day	4.00E-05	7.30E-05	1.24E-04	1.77E-04	2.21E-04	2.48E-04	3.03E-04
	14-day	2.40E-05	5.00E-05	8.70E-05	1.37E-04	1.84E-04	2.16E-04	2.85E-04
4F (1y)	7-day	3.70E-05	7.10E-05	1.18E-04	1.76E-04	2.33E-04	2.67E-04	3.64E-04
	14-day	3.10E-05	5.30E-05	9.20E-05	1.42E-04	1.97E-04	2.31E-04	3.44E-04
5S (3m)	7-day	4.40E-05	8.80E-05	1.30E-04	1.70E-04	2.01E-04	2.16E-04	2.46E-04
	14-day	4.30E-05	7.40E-05	1.10E-04	1.49E-04	1.78E-04	1.93E-04	2.29E-04
5S (1y)*	7-day	4.78E-05	8.86E-05	1.30E-04	1.70E-04	2.01E-04	2.16E-04	2.55E-04
	14-day	4.25E-05	7.46E-05	1.09E-04	1.46E-04	1.77E-04	1.94E-04	2.29E-04
6S (3m)	7-day	4.20E-05	8.40E-05	1.23E-04	1.56E-04	1.83E-04	1.95E-04	2.16E-04
	14-day	3.30E-05	7.10E-05	1.12E-04	1.41E-04	1.64E-04	1.76E-04	1.93E-04
6S (1y)*	7-day	4.96E-05	8.75E-05	1.21E-04	1.55E-04	1.98E-04	2.41E-04	2.05E-04
	14-day	4.44E-05	7.33E-05	1.08E-05	1.51E-04	1.75E-04	1.98E-04	1.99E-04
7S (3m)	7-day	3.90E-05	8.10E-05	1.26E-04	1.70E-04	2.02E-04	2.23E-04	2.55E-04
	14-day	3.80E-05	7.30E-05	1.11E-04	1.48E-04	1.84E-04	2.04E-04	2.40E-04
7S (1y)*	7-day	4.46E-05	7.75E-05	1.11E-04	1.53E-04	2.01E-04	2.54E-04	2.65E-04
	14-day	4.93E-05	6.78E-05	7.45E-05	9.28E-05	1.21E-04	2.03E-04	2.61E-04
8S (1y)*	7-day	5.08E-05	9.82E-05	1.54E-04	2.18E-04	2.76E-04	3.08E-04	5.52E-04
	14-day	3.13E-05	6.60E-05	1.05E-04	1.43E-04	1.74E-04	1.90E-04	4.58E-04
8S (3m)	7-day	7.30E-05	1.23E-04	1.61E-04	1.94E-04	2.28E-04	2.50E-04	2.43E-04
	14-day	5.00E-05	9.80E-05	1.36E-04	1.69E-04	2.02E-04	2.30E-04	2.20E-04
9LF (1y)	7-day	4.90E-05	9.60E-05	1.34E-04	2.25E-04	2.87E-04	3.22E-04	3.95E-04
	14-day	4.60E-05	8.30E-05	1.34E-04	1.84E-04	2.41E-04	2.76E-04	3.49E-04
10LS (1y)	7-day	6.70E-05	1.30E-04	1.98E-04	2.60E-04	3.20E-04	3.58E-04	4.22E-04
	14-day	3.80E-05	9.00E-05	1.52E-04	2.09E-04	2.80E-04	3.17E-04	3.96E-04
1GF (1y)*	7-day	1.18E-04	6.76E-05	1.52E-05	1.22E-04	1.69E-04	2.30E-04	2.23E-04
	14-day	1.99E-04	6.78E-05	9.24E-05	1.38E-04	1.77E-04	2.32E-04	1.98E-04
1GF (3m)*	7-day	9.90E-05	1.50E-04	3.50E-05	7.67E-05	1.47E-04	1.65E-04	2.23E-04
	14-day	2.16E-05	4.42E-05	6.83E-05	1.00E-04	1.32E-04	1.51E-04	1.98E-04
2GF (1y)	7-day	---	---	---	---	---	---	---
	14-day	3.20E-05	6.10E-05	1.09E-04	1.61E-04	2.04E-04	2.31E-04	2.83E-04
2GF (3m)	7-day	3.34E-05	5.00E-05	8.34E-05	1.33E-04	2.08E-04	2.32E-04	3.18E-04
	14-day	2.78E-05	2.56E-05	7.23E-05	1.11E-04	1.91E-04	2.20E-04	3.08E-04
3GF (1y)	7-day	---	---	---	---	---	---	---
	14-day	2.90E-05	5.40E-05	8.40E-05	1.23E-04	1.57E-04	1.82E-04	2.62E-04

Table 6-1. Continued . . .

Mix Number	Moist Curing Time	Age of Testing						Predicted Ultimate Shrinkage Strain
		3 days	7 days	14 days	28 days	56 days	91 days	
3GF (3m)*	7-day	2.08E-05	4.33E-05	7.34E-05	1.13E-04	1.55E-04	1.81E-04	2.49E-04
	14-day	2.03E-05	4.04E-05	6.76E-05	1.05E-04	1.48E-04	1.77E-04	2.70E-04
4GF (1y)*	7-day	4.11E-05	9.32E-05	1.19E-04	1.61E-04	1.96E-04	2.39E-04	2.89E-04
	14-day	6.79E-05	1.07E-04	2.14E-04	1.92E-04	3.03E-04	2.77E-04	3.38E-04
4GF (3m)	7-day	5.46E-05	9.02E-05	1.25E-04	1.60E-04	2.21E-04	2.35E-04	2.89E-04
	14-day	9.25 E-05	1.34E-04	2.14E-04	2.79E-04	3.41E-04	2.53E-04	3.38E-04
5GS (3m)*	7-day	7.90E-05	9.33E-05	1.18E-04	1.49E-04	1.88E-04	2.25E-04	2.35E-04
	14-day	5.68E-05	7.56E-05	1.05E-04	1.40E-04	1.86E-04	2.20E-04	2.35E-04
6GS (1y)*	7-day	8.91E-06	5.53E-05	9.36E-05	1.29E-04	1.41E-04	2.35E-04	1.23E-04
	14-day	3.12E-05	5.77E-05	1.04E-04	1.38E-04	2.04E-04	2.64E-04	1.50E-04
6GS (3m)	7-day	2.45E-05	3.45E-05	5.56E-05	8.12E-05	1.76E-04	1.84E-04	1.23E-04
	14-day	6.33E-05	9.34E-05	1.13E-04	1.29E-04	1.40E-04	1.60E-04	1.50E-04
7GS (1y)	7-day	---	---	---	---	---	---	---
	14-day	4.30E-05	7.40E-05	1.00E-04	1.31E-04	1.63E-04	1.81E-04	2.19E-04
7GS (3m)*	7-day	5.63E-05	8.30E-05	1.11E-04	1.43E-04	1.75E-04	1.95E-04	2.48E-04
	14-day	4.78E-05	7.07E-05	9.56E-05	1.26E-04	1.58E-04	1.80E-04	2.49E-04
8GS (1y)*	7-day	7.54E-05	7.03E-05	1.21E-05	1.43E-04	1.91E-04	2.30E-04	2.34E-04
	14-day	1.51E-05	3.14E-05	6.40E-05	8.29E-05	1.27E-04	1.53E-04	2.10E-04
8GS (3m)*	7-day	5.33E-05	8.82E-05	1.24E-04	1.34E-04	1.88E-04	2.03E-04	2.34E-04
	14-day	2.39E-05	4.57E-05	7.26E-05	1.06E-04	1.40E-04	1.60E-04	7.54E-05

* Data have been modified to correct for measurement errors.

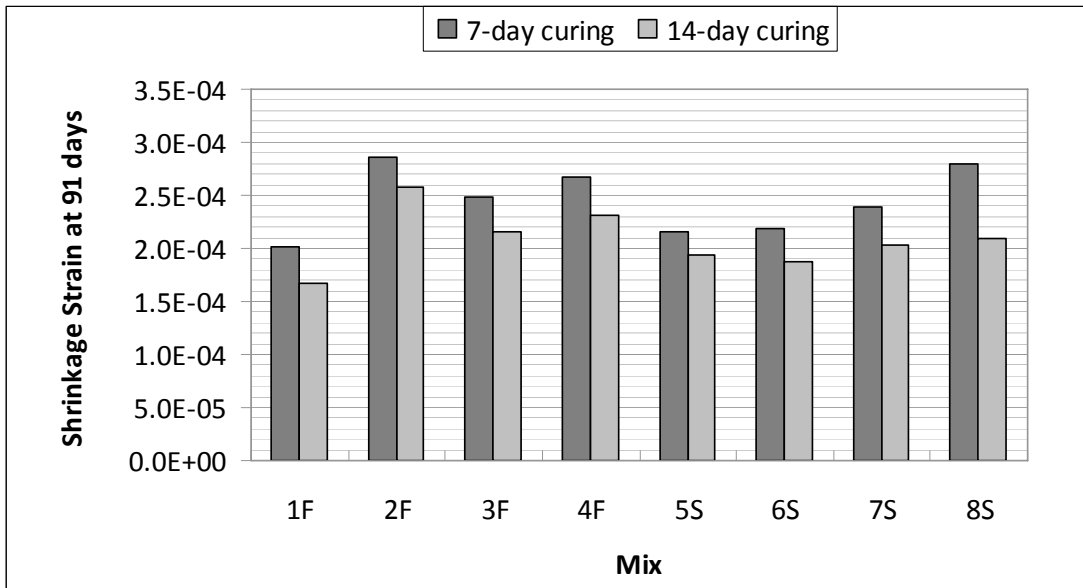


Figure 6-1. Effects of curing condition on shrinkage strain of concrete mixtures containing Miami Oolite limestone aggregate at 91 days.

difference was 19.0%, 10.3%, 13.8%, and 14.5% for Mixes 1F, 2F, 3F, and 4F, respectively. For the mixes containing slag, the percent difference was 11.2%, 15.3%, 15.8%, and 28.2% for Mixes 5S, 6S, 7S and 8S, respectively.

Figure 6-2 shows the comparison of shrinkage strains at 91 days for the 7-day and 14-day curing conditions for the concrete mixes containing Georgia granite as aggregate. The differences in shrinkage strains for these two curing conditions were generally small and did not show a consistent trend.

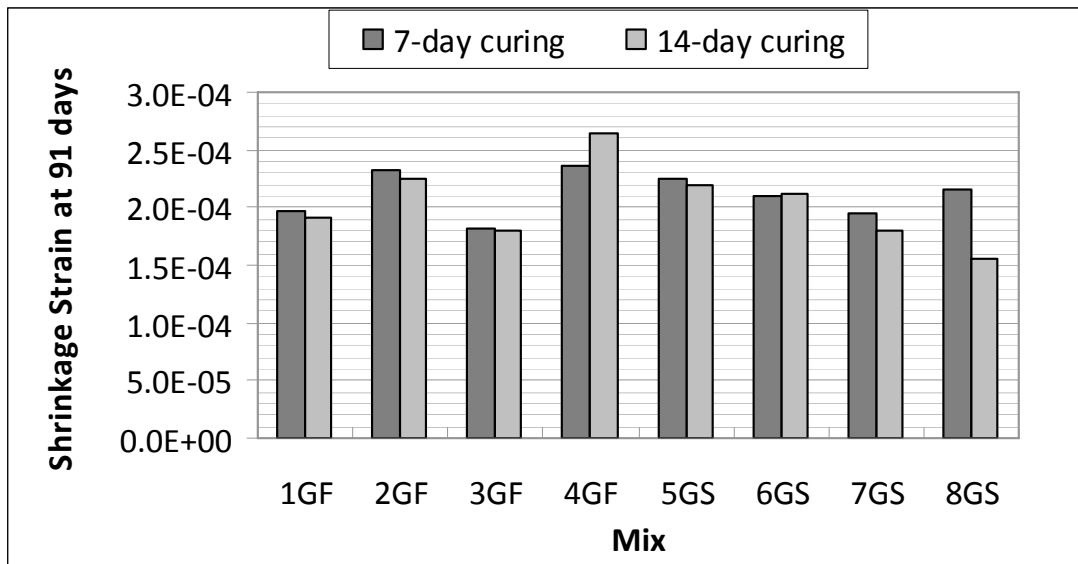


Figure 6-2. Effects of curing condition on shrinkage strain of concrete mixtures containing Georgia granite aggregate at 91 days.

Figure 6-3 shows the comparison of shrinkage strains at 91 days for the 7-day and 14-day curing conditions for the concrete mixes containing Stalite lightweight aggregate. Shrinkage strains for the 7-day moist curing condition were significantly higher than those for the 14-day moist curing condition. The percent difference was 15.4% and 12.1% for Mixes 9LF and 10LS, respectively. Overall, the mixes containing lightweight aggregate show the highest shrinkage

strain at 91 days as compared with the mixes containing Miami Oolite limestone or Georgia granite as aggregate.

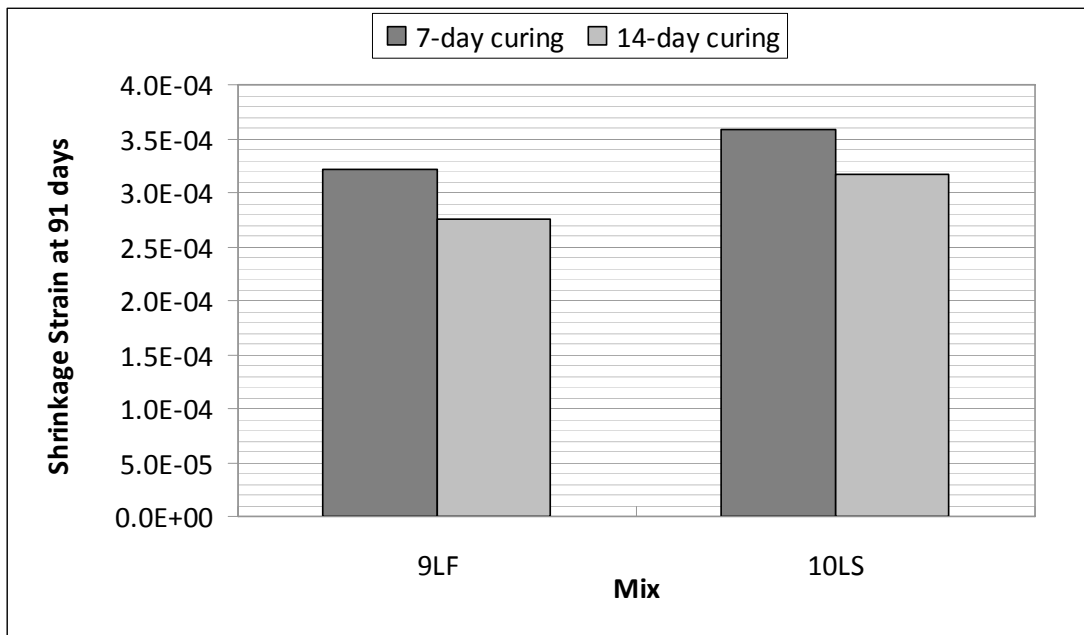


Figure 6-3. Effects of curing condition on shrinkage strain of concrete mixtures containing lightweight aggregate at 91 days.

6.2.2 Effects of Mineral Additives on Shrinkage Behavior

Further investigation of Figures 6-1 and 6-2 shows an interesting observation on the effects of mineral additives on shrinkage behavior of concrete: by comparing mixes with the same water-to-cementitious materials ratio, one can see that mixes that contain fly ash generally experience higher shrinkage strains at 91 days as compared with the concrete mixtures containing slag. For example, Mixes 2F and 5S both have a w/c materials ratio of 0.33. For the 7-day curing condition, Mix 2F exhibits a shrinkage strain of 2.86×10^{-4} at 91 days, while Mix 5S exhibits a shrinkage strain of 2.16×10^{-4} at 91 days; a difference of 27.9%. For the 14-day curing condition, this percent difference is 28.8% between 2.58×10^{-4} for Mix 2F and 1.93×10^{-4} for Mix 5S. Similar trends can also be observed in the comparison between Mixes 3F and 7S,

and in the comparison between Mixes 2GF and 5GS. However, this trend is not observed in the comparison between Mixes 3GF and 7GS. Mix 7GF (which contains fly ash) shows slightly lower shrinkage strains at 91 days than Mix 7GS (which contains slag).

6.2.3 Effects of Water Content on Shrinkage Behaviors

Figure 6-4 shows a plot of the shrinkage strain at 91 days for each mix against its corresponding water content in pounds per cubic yard (lb/yd³ or lb/cy). The regression line which is drawn through these plotted points shows that shrinkage strain generally increases as the water content increases. However, the plot also shows a great scattering of the data around the regression line. This could possibly mean that the shrinkage strain is not entirely dependent on the water content of concrete, but rather a combination of other factors.

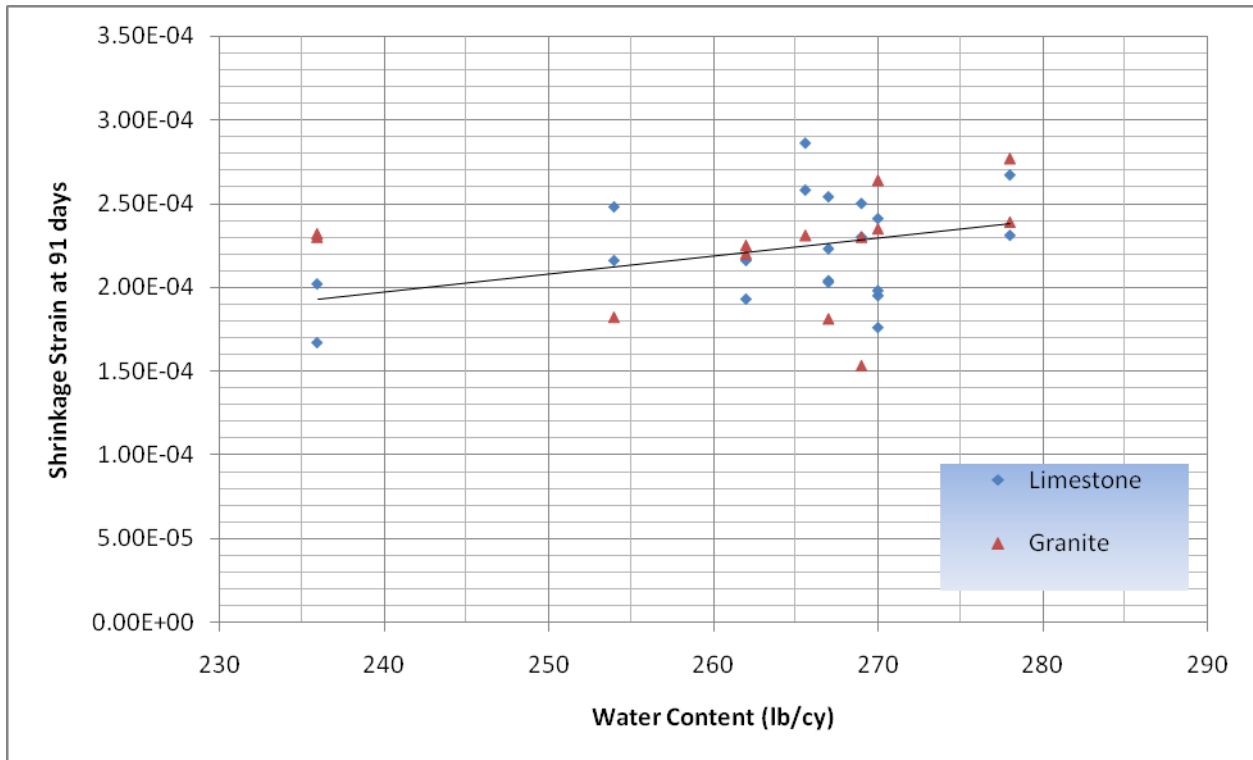


Figure 6-4. Effects of water content on shrinkage strain at 91 days.

6.2.4 Effects of Aggregate Types on Shrinkage Behavior

Figure 6-5 shows the comparison of the shrinkage strain at 91 days for each mix using Miami Oolite limestone with its corresponding identical mix using Georgia granite. The results were mixed. Half of the mixes containing Georgia granite shrank less, while the other half shrank more than the corresponding identical mixes containing Miami Oolite. Thus, from this set of data alone, the findings are inconclusive.

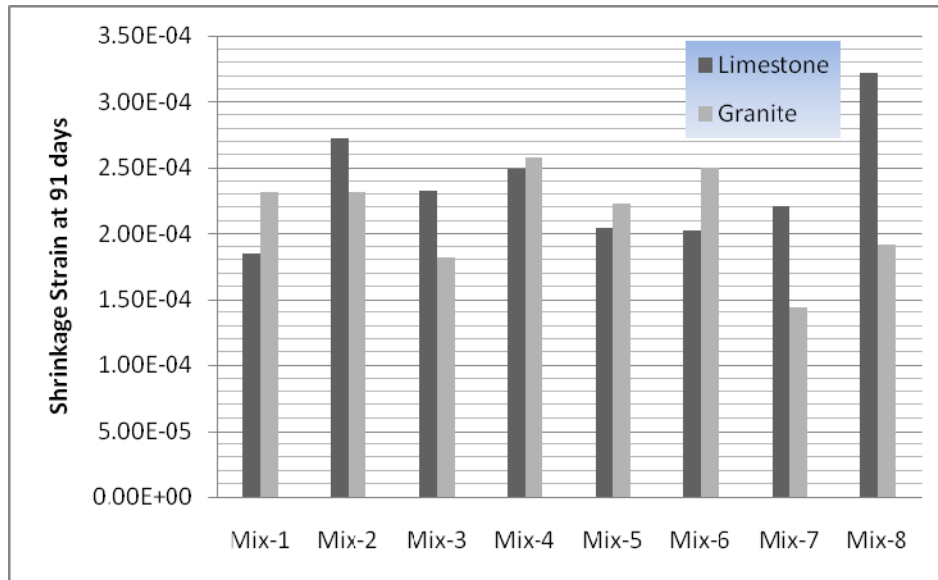


Figure 6-5. Effects of coarse aggregate type on shrinkage behavior of concrete.

6.2.5 Relationship Between Compressive Strength and Shrinkage Strain

Over the past decades, the study on shrinkage behavior of concrete has been carried out extensively. The effects of various factors, such as water-to-cement ratio, aggregate type, aggregate content, mineral additives, and cement content on shrinkage behavior have been considered. However, since concrete is a complicated composite material, the effects of various components and their proportions on shrinkage behavior are inter-twisted together. Also, because of the massive introduction of chemical admixtures to concrete, such as air entraining

and water reducing admixtures, the shrinkage behavior of concrete becomes more complex. Thus, shrinkage behavior of concrete cannot be reasonably estimated based on a simple addition of every individual factor's function. Therefore, it is desirable to relate the shrinkage behavior of concrete to one or more fundamental properties of concrete, for example, compressive strength, tensile strength, or elastic modulus at a particular age. In doing so, it assumes that the fundamental properties of concrete are closely related to one another, i.e., one fundamental property can be predicted from another. In doing so, a complicated fundamental property can be estimated by a simple fundamental property without using a complicated and time-consuming test.

In trying to find out the relationship between compressive strength and shrinkage behavior of concrete, compressive strength at the age when the shrinkage test was started was plotted against shrinkage strain at 91 days in Figure 6-6.

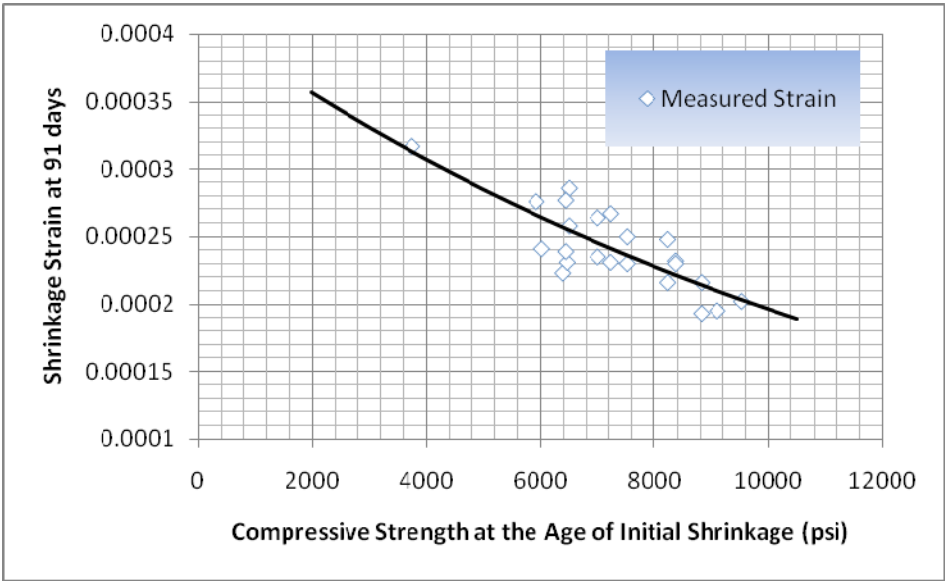


Figure 6-6. Relationship between compressive strength and shrinkage strain at 91 days.

As shown in Figure 6-6, it appears that there exists a very pleasing relationship between the shrinkage strains at 91 days and compressive strength regardless of which type of coarse aggregate was used for the concrete. Then, a regression analysis was carried out using an exponential function with two unknown parameters, given as follows. The regression analysis results are provided in Table 6-2.

$$\varepsilon_{sh} = \alpha \cdot e^{-\beta \cdot f_c} \quad (6-1)$$

In this formula, f_c is the compressive strength of concrete at the age of initial shrinkage test. As can be seen in Table 6-2, the best fit value of α is 4.139×10^{-4} and 7.454×10^{-5} for β , and R^2 has a value of 0.6469. This regression line has been plotted on Figure 6-6 and it seems to be a fairly good estimation considering all the other components in concrete such as admixtures, aggregate type, as well as two different curing conditions.

Table 6-2. Results of Regression Analysis on Relationship of Compressive Strength to Shrinkage Strain

Regression Results	Best-fit Value	Standard Error (SE)	95% Confidence Interval	R^2	Absolute Sum of Square Root due to Error (SSE)
α	4.139E-04	5.973E-05	3.54E-04 ~ 4.74 E-04	0.6469	7.067E-09
β	7.454E-05	1.194E-05	5.44E-05 ~ 9.47E-05		

It would be very useful to combine data from other data banks to develop a better and more representative model for estimation of shrinkage strains, especially because, as mentioned before, the shrinkage strain tests can be very time consuming.

6.2.6 Relationship Between Elastic Modulus and Shrinkage Strain

Since a close relationship has been found between compressive strength and shrinkage of concrete, and since there is a direct relationship between compressive strength and elastic modulus, elastic modulus and shrinkage should be related to each other as well.

As shown in Figure 6-7, shrinkage strains at 91 days for all the concretes investigated in this study, including normal-weight aggregate concrete and lightweight aggregate concrete, were plotted against elastic modulus at the age of the concrete when the shrinkage test was started. There is no surprise that a similar relationship to compressive strength and shrinkage can be found between elastic modulus and shrinkage. The regression analysis was performed using exponential function with two unknown parameters, given as follows, and the analyzed results are presented in Table 6-3.

$$\varepsilon_{sh} = \alpha \cdot e^{-\beta \cdot E_c} \quad (6-2)$$

In this equation, E_c is the elastic modulus of concrete at the age of shrinkage test starts.

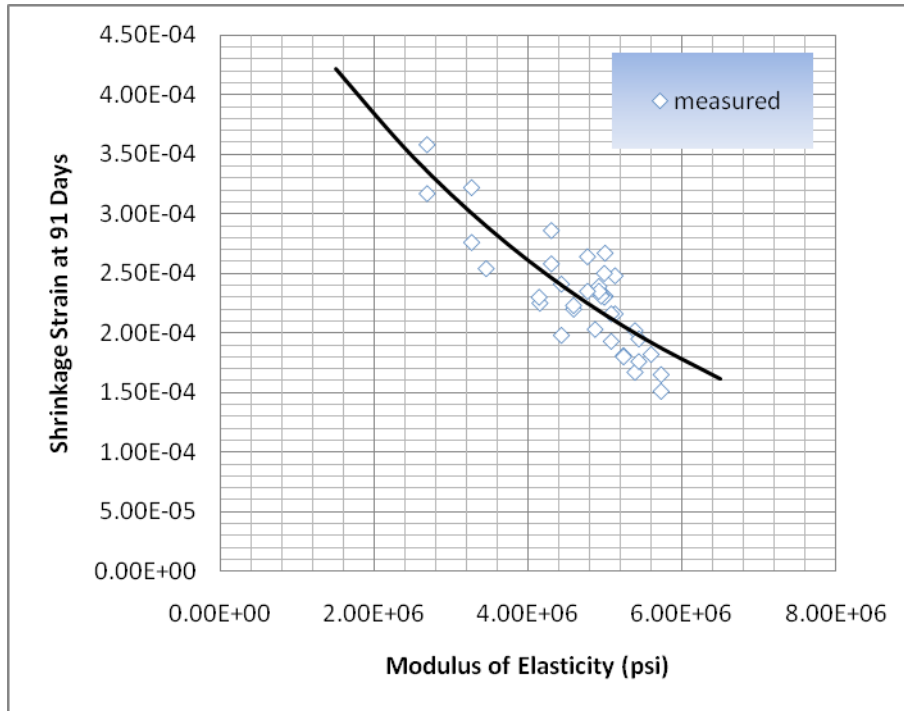


Figure 6-7. Relationship between shrinkage strain at 91 days and modulus of elasticity.

Table 6-3. Results of Regression Analysis on Relationship of Elastic Modulus to Shrinkage Strain

Regression Results	Best-fit Value	Standard Error (SE)	95% Confidence Interval	R^2	Absolute Sum of Square Root due to Error (SSE)
α	5.616E-04	1.024E-04	4.592E-04 ~ 6.460E-04	0.7065	2.136E-08
β	1.916E-07	4.0102E-08	1.515E-07 ~ 2.317E-07		

6.3 Evaluation on Shrinkage Prediction Models

In this study, the ACI 209 and CEB-FIP models were evaluated on their effectiveness and accuracy in prediction of shrinkage behaviors of typical concretes used in Florida.

6.3.1 ACI 209 Model

The concrete shrinkage prediction model recommended by ACI 209 (1992) is given as follows:

$$(\varepsilon_{sh})_t = \frac{t}{35+t}(\varepsilon_{sh})_u \quad (6-3)$$

where $(\varepsilon_{sh})_t$ = time dependent shrinkage strain;

$(\varepsilon_{sh})_u$ = ultimate shrinkage strain; and

t = time variable in days.

If there is no available shrinkage data from the specific concrete mixture, the ultimate shrinkage strain, $(\varepsilon_{sh})_u$, can be assumed to be the following:

$$(\varepsilon_{sh})_u = 780 \times 10^{-6} \times \gamma_{sh} \quad (6-4)$$

where γ_{sh} represents the product of all the applicable correction factors for the testing conditions other than the standard condition. Under standard testing condition, $\gamma_{sh} = \text{one (1)}$.

The value for γ_{sh} is obtained by multiplying the ultimate shrinkage strain under the standard condition by the appropriate correction factors, such as a correction factor for the effect

of initial moist curing; a correction factor for the effect of ambient relative humidity; a correction factor for the effects of specimen size; a correction factor for concrete composition; and so on.

In this study, γ_{sh} is calculated as follows:

$$\gamma_{sh} = \gamma_{la} \cdot \gamma_{rh} \cdot \gamma_s \cdot \gamma_a \cdot \gamma_{at} \cdot \gamma_p \quad (6-5)$$

The detailed correction factors involved in this study are provided in Table 6-4.

Table 6-4. Correction Factors for the ACI 209 Model on Shrinkage Prediction

Mix	γ_{la}		γ_{λ}	γ_s	γ_a	γ_h	γ_{ψ}	γ_{sh}	
	7-day moist	14-day moist						7-day moist	14-day moist
1F	0.994	0.916	0.70	1.21	0.96	0.97	0.97	0.76	0.7
2F	0.994	0.916	0.70	1.13	1	0.97	0.97	0.74	0.68
3F	0.994	0.916	0.70	0.96	0.97	0.97	0.98	0.62	0.57
4F	0.994	0.916	0.70	1.01	0.96	0.97	0.97	0.63	0.58
5S	0.994	0.916	0.70	1.22	1	0.97	0.98	0.81	0.74
6S	0.994	0.916	0.70	1.03	0.98	0.97	0.98	0.67	0.62
7S	0.994	0.916	0.70	1.08	1	0.97	0.98	0.71	0.66
8S	0.994	0.916	0.70	1.06	0.99	0.97	0.98	0.69	0.64
9LF	0.994	0.916	0.70	1.02	0.98	0.97	0.99	0.67	0.62
10LS	0.994	0.916	0.70	1.02	0.99	0.97	0.98	0.67	0.62
1GF	0.994	0.916	0.70	0.95	0.97	0.97	0.96	0.6	0.55
2GF	0.994	0.916	0.70	1.12	0.99	0.97	0.96	0.72	0.66
3GF	0.994	0.916	0.70	1.11	0.97	0.97	0.97	0.7	0.65
4GF	0.994	0.916	0.70	1.12	0.97	0.97	0.97	0.71	0.66
5GS	0.994	0.916	0.70	1.17	1.01	0.97	0.97	0.77	0.71
6GS	0.994	0.916	0.70	1.03	0.97	0.97	0.97	0.65	0.6
7GS	0.994	0.916	0.70	1.05	0.98	0.97	0.97	0.67	0.62
8GS	0.994	0.916	0.70	1.15	0.99	0.97	0.97	0.75	0.69

6.3.2 CEB-FIP Model

In the CEB-FIP model, the effects of cement type, ambient relative humidity, compressive strength of concrete, and size effect of specimen on shrinkage strain of concrete are taken into consideration. The total shrinkage strain may be estimated with the following equation:

$$\varepsilon_{cs}(t, t_s) = \varepsilon_{cs0} \cdot \beta_s(t - t_s) \quad (6-6)$$

where $\varepsilon_{cs}(t, t_s)$ = time dependent total shrinkage strain;

ε_{cs0} = notational shrinkage coefficient; and

$\beta_s(t - t_s)$ = coefficient to describe the development of shrinkage with time.

The value of ε_{cs0} can be estimated by the following equation:

$$\varepsilon_{cs0} = \left(160 + 10\beta_{sc} \left(9 - \left(\frac{f_{cm}}{f_{cmo}} \right) \right) \right) \times 10^{-6} \times \beta_{RH} \quad (6-7)$$

where β_{sc} , = a coefficient depending on the type of cement (In this study, it is equal to 5 for normal or rapid hardening cements);

f_{cm} = mean compressive strength of concrete at the age of initial shrinkage tests; and

f_{cmo} = a constant equal to 10 MPa.

The value of β_{RH} can be computed as follows:

$$\beta_{RH} = -1.55 \left(1 - \left(\frac{RH}{RH_0} \right)^3 \right) \text{ for } 40\% \leq RH < 99\% \quad (6-8)$$

with RH equal to 75% in this study and RH_0 equal to 100%, then,

$$\varepsilon_{cs0} = \left(160 + 10\beta_{sc} \left(9 - \left(\frac{f_{cm}}{f_{cmo}} \right) \right) \right) \times 10^{-6} \times 0.8959 \quad (6-9)$$

The value for $\beta_s(t - t_s)$ can be estimated by the following equation:

$$\beta_s(t - t_s) = \left(\frac{\frac{(t - t_s)}{t_1}}{350 \cdot \left(\frac{h}{h_0} \right)^2 + \frac{t - t_s}{t_1}} \right)^{0.5} \quad (6-10)$$

where $h = \frac{2A_c}{u}$ = notational size of member (in mm);

A_c = cross-sectional area (mm²);

u = perimeter (mm) of the member circular cross section ($2\pi r$) in contact with the atmosphere;

H = 1.5 for 6" × 12" cylinder;

h_0 = 100 mm; and

t_1 = one (1) day.

Therefore, the above equation can be simplified as follows:

$$\beta_s(t) = \left(\frac{t}{203.23 + t} \right)^{0.5} \quad (6-11)$$

The shrinkage strains at 91 days for all the concrete mixtures investigated in this study were compared with the calculated results using the ACI 209 and CEB-FIP models in Figure 6-8. As shown in Figure 6-8, the CEB-FIP model gives better prediction in comparison with the ACI 209 model.

6.4 Prediction of Ultimate Shrinkage Strain

Shrinkage of concrete lasts for a long time with decreasing shrinkage rate. Generally, it is assumed that concrete will shrink with time to a limiting value, called ultimate shrinkage strain, which is a very important parameter in concrete structural design. In this study, an asymptotic equation, given as follows, was used to fit the experimental data.

$$(\varepsilon_{sh})_t = \left(\frac{t}{\gamma + t} \right)^\alpha \cdot \beta \quad (6-12)$$

As can be seen from the above equation, shrinkage strain will approach its limiting value β as time goes to infinite value, thus β is the ultimate shrinkage strain.

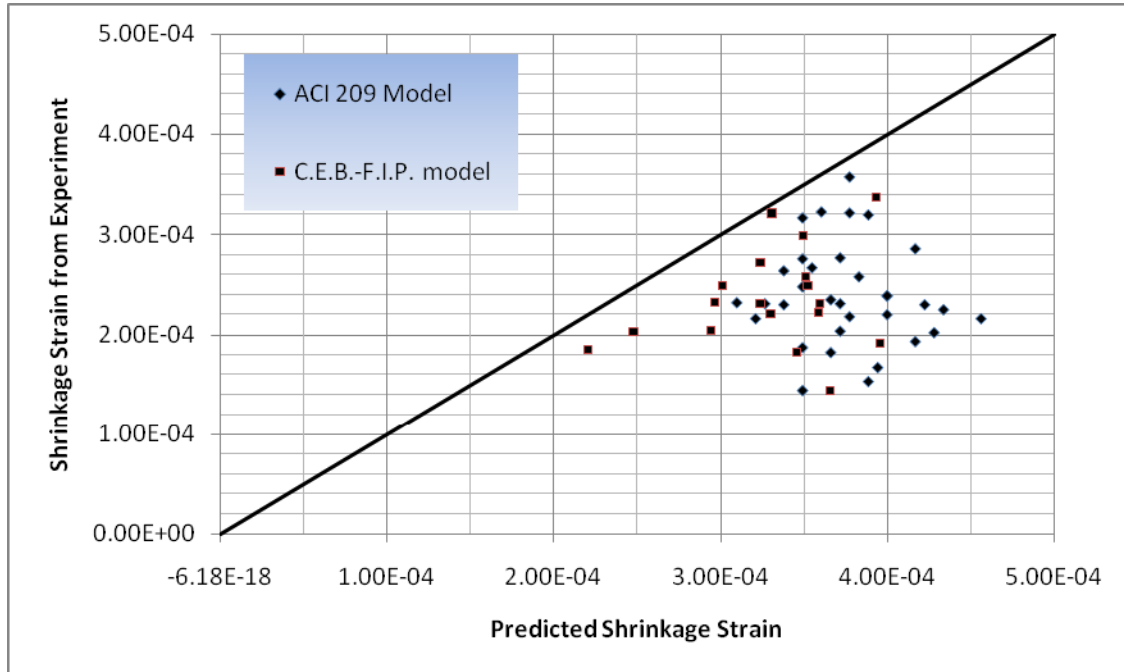


Figure 6-8. Comparison between the shrinkage strain at 91 days and the shrinkage strain calculated by the ACI 209 model and the CEB-FIP model.

Table 6-5 shows the results of the regression analysis for all the mixes in this study. The replicates of Mixes 8S and 8GS were significantly different in shrinkage strains, thus they are presented separately instead of combined. The ultimate shrinkage is the limiting value β , which is also presented in Table 6-5. Most mixes have a value close to 1 for α and the average of γ is 29.8. The average for α is 0.91. The maximum average ultimate shrinkage strain is in the order of 3.34×10^{-4} for normal-weight concrete and 4.50×10^{-4} for light-weight aggregate concrete. The comparison of the predicted ultimate shrinkage strains of the concrete made with Miami Oolite limestone and those made with Georgia granite is shown in Figure 6-9. It can be seen that the ultimate strains for the limestone concrete are consistently higher than those for the granite concrete.

Table 6-5. Results of Regression Analysis for Prediction of Shrinkage Strain

Mix	α	SE	β	SE	γ	SE	R^2	SSE
1F	0.983	0.024	2.66E-04	2.70E-06	31.18	1.804	0.9997	1.20×10^{-6}
	1.122	0.049	2.27E-04	4.31E-06	31.10	3.117	0.9992	1.67×10^{-6}
2F	1.027	0.021	3.39E-04	1.51E-06	16.48	0.649	0.9998	1.27×10^{-6}
	1.137	0.042	3.21E-04	3.35E-06	19.13	1.515	0.9994	1.23×10^{-6}
3F	1.011	0.022	3.03E-04	1.69E-06	20.05	0.869	0.9998	1.19×10^{-6}
	0.920	0.031	2.85E-04	3.89E-06	31.74	2.545	0.9994	1.81×10^{-6}
4F	0.867	0.013	3.44E-04	2.74E-06	27.84	1.530	0.9999	1.10×10^{-7}
	0.855	0.032	3.24E-04	8.93E-06	32.44	3.910	0.9990	2.45×10^{-6}
5S	0.871	0.634	2.55E-04	2.99E-05	16.81	23.24	0.9652	1.64×10^{-5}
	0.812	0.026	2.29E-04	1.86E-05	20.88	1.427	0.9994	1.50×10^{-6}
6S	1.243	0.709	2.05E-04	1.13E-05	6.59	5.74	0.9890	7.93×10^{-6}
	1.282	0.484	1.99E-04	7.94E-06	7.53	4.48	0.9949	5.18×10^{-6}
7S	0.849	0.143	2.65E-04	9.83E-06	21.91	7.31	0.9964	5.03×10^{-6}
	0.732	0.315	2.61E-04	2.62E-05	24.27	22.64	0.9764	1.33×10^{-5}
8S (3m)	1.325	0.087	2.43E-04	1.82E-06	7.822	0.789	0.9989	2.42×10^{-6}
	1.232	0.089	2.20E-04	2.52E-06	11.61	1.406	0.9984	2.56×10^{-6}
8S (1y)	0.960	0.473	5.52E-04	9.28E-05	42.90	45.04	0.9842	2.06×10^{-5}
	0.981	0.234	4.58E-04	1.41E-05	26.27	10.30	0.9994	4.22×10^{-6}
9LF	0.836	0.030	3.95E-04	3.09E-06	20.53	1.220	0.9996	2.11×10^{-6}
	1.018	0.030	3.49E-04	4.89E-06	31.49	2.756	0.9992	2.51×10^{-6}
10LS	1.055	0.026	4.22E-04	3.30E-06	21.74	1.349	0.9983	4.42×10^{-6}
	0.851	0.066	3.96E-04	7.12E-06	21.04	2.796	0.9995	2.05×10^{-6}
1GF	0.857	0.920	2.23E-04	1.17E-04	38.74	108.23	0.8850	2.16×10^{-5}
	0.628	0.185	1.98E-04	2.69E-05	51.35	44.50	0.9919	6.11×10^{-6}
2GF	1.109	0.4871	3.18E-04	6.94E-05	27.16	27.44	0.9900	7.21×10^{-6}
	0.903	0.3142	3.08E-04	5.33E-05	36.26	31.81	0.9895	7.85×10^{-6}
3GF	0.981	0.266	2.49E-04	4.05E-05	34.64	24.09	0.9966	3.38×10^{-6}
	0.961	0.525	2.70E-04	9.88E-05	46.83	57.38	0.9600	1.13×10^{-5}
4GF	0.625	0.260	2.89E-04	3.44E-05	38.24	38.63	0.9624	1.53×10^{-5}
	0.509	0.544	3.38E-04	7.87E-05	36.81	95.71	0.8587	3.57×10^{-5}
5GS	0.320	0.060	2.35E-04	2.35E-05	90.95	75.46	0.9904	6.59×10^{-6}
	0.703	0.122	2.35E-04	1.12E-05	30.96	12.03	0.9969	4.10×10^{-6}
6GS	1.169	1.176	1.23E-04	3.20E-05	12.31	23.45	0.9696	5.50×10^{-6}
	1.348	2.504	1.50E-04	1.38E-05	3.46	8.52	0.9886	4.53×10^{-6}
7GS	0.496	0.245	2.48E-04	6.93E-05	56.34	99.71	0.9869	8.04×10^{-6}
	0.487	0.064	2.49E-04	2.88E-05	85.98	49.25	0.9964	3.64×10^{-6}
8GS (1y)	0.740	0.415	2.34E-04	1.66E-05	17.48	19.17	0.9801	1.10×10^{-6}
	0.868	0.500	2.10E-04	2.82E-05	33.61	41.36	0.9833	9.77×10^{-6}
8GS (3m)	0.632	0.197	7.54E-05	1.23E-05	30.99	28.94	0.9953	1.22×10^{-6}

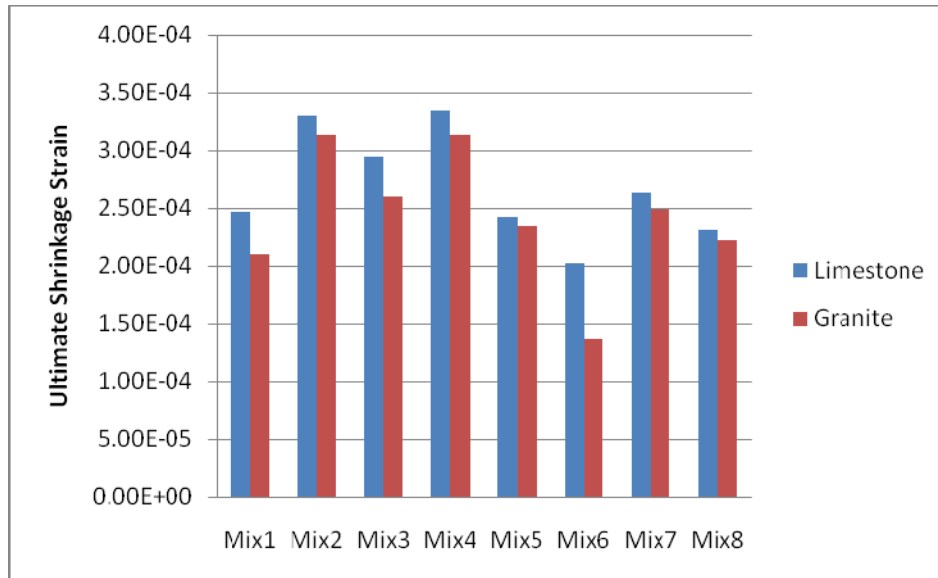


Figure 6-9. Predicted ultimate shrinkage strains of limestone and granite concretes.

6.5 Summary of Findings

This chapter has presented the results of shrinkage tests on the concrete mixtures investigated in this study. A summary of the major findings is provided as follows:

- 1) Fly ash concrete mixtures had slightly higher shrinkage strain at 91 days than slag concretes. This is due probably to the slow hydration rate of fly ash in comparison with that of slag. As a result of the slower rate of hydration, there was more free water evaporating from the interior concrete outward causing the concrete to shrink more. Thus, it is recommended that using a longer wet curing time would be helpful to reduce shrinkage in fly ash concrete.
- 2) Water content has a significant effect on drying shrinkage strain of concrete. The higher the water content, the more the concrete tends to shrink. However, no clear trend can be seen on the effects of the water-to-cementitious materials ratio on shrinkage of concrete.
- 3) The predicted ultimate shrinkage strain of concrete made with Georgia granite is slightly lower than that of the corresponding concrete made with Miami Oolite limestone aggregate. Lightweight aggregate concrete shrinks more than normal weight aggregate concrete. This might be explained by their difference in elastic modulus. The concrete with a higher elastic modulus would have a stronger resistance to the movement caused by shrinkage of the cement paste.

- 4) For the concretes tested, there appeared to be a relationship between the compressive strength (f'_c) at the age when shrinkage test was started and the shrinkage strain (ϵ_{sh}) at 91 days as follows:

$$\epsilon_{sh} = .0.000414 \cdot e^{-0.0000745 \cdot f'_c}$$

where f'_c is in units of psi.

- 5) For the concretes tested, there appeared to be a relationship between elastic modulus (E_c) at the age when the shrinkage test was started and the shrinkage strain (ϵ_{sh}) at 91 days as follows:

$$\epsilon_{sh} = 0.000562 \cdot e^{-1.92 \times 10^{-7} \cdot E_c}$$

where E_c is in units of psi.

- 6) According to the shrinkage test results from this study, the CEB-FIP model (as shown in Equation 6-6) appeared to give better prediction than the ACI 209 model (as shown in Equation 6-3). Using the ACI 209 model may result in over-estimation of the ultimate shrinkage strain.
- 7) For the concrete investigated in this study, the ultimate shrinkage strain ranged from 1.37×10^{-4} to 3.14×10^{-4} for the concrete with Georgia granite aggregate; from 2.02×10^{-4} to 3.34×10^{-4} for the concrete with Miami Oolite limestone aggregate; and from 3.49×10^{-4} to 4.22×10^{-4} for the concrete with Stalite lightweight aggregate concrete.

CHAPTER 7 ANALYSIS OF CREEP TEST

7.1 Introduction

This chapter presents the results from creep tests on the eighteen (18) concrete mixes evaluated in this study. The effects of various factors on creep behavior of concrete were analyzed. Empirical equations relating creep behavior to other fundamental properties, such as compressive strength and elastic modulus, were established through regression analysis. Evaluation was made on the CEB-FIP model and ACI 209 model for their effectiveness and accuracy in creep prediction. Finally, ultimate creep strain was predicted using a three-parameter asymptotic equation to fit experimental data, and ultimate creep coefficient was computed from this predicted ultimate creep strain.

7.2 Analysis of Creep Coefficients

The measured and calculated results from the creep tests on the eighteen concrete mixes evaluated in this study were presented in Table B-1 in Appendix B. The results presented include the total measured strain, measured shrinkage strain, measured instantaneous elastic strain, creep strain and creep modulus at various loading ages. As described in Chapter 4, the creep strain was calculated by subtracting the measured shrinkage strain and measured elastic strain from the total measured strain. The creep modulus was computed by dividing the applied stress by the creep strain.

As described in Chapter 4, the eighteen concrete mixes were loaded to either 40% or 50% of their compressive strengths at the time of load. Since the different concrete mixes were loaded to different stresses in the creep test, comparing their creep behavior based on just the creep strain or the creep modulus values would not give a fair comparison between them. For

this reason, comparisons of the creep behavior of different concrete mixes were made based on the creep coefficient.

Creep coefficient was calculated by dividing the creep strain by the elastic strain caused by the creep load. The elastic strain was computed by dividing the applied creep stress by the elastic modulus of the concrete at the time of load. The elastic modulus of the concrete and the computed elastic strain at the time of the load are also given in Table B-1, along with the computed creep coefficients at various loading ages.

7.2.1 Effects of Stress Level on Creep Coefficient

The concrete mixes in this study were loaded in the creep frames at 40% and 50% of their compressive strengths. Were the creep coefficients affected by the level of the applied stress? The next three figures show the comparison of creep coefficients at 40% stress level with those at 50% stress level. Figure 7-1 shows the comparison of creep coefficients at 91 days of concrete mixes when loaded to 40% of their compressive strengths, with those of the same concrete mixes when loaded to 50% of their compressive strength, for the specimens which had been moist-cured for 7 days before loading. Figure 7-2 shows similar comparison for the specimens which had been moist-cured for 14 days before loading. Figure 7-3 shows the comparison of creep coefficients at 360 days of concrete mixes when loaded to 40% stress level, with those of the same concrete when loaded to 50% stress level, for the specimens which had been moist-cured for 14 days before loading.

From these three figures, it can be observed that the two different stress levels had nearly no effect on the creep coefficients of all the concrete mixtures. In some cases, the creep coefficient was slightly higher at 40% stress level, while in others, it was slightly higher at 50% stress level.

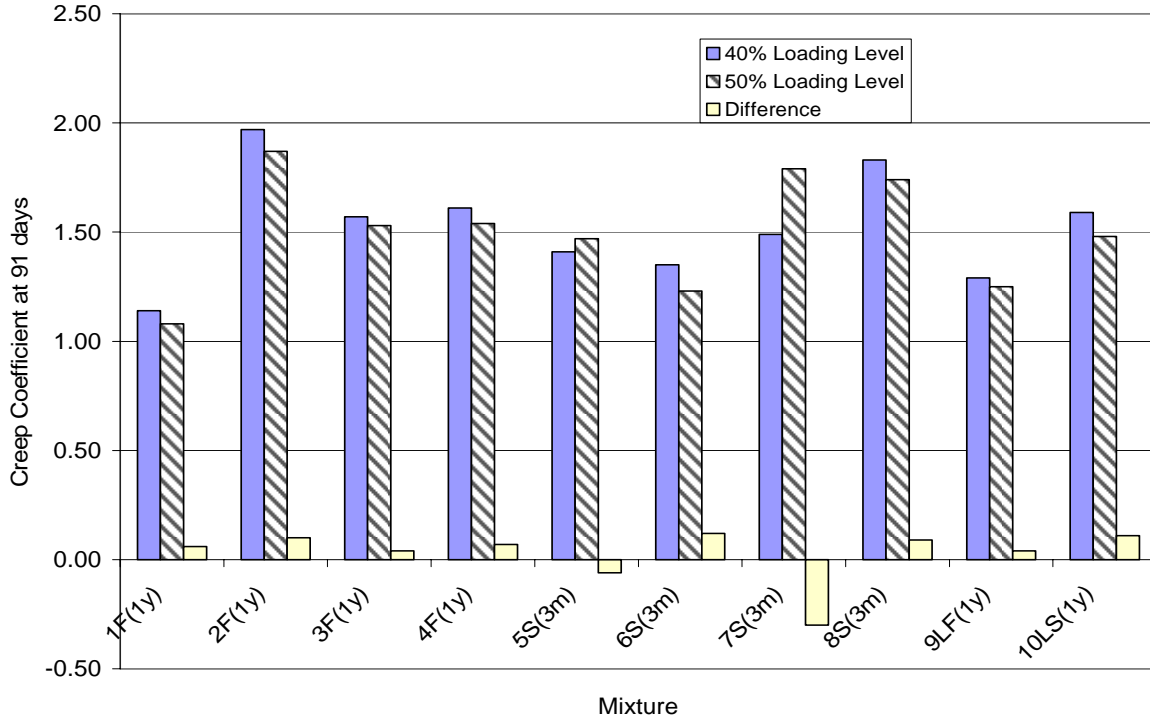


Figure 7-1. Effects of stress level on creep coefficient at 91 days of concrete moist-cured for 7 days.

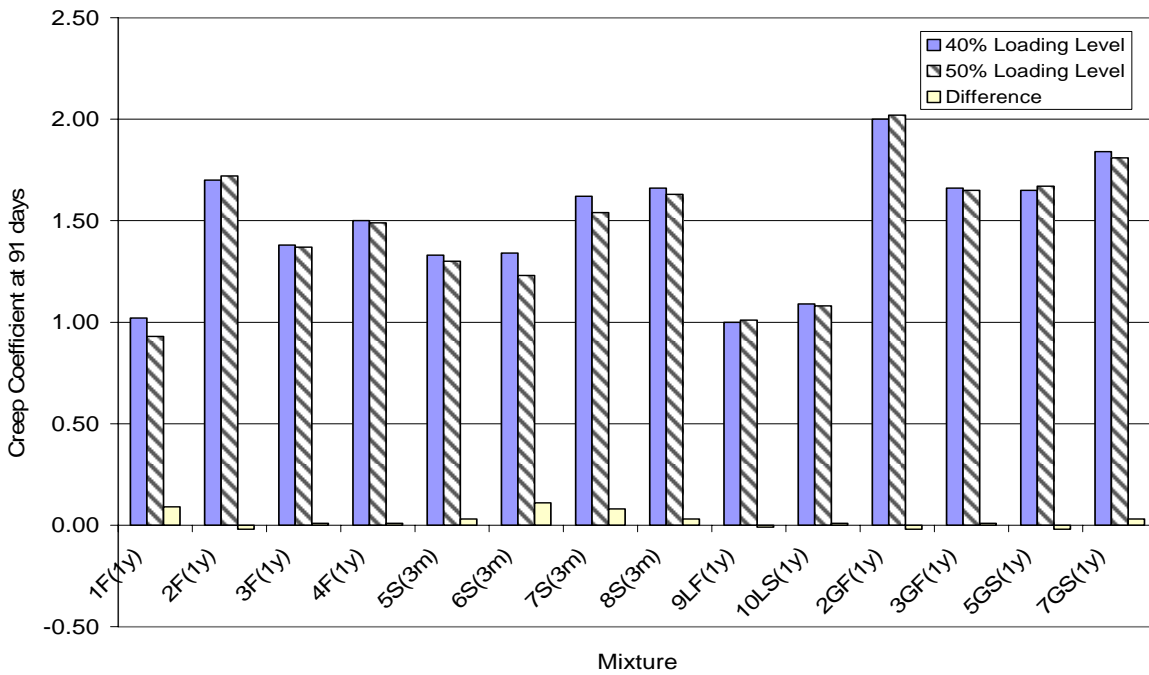


Figure 7-2. Effects of stress level on creep coefficient at 91 days of concrete moist-cured for 14 days.

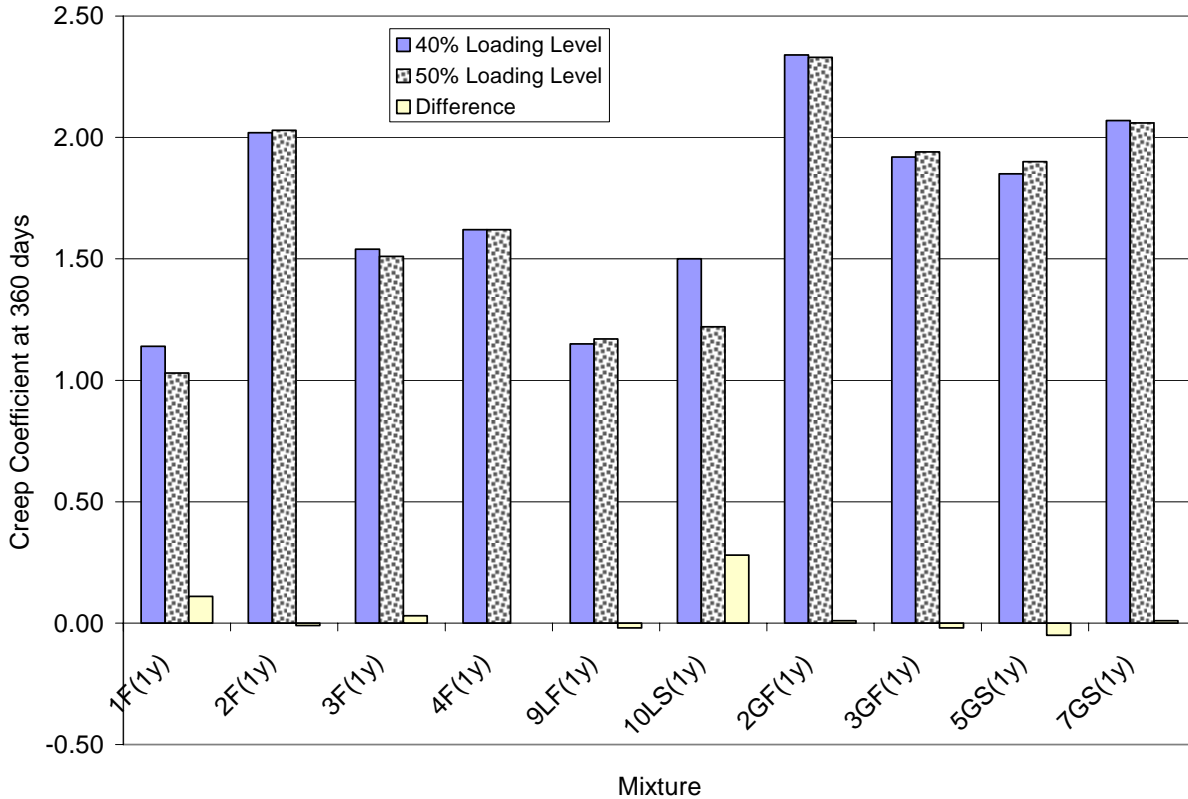


Figure 7-3. Effects of stress level on creep coefficient at 360 days of concrete moist-cured for 14 days.

7.2.2 Effects of Curing Conditions on Creep Coefficient

Figure 7-4 shows the comparison of creep coefficients at 91 days of the concrete mixes which had been moist-cured for 7 days before loading, with those of the same concrete mixes which had been moist-cured for 14 days before loading. Figure 7-5 shows similar comparison of creep coefficients at 360 days. It can be observed from both figures that the creep coefficients decreased substantially when the moist-curing time was increased from 7 days to 14 days.

The effects of curing condition on creep coefficient of lightweight aggregate concrete are substantial as well, as can be seen from Mixes 9LF and 10LS.

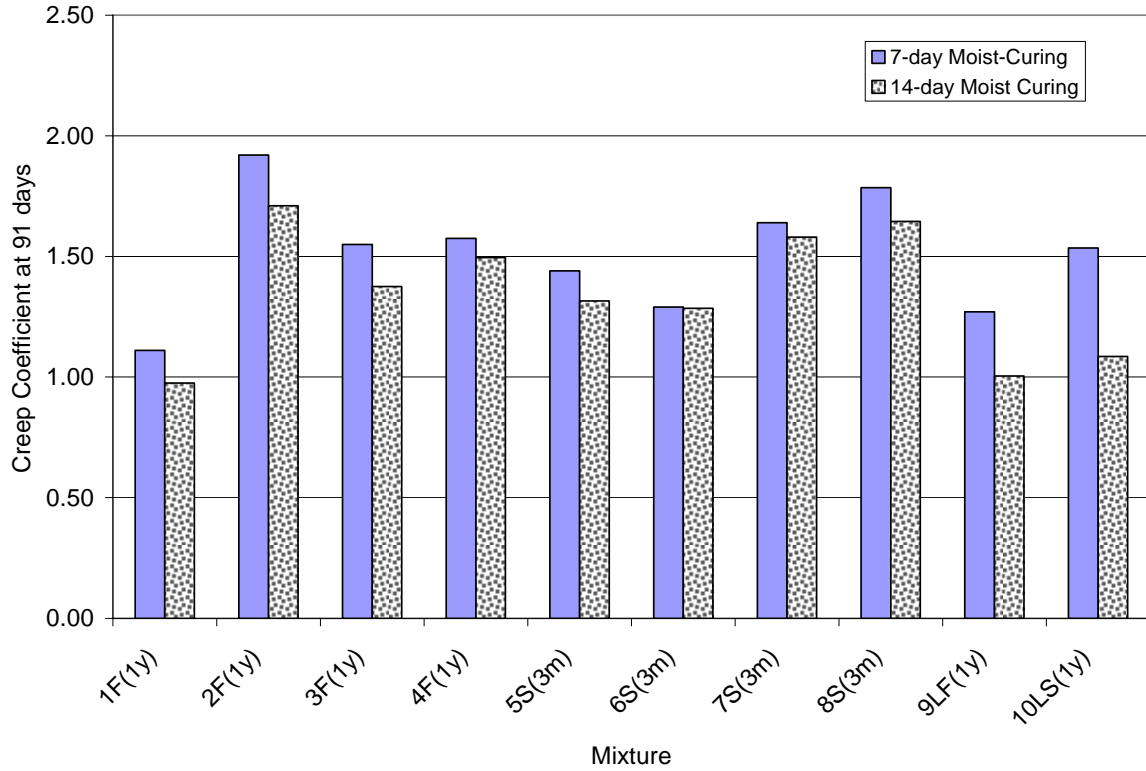


Figure 7-4. Effects of curing condition on creep coefficient of concrete at 91 days.

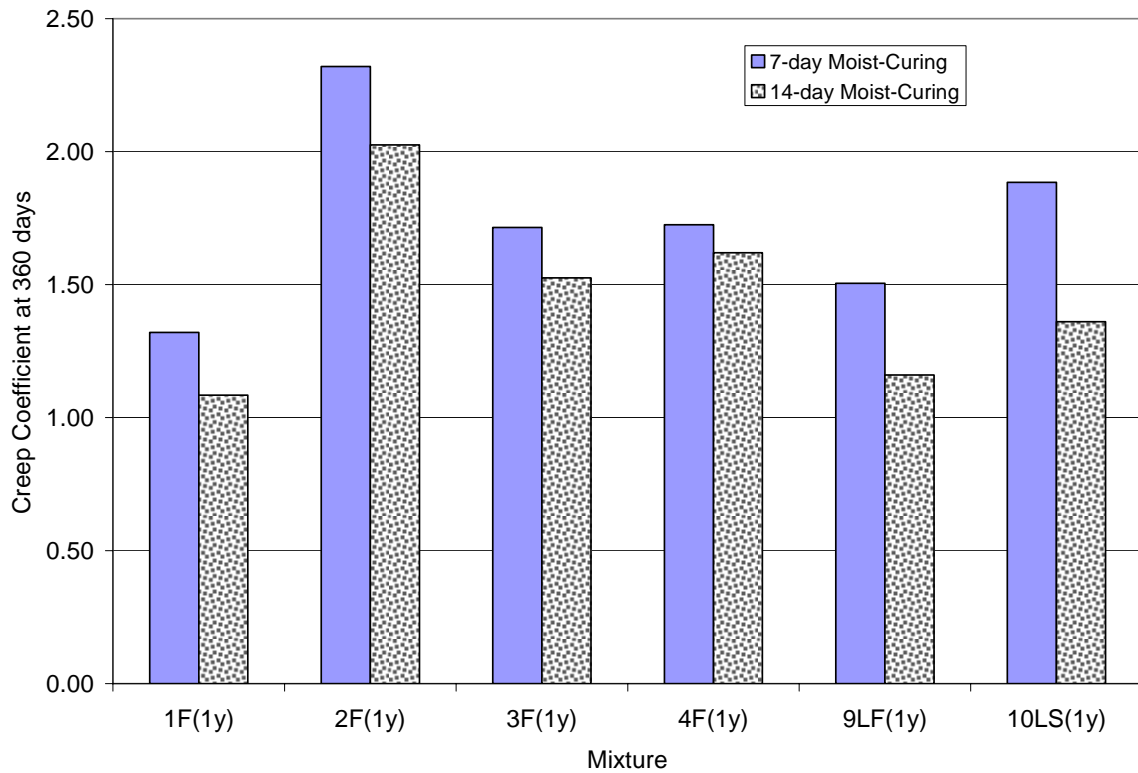


Figure 7-5. Effects of curing condition on creep coefficient of concrete at 360 days.

7.2.3 Effects of Water Content on Creep Coefficient

Since water content of fresh concrete significantly affects the drying creep of concrete, it should have considerable impact on the creep coefficient as well. Figure 7-6 shows a plot of the creep coefficient at 91 days versus the water content of the concrete mixes. It can be seen that as the water content of a concrete increased, the creep coefficient increased accordingly.

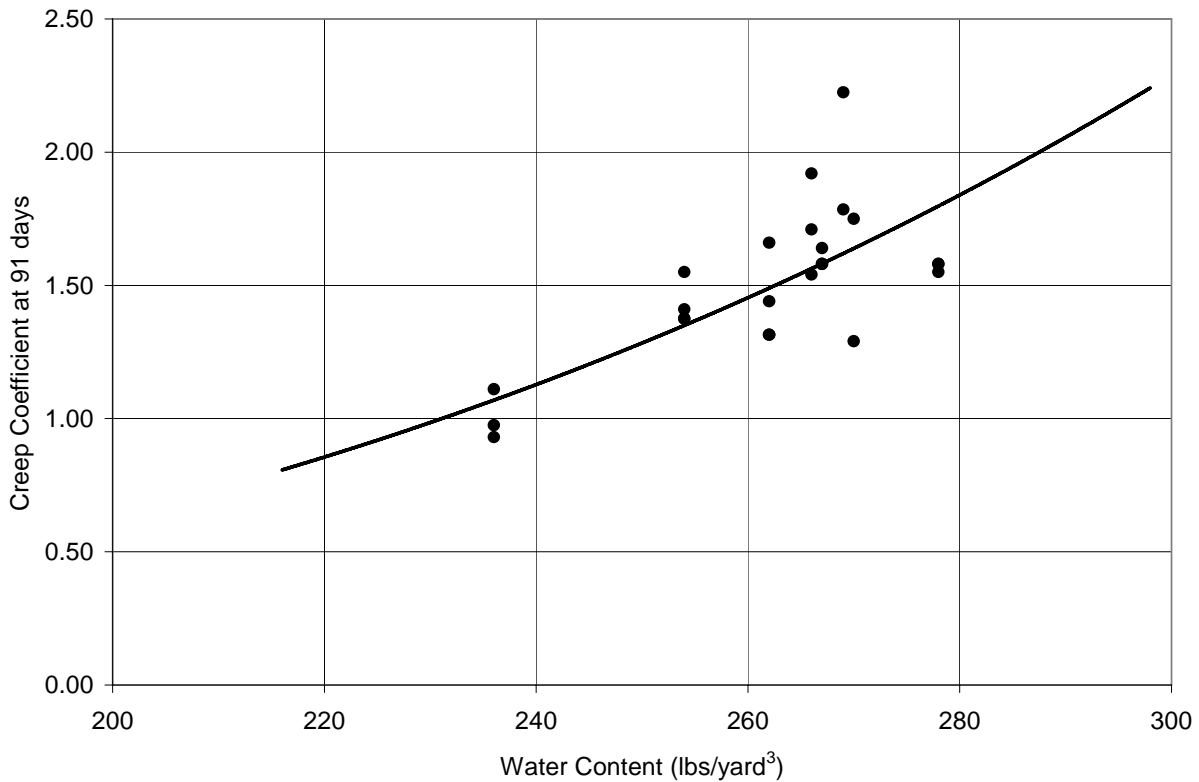


Figure 7-6. Effects of water content on creep coefficient at 91 days.

7.2.4 Effects of Compressive Strength at Loading Age on Creep Coefficient

To find out how the compressive strength of concrete at loading age was related to the creep coefficient, compressive strength at loading age was plotted against the corresponding creep coefficient of the concrete. Figure 7-7 shows a plot of creep coefficient at 91 days of the concrete loaded at 14 days versus the compressive strength of the concrete at the time of loading (14 days). Figure 7-8 shows a similar plot for the concrete loaded at 28 days. It can be seen that

the creep coefficient decreased as the compressive strength of the concrete at the time of loading increased.

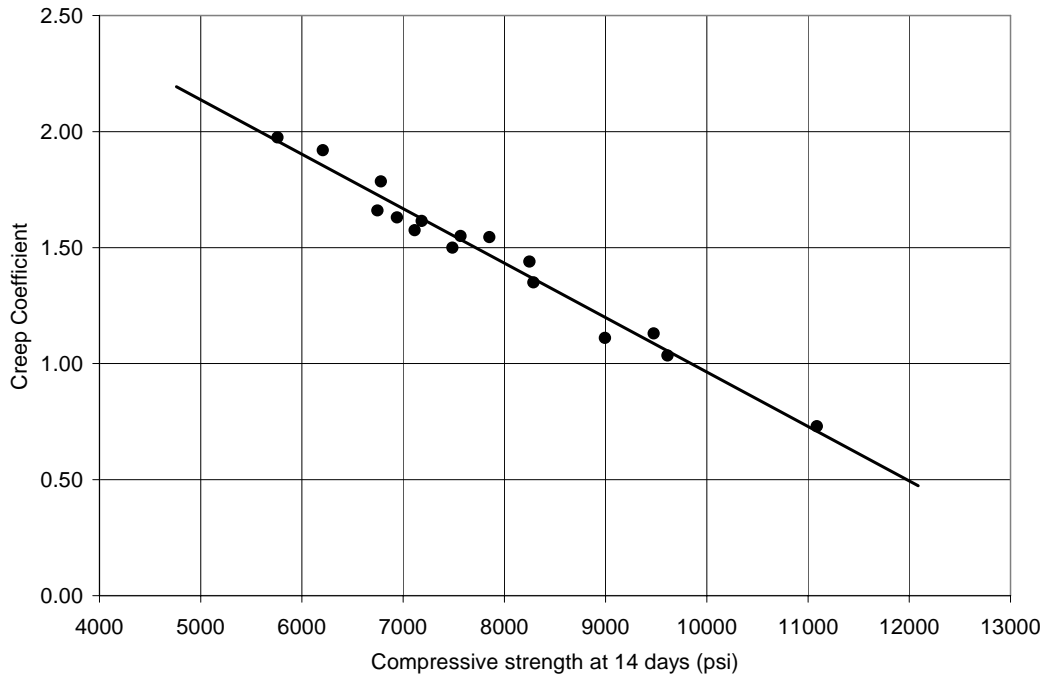


Figure 7-7. Relationship between compressive strength and creep coefficient at 91 days for specimens loaded at 14 days.

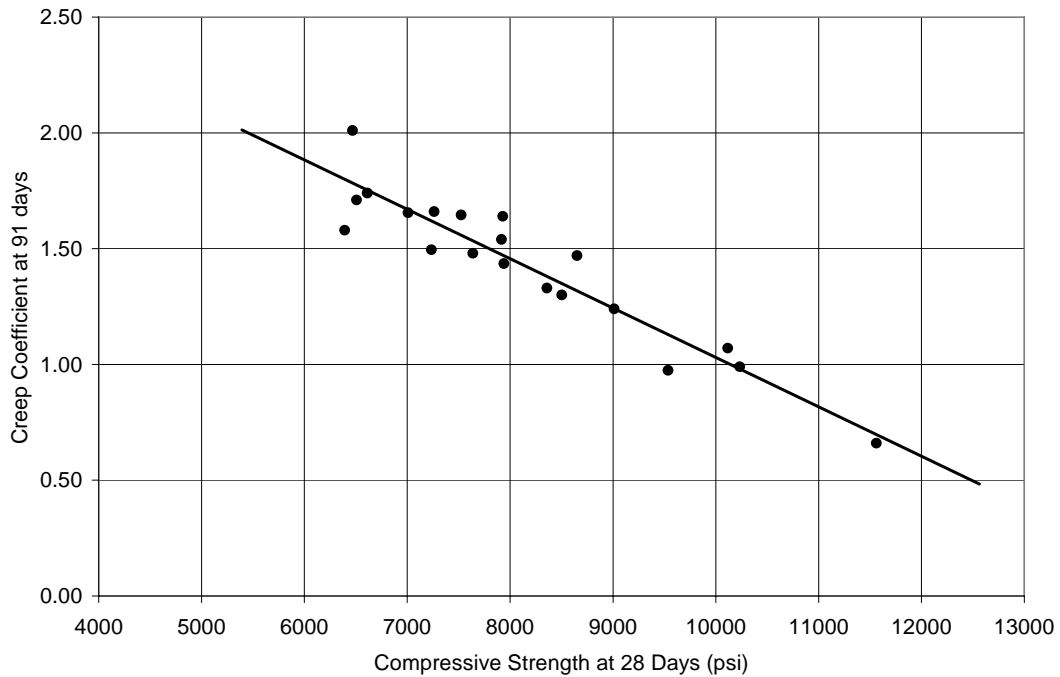


Figure 7-8. Relationship between compressive strength and creep coefficient at 91 days for specimens loaded at 28 days.

Figure 7-9 shows the combined plot of creep coefficient at 91 days of all the concrete versus the compressive strength of the concrete at the time of loading. It can be seen that the creep coefficient was a function of the compressive strength of the concrete at time of loading.

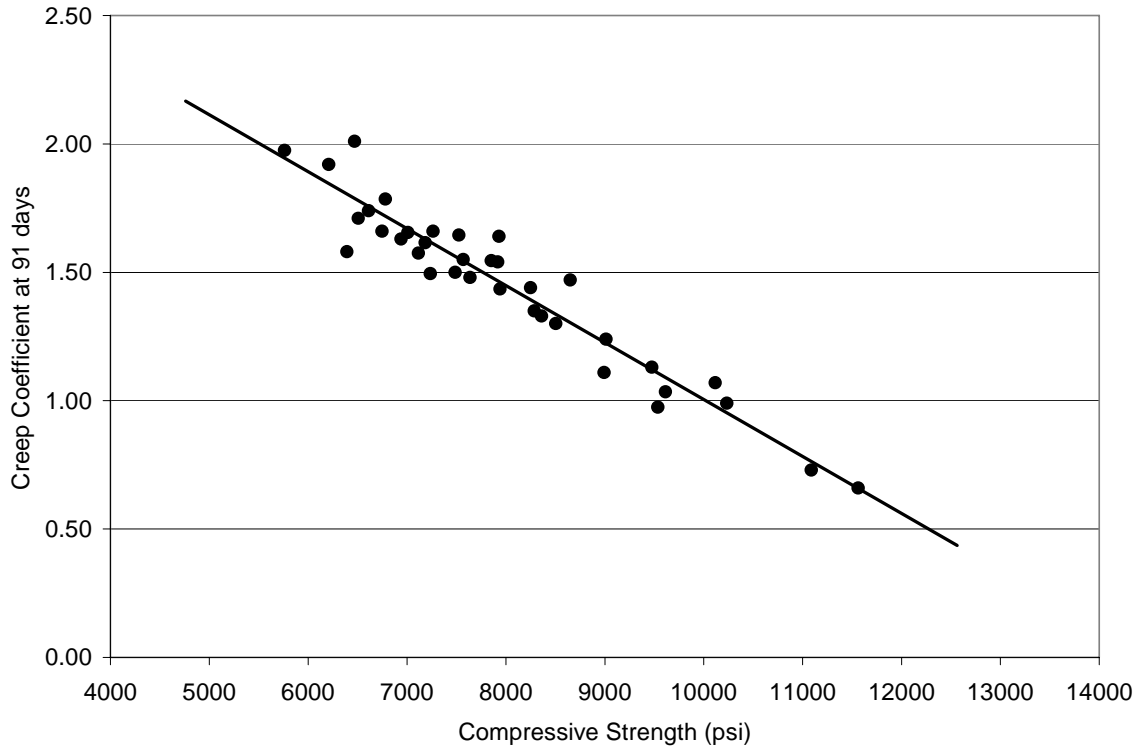


Figure 7-9. Relationship between compressive strength at loading age and corresponding creep coefficient at 91 days.

A linear regression analysis was performed to relate the creep coefficient at 91 days of the concrete to its compressive at the time of loading, using the following equation:

$$\varphi_c = \alpha \cdot f_c + \beta \tag{7-1}$$

where φ_c = creep coefficient;

f_c = compressive strength; and

α and β = slope and interception of linear equation.

The results of the regression analysis are provided in Table 7-1.

Table 7-1. Regression Analysis on Relationship of Compressive Strength to Creep Coefficient at 91 Days

Curing condition	α	95% Confidence Interval	β	95% Confidence Interval	R ²	S _{y,x}
14-day curing	-2.347E-04	-2.57E-04 ~ -2.21E-04	3.311	3.132 ~ 3.489	0.9729	0.0567
28-day curing	-2.132E-04	-2.514E-04 ~ -1.750E-04	3.162	2.848 ~ 3.477	0.8843	0.1115
All curing conditions	-2.217E-04	-2.442E-04 ~ -1.993E-04	3.222	3.039 ~ 3.404	0.9221	0.0909

As can be seen from Table 7-1 as well as Figures 7-7 through 7-9, the compressive strength of the concrete at the time of loading was nearly linearly related to the creep coefficient at 91 days. This situation was true for the specimens under two different curing conditions. Also, it is of great importance to realize that the slope and interception of linear regression equation were nearly identical to one another for the specimens under two different curing conditions. That is to say, once compressive strengths of specific concrete mixtures are given, the creep coefficient can be computed using the linear relationship between compressive strength and creep coefficient at 91 days regardless of what curing condition was applied to the specimens.

Therefore, linear regression analysis was carried out on the experimental data obtained from both curing conditions. The analyzed results are plotted in Figure 7-9 and presented in Table 7-1 as well. As can be seen from Table 7-1, the slope and interception of linear regression equation from combined analysis were nearly the average of slopes and interceptions from separate analyses. That means the combined linear equation could give reliable estimation of the creep coefficient obtained under two different curing conditions.

The same regression analysis was also carried out between compressive strength at loading age and creep coefficients at 360 days. The analyzed results are presented in Table 7-2, and the relationship between compressive strength at loading age and creep coefficient at 360

days is plotted in Figure 7-10. As can be seen from Table 7-2 as well as Figure 7-10, the creep coefficients of concretes at 360 days were linearly related to the compressive strengths at loading age.

Table 7-2. Regression Analysis on Relationship of Compressive Strength to Creep Coefficient at 360 Days

Curing condition	α	95% Confidence Interval	β	95% Confidence Interval	R ²	S _{y,x}
All curing conditions	-3.394E-04	-4.164E-04 ~ -2.624E-04	4.302	3.729 ~ 4.876	0.9061	0.1211

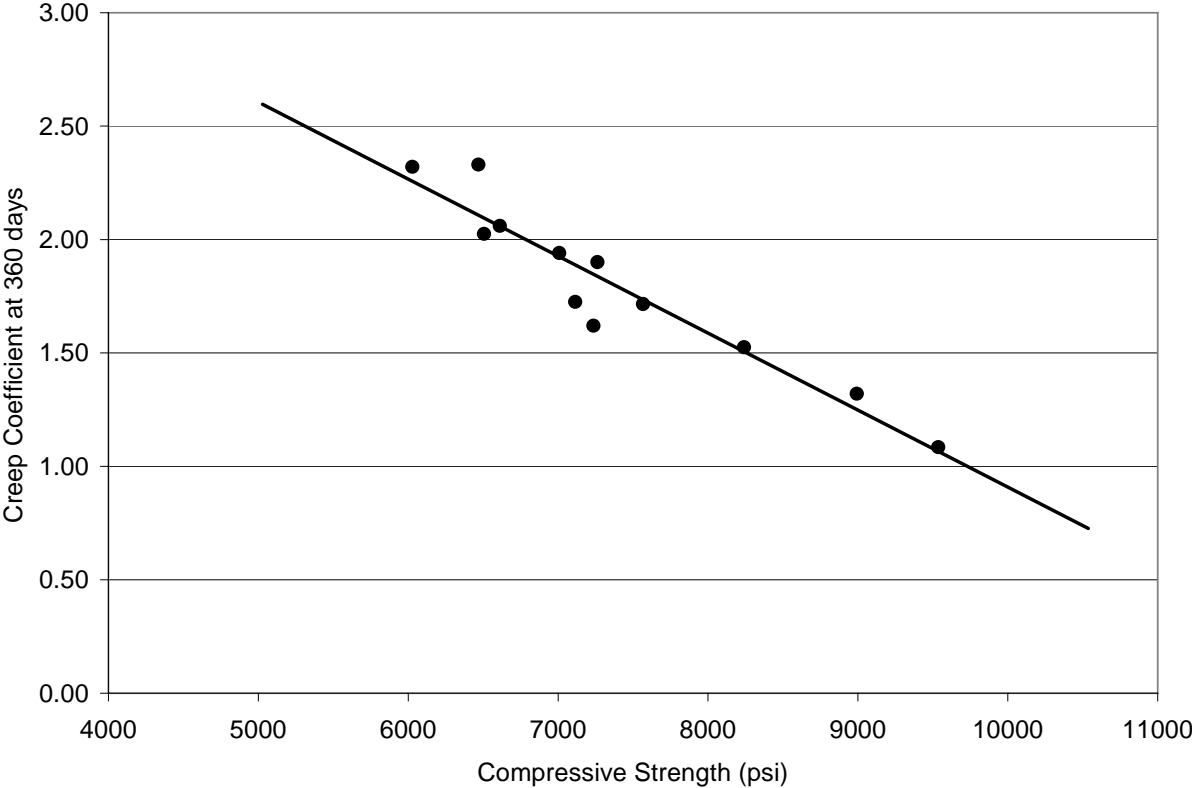


Figure 7-10. Relationship between compressive strength at loading age and corresponding creep coefficient at 360 days.

7.2.5 Effects of Coarse Aggregate Type on Creep Coefficient

Figure 7-11 shows the comparison of creep coefficient at 91 days of the concrete made with Miami Oolite with those of the corresponding concrete made with Georgia granite. It can

be seen that the creep coefficients of concretes made with Georgia granite were higher than those of the corresponding concretes with Miami Oolite limestone aggregate. This is due probably to the lower elastic deformation of concretes with Georgia granite aggregate in comparison with those with Miami Oolite limestone aggregate. Therefore, the ratio of creep strain to elastic strain was larger for the concrete made with Georgia granite.

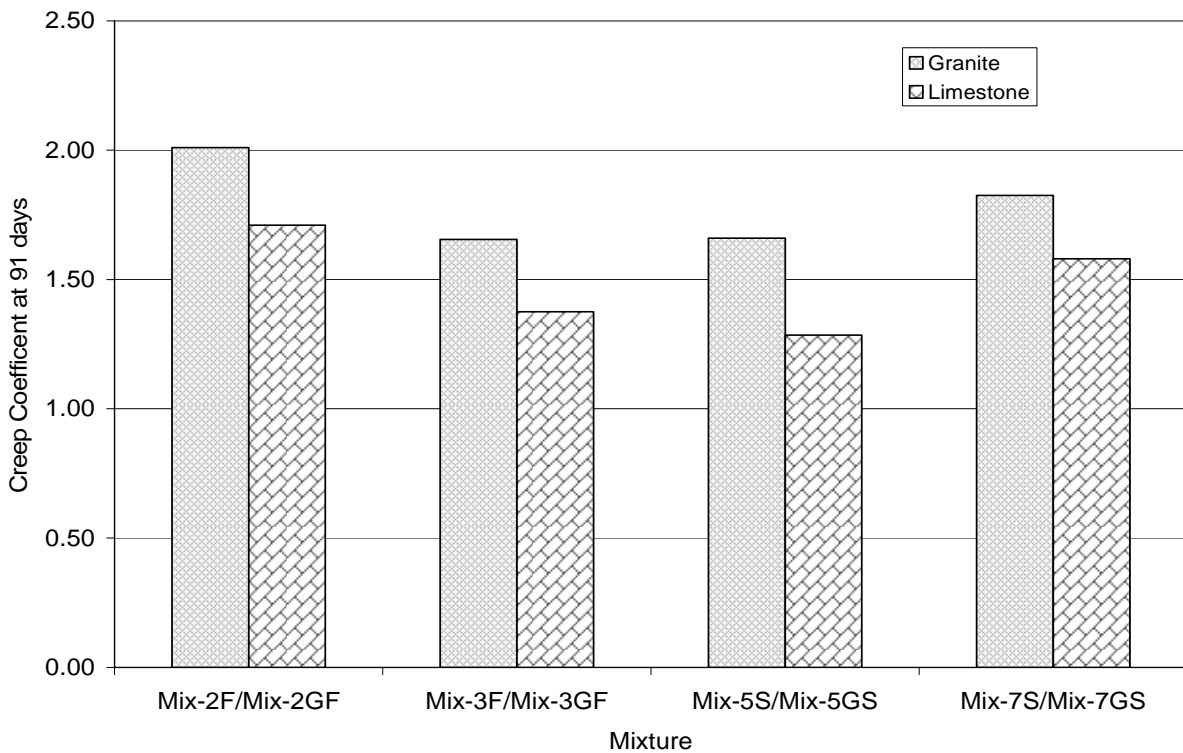


Figure 7-11. Effects of coarse aggregate type on creep coefficient at 91 days.

7.3 Prediction of Ultimate Creep Strain

It was assumed that creep rate for concrete materials was decreasing, and creep strain would approach the limiting value after an infinite time under load. The study by Troxell et al. [1958] indicates that the average value of creep strain after 30 years is 1.36 times the one-year creep strain. Thus, in the point of view of engineering practice, it is often assumed that the 30-year creep strain represents the ultimate creep strain.

The ultimate creep strain of concrete investigated in this study was determined using asymptotic equation, given as follows, to fit the experimental data:

$$\varepsilon_c = \alpha \cdot \left(\frac{t}{t + \gamma} \right)^\beta \quad (7-2)$$

This equation is the ratio of two polynomials. As the time variable approaches infinity, the ratio of two polynomials is equal to 1. Therefore, ultimate creep strain is equal to α .

In this equation, α and β are two parameters to be determined from curve-fitting, and γ , which is the factor borrowed from CEB-FIP equation, reflects the effect of geometrical characteristics of the specimen and relative humidity on creep behavior of concrete. The relative humidity was controlled at 75% in this study, and a 6" \times 12" cylinder was used for the creep test, thus, the geometrical characteristic of the testing specimen, h , was computed as follows:

$$h = \frac{2A_c}{u} = \frac{2 \times \pi \times 3^2}{\pi \times 6} = 3 \text{ in.} = 76.2 \text{ mm} \quad (7-3)$$

Then, γ was obtained as follows:

$$\gamma = 150 \cdot \left[1 + \left(1.2 \cdot \frac{75\%}{100\%} \right)^{18} \right] \cdot \frac{h}{100} + 250 = 381.5 \leq 1500 \quad (7-4)$$

Thus, the equation used to fit the experimental data became

$$\varepsilon_c = \alpha \cdot \left(\frac{t}{t + 381.5} \right)^\beta \quad (7-5)$$

The least squares method of curve fitting was used to determine two unknown parameters, α and β . Ultimate creep strains and ultimate creep coefficient, based on the measurements up to 91 days from the regression analysis, are presented in Table 7-3. The ultimate creep strain and ultimate creep coefficient based on the measurements up to 360 days are given in Table 7-4.

Table 7-3. Predicted Ultimate Creep Strain and Creep Coefficient Based on Creep Measurements up to 91 Days

Mix	Predicted Ultimate Creep Strain				Predicted Ultimate Creep Coefficient			
	Curing Condition 1		Curing Condition 2		Curing Condition 1		Curing Condition 2	
	40% Load	50% Load	40% Load	50% Load	40% Load	50% Load	40% Load	50% Load
1F	1.06E-03	1.30E-03	0.88E-03	1.03E-03	1.46	1.53	1.21	1.19
2F	1.93E-03	2.08E-03	1.66E-03	2.11E-03	3.27	2.84	2.68	2.74
3F	1.45E-03	1.86E-03	1.39E-03	1.56E-03	2.42	2.48	2.59	1.95
4F	1.37E-03	1.59E-03	1.24E-03	1.63E-03	2.35	2.15	2.15	2.36
5S	1.40E-03	1.84E-03	1.25E-03	1.64E-03	2.07	2.18	1.87	1.96
6S	1.68E-03	1.87E-03	1.55E-03	1.75E-03	2.63	2.34	2.30	2.12
7S	1.41E-03	1.69E-03	1.46E-03	1.60E-03	2.70	2.59	2.60	2.36
8S	1.58E-03	1.97E-03	1.45E-03	1.95E-03	2.82	2.87	2.46	2.52
9LF	1.11E-03	1.40E-03	0.99E-03	1.16E-03	1.69	1.71	1.30	1.32
10LS	0.94E-03	1.19E-03	0.76E-03	0.97E-03	1.89	1.91	1.44	1.39
1GF	0.87E-03*		0.63E-03		1.49		1.09	
2GF	---	---	1.80E-03	2.10E-03	---	---	3.45	3.22
3GF	---	---	1.57E-03	1.81E-03	---	---	3.14	2.90
4GF	0.93E-03*		0.81E-03		1.73		1.50	
5GS			1.41E-03	1.82E-03			2.51	2.59
6GS	0.88E-03*		0.96E-03		1.71*		1.77	
7GS	---	---	1.49E-03	1.76E-03	---	---	2.96	2.51

Table 7-4. Predicted Ultimate Creep Strain and Creep Coefficient Based on Creep Measurements up to at 360 Days

Mix	Predicted Ultimate Creep Strain				Predicted Ultimate Creep Coefficient			
	Curing Condition 1		Curing Condition 2		Curing Condition 1		Curing Condition 2	
	40% Load	50% Load	40% Load	50% Load	40% Load	50% Load	40% Load	50% Load
1F	1.04E-03	1.28E-03	0.84E-03	0.98E-03	1.43	1.51	1.16	1.13
2F	1.85E-03	2.05E-03	1.55E-03	1.95E-03	3.13	2.80	2.50	2.53
3F	1.35E-03	1.65E-03	1.23E-03	1.46E-03	2.25	2.20	1.92	1.82
4F	1.27E-03	1.46E-03	1.14E-03	1.48E-03	2.18	1.97	1.97	2.14
5S	1.10E-03	---	1.34E-03	---	2.20	---	2.67	---
6S	1.58E-03	---	1.23E-03	---	2.90	---	2.26	---
7S	1.40E-03	---	1.47E-03	---	2.28	---	2.40	---
8S	1.60E-03	---	1.97E-03	---	3.22	---	3.96	---
9LF	1.13E-03	1.38E-03	0.94E-03	1.16E-03	1.72	1.68	1.24	1.32
10LS	1.00E-03	1.22E-03	0.81E-03	1.02E-03	2.01	1.96	1.54	1.47
1GF	---	---	---	---	---	---	---	---
2GF	---	---	1.58E-03	1.93E-03	---	---	3.03	2.96
3GF	---	---	1.30E-03	1.58E-03	---	---	2.60	2.53
4GF	1.14E-03		0.97E-03	---	2.12	---	1.80	---
5GS	---	---	1.29E-03	1.63E-03	---	---	2.30	2.32
6GS	---	---	1.76E-03	---	---	---	3.74	---
7GS	---	---	1.34E-03	1.60E-03	---	---	2.66	2.54

As shown in Tables 7-3 and 7-4, it is of great importance to realize that many concretes investigated in this study had ultimate creep coefficient higher than 2.0, particularly the mixtures with granite aggregate. In addition, the predicted ultimate creep strains and ultimate creep coefficients based on the measurements up to 91 days were slightly higher than those based on the measurement up to 360 days.

7.4 Evaluation on Creep Prediction Models

The effectiveness of other creep prediction models, such as Burgers model, the CEB-FIP model and ACI 209 model, were evaluated in this study.

7.4.1 Burgers Model

Burgers model or four-element model, as shown in Figure 7-12, was also used to fit the experimental data. Then, extrapolation was carried out using Burgers model with unknown parameters determined from regression analysis to evaluate the feasibility of Burgers model to predict creep strain of concrete at 30 years, based on the experimental data obtained in three months.

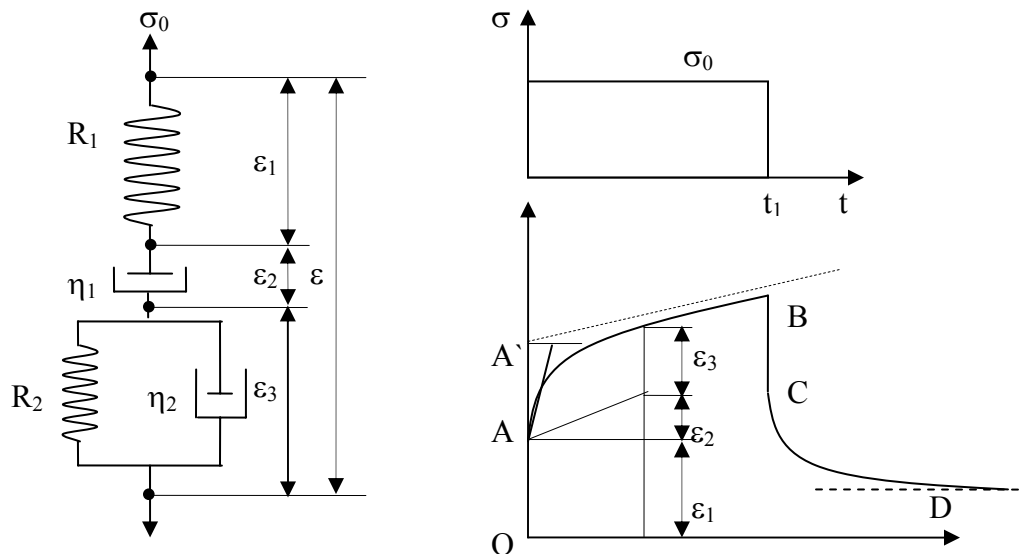


Figure 7-12. Behavior of a Burgers model.

The total strain of Burgers model can be derived by considering the strain responses of each element under the constant load in the model, and it can be expressed as the following equation:

$$\varepsilon = \varepsilon_1 + \varepsilon_2 + \varepsilon_3 \quad (7-6)$$

where ε_1 is the elastic strain of spring in Maxwell model, and it can be given as

$$\varepsilon_1 = \frac{\sigma}{R_1} \quad (7-7)$$

ε_2 is viscous flow of dash-pot in Maxwell model, and its rate type formula can be expressed as

$$\dot{\varepsilon}_2 = \frac{\sigma}{\eta_1} \quad (7-8)$$

And ε_3 is the strain of Kelvin unit, and it can be derived from

$$\dot{\varepsilon}_3 + \frac{R_2}{\eta_2} \cdot \varepsilon_3 = \frac{\sigma}{\eta_2} \quad (7-9)$$

Eliminating ε_1 , ε_2 , and ε_3 from the above four equations, the constitutive relationship between ε and σ for Burgers model can be obtained

$$\sigma + \left(\frac{\eta_1}{R_1} + \frac{\eta_1}{R_2} + \frac{\eta_2}{R_2} \right) \cdot \dot{\sigma} + \frac{\eta_1 \eta_2}{R_1 R_2} \ddot{\sigma} = \eta_1 \dot{\varepsilon} + \frac{\eta_1 \eta_2}{R_2} \ddot{\varepsilon} \quad (7-10)$$

Solving the above second order differential equation with initial conditions of

$$\begin{aligned} \varepsilon &= \varepsilon_1 = \frac{\sigma_0}{R_1} \\ t = 0 \rightarrow \varepsilon_2 &= \varepsilon_3 = 0 \\ \dot{\varepsilon} &= \frac{\sigma_0}{\eta_1} + \frac{\sigma_0}{\eta_2} \end{aligned} \quad (7-11)$$

the creep behavior of Burgers model under the constant stress can be derived

$$\varepsilon(t) = \frac{\sigma_0}{R_1} + \frac{\sigma_0}{\eta_1} t + \frac{\sigma_0}{R_2} \left(1 - \exp \left(-\frac{R_2}{\eta_2} t \right) \right) \quad (7-12)$$

In this study, just creep strain was considered. Thus, the first term in Equation 7-9 can be eliminated. Therefore, the Burgers model becomes:

$$\varepsilon(t) = \frac{\sigma_0}{\eta_1} t + \frac{\sigma_0}{R_2} \left(1 - \exp \left(-\frac{R_2}{\eta_2} t \right) \right) \quad (7-13)$$

Three material constants, R_2 , η_1 and η_2 , can be easily determined by curve-fitting Equation 7-13 to the experimental data.

As can be seen from Equation 7-13, after a certain time the second term on the right side of the equation will decay and approach $\frac{\sigma_0}{R_2}$, and creep rate becomes a constant number, i.e., $\frac{\sigma_0}{\eta_1}$.

Then, after a long time creep test, Burgers model can be simplified as straight line as follows,

$$\varepsilon(t) = \frac{\sigma_0}{\eta_1} t + \frac{\sigma_0}{R_2} \quad (7-14)$$

Burgers model with constitutive parameters determined from regression analysis was plotted in Figure 7-13. As can be seen from Figure 7-13, Burger's model is very capable of simulating the development trend of creep of concrete. However, it indicates that the extrapolation made by Burgers model extremely overestimates the ultimate creep strain. That is to say, if not impossible, the reasonable projection by Burgers model cannot be expected without longer term experimental data available to determine constitutive parameters accurately, while the regression model (Equation 7-2) appears to give a relatively safe extrapolation by using the

creep data obtained in 91 days. This can be seen from Figure 7-13, since the regression model (7-2) had a continuous decreasing creep rate.

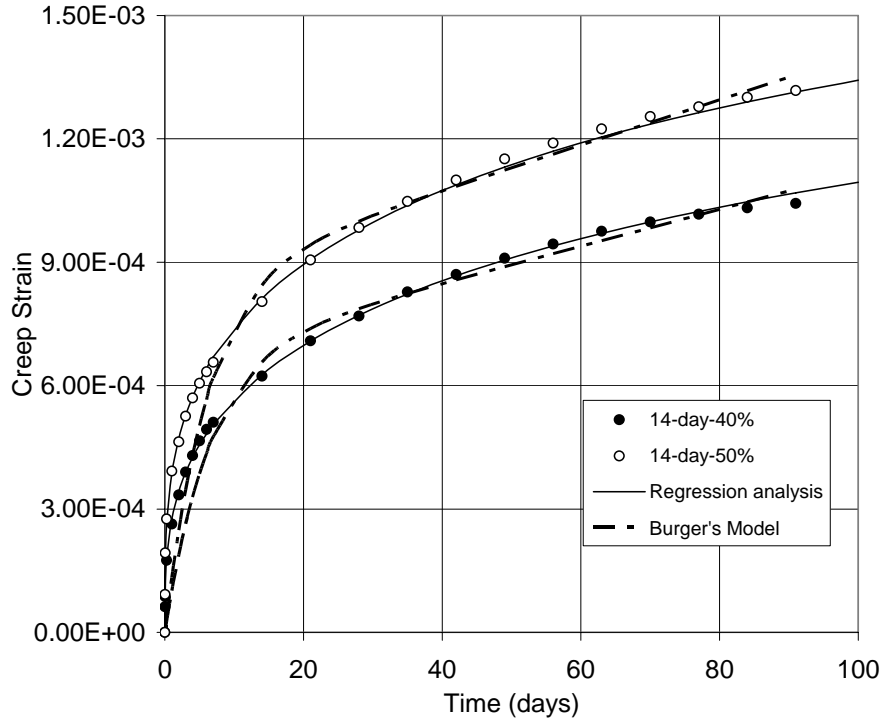


Figure 7-13. Evaluation on Burgers model.

7.4.2 CEB-FIP Model (1990)

The CEB-FIP model is an empirical model recommended by the European Union in 1990. In this model, creep strain can be predicted based on the information from ultimate compressive strength and modulus of elasticity at loading age, and a time function determined according to the mechanical properties of a specific concrete mixture, the geometry of specimen, and the curing conditions applied to the specimen, and so on. The general equation is given as follows:

$$\varepsilon_{cr}(t, t_0) = \frac{\sigma_c(t_0)}{E_{ci}} \cdot \phi_{ci}(t, t_0) \quad (7-15)$$

For a detailed description of the CEB-FIP model, please refer to the literature review in Chapter 2.

Finally, by putting all the equations together and simplifying them, the following equation was used to predict the development of creep strain with time.

$$\varepsilon_{cr}(t, t_0) = \frac{\sigma_c(t_0)}{E_{ci}} \cdot \left(1 + \frac{1 - RH / RH_0}{0.46 \cdot (h / h_0)^{1/3}} \right) \cdot \left(\frac{5.3}{\sqrt{f_{cm} / f_{cmo}}} \right) \cdot \left(\frac{1}{0.1 + (t_0 / t_1)^{0.2}} \right) \cdot \left[\frac{(t - t_0) / t_1}{\beta_H + (t - t_0) / t_1} \right]^{0.3} \quad (7-16)$$

In this study, the relative humidity was controlled at 75%. For a 6" × 12"-cylinder, the geometrical characteristic of the testing specimen, h , was computed as follows:

$$h = \frac{2A_c}{u} = \frac{2 \times \pi \times 3^2}{\pi \times 6} = 3" = 76.2 \text{ mm} \quad (7-17)$$

Then, β_h could be obtained as follows:

$$\beta_H = 150 \cdot \left[1 + \left(1.2 \cdot \frac{75\%}{100\%} \right)^{18} \right] \cdot \frac{76.2}{100} + 250 = 381.5 \leq 1500 \quad (7-18)$$

Then, the prediction formula for concrete cured for 14 days was simplified as follows:

$$\varepsilon_{cr}(t, t_0) = \frac{\sigma_c(t_0)}{E_{c14}} \cdot \left(\frac{18.55}{\sqrt{f_{cm}}} \right) \cdot \left[\frac{(t - 14)}{381.5 + (t - 14)} \right]^{0.3} \quad (7-19)$$

The above equation is an asymptotic function. As the time argument approaches an infinite number, creep strain reaches ultimate creep strain $(\sigma_c(t_0) / E_{ci}) (18.55 / \sqrt{f_{cm}})$.

Similarly, for the concrete specimen cured for 28 days, the prediction equation became

$$\varepsilon_{cr}(t, t_0) = \frac{\sigma_c(t_0)}{E_{c28}} \left(\frac{18.55}{\sqrt{f_{cm}}} \right) \cdot \left[\frac{(t-28)}{381.5 + (t-28)} \right]^{0.3} \quad (7-20)$$

As can be seen from the above equation, this asymptotic equation approaches a limiting value as time approaches infinity. Therefore, ultimate creep strain can be computed by the following formula:

$$\varepsilon_{ult} = \frac{\sigma_c(t_0)}{E_{c28}} \left(\frac{18.55}{\sqrt{f_{cm}}} \right) \quad (7-21)$$

To evaluate the effectiveness of the CEB-FIP model, the CEB-FIP equation was plotted in Figure 7-14. It indicates that the CEB-FIP model gave a very pleasing prediction. To clarify this conclusion, the creep strain at 91 days from experimental measurements was plotted against the creep strain computed according to the CEB-FIP model in Figure 7-15. It clearly shows that the measurements agree very well with the prediction made by the CEB-FIP model.

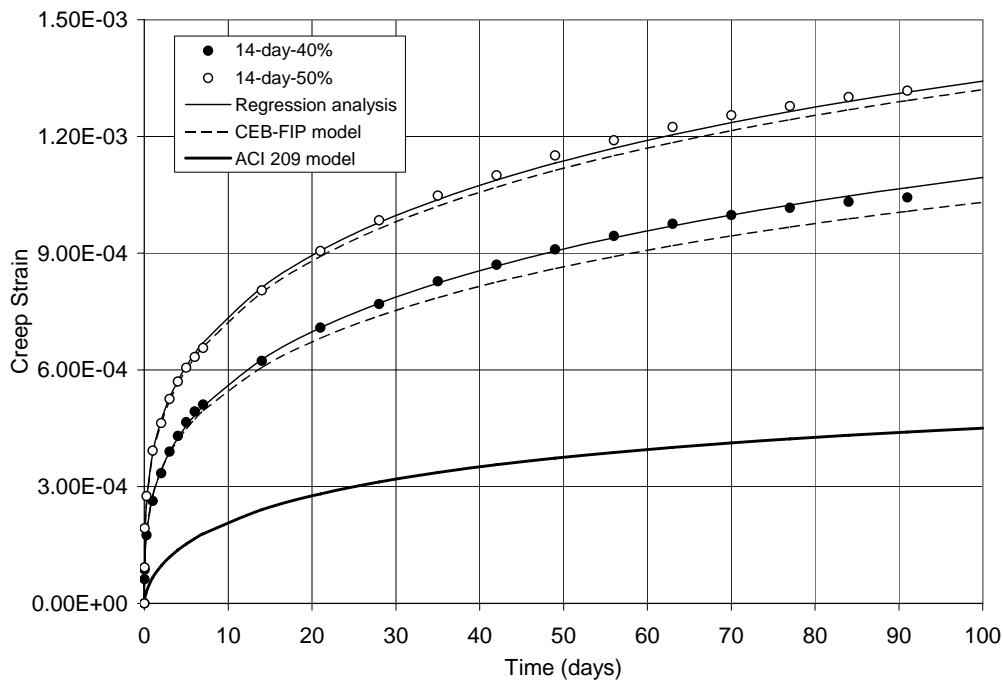


Figure 7-14. Comparison on the effectiveness of the CEB-FIP model and ACI model.

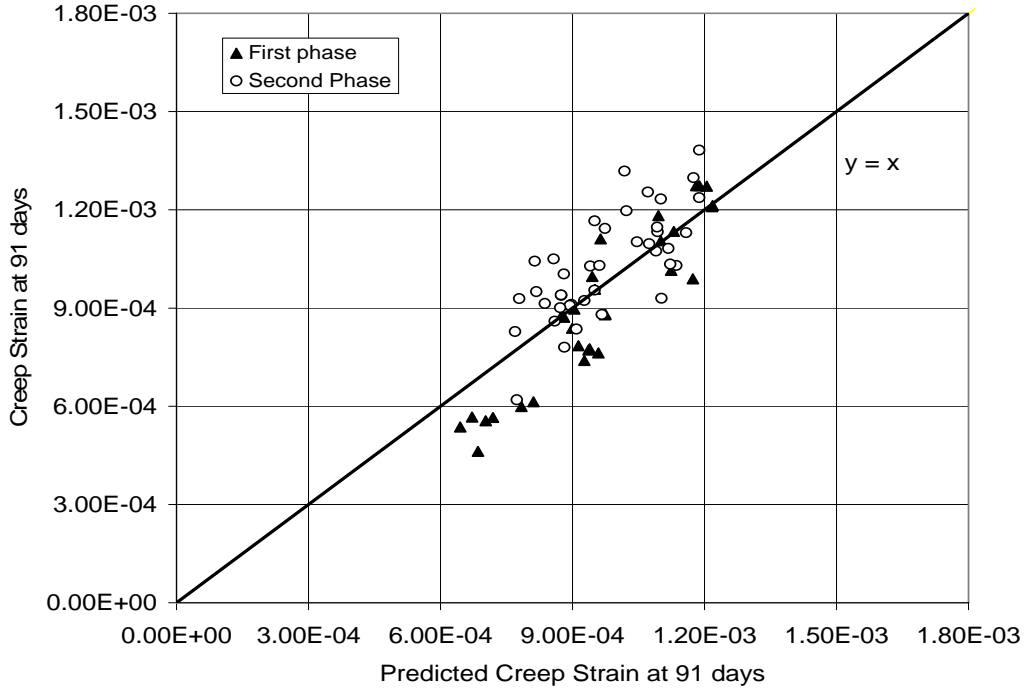


Figure 7-15. Comparison between the creep strain at 91 days from experimental data and the predicted creep strain using the CEB-FIP model.

Also, in order to verify the simple linear relationship between creep strain and $\sigma / (E \cdot \sqrt{f_{cm}})$, the creep strain at 91 days was plotted against $\sigma / (E \cdot \sqrt{f_{cm}})$, where σ was stress applied to the specimen; E was the elastic modulus of the concrete at loading age; and f_{cm} was the characteristic strength of concrete at loading age (see Figure 7-16). Then, linear regression analysis was performed to determine the relationship between creep strain at 91 days and $\sigma / (E \cdot \sqrt{f_{cm}})$, and the analyzed results are provided in Table 7-5. As can be seen in Figure 7-16, the creep strain at 91 days was linearly related to $\sigma / (E \cdot \sqrt{f_{cm}})$. The regression equation is given as follows:

$$\varepsilon_{c91} = 13.40 \cdot \frac{\sigma}{E \cdot \sqrt{f_{cm}}} - 1.758 \times 10^{-4} \quad (7-22)$$

Table 7-5. Regression Analysis on Relation of Creep Coefficient to f_c/E

α	95% Confidence Interval	β	95% Confidence Interval	R^2	SSE
13.40	11.21 ~ 15.58	-1.758E-04	-3.649E-04 ~ -1.333E-04	0.6848	1.193E-04

In addition, the ultimate creep strains predicted by curve-fitting to experimental data were depicted against the creep strains calculated using the original CEB-FIP model in Figure 7-17. It indicated that original CEB-FIP model yielded very pleasing prediction of the typical concrete mixtures investigated in this study.

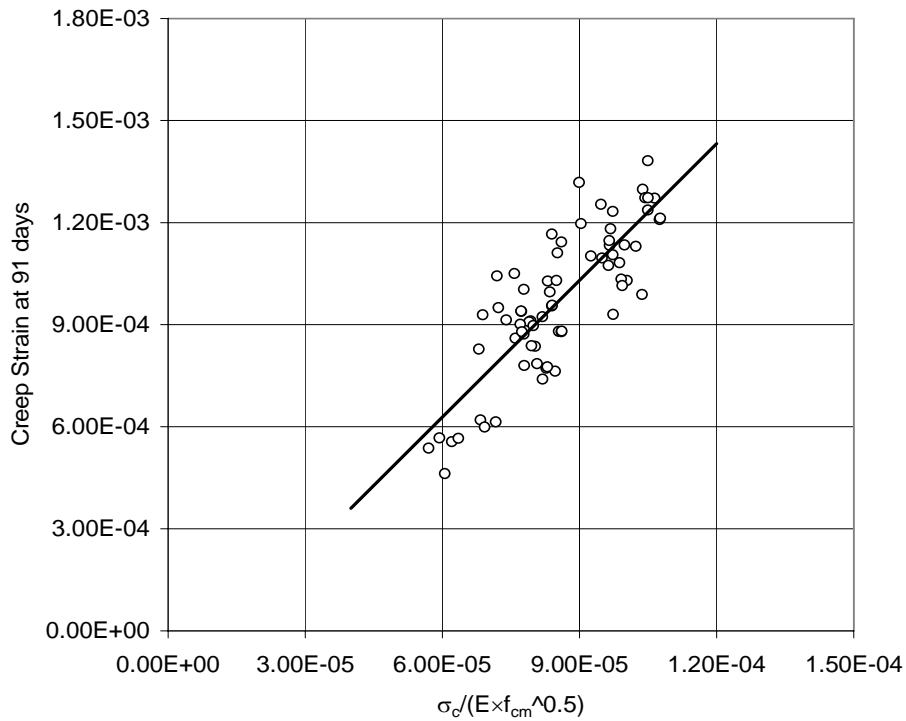


Figure 7-16. Relationship between creep strain and mechanical properties at loading age.

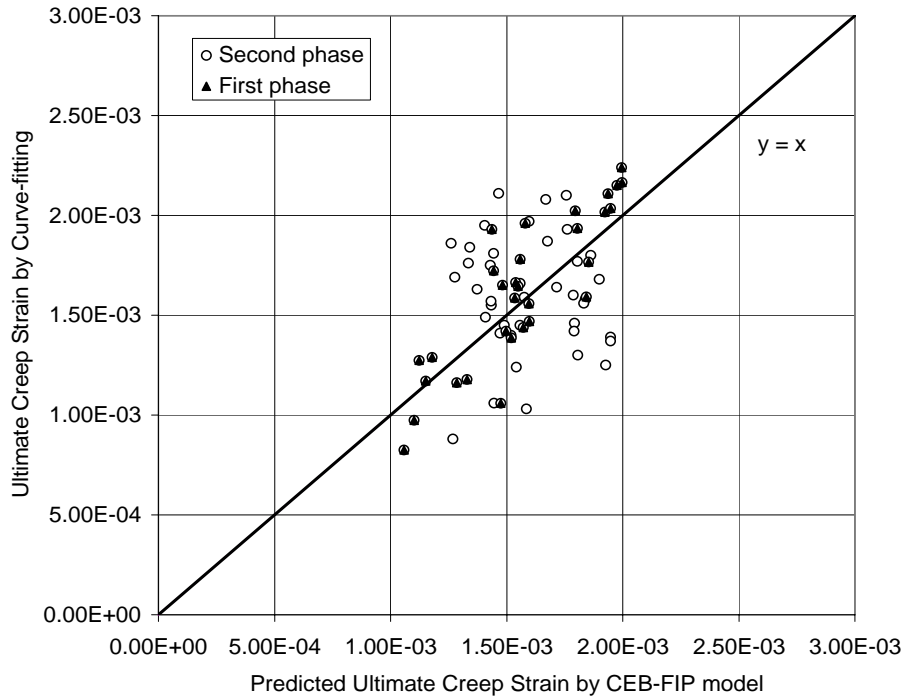


Figure 7-17. Comparison between the ultimate creep strain calculated by CEB-FIP model and that by curve-fitting.

7.4.3 ACI-209R Model

Evaluation of the ACI 209 model was performed in this study. The ACI 209 (1992) model is given as follows:

$$\phi_{28}(t, t_0) = \phi_{\infty}(t_0) \cdot \frac{(t-t_0)^{0.6}}{10 + (t-t_0)^{0.6}} \quad (7-23)$$

where $\phi_{28}(t, t_0)$ = creep coefficient at time t ;

$\phi_{\infty}(t_0)$ = ultimate creep coefficient; and

t_0 = time of loading (in this study, $t_0 = 14$ days for concrete cured for 14 days before loading; and $t_0 = 28$ days for concrete cured for 28 days before loading).

The ultimate creep coefficient can be expressed as:

$$\phi_{\infty}(t_0) = \gamma_c \cdot \phi_{\infty} \quad (7-24)$$

The constant $\phi_{\infty} = 2.35$ is recommended. The correction factor (γ_c) consists of the following terms:

$$\gamma_c = \gamma_{la} \cdot \gamma_{RH} \cdot \gamma_{at} \cdot \gamma_s \cdot \gamma_p \cdot \gamma_a \quad (7-25)$$

where γ_{la} = correction factor for loading age (0.916 for specimen cured for 14 days, and 0.814 for specimen cured for 28 days);

γ_{RH} = correction factor for ambient relative humidity (for this study, the ambient relative humidity is 75%, so $\gamma_{RH} = 0.77$);

γ_s = correction factor for slump of fresh concrete ($\gamma_s = 0.82 + 0.00264 \cdot S_l$) (S_l is slump in mm);

γ_p = correction factor for fine-to-total aggregate ratio ($\gamma_p = 0.88 + 0.0024 \cdot \rho_a$) (ρ_a is fine-to-total aggregate ratio);

γ_a = correction factor for air content ($\gamma_a = 0.46 + 0.09 \cdot a_a$) (a_a is air content); and

γ_{at} = correction factor for thickness of member (in this study, the volume-surface ratio method was used to obtain γ_{at} :

$$\gamma_{at} = \frac{2}{3} \cdot \left[1 + 1.13 \cdot e^{-0.0213 \cdot \left(\frac{v}{s}\right)} \right] \quad (7-26)$$

where v/s = volume-to-surface ratio in mm.

The correction factors based on the concrete mixtures, geometry of specimen, and ambient conditions employed in this study for the ACI 209 model are provided in Table 7-6.

Table 7-6. Correction Factors for the ACI 209 Model

Mix	γ_{la}		γ_{RH}	γ_s	γ_a	γ_{at}	γ_p	γ_c	
	7-day moist	14-day moist						7-day moist	14-day moist
1F	0.916	0.814	0.77	1.34	0.57	1.00	0.88	0.30	0.27
2F	0.916	0.814	0.77	1.32	0.87	1.00	0.88	0.45	0.40
3F	0.916	0.814	0.77	0.92	0.69	1.00	0.88	0.36	0.32
4F	0.916	0.814	0.77	1.02	0.64	1.00	0.88	0.33	0.29
5S	0.916	0.814	0.77	1.31	0.80	1.00	0.88	0.42	0.37
6S	0.916	0.814	0.77	1.05	0.66	1.00	0.88	0.34	0.30
7S	0.916	0.814	0.77	1.09	0.96	1.00	0.88	0.50	0.44
8S	0.916	0.814	0.77	1.00	0.80	1.00	0.88	0.41	0.37
9LF	0.916	0.814	0.77	0.82	0.73	1.00	0.88	0.38	0.33
10LS	0.916	0.814	0.77	0.82	0.93	1.00	0.88	0.48	0.43
2GF	0.916	0.814	0.77	1.12	1.13	1.00	0.88	0.58	0.52
3GF	0.916	0.814	0.77	0.99	0.60	1.00	0.88	0.31	0.27
5GS	0.916	0.814	0.77	1.26	0.96	1.00	0.88	0.50	0.44
7GS	0.916	0.814	0.77	0.97	0.80	1.00	0.88	0.41	0.37

As can be seen from Figure 7-18, the ACI 209 model extremely underestimates the creep strain of concretes investigated in this study.

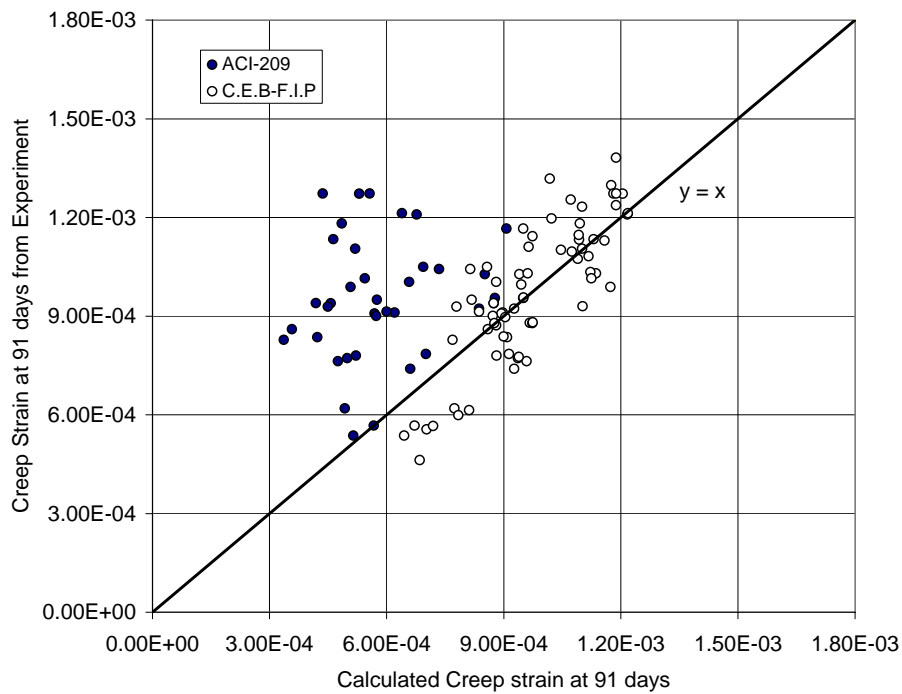


Figure 7-18. Evaluation on ACI-209 model and CEB-FIP model.

7.5 Summary of Findings

This chapter has presented the results of the creep tests conducted in this study. The following is a summary of the major findings from the creep tests:

- 1) Curing condition had a significant effect on the creep behavior of concrete evaluated in this study. Concretes which had been moist-cured for 14 days had substantially lower creep coefficients than those which had been moist-cured for only 7 days.
- 2) For the stress levels used (40% and 50% of compressive strength), the measured creep strain was linearly proportional to the stress applied. Thus, the computed creep coefficients were not affected by the stress level in this study.
- 3) The creep coefficient of the concrete using Georgia granite was much higher than that of the concrete using Miami Oolite limestone aggregate.
- 4) A linear relationship was found between creep coefficient at 365 days and compressive strength (f'_c). The regression equation which related compressive strength at loading age to creep coefficient at 360 days (ϕ_c) is given as follows:

$$\phi_c = \alpha \cdot f'_c + \beta \quad (7-1)$$

where α is equal to -3.39×10^{-4} and β is equal to 4.302. f'_c is in unit of psi.

- 5) Ultimate creep coefficient of some of the concretes appeared to exceed 2.0. These concrete mixtures included Mixes 2F, 3F, 4F, 5S, 6S, 7S, 8S, 2GF, 3GF, 5GS, 6GS, and 7GS.
- 6) The CEB-FIP model (as shown in Equation 7-16) appeared to give better prediction on the creep behaviors of concretes investigated in this study than ACI 209 model (as shown in Equation 7-22).

CHAPTER 8 CONCLUSIONS AND RECOMMENDATIONS

8.1 Design of Creep Apparatus

Performance and characteristics of the creep apparatus designed for this study are presented as follows:

- 1) The creep apparatus designed in this study was capable of applying and maintaining a load up to 145,000 lb on the test specimens with an error of less than 2%.
- 2) Three specimens could be stacked for simultaneous loading.
- 3) When a maximum load of 145,000 lb was applied, the deflection of bearing surfaces of the header plates was less than 0.001", and the pressure distribution on the test specimen varied by less than 0.026%, or 1.5 psi.
- 4) The creep testing procedures developed in this study were found to work very well. Details are given in Section 4.3.

8.2 Findings from This Study

8.2.1 Strength and Elastic Modulus

- 1) The splitting tensile strength of the concrete mixtures using granite aggregate was significantly lower than that of mixtures using Miami Oolite limestone aggregate. This is probably due to the poor bonding condition between hardened cement paste and granite aggregate.
- 2) The compressive strength of concretes with granite aggregate was comparable to or lower than that of concretes with Miami Oolite limestone aggregate.
- 3) The concrete with granite aggregate had higher elastic modulus than that with Miami Oolite limestone aggregate, while the lightweight aggregate concretes had lower elastic modulus than the normal weight concretes.
- 4) Fly ash concretes developed compressive strength and splitting tensile strength at a slower rate than the slag concretes. Fly ash concrete showed significant strength gain after 28 days, while this was not seen in the slag concrete mixtures.

- 5) The relationship between compressive strength (f'_c) and splitting tensile strength (f_{ct}) was established for the concrete mixtures investigated in this study. The Carino and Lew model, given as follows,

$$f_{ct} = 1.15(f'_c)^{0.71}$$

was modified to the following equation:

$$f_{ct} = 2.4(f'_c)^{0.62}$$

where f'_c and f_{ct} are in units of psi.

- 6) The relationship between compressive strength and modulus of elasticity was refined in this study using least square of curve-fitting technique. The ACI 318-89 equation, which is

$$E_c = 57000\sqrt{f'_c}$$

was modified to the following equation:

$$E_c = \alpha\sqrt{f'_c}$$

where α is equal to 55,824 for Miami Oolite limestone aggregate; 63,351 for Georgia granite aggregate; and 43,777 for Stalite lightweight aggregate, and f'_c and E_c are in units of psi.

- 7) For all three aggregate types investigated in this study, a modified ACI 318-95 prediction equation was developed:

$$E = 31.92 \cdot w^{1.5} \cdot \sqrt{f'_c} + 345300$$

where w is the density of concrete in pound per cubic foot, and f'_c and E_c are in units of psi.

8.2.2 Shrinkage Characteristics of Concretes Investigated

- 1) Fly ash concrete mixtures had slightly higher shrinkage strain at 91 days than slag concretes. This is probably due to the slow hydration rate of fly ash in comparison with that of slag. As a result of a slower rate of hydration, there is more free water evaporating from the interior of

the concrete, which may cause the concrete to shrink more. Thus, it is recommended that using a longer wet-curing time would be helpful to reduce shrinkage of fly ash concrete.

- 2) Water content had a significant effect on drying shrinkage strain of concrete. The higher the water content, the more the concrete tended to shrink. However, no clear trend can be seen on the effects of the water-to-cementitious materials ratio on shrinkage of concrete.
- 3) The predicted ultimate shrinkage strain of concrete made with Georgia granite was slightly lower than that of the corresponding concrete made with Miami Oolite limestone aggregate. Lightweight aggregate concrete shrank more than the normal weight aggregate concrete. This might be explained by their difference in elastic modulus. The concrete with higher elastic modulus had a stronger resistance to the movement caused by shrinkage of the cement paste.
- 4) For the concretes tested, there appeared to be a relationship between the compressive strength (f'_c) at the age when the shrinkage test was started and the shrinkage strain (ϵ_{sh}) at 91 days as follows:

$$\epsilon_{sh} = 0.000414 \cdot e^{-0.0000745 \cdot f'_c}$$

where f'_c is in unit of psi.

- 5) For the concretes tested, there appeared to be a relationship between elastic modulus (E_c) at the age when the shrinkage test was started and the shrinkage strain (ϵ_{sh}) at 91 days as follows:

$$\epsilon_{sh} = 0.000562 \cdot e^{-1.92 \times 10^{-7} \cdot E_c}$$

where E_c is in unit of psi.

- 6) According to the shrinkage test results from this study, the CEB-FIP model (as shown in Equation 6-6) appeared to give better prediction than the ACI 209 model (as shown in Equation 6-3). Using the ACI 209 model may result in over-estimation of the ultimate shrinkage strain.
- 7) For the concrete investigated in this study, the ultimate shrinkage strain ranged from 1.37×10^{-4} to 3.14×10^{-4} for the concrete with Georgia granite aggregate; from 2.02×10^{-4}

to 3.34×10^{-4} for the concrete with Miami Oolite limestone aggregate; and from 3.49×10^{-4} to 4.22×10^{-4} for the concrete with Stalite lightweight aggregate concrete.

8.2.3 Creep Characteristics of Concretes Investigated

- 1) Curing condition had a significant effect on the creep behavior of concrete evaluated in this study. The concretes which had been moist-cured for 14 days had substantially lower creep coefficients than those which had been moist-cured for only 7 days.
- 2) For the stress levels used (40% and 50% of compressive strength), the measured creep strain was linearly proportional to the stress applied. Thus, the computed creep coefficients were not affected by the stress level in this study.
- 3) The creep coefficient of the concrete using Georgia granite was much higher than that of the concrete using Miami Oolite limestone aggregate.
- 4) Linear relationship was found between creep coefficient at 365 days and compressive strength (f'_c). The regression equation which related compressive strength at loading age to creep coefficient at 360 days (ϕ_c) is given as follows:

$$\phi_c = \alpha \cdot f'_c + \beta$$

where α is equal to -3.39×10^{-4} ; β equal to 4.302, and f'_c is in unit of psi.

- 5) Ultimate creep coefficient of some of the concretes appeared to exceed 2.0. These concrete mixtures included Mixes 2F, 3F, 4F, 5S, 6S, 7S, 8S, 2GF, 3GF, 5GS, 6GS, and 7GS.
- 6) The CEB-FIP model (as shown in Equation 7-16) appeared to give better prediction on the creep behaviors of concretes investigated in this study than the ACI 209 model (as shown in Equation 7-22).

8.3 Recommendations

Based on this study, the following recommendations are given:

- 1) Further study on effects of aggregate gradation on shrinkage and creep of concrete. Since the gradation of aggregate has a great effect on the compressive strength of concrete and compressive strength was found to be related to shrinkage and creep in the present study, the effects of aggregate gradation on shrinkage and creep behavior of concrete should be studied

in order to have a better understanding of the effect of this factor on shrinkage and creep of concrete.

- 2) Further study on the optimization of mix proportion. The optimization of mix proportion should be studied for reducing shrinkage and creep of concrete.
- 3) Further study on the interfacial characteristics between coarse aggregate and mortar paste in order to have a better interpretation on the effects of different aggregate types on strength of concrete.
- 4) Further study on rheological properties of concrete under sustained load in order to have a better understanding about the creep behavior of concrete.

REFERENCES

- AASHTO (American Association of State Association of State Highway and Transportation Officials). (2001). *AASHTO LRFD Bridge Construction Specifications-2001 Interim Revisions*. AASHTO, Washington, D.C.
- ACI 209 (American Concrete Institute). (1992). "Prediction of Creep, Shrinkage, and Temperature Effects in Concrete Structures," *ACI Manual of Concrete Practice*. ACI Committee 209, Detroit, Michigan, Part 1, pp.47.
- ACI 318 (American Concrete Institute). (1983). *Building Code Requirements for Reinforced Concrete*. ACI, Detroit, Michigan, November.
- ACI 363 (American Concrete Institute). (1992). *State-of-the-Art Report on High-Strength Concrete*. ACI Committee 363, Detroit, Michigan.
- Aitcin, P-C., and Mehta, P. K. (1990). "Effect of Coarse Aggregate Characteristics on Mechanical Properties of High Strength Concrete." *ACI Materials Journal*, Vol. 87, No. 2, Mar.-Apr., pp. 103-107.
- Alexander, M. G. (1996). "Aggregates and the Deformation Properties of Concrete." *Materials Journal*, Vol. 93, Issue 6, Nov 1.
- Alexander, M. G., and Addis, B. J. (1992). "Properties of High Strength Concrete Influenced by Aggregates and Interfacial Bond." *Proceedings*, CEB International Conference on Bond in Concrete: From Research to Practice, Oct. 15-17, Riga Technical University, Riga, Latvia, Vol. 2, Topics 3-7, pp. 4-19 – 4-26.
- Alfes, C. (1992). "Modulus of Elasticity and Drying Shrinkage of High-Strength Concrete Containing Silica Fume." *Proceedings*, 4th International Conference on Use of Fly Ash, Silica Fume, Slag, and Natural Pozzolans in Concrete, May 3-8, 1992, Istanbul, Turkey, Sponsored by CANMET in association with the American Concrete Institute and others. V. M. Malhotra, Ed. American Concrete Institute, Detroit, Michigan, ACI SP-132, Vol. 2, pp. 1651-71.
- Aykut, C., and Carrasquillo, R. L. (1998). "High-Performance Concrete: Influence of Coarse Aggregates on Mechanical Properties." *Materials Journal*, Vol. 95, Issue 3, May 1.
- Baalbaki, W., Benmokrane, B., Chaallal, O., and Aitcin, P-C. (1991). "Influence of Coarse Aggregate on Elastic Properties of High Performance Concrete." *ACI Materials Journal*, Vol. 88, No. 5, Sep.-Oct., pp. 499-503.
- Bazant, Z. P., and Carol, I. (Eds.). (1993). *Creep and Shrinkage of Concrete*. Spon, London.
- Beshr, H., Almusallam, A., and Maslehuddin, M. (2003). "Effect of Coarse Aggregate Quality on the Mechanical Properties of High Strength Concrete." *Construction and Building Materials*, Vol. 17, No. 2, Mar., pp. 97-103 (7).

- Bisschop, J., and Van Mier, J. G. M. (2000). Effect of Aggregates on Drying Shrinkage Micro-cracking in Cement-based Materials. *Proceedings, United Engineering Foundation (UEF) Conference, Mt.-Tremblant, Canada, August (Con. Sc. Techn).*
- Carino, N. J., and Lew, H. S. (1982). "Re-examination of the Relation Between Splitting Tensile and Compressive Strength of Normal Weight Concrete." *Journal of American Concrete Institute*, Vol. 79, No. 3, May-Jun., pp. 214-219.
- CEB-FIP (Comité Euro-International du Béton-Federation Internationale de la Precontrainte). (1990). "Model Code for Concrete Structures." First draft. *Bulletin d' information No. 195*, Paris.
- Chi, J. M., Huang, R., Yang, C. C., and Chang, J. J. (2003). "Effect of Aggregate Properties on the Strength and Stiffness of Lightweight Concrete." *Cement & Concrete Composites*, Vol. 25, pp. 197-205.
- Collins, T. M. (1989). "Proportioning High-Strength Concrete to Control Creep and Shrinkage." *ACI Materials Journal*, Vol. 86, No. 6, Nov.-Dec., pp. 576-580.
- El-Hindy, E., Miao, B. O., Chaallal, O., and Aitcin, P. C. (1994). "Drying Shrinkage of Ready Mixed High-performance Concrete." *ACI Materials Journal*, Vol. 91, p. 300.
- Ezeldin, A. S., and Aitcin, P-C. (1991). "Effect of Coarse Aggregate on the Behavior of Normal and High Strength Concretes." *Cement, Concrete and Aggregates*, Vol. 13, No. 2, Winter, pp. 121-124.
- FDOT (Florida Department of Transportation). (2002). *Structural Design Guidelines for Load and Resistance Factor Design*. Structural Design Office, Tallahassee, Florida.
- Gesoğlu, M., Zturan, T., and Güneyisi, E. (2004). Shrinkage Cracking of Lightweight Concrete Made with Cold-bonded Fly Ash Aggregates. *Cement and Concrete Research*, Vol. 34, pp. 1121-1130.
- Giaccio, G., Rocco, C., Violini, D., Zappitelli, J., and Zerbino, R. (1992). "High Strength Concrete Incorporating Different Coarse Aggregates." *ACI Materials Journal*, Vol. 89, No. 3, May-Jun., pp. 242-246.
- Hermite, R. L. (1960). "Volume Changes of Concrete." *Proceedings, 4th International Symposium on the Chemistry of Cement*, Washington D.C., pp. 659-694.
- Hua, C., Acker, P., and Ehrlacher, A. (1995). "Analysis and Modeling of the Autogenous Shrinkage of Hardening Cement Paste: I. Modeling at Macroscopic Scale." *Cement and Concrete Research*, Vol. 25, No. 7, pp. 1457-1468.
- Huo, X., Al-Omaishi, N., and Tadros, M. K. (2001). "Creep, Shrinkage and Modulus of Elasticity of High Performance Concrete." *ACI Materials Journal*, Vol. 98, No. 6, pp. 440-449.

- Leming, M. L. (1990). "Comparison of Mechanical Properties of High Strength Concrete Made with Different Raw Materials." In *Transportation Research Record (TRR): Journal of the Transportation Research Board (TRB)*, No. 1284, TRB of the National Academies, Washington, D.C., pp. 23-30.
- Lindgard, J., and Smeplass, S. (1993). "High Strength Concrete Containing Silica Fume—Impact of Aggregate Type on Compressive Strength and Elastic Modulus." *Proceedings*, 4th International Conference on Use of Fly Ash, Silica Fume, Slag, and Natural Pozzolans in Concrete, May 3-8, 1992, Istanbul, Turkey, Sponsored by CANMET in association with the American Concrete Institute and others. V. M. Malhotra, Ed. American Concrete Institute, Detroit, Michigan, ACI SP-132, Vol. 2, pp. 1061-1074.
- McQueen, R. D., Rapol, J., and Flynn, R. (2002). "Development of Material Requirements for Portland Cement Concrete Pavements at the FAA National Airport Pavement Test Facility." *Proceedings*, 2002 FAA Worldwide Airport Technology Transfer Conference, Atlantic City, New Jersey, USA.
- Neville, A. M. (1996). *Properties of Concrete*. (Fourth and Final Edition). John Wiley & Sons, Inc., New York.
- Nilsen, A. U., and Aitcin, P-C. (1992). "Properties of High Strength Concrete Containing Light, Normal, and Heavyweight Aggregate." *Cement, Concrete, and Aggregates*, Vol. 14, No. 1, Summer, pp. 8-12.
- Ozyildirim, C. (2000). "Evaluation of High-Performance Concrete Pavement in Newport News, VA." *Draft Interim Report*, Virginia Transportation Research Council, Charlottesville.
- Persson, B. (2001). "A Comparison Between Mechanical Properties of Self-compacting Concrete and the Corresponding Properties of Normal Concrete." *Cement and Concrete Research*, Vol. 31, pp. 193 –198.
- Pichett, G. (1956). "Effect of Aggregate on Shrinkage of Concrete and Hypothesis Concerning Shrinkage." *Journal of American Concrete Institute*, Vol. 52, pp. 581-590.
- Rashid, M. A., Mansur, M., and Paramasivam, P. (2002). "Correlations Between Mechanical Properties of High-Strength Concrete." *Materials Journal*, Vol. 14, Issue 3, May/June, pp. 230-238.
- Reichard, T. W. (1964). "Creep and Drying Shrinkage of Lightweight and Normal Weight Concretes." *National Bureau of Standards Monograph No. 74*, Washington D.C., March.
- Rüsch, H., Kordina, K., and Hilsdorf, H. (1963). "Der Einfluss des Mineralogischen Charakters der Zuschläge auf das Kriechen von Beton." *Deutscher Ausschuss für Stahlbeton*, No. 146, pp. 19-133.

- Sarkar, S. L., and Aitcin, P.-C. (1990). "Importance of Petrological, Petrographical and Mineralogical Characteristics of Aggregates in Very High Strength Concrete." *ASTM Special Technical Publication*, No. 1061, pp. 129-144.
- Schlumpf, J. (2004). "Self-compacting Concrete Structures in Switzerland." *Tunneling and Underground Space Technology*, Vol. 19, p. 480.
- Shideler, J. J. (1957). "Lightweight Aggregate Concrete for Structural Use." *Journal of American Concrete Institute*, Vol. 54, pp. 299-328.
- Shih, T. S., Lee, G. C., and Chang, K. C. (1989). "On Static Modulus of Elasticity of Normal Weight Concrete." *Journal of Structural Engineering*, Vol. 115, No. 10, Oct., pp. 2579-2587.
- Stock, A.F., Hannant, D. J., and Williams, R.I.T. (1979). "The Effect of Aggregate Concentration upon the Strength and Modulus of Elasticity of Concrete." *Magazine of Concrete Research*, Vol. 31, No. 109, pp. 225-234.
- Troxell, G.E., Raphael, J. M., and Davis, R. E. (1958). "Long-time Creep and Shrinkage Tests of Plain and Reinforced Concrete." *Proceedings, American Society for Testing and Materials (ASTM)*, Vol. 58, pp. 1101-1120.
- Wu, K.-R., Chen, B., Yao, W., and Zhang, D. (2001). "Effect of Coarse Aggregate Type on Mechanical Properties of High-performance Concrete." *Cement and Concrete Research*, Vol. 31, No. 10, Oct., pp. 1421-1425 (5).
- Zhou, F. P., Lydon, F. D., and Barr, B. I. G. (1995). "Effect of Coarse Aggregate on Elastic Modulus and Compressive Strength of High Performance Concrete." *Cement and Concrete Research*, Vol. 25, No. 1, pp. 177-186.
- Zia, P., Ahmad, S. H., Leming, M. L., Schemmel, J. J., and Elliott, R. P. (1993a). *Mechanical Behavior of High Performance Concretes, Volume 3: Very Early Strength Concrete*. Strategic Highway Research Program (SHRP), National Research Council (NRC), Washington, D.C., SHRP-C-363, xi, 116 pp.
- Zia, P., Ahmad, S. H., Leming, M. L., Schemmel, J. J., and Elliott, R. P. (1993b). *Mechanical Behavior of High Performance Concretes, Volume 4: High Early Strength Concrete*. SHRP, NRC, Washington, D. C., SHRP-C-364, xi, 179 pp.
- Zia, P., Ahmad, S. H., Leming, M. L., Schemmel, J. J., and Elliott, R. P. (1993c). *Mechanical Behavior of High Performance Concretes, Volume 5: Very High Strength Concrete*. SHRP, NRC, Washington, D. C., SHRP-C-365, xi, 101 pp.

APPENDIX A

MEASUREMENTS FROM STRENGTH TESTS

Table A-1. Results of Compressive Strength Tests (psi)

No. of mix	Age of Testing (days)																	
	3			7			14			28			56			91		
	1	2	3	1	2	3	1	2	3	1	2	3	1	2	3	1	2	3
1F(1r)	8018	8091	8123	8556	8554	8607	8929	8869	9182	9319	9811	9479	10665	10799	10847	11123	11302	11376
2F(1y)	4110	4195	3927	4660	4680	4635	6053	6032	5999	6499	6268	6752	6661	6604	6648	7631	7582	7609
3F(1y)	5325	5424	5118	6448	6449	6512	7475	7649	7578	8229	8147	8349	8479	8400	8468	9415	9496	9366
4F(1y)	5669	5783	5684	7075	6762	6922	7224	7208	6910	7038	7509	7160	8668	8994	9325	9273	9072	9467
5S(1y)	4359	4238	4549	5058	5094	5657	5553	5911	6232	5401	5919	5401	-	-	-	6148	6585	6643
5S(3m)	5351	5772	5539	7059	7739	6908	7995	8208	8541	8684	8924	8888	9071	9255	9092	9348	9615	9406
6S(1y)	5373	5590	4795	6060	5536	5852	6232	5748	5764	5707	6657	5754	-	-	-	-	-	-
6S(3m)	6300	6402	6423	7776	7316	8004	8211	8481	8169	8684	9127	9223	9604	9540	9593	9779	9734	9770
7S(1y)	3839	3759	3329	3570	3778	4255	4138	4381	4260	5065	4754	6077	4664	4480	4723	3778	5072	3442
7S(3m)	4323	4482	4166	5311	5435	5375	5993	5902	5886	6346	6441	6389	6773	6812	6798	6990	6837	6923
8S(1y)	2297	3517	3490	3620	4062	4183	4429	4375	4746	4806	4971	4602	4723	4551	5367	4008	5076	4560
8S(3m)	4415	5017	4954	5831	6202	6308	6879	6967	6971	7544	7282	7749	7856	8253	8249	8262	8148	8214
9LF(1y)	3019	3007	3092	3911	3939	3974	5039	5174	5194	5981	5999	5806	6655	6953	6462	7043	7092	6750
10LS(1y)	1486	1411	1504	2175	2310	2088	2749	2860	3201	3760	3811	3660	4496	4204	4236	4863	4725	4595
1GF(1y)	6627	7306	6889	7931	6918	7153	7059	7381	7297	8719	7850	8567	7820	8751	8827	-	-	-
1GF(3m)	6341	6811	6505	7483	7854	7219	7119	7361	5579	7572	7776	8513	8797	8752	8541	-	-	-
2GF(1y)	3982	3867	3807	4922	5046	4888	5874	5812	5735	6440	6388	6579	6887	7001	6969	7387	6909	7308
2GF(3m)	4041	3792	3733	4787	4107	4372	5133	5065	4555	5594	5880	5488	6163	6181	6524	6399	7006	6380
3GF(1y)	2960	2865	3099	4810	4612	4655	5468	5778	5829	6816	7075	7134	7818	7801	7943	7862	7915	8105
3GF(3m)	3971	3824	3971	4525	4711	4332	5101	5230	5195	5854	5815	5574	5598	7137	6451	6879	6631	6906
4GF(1y)	4787	4930	4950	4913	4910	5139	5804	5858	5258	6377	6565	6397	7711	7060	7814	-	-	-
4GF(3m)	4173	4154	4404	5321	3276	5832	5658	5424	5732	6117	6191	6348	7258	6967	7991	-	-	-
5GS(1y)	3746	3861	3847	5098	5211	5145	6196	6087	6127	7000	7409	7377	7895	7683	7769	8047	8090	7986
5GS(3m)	2731	2789	2618	4213	4462	4111	4419	4467	4621	5711	5362	4416	5702	6737	5254	4781	5305	5305
6GS(1y)	2686	2625	2650	3291	3873	3549	4842	5031	5466	5166	5885	5834	6947	7164	6841	-	-	-
6GS(3m)	-	-	-	4998	4961	5177	5650	6432	6058	7051	6870	6931	6424	6984	6900	7301	7617	6840
7GS(1y)	2249	2205	2346	4433	4178	4298	5308	5182	5175	6601	6603	6632	7072	6629	7176	7226	7200	7273
7GS(3m)	2335	2295	2202	3599	3509	3597	3956	4142	4009	5154	5173	4936	5279	4614	5728	5471	6288	5659
8GS(1y)	1989	2165	2214	-	-	-	4050	3658	3840	5003	4772	5208	5873	6540	6360	-	-	-
8GS(3m)	-	-	-	3666	3433	3536	3807	3986	3905	4541	5023	4803	5568	5024	5320	5162	5316	5417

Table A-2. Normalized Compressive Strength Development Characteristics of the Concrete Mixtures Evaluated

Mix Number	W/C	Fly ash	Slag	Age of Testing (days)					
				3	7	14	28	56	91
1F(1y)	0.24	20%	---	0.72	0.76	0.80	0.85/0.93*	0.96	1.00
2F(1y)	0.33	20%	---	0.54	0.61	0.79	0.86/0.87*	0.90	1.00
3F(1y)	0.41	20%	---	0.56	0.69	0.80	0.87/0.85*	0.90	1.00
4F(1y)	0.37	20%	---	0.62	0.75	0.77	0.78/0.87*	0.97	1.00
5S(1y)	0.33	---	50%	0.68	0.82	0.91	0.86	0.95	1.00
5S(3m)	0.33	---	50%	0.59	0.77	0.87	0.93/0.99*	0.97	1.00
6S(1y)	0.36	---	50%	0.75	0.83	0.84	0.86	---	1.00
6S(3m)	0.36	---	50%	0.66	0.80	0.89	0.94/0.95*	0.99	1.00
7S(1y)	0.41	---	70%	0.89	0.94	1.04	1.29	1.13	1.00
7S(3m)	0.41	---	70%	0.63	0.78	0.86	0.92/0.93*	0.98	1.00
8S(1y)	0.44	---	50%	0.68	0.87	0.99	1.05	1.07	1.00
8S(3m)	0.44	---	50%	0.58	0.74	0.85	0.92/0.92*	0.99	1.00
9LF(1y)	0.31	20%	---	0.44	0.57	0.74	0.85/0.84*	0.96	1.00
10LS(1y)	0.39	---	60%	0.31	0.46	0.62	0.79/0.85*	0.91	1.00
1GF(1y)	0.24	20%	---	---	---	---	---	---	---
1GF(3m)	0.24	20%	---	---	---	---	---	---	---
2GF(1y)	0.33	20%	---	0.54	0.69	0.81	0.90	0.97	1.00
2GF(3m)	0.33	20%	---	0.58	0.67	0.75	0.86	0.95	1.00
3GF(1y)	0.41	20%	---	0.47	0.64	0.76	0.90	0.97	1.00
3GF(3m)	0.41	20%	---	0.58	0.66	0.76	0.84	0.94	1.00
4GF(1y)	0.37	20%	---	---	---	---	---	---	---
4GF(3m)	0.37	20%	---	0.57	0.65	0.76	0.84	0.94	1.00
5GS(1y)	0.33	---	50%	0.37	0.58	0.70	0.86	0.97	1.00
5GS(3m)	0.33	---	50%	0.53	0.83	0.88	1.01	1.15	1.00
6GS(1y)	0.36	---	50%	0.41	0.55	0.78	0.86	1.07	1.00
6GS(3m)	0.36	---	50%	---	0.70	0.83	0.96	0.93	1.00
7GS(1y)	0.41	---	70%	0.31	0.59	0.72	0.91	0.93	1.00
7GS(3m)	0.41	---	70%	0.39	0.61	0.70	0.88	0.90	1.00
8GS(1y)	0.44	---	50%	0.34	---	0.64	0.81	1.02	1.00
8GS(3m)	0.44	---	50%	---	0.67	0.74	0.90	1.00	1.00

Table A-3. Results of Splitting Tensile Strength Tests (psi)

No. of Mix	Age of Testing (days)																	
	3			7			14			28			56			91		
	1	2	3	1	2	3	1	2	3	1	2	3	1	2	3	1	2	3
1F(1y)	621	573	582	657	613	614	673	768	706	823	794	770	833	826	844	863	834	851
2F(1r)	397	428	401	501	484	468	551	521	515	545	542	539	650	596	617	675	645	658
3F(1y)	503	527	510	550	502	568	579	541	567	644	620	608	678	673	671	740	722	731
4F(1y)	480	434	459	604	440	517	581	455	663	678	684	647	776	737	764	796	748	766
5S(1y)	389	475	498	435	387	605	636	665	562	508	676	659	-	-	-	661	629	703
5S(3m)	492	429	405	567	557	599	724	507	677	757	615	697	716	704	713	748	772	695
6S(1y)	673	651	679	655	486	544	648	595	571	635	632	655	483	703	685	454	520	616
6S(3m)	607	523	580	633	586	589	616	755	575	696	658	663	711	654	707	728	708	719
7S(1y)	359	330	413	438	448	408	487	487	391	500	388	443	530	464	476	422	527	539
7S(3m)	430	415	434	467	476	475	553	509	493	567	604	473	489	657	625	572	602	616
8S(1y)	416	410	370	379	460	327	540	537	531	504	476	507	515	513	412	504	455	437
8S(3m)	324	383	409	428	512	557	555	530	564	617	603	681	702	691	686	696	709	704
9LF(1y)	283	369	399	425	350	438	470	460	416	472	486	512	563	549	542	579	601	552
10LS(1y)	211	203	222	316	295	253	366	351	376	413	404	400	433	401	420	444	433	414
1GF(1y)	619	665	599	684	627	717	768	559	671	649	728	701	717	790	850	781	831	813
1GF(3m)	458	534	464	453	613	614	642	615	610	637	711	616	-	-	-	-	-	-
2GF(1y)	350	340	366	425	429	408	518	446	502	541	557	535	557	550	539	585	606	595
2GF(3m)	420	414	413	485	426	478	518	497	480	529	501	553	614	582	623	680	598	591
3GF(1y)	283	288	276	433	411	417	442	522	422	521	508	547	516	646	611	617	646	684
3GF(3m)	381	384	408	442	413	407	459	443	474	510	545	485	537	547	594	643	554	623
4GF(1y)	433	474	440	454	427	461	496	559	550	572	597	518	629	626	707	773	709	770
4GF(3m)	434	436	416	429	472	463	493	472	494	635	630	570	-	-	-	-	-	-
5GS(1y)	364	410	372	381	391	456	507	509	494	563	564	553	621	600	578	652	642	659
5GS(3m)	247	325	306	431	521	439	344	360	381	480	533	540	472	503	462	533	500	573
6GS(1y)	297	228	295	363	389	383	469	388	464	522	501	518	516	461	414	-	-	-
6GS(3m)	-	-	-	469	403	490	563	524	579	656	534	589	613	637	652	573	561	581
7GS(1y)	234	258	245	363	353	371	411	418	460	540	582	515	566	623	607	555	584	593
7GS(3m)	255	273	255	367	365	366	398	430	424	404	392	380	459	476	478	412	477	407
8GS(1y)	192	233	226	316	292	329	378	456	368	433	524	467	445	418	434	-	-	-
8GS(3m)	-	-	-	344	332	374	414	491	419	455	474	432	478	526	455	470	494	469

Table A-4. Normalized Splitting Tensile Strength Development Characteristics of the Concrete Mixtures Evaluated

Mix Number	W/C	Fly ash	Slag	Age of Testing (days)					
				3	7	14	28	56	91
1F(1y)	0.24	20%	---	0.70	0.74	0.84	0.94/0.86*	0.98	1.00
2F(1y)	0.33	20%	---	0.62	0.73	0.80	0.82/0.87*	0.94	1.00
3F(1y)	0.41	20%	---	0.70	0.74	0.77	0.85/0.83*	0.92	1.00
4F(1y)	0.37	20%	---	0.59	0.68	0.74	0.87/0.80*	0.99	1.00
5S(1y)	0.33	---	50%	0.68	0.72	0.94	0.92	0.97	1.00
5S(3m)	0.33	---	50%	0.60	0.78	0.86	0.93/0.92*	0.96	1.00
6S(1y)	0.36	---	50%	1.26	1.06	1.14	1.21	1.18	1.00
6S(3m)	0.36	---	50%	0.79	0.84	0.90	0.94/0.87*	0.96	1.00
7S(1y)	0.41	---	70%	0.74	0.87	0.92	0.90	0.99	1.00
7S(3m)	0.41	---	70%	0.71	0.79	0.87	0.92/0.87*	0.99	1.00
8S(1y)	0.44	---	50%	0.86	0.84	1.15	1.07	1.03	1.00
8S(3m)	0.44	---	50%	0.53	0.71	0.78	0.90/0.93*	0.99	1.00
9LF(1y)	0.31	20%	---	0.61	0.70	0.78	0.85	0.95	1.00
10LS(1y)	0.39	---	60%	0.49	0.67	0.85	0.94/0.82*	0.97	1.00
1GF(1y)	0.24	20%	---	0.78	0.84	0.82	0.86	0.97	1.00
1GF(3m)	0.24	20%	---	0.65	0.75	0.84	0.88	0.92	1.00
2GF(1y)	0.33	20%	---	0.59	0.71	0.82	0.89	0.92	1.00
2GF(3m)	0.33	20%	---	0.67	0.74	0.80	0.85	0.97	1.00
3GF(1y)	0.41	20%	---	0.59	0.63	0.77	0.86	0.92	1.00
3GF(3m)	0.41	20%	---	0.64	0.69	0.76	0.85	0.92	1.00
4GF(1y)	0.37	20%	---	0.60	0.60	0.71	0.75	0.87	1.00
4GF(3m)	0.37	20%	---	0.66	0.70	0.75	0.94	0.96	1.00
5GS(1y)	0.33	---	50%	0.43	0.65	0.71	0.81	0.91	1.00
5GS(3m)	0.33	---	50%	0.55	0.87	0.68	0.97	0.90	1.00
6GS(1y)	0.36	---	50%	0.55	0.76	0.88	1.03	0.93	1.00
6GS(3m)	0.36	---	50%	---	0.79	0.97	1.04	1.11	1.00
7GS(1y)	0.41	---	70%	0.42	0.63	0.75	0.87	0.96	1.00
7GS(3m)	0.41	---	70%	0.60	0.85	0.97	0.91	1.09	1.00
8GS(1y)	0.44	---	50%	0.50	0.72	0.93	1.10	1.00	1.00
8GS(3m)	0.44	---	50%	---	0.73	0.92	0.95	1.02	1.00

Table A-5. Results of Elastic Modulus Tests ($\times 10^6$ psi)

No. of Mix	Age of Testing (days)											
	3		7		14		28		56		91	
	1	2	1	2	1	2	1	2	1	2	1	2
1F(1y)	4.71	4.77	4.92	4.94	5.20	5.25	5.37	5.43	5.56	5.52	5.57	5.59
2F(1y)	3.47	3.38	3.72	3.82	4.11	4.04	4.28	4.34	4.46	4.40	4.77	4.50
3F(1y)	4.37	4.42	4.87	4.83	5.02	5.07	5.08	5.19	5.38	5.18	5.66	5.73
4F(1y)	4.50	4.47	4.63	4.59	4.85	4.90	4.98	5.03	5.16	5.14	5.33	5.25
5S(1y)	3.65	3.60	3.85	4.00	4.10	3.95	4.23	4.68	-	-	4.45	4.25
5S(3m)	4.11	4.11	4.53	4.78	4.86	4.89	5.06	5.12	5.19	5.26	5.23	5.22
6S(1y)	4.13	4.00	4.13	4.28	4.45	4.13	4.45	4.43	-	-	-	-
6S(3m)	4.42	4.11	4.97	4.86	5.08	5.28	5.23	5.67	5.48	5.75	5.54	5.78
7S(1y)	3.20	3.15	3.40	3.45	3.50	3.60	3.53	3.40	3.73	3.63	3.65	4.65
7S(3m)	3.99	3.80	4.30	4.30	4.53	4.51	4.59	4.61	4.75	4.71	4.78	4.74
8S(1y)	3.10	3.10	3.30	3.30	3.50	3.70	3.90	3.83	4.18	4.03	4.20	3.90
8S(3m)	3.87	4.04	4.43	4.35	4.90	4.78	5.02	4.98	5.14	5.12	5.16	5.15
9LF(1y)	2.71	2.81	2.94	2.90	3.16	3.10	3.29	3.25	3.34	3.36	3.69	3.31
10LS(1y)	1.77	1.73	2.01	1.74	2.40	2.32	2.73	2.65	3.07	2.94	2.98	3.09
1GF(1y)	5.23	5.18	5.18	5.40	5.45	5.48	5.63	5.85	5.78	5.78	-	-
1GF(3m)	5.10	4.98	5.53	5.30	5.43	5.80	5.48	5.53	5.83	5.65	-	-
2GF(1y)	3.61	3.99	4.10	4.33	4.59	4.63	4.85	5.07	5.17	5.06	5.25	5.12
2GF(3m)	4.33	3.80	4.53	4.25	4.45	4.55	5.05	4.93	4.95	5.18	5.55	5.50
3GF(1y)	4.08	4.21	4.28	4.95	5.56	5.48	5.62	5.59	5.83	6.03	5.95	5.97
3GF(3m)	4.23	4.25	4.48	4.63	4.88	4.83	5.05	5.15	5.60	5.50	5.40	5.93
4GF(1y)	4.45	4.15	4.38	4.45	4.68	4.60	5.05	4.80	5.30	5.38	-	-
4GF(3m)	4.63	4.35	3.05	5.15	4.78	4.93	5.10	5.10	5.58	5.85	-	-
5GS(1y)	3.24	3.06	3.66	3.97	4.54	4.76	5.42	4.92	5.48	5.26	5.47	5.64
5GS(3m)	2.85	2.85	4.08	3.75	4.25	4.15	4.30	4.03	4.78	4.05	4.10	4.10
6GS(1y)	2.75	2.85	3.53	3.45	4.25	4.05	4.75	4.80	5.45	5.25	-	-
6GS(3m)	-	-	4.15	4.55	4.95	5.10	5.38	5.45	5.60	5.65	5.70	5.75
7GS(1y)	2.63	2.74	3.28	3.48	4.05	4.14	5.17	5.33	5.64	5.56	5.77	5.68
7GS(3m)	2.55	2.30	3.05	3.65	3.93	3.60	4.43	4.50	4.90	4.90	4.75	4.70
8GS(1y)	2.75	2.58	-	-	3.95	3.83	4.10	4.20	5.00	4.70	-	-
8GS(3m)	-	-	3.30	3.80	4.40	4.30	4.95	4.80	5.05	4.95	4.85	4.90

APPENDIX B

MEASURED AND CALCULATED RESULTS FROM CREEP TESTS

Table B-1. Measured and Calculated Results from Creep Tests

No. of Mix	Curing condition	Load level	Strain	Age of testing (days)									
				3	7	14	28	56	91	180	270	360	
1F (1y) (W/C)=0.24	7-day moist cure	40% (3797 psi)	Total	1.16E-03	1.24E-03	1.33E-03	1.46E-03	1.60E-03	1.70E-03	1.80E-03	1.82E-03	1.83E-03	
			Shrinkage	2.11E-05	4.33E-05	7.56E-05	1.18E-04	1.63E-04	2.01E-04	2.31E-04	2.41E-04	2.44E-04	
			Elastic	7.16E-04	7.16E-04	7.16E-04	7.16E-04	7.16E-04	7.16E-04	7.16E-04	7.16E-04	7.16E-04	
			Creep	4.28E-04	4.84E-04	5.43E-04	6.22E-04	7.19E-04	7.84E-04	8.49E-04	8.68E-04	8.73E-04	
			Creep Modulus	3.32E+06	3.16E+06	3.02E+06	2.84E+06	2.65E+06	2.53E+06	2.43E+06	2.40E+06	2.39E+06	
			Creep Coefficient (computed)	0.59	0.67	0.75	0.86	0.99	1.08	1.17	1.20	1.20	
		Elastic Modulus at Time of Load: 5.23E+06 psi											
		Computed Elastic Strain at Time of Load: 7.26E-04											
		50% (4447 psi)	Total	1.31E-03	1.42E-03	1.52E-03	1.66E-03	1.84E-03	1.97E-03	2.09E-03	2.12E-03	2.14E-03	
			Shrinkage	2.11E-05	4.33E-05	7.56E-05	1.18E-04	1.63E-04	2.01E-04	2.31E-04	2.41E-04	2.44E-04	
			Elastic	8.39E-04	8.39E-04	8.39E-04	8.39E-04	8.39E-04	8.39E-04	7.16E-04	7.16E-04	7.16E-04	
			Creep	4.53E-04	5.34E-04	6.08E-04	7.04E-04	8.37E-04	9.29E-04	1.14E-03	1.17E-03	1.18E-03	
			Creep modulus	3.44E+06	3.24E+06	3.07E+06	2.88E+06	2.65E+06	2.52E+06	2.40E+06	2.36E+06	2.35E+06	
			Creep Coefficient (computed)	0.53	0.63	0.72	0.83	0.98	1.09	1.34	1.37	1.39	
		Elastic Modulus at Time of Load: 5.23E+06 psi											
		Computed Elastic Strain at Time of Load: 8.50E-04											

No. of Mix	Curing condition	Load level	Strain	Age of testing (days)									
				3	7	14	28	56	91	180	270	360	
1F (1y) (W/C) =0.24	14-day moist cure	40% (3915 psi)	Total	1.27E-03	1.35E-03	1.48E-03	1.57E-03	1.69E-03	1.77E-03	1.87E-03	1.89E-03	1.89E-03	
			Shrinkage	1.44E-05	3.33E-05	6.33E-05	1.00E-04	1.36E-04	1.67E-04	1.96E-04	2.04E-04	2.06E-04	
			Elastic	8.83E-04	8.83E-04	8.83E-04	8.83E-04	8.83E-04	8.83E-04	8.83E-04	8.83E-04	8.83E-04	
			Creep	3.77E-04	4.37E-04	5.36E-04	5.91E-04	6.71E-04	7.23E-04	7.90E-04	8.00E-04	8.03E-04	
			Creep modulus	3.11E+06	2.97E+06	2.76E+06	2.66E+06	2.52E+06	2.44E+06	2.34E+06	2.33E+06	2.32E+06	
			Creep Coefficient (computed)	0.52	0.60	0.74	0.82	0.93	1.00	1.09	1.10	1.11	
			Elastic Modulus at Time of Load: 5.40E+06 psi										
		Computed Elastic Strain at Time of Load: 7.25E-04											
		50% (4668 psi)	Total	1.16E-03	1.24E-03	1.33E-03	1.46E-03	1.60E-03	1.70E-03	1.80E-03	1.82E-03	1.83E-03	
			Shrinkage	1.44E-05	3.33E-05	6.33E-05	1.00E-04	1.36E-04	1.67E-04	1.96E-04	2.04E-04	2.06E-04	
			Elastic	7.16E-04	7.16E-04	7.16E-04	7.16E-04	7.16E-04	7.16E-04	7.16E-04	7.16E-04	7.16E-04	
			Creep	4.34E-04	4.94E-04	5.56E-04	6.40E-04	7.47E-04	8.19E-04	8.84E-04	9.04E-04	9.12E-04	
			Creep modulus	4.06E+06	3.86E+06	3.67E+06	3.44E+06	3.19E+06	3.04E+06	2.92E+06	2.88E+06	2.87E+06	
			Creep Coefficient (computed)	0.50	0.57	0.64	0.74	0.86	0.95	1.02	1.05	1.06	
	Elastic Modulus at Time of Load: 5.40E+06 psi												
	Computed Elastic Strain at Time of Load: 8.64E-04												

No. of Mix	Curing condition	Load level	Strain	Age of testing (days)									
				3	7	14	28	56	91	180	270	360	
2F (1y) (W/C) =0.33	7-day moist cure	40% (2411 psi)	Total	1.14E-03	1.31E-03	1.50E-03	1.73E-03	1.97E-03	2.14E-03	2.34E-03	2.42E-03	2.48E-03	
			Shrinkage	5.11E-05	9.67E-05	1.58E-04	2.14E-04	2.71E-04	3.13E-04	3.57E-04	3.67E-04	3.80E-04	
			Elastic	6.63E-04	6.63E-04	6.63E-04	6.63E-04	6.63E-04	6.63E-04	6.63E-04	6.63E-04	6.63E-04	
			Creep	4.27E-04	5.53E-04	6.83E-04	8.51E-04	1.04E-03	1.17E-03	1.32E-03	1.39E-03	1.44E-03	
			Creep Modulus	2.21E+06	1.98E+06	1.79E+06	1.59E+06	1.42E+06	1.32E+06	1.21E+06	1.17E+06	1.15E+06	
			Creep Coefficient (computed)	0.72	0.94	1.16	1.44	1.75	1.97	2.24	2.35	2.43	
		Elastic Modulus at Time of Load: 4.08E+06 psi											
		Computed Elastic Strain at Time of Load: 5.91E-04											
		50% (2984 psi)	Total	1.47E-03	1.61E-03	1.82E-03	2.06E-03	2.32E-03	2.50E-03	2.70E-03	2.76E-03	2.82E-03	
			Shrinkage	5.11E-05	9.67E-05	1.58E-04	2.14E-04	2.71E-04	3.13E-04	3.56E-04	3.69E-04	3.82E-04	
			Elastic	8.03E-04	8.03E-04	8.03E-04	8.03E-04	8.03E-04	8.03E-04	8.03E-04	8.03E-04	8.03E-04	
			Creep	6.17E-04	7.14E-04	8.57E-04	1.04E-03	1.24E-03	1.38E-03	1.54E-03	1.59E-03	1.63E-03	
			Creep modulus	2.10E+06	1.97E+06	1.80E+06	1.61E+06	1.46E+06	1.37E+06	1.27E+06	1.25E+06	1.23E+06	
			Creep Coefficient (computed)	0.84	0.98	1.17	1.43	1.70	1.89	2.10	2.18	2.23	
		Elastic Modulus at Time of Load: 4.08E+06 psi											
		Computed Elastic Strain at Time of Load: 7.31E-04											

No. of Mix	Curing condition	Load level	Strain	Age of testing (days)									
				3	7	14	28	56	91	180	270	360	
2F (1y) (W/C) =0.33	14-day moist cure	40% (2673 psi)	Total	1.11E-03	1.23E-03	1.38E-03	1.59E-03	1.82E-03	1.96E-03	2.10E-03	2.15E-03	2.19E-03	
			Shrinkage	2.44E-05	6.00E-05	1.00E-04	1.64E-04	2.23E-04	2.62E-04	2.82E-04	2.97E-04	3.04E-04	
			Elastic	6.69E-04	6.69E-04	6.69E-04	6.69E-04	6.69E-04	6.69E-04	6.69E-04	6.69E-04	6.69E-04	6.69E-04
			Creep	4.14E-04	5.06E-04	6.09E-04	7.59E-04	9.32E-04	1.03E-03	1.15E-03	1.19E-03	1.22E-03	
			Creep modulus	2.47E+06	2.28E+06	2.09E+06	1.87E+06	1.67E+06	1.58E+06	1.47E+06	1.44E+06	1.42E+06	
			Creep Coefficient (computed)	0.67	0.82	0.98	1.22	1.50	1.66	1.86	1.91	1.97	
		Elastic Modulus at Time of Load: 4.31E+06 psi											
		Computed Elastic Strain at Time of Load: 6.20E-04											
		50% (3323 psi)	Total	1.38E-03	1.55E-03	1.75E-03	1.96E-03	2.22E-03	2.40E-03	2.61E-03	2.66E-03	2.70E-03	
			Shrinkage	2.44E-05	6.00E-05	1.00E-04	1.64E-04	2.23E-04	2.62E-04	3.04E-04	3.14E-04	3.28E-04	
			Elastic	8.42E-04	8.42E-04	8.42E-04	8.42E-04	8.42E-04	8.42E-04	8.42E-04	8.42E-04	8.42E-04	8.42E-04
			Creep	5.12E-04	6.46E-04	8.06E-04	9.57E-04	1.16E-03	1.30E-03	1.46E-03	1.50E-03	1.53E-03	
			Creep modulus	2.45E+06	2.23E+06	2.02E+06	1.85E+06	1.66E+06	1.55E+06	1.44E+06	1.42E+06	1.40E+06	
			Creep Coefficient (computed)	0.66	0.84	1.04	1.24	1.50	1.68	1.89	1.95	1.98	
		Elastic Modulus at Time of Load: 4.31E+06 psi											
		Computed Elastic Strain at Time of Load: 7.71E-04											

No. of Mix	Curing condition	Load level	Strain	Age of testing (days)								
				3	7	14	28	56	91	180	270	360
3F (1y) (W/C) =0.41	7-day moist cure	40% (3027 psi)	Total	1.03E-03	1.17E-03	1.33E-03	1.50E-03	1.71E-03	1.84E-03	1.97E-03	2.00E-03	2.00E-03
			Shrinkage	4.00E-05	7.56E-05	1.37E-04	2.03E-04	2.61E-04	2.96E-04	3.33E-04	3.41E-04	3.43E-04
			Elastic	6.09E-04	6.09E-04	6.09E-04	6.09E-04	6.09E-04	6.09E-04	6.09E-04	6.09E-04	6.09E-04
			Creep	3.83E-04	4.83E-04	5.85E-04	6.91E-04	8.39E-04	9.39E-04	1.03E-03	1.05E-03	1.04E-03
			Creep Modulus	3.05E+06	2.77E+06	2.53E+06	2.33E+06	2.09E+06	1.96E+06	1.85E+06	1.83E+06	1.83E+06
			Creep Coefficient (computed)	0.64	0.81	0.98	1.15	1.40	1.57	1.72	1.75	1.74
			Elastic Modulus at Time of Load: 5.05E+06 psi									
		Computed Elastic Strain at Time of Load: 5.99E-04										
		50% (3784 psi)	Total	1.22E-03	1.39E-03	1.59E-03	1.79E-03	2.03E-03	2.18E-03	2.32E-03	2.34E-03	2.34E-03
			Shrinkage	4.00E-05	7.56E-05	1.37E-04	2.03E-04	2.61E-04	2.96E-04	3.33E-04	3.41E-04	3.43E-04
			Elastic	7.51E-04	7.51E-04	7.51E-04	7.51E-04	7.51E-04	7.51E-04	7.51E-04	7.51E-04	7.51E-04
			Creep	4.30E-04	5.67E-04	7.00E-04	8.36E-04	1.02E-03	1.13E-03	1.23E-03	1.24E-03	1.25E-03
			Creep modulus	3.20E+06	2.87E+06	2.61E+06	2.38E+06	2.14E+06	2.01E+06	1.91E+06	1.90E+06	1.89E+06
			Creep Coefficient (computed)	0.58	0.77	0.95	1.13	1.38	1.53	1.67	1.68	1.69
	Elastic Modulus at Time of Load: 5.05E+06 psi											
	Computed Elastic Strain at Time of Load: 7.39E-04											

No. of Mix	Curing condition	Load level	Strain	Age of testing (days)									
				3	7	14	28	56	91	180	270	360	
3F (1y) (W/C) =0.41	14-day moist cure	40% (3297 psi)	Total	9.57E-04	1.09E-03	1.22E-03	1.38E-03	1.56E-03	1.69E-03	1.79E-03	1.81E-03	1.82E-03	
			Shrinkage	2.11E-05	4.67E-05	8.67E-05	1.37E-04	1.82E-04	2.17E-04	2.48E-04	2.57E-04	2.59E-04	
			Elastic	6.33E-04	6.33E-04	6.33E-04	6.33E-04	6.33E-04	6.33E-04	6.33E-04	6.33E-04	6.33E-04	6.33E-04
			Creep	3.02E-04	4.13E-04	4.97E-04	6.11E-04	7.41E-04	8.36E-04	9.06E-04	9.20E-04	9.28E-04	
			Creep modulus	3.52E+06	3.15E+06	2.92E+06	2.65E+06	2.40E+06	2.24E+06	2.14E+06	2.12E+06	2.11E+06	
			Creep Coefficient (computed)	0.50	0.68	0.82	1.01	1.23	1.38	1.50	1.52	1.54	
		Elastic Modulus at Time of Load: 5.14E+06 psi											
		Computed Elastic Strain at Time of Load: 6.04E-04											
		50% (4121 psi)	Total	1.25E-03	1.39E-03	1.54E-03	1.70E-03	1.89E-03	2.02E-03	2.15E-03	2.18E-03	2.18E-03	
			Shrinkage	2.11E-05	4.67E-05	8.67E-05	1.37E-04	1.82E-04	2.10E-04	2.48E-04	2.57E-04	2.59E-04	
			Elastic	7.76E-04	7.76E-04	7.76E-04	7.76E-04	7.76E-04	7.76E-04	7.76E-04	7.76E-04	7.76E-04	
			Creep	4.58E-04	5.67E-04	6.74E-04	7.88E-04	9.32E-04	1.04E-03	1.13E-03	1.14E-03	1.14E-03	
			Creep modulus	3.34E+06	3.07E+06	2.84E+06	2.64E+06	2.41E+06	2.27E+06	2.16E+06	2.15E+06	2.15E+06	
			Creep Coefficient (computed)	0.61	0.75	0.89	1.04	1.23	1.37	1.50	1.52	1.51	
		Elastic Modulus at Time of Load: 5.14E+06 psi											
		Computed Elastic Strain at Time of Load: 7.55E-04											

No. of Mix	Curing condition	Load level	Strain	Age of testing (days)								
				3	7	14	28	56	91	180	270	360
4F (1y) (W/C) =0.37	7-day moist cure	40% (2846 psi)	Total	1.06E-03	1.20E-03	1.34E-03	1.51E-03	1.68E-03	1.81E-03	1.90E-03	1.93E-03	1.93E-03
			Shrinkage	3.67E-05	7.33E-05	1.16E-04	1.74E-04	2.32E-04	2.71E-04	3.00E-04	3.03E-04	3.06E-04
			Elastic	5.98E-04	5.98E-04	5.98E-04	5.98E-04	5.98E-04	5.98E-04	5.98E-04	5.98E-04	5.98E-04
			Creep	4.23E-04	5.33E-04	6.29E-04	7.39E-04	8.51E-04	9.41E-04	1.00E-03	1.03E-03	1.03E-03
			Creep Modulus	2.79E+06	2.52E+06	2.32E+06	2.13E+06	1.96E+06	1.85E+06	1.78E+06	1.75E+06	1.75E+06
			Creep Coefficient (computed)	0.73	0.91	1.08	1.27	1.46	1.61	1.72	1.77	1.77
			Elastic Modulus at Time of Load: 4.88E+06 psi									
		Computed Elastic Strain at Time of Load: 5.83E-04										
		50% (3617 psi)	Total	1.34E-03	1.47E-03	1.62E-03	1.78E-03	1.96E-03	2.10E-03	2.20E-03	2.22E-03	2.23E-03
			Shrinkage	3.67E-05	7.33E-05	1.16E-04	1.74E-04	2.32E-04	2.71E-04	3.00E-04	3.03E-04	3.06E-04
			Elastic	7.03E-04	7.03E-04	7.03E-04	7.03E-04	7.03E-04	7.03E-04	7.03E-04	7.03E-04	7.03E-04
			Creep	5.98E-04	6.90E-04	8.03E-04	9.07E-04	1.03E-03	1.13E-03	1.19E-03	1.22E-03	1.22E-03
			Creep modulus	2.78E+06	2.60E+06	2.40E+06	2.25E+06	2.09E+06	1.98E+06	1.91E+06	1.88E+06	1.88E+06
			Creep Coefficient (computed)	0.82	0.95	1.10	1.24	1.41	1.54	1.64	1.67	1.68
	Elastic Modulus at Time of Load: 4.88E+06 psi											
	Computed Elastic Strain at Time of Load: 7.29E-04											

No. of Mix	Curing condition	Load level	Strain	Age of testing (days)									
				3	7	14	28	56	91	180	270	360	
4F (1y) (W/C) =0.37	14-day moist cure	40% (2894 psi)	Total	1.02E-03	1.13E-03	1.25E-03	1.39E-03	1.54E-03	1.66E-03	1.74E-03	1.76E-03	1.77E-03	
			Shrinkage	2.11E-05	4.22E-05	8.00E-05	1.32E-04	1.86E-04	2.23E-04	2.49E-04	2.56E-04	2.60E-04	
			Elastic	5.71E-04	5.71E-04	5.71E-04	5.71E-04	5.71E-04	5.71E-04	5.71E-04	5.71E-04	5.71E-04	
			Creep	4.26E-04	5.12E-04	5.98E-04	6.82E-04	7.87E-04	8.65E-04	9.16E-04	9.32E-04	9.35E-04	
			Creep modulus	2.90E+06	2.67E+06	2.48E+06	2.31E+06	2.13E+06	2.02E+06	1.95E+06	1.93E+06	1.92E+06	
			Creep Coefficient (computed)	0.74	0.89	1.03	1.18	1.36	1.50	1.58	1.61	1.62	
		Elastic Modulus at Time of Load: 5.01E+06 psi											
		Computed Elastic Strain at Time of Load: 5.78E-04											
		50% (3457 psi)	Total	1.21E-03	1.35E-03	1.51E-03	1.69E-03	1.88E-03	2.01E-03	2.10E-03	2.13E-03	2.13E-03	
			Shrinkage	3.11E-05	5.22E-05	9.00E-05	1.42E-04	1.96E-04	2.33E-04	2.49E-04	2.56E-04	2.60E-04	
			Elastic	7.02E-04	7.02E-04	7.02E-04	7.02E-04	7.02E-04	7.02E-04	7.02E-04	7.02E-04	7.02E-04	
			Creep	4.75E-04	6.00E-04	7.16E-04	8.45E-04	9.78E-04	1.07E-03	1.15E-03	1.17E-03	1.17E-03	
			Creep modulus	2.94E+06	2.65E+06	2.44E+06	2.24E+06	2.06E+06	1.95E+06	1.87E+06	1.85E+06	1.85E+06	
			Creep Coefficient (computed)	0.66	0.83	0.99	1.17	1.35	1.49	1.59	1.62	1.62	
		Elastic Modulus at Time of Load: 5.01E+06 psi											
		Computed Elastic Strain at Time of Load: 7.22E-04											

No. of Mix	Curing condition	Load level	Strain	Age of testing (days)								
				3	7	14	28	56	91	180	270	360
5S (1y) (W/C) =0.33	7-day moist cure	40% (2230 psi)	Total	9.08E-04	1.03E-03	1.16E-03	1.31E-03	1.48E-03	1.60E-03	1.56E-03	-	1.73E-03
			Shrinkage	5.09E-05	8.82E-05	1.28E-04	1.68E-04	2.03E-04	2.21E-04	2.38E-04	-	2.47E-04
			Elastic	5.86E-04	5.86E-04	5.86E-04	5.86E-04	5.86E-04	5.86E-04	5.86E-04	5.86E-04	5.86E-04
			Creep	2.71E-04	3.59E-04	4.49E-04	5.59E-04	6.90E-04	7.93E-04	7.38E-04	-	8.95E-04
			Creep Modulus	2.60E+06	2.36E+06	2.15E+06	1.95E+06	1.75E+06	1.62E+06	1.68E+06	-	1.51E+06
			Creep Coefficient (computed)	0.54	0.72	0.90	1.12	1.38	1.58	1.47	-	1.79
			Elastic Modulus at Time of Load: 4.45E+06 psi									
	Computed Elastic Strain at Time of Load: 5.01E-04											
	14-day moist cure	40% (2230 psi)	Total	9.13E-04	1.04E-03	1.15E-03	1.28E-03	1.42E-03	1.52E-03	1.73E-03	-	1.91E-03
			Shrinkage	7.23E-05	1.15E-04	1.53E-04	1.88E-04	2.13E-04	2.25E-04	2.36E-04	-	2.41E-04
			Elastic	6.88E-04	6.88E-04	6.88E-04	6.88E-04	6.88E-04	6.88E-04	6.88E-04	6.88E-04	6.88E-04
			Creep	1.54E-04	2.35E-04	3.10E-04	4.02E-04	5.17E-04	6.12E-04	8.04E-04	-	9.86E-04
			Creep modulus	2.65E+06	2.42E+06	2.23E+06	2.05E+06	1.85E+06	1.72E+06	1.49E+06	-	1.33E+06
			Creep Coefficient (computed)	0.31	0.47	0.62	0.80	1.03	1.22	1.61	-	1.97
			Elastic Modulus at Time of Load: 4.45E+06 psi									
	Computed Elastic Strain at Time of Load: 5.01E-04											

No. of Mix	Curing condition	Load level	Strain	Age of testing (days)									
				3	7	14	28	56	91	180	270	360	
5S (3m) (W/C) =0.33	7-day moist cure	40% (3299 psi)	Total	1.17E-03	1.30E-03	1.42E-03	1.59E-03	1.74E-03	1.84E-03	-	-	-	
			Shrinkage	4.40E-05	8.80E-05	1.30E-04	1.70E-04	2.01E-04	2.16E-04	-	-	-	
			Elastic	6.69E-04	6.69E-04	6.69E-04	6.69E-04	6.69E-04	6.69E-04	-	-	-	
			Creep	4.55E-04	5.42E-04	6.24E-04	7.48E-04	8.74E-04	9.55E-04	-	-	-	
			Creep Modulus	2.99E+06	2.69E+06	2.49E+06	2.28E+06	2.09E+06	1.98E+06	-	-	-	
			Creep Coefficient (computed)	0.67	0.80	0.92	1.11	1.29	1.41	-	-	-	
		Elastic Modulus at Time of Load: 4.88E+06 psi											
		Computed Elastic Strain at Time of Load: 6.76E-04											
		50% (4124 psi)	Total	1.46E-03	1.62E-03	1.78E-03	1.98E-03	2.18E-03	2.30E-03	-	-	-	
			Shrinkage	4.40E-05	8.80E-05	1.30E-04	1.70E-04	2.01E-04	2.16E-04	-	-	-	
			Elastic	8.46E-04	8.46E-04	8.46E-04	8.46E-04	8.46E-04	8.46E-04	-	-	-	
			Creep	5.65E-04	6.86E-04	8.07E-04	9.61E-04	1.13E-03	1.24E-03	-	-	-	
			Creep modulus	2.99E+06	2.69E+06	2.49E+06	2.28E+06	2.09E+06	1.98E+06	-	-	-	
			Creep Coefficient (computed)	0.67	0.81	0.96	1.14	1.34	1.47	-	-	-	
		Elastic Modulus at Time of Load: 4.88E+06 psi											
		Computed Elastic Strain at Time of Load: 8.45E-04											

No. of Mix	Curing condition	Load level	Strain	Age of testing (days)									
				3	7	14	28	56	91	180	270	360	
5S (3m) (W/C) =0.33	14-day moist cure	40% (3401 psi)	Total	1.22E-03	1.32E-03	1.44E-03	1.59E-03	1.75E-03	1.83E-03	-	-	-	
			Shrinkage	4.30E-05	7.40E-05	1.10E-04	1.49E-04	1.78E-04	1.93E-04	-	-	-	
			Elastic	7.18E-04	7.18E-04	7.18E-04	7.18E-04	7.18E-04	7.18E-04	-	-	-	
			Creep	4.61E-04	5.31E-04	6.11E-04	7.27E-04	8.51E-04	9.23E-04	-	-	-	
			Creep modulus	3.00E+06	2.79E+06	2.60E+06	2.38E+06	2.19E+06	2.11E+06	-	-	-	
			Creep Coefficient (computed)	0.66	0.77	0.88	1.05	1.23	1.33	-	-	-	
		Elastic Modulus at Time of Load: 5.09E+06 psi											
		Computed Elastic Strain at Time of Load: 6.94E-04											
		50% (4251 psi)	Total	1.46E-03	1.60E-03	1.75E-03	1.94E-03	2.12E-03	2.21E-03	-	-	-	
			Shrinkage	4.30E-05	7.40E-05	1.10E-04	1.49E-04	1.78E-04	1.93E-04	-	-	-	
			Elastic	8.89E-04	8.89E-04	8.89E-04	8.89E-04	8.89E-04	8.89E-04	-	-	-	
			Creep	5.32E-04	6.33E-04	7.48E-04	8.99E-04	1.05E-03	1.13E-03	-	-	-	
			Creep modulus	2.99E+06	2.79E+06	2.60E+06	2.38E+06	2.19E+06	2.11E+06	-	-	-	
			Creep Coefficient (computed)	0.61	0.73	0.86	1.04	1.21	1.30	-	-	-	
		Elastic Modulus at Time of Load: 5.09E+06 psi											
		Computed Elastic Strain at Time of Load: 8.68E-04											

No. of Mix	Curing condition	Load level	Strain	Age of testing (days)								
				3	7	14	28	56	91	180	270	360
6S (1y) (W/C) =0.36	7-day moist cure	40% (2416 psi)	Total	1.03E-03	1.11E-03	1.17E-03	1.24E-03	1.30E-03	1.37E-03	1.66E-03	1.92E-03	2.02E-03
			Shrinkage	6.31E-05	8.48E-05	1.07E-04	1.33E-04	1.62E-04	1.83E-04	1.98E-04	2.23E-04	2.25E-04
			Elastic	8.68E-04	8.68E-04	8.68E-04	8.68E-04	8.68E-04	8.68E-04	8.68E-04	8.68E-04	8.68E-04
			Creep	9.64E-05	1.53E-04	1.97E-04	2.40E-04	2.72E-04	3.20E-04	5.97E-04	8.32E-04	9.32E-04
			Creep Modulus	2.52E+06	2.38E+06	2.28E+06	2.19E+06	2.13E+06	2.04E+06	1.65E+06	1.42E+06	1.34E+06
			Creep Coefficient (computed)	0.18	0.28	0.36	0.44	0.50	0.59	1.10	1.53	1.71
			Elastic Modulus at Time of Load: 4.44E+06 psi									
	Computed Elastic Strain at Time of Load: 5.44E-04											
	14-day moist cure	40% (2416 psi)	Total	1.36E-03	1.46E-03	1.55E-03	1.64E-03	1.72E-03	1.81E-03	2.05E-03	2.15E-03	2.17E-03
			Shrinkage	3.82E-05	6.65E-05	9.81E-05	1.33E-04	1.60E-04	1.83E-04	2.00E-04	2.06E-04	2.09E-04
			Elastic	9.00E-04	9.00E-04	9.00E-04	9.00E-04	9.00E-04	9.00E-04	9.00E-04	9.00E-04	9.00E-04
			Creep	4.24E-04	4.95E-04	5.50E-04	6.06E-04	6.60E-04	7.25E-04	9.47E-04	1.04E-03	1.06E-03
			Creep modulus	1.79E+06	1.70E+06	1.63E+06	1.57E+06	1.52E+06	1.46E+06	1.28E+06	1.22E+06	1.20E+06
			Creep Coefficient (computed)	0.78	0.91	1.01	1.11	1.21	1.33	1.74	1.91	1.96
			Elastic Modulus at Time of Load: 4.44E+06 psi									
	Computed Elastic Strain at Time of Load: 5.44E-04											

No. of Mix	Curing condition	Load level	Strain	Age of testing (days)									
				3	7	14	28	56	91	180	270	360	
6S (3m) (W/C) =0.36	7-day moist cure	40% (3315 psi)	Total	9.75E-04	1.11E-03	1.26E-03	1.41E-03	1.60E-03	1.76E-03	-	-	-	
			Shrinkage	4.20E-05	8.20E-05	1.23E-04	1.57E-04	1.83E-04	1.96E-04	-	-	-	
			Elastic	6.70E-04	6.70E-04	6.70E-04	6.70E-04	6.70E-04	6.70E-04	-	-	-	
			Creep	2.63E-04	3.53E-04	4.62E-04	5.88E-04	7.47E-04	8.92E-04	-	-	-	
			Creep Modulus	3.32E+06	3.16E+06	3.02E+06	2.84E+06	2.65E+06	2.53E+06	-	-	-	
			Creep Coefficient (computed)	0.40	0.53	0.70	0.89	1.13	1.35	-	-	-	
		Elastic Modulus at Time of Load: 5.18E+06 psi											
		Computed Elastic Strain at Time of Load: 6.63E-04											
		50% (4144 psi)	Total	1.19E-03	1.39E-03	1.55E-03	1.71E-03	1.90E-03	2.05E-03	-	-	-	
			Shrinkage	4.20E-05	8.20E-05	1.23E-04	1.57E-04	1.83E-04	1.96E-04	-	-	-	
			Elastic	8.37E-04	8.37E-04	8.37E-04	8.37E-04	8.37E-04	8.37E-04	-	-	-	
			Creep	3.25E-04	4.72E-04	5.70E-04	7.13E-04	8.91E-04	1.02E-03	-	-	-	
			Creep modulus	3.54E+06	3.15E+06	2.89E+06	2.62E+06	2.31E+06	2.30E+06	-	-	-	
			Creep Coefficient (computed)	0.39	0.57	0.69	0.86	1.07	1.23	-	-	-	
		Elastic Modulus at Time of Load: 5.18E+06 psi											
		Computed Elastic Strain at Time of Load: 8.29E-04											

No. of Mix	Curing condition	Load level	Strain	Age of testing (days)									
				3	7	14	28	56	91	180	270	360	
6S (3m) (W/C) =0.36	14-day moist cure	40% (3680 psi)	Total	1.04E-03	1.16E-03	1.29E-03	1.45E-03	1.65E-03	1.80E-03	-	-	-	
			Shrinkage	3.80E-05	7.60E-05	1.14E-04	1.41E-04	1.63E-04	1.77E-04	-	-	-	
			Elastic	6.92E-04	6.92E-04	6.92E-04	6.92E-04	6.92E-04	6.92E-04	-	-	-	
			Creep	3.07E-04	3.96E-04	4.85E-04	6.15E-04	7.93E-04	9.27E-04	-	-	-	
			Creep modulus	3.70E+06	3.40E+06	3.15E+06	2.87E+06	2.56E+06	2.21E+06	-	-	-	
			Creep Coefficient (computed)	0.44	0.57	0.70	0.89	1.14	1.34	-	-	-	
		Elastic Modulus at Time of Load: 5.45E+06 psi											
		Computed Elastic Strain at Time of Load: 6.94E-04											
		50% (4506 psi)	Total	1.26E-03	1.47E-03	1.57E-03	1.73E-03	1.94E-03	2.10E-03	-	-	-	
			Shrinkage	3.80E-05	7.60E-05	1.14E-04	1.41E-04	1.63E-04	1.77E-04	-	-	-	
			Elastic	8.54E-04	8.54E-04	8.54E-04	8.54E-04	8.54E-04	8.54E-04	-	-	-	
			Creep	3.71E-04	5.37E-04	5.99E-04	7.32E-04	9.24E-04	1.07E-03	-	-	-	
			Creep modulus	3.69E+06	3.35E+06	3.12E+06	2.85E+06	2.51E+06	2.10E+06	-	-	-	
			Creep Coefficient (computed)	0.43	0.62	0.69	0.84	1.06	1.23	-	-	-	
		Elastic Modulus at Time of Load: 5.45E+06 psi											
		Computed Elastic Strain at Time of Load: 8.68E-04											

No. of Mix	Curing condition	Load level	Strain	Age of testing (days)									
				3	7	14	28	56	91	180	270	360	
7S (1y) (W/C) =0.41	7-day moist cure	40% (2120 psi)	Total	8.62E-04	9.70E-04	1.07E-03	1.18E-03	1.27E-03	1.39E-03	1.62E-03	-	1.96E-03	
			Shrinkage	4.43E-05	7.93E-05	1.18E-04	1.61E-04	1.93E-04	2.18E-04	2.37E-04	2.37E-04	-	2.47E-04
			Elastic	5.32E-04	5.32E-04	5.32E-04	5.32E-04	5.32E-04	5.32E-04	5.32E-04	5.32E-04	5.32E-04	5.32E-04
			Creep	2.86E-04	3.59E-04	4.18E-04	4.83E-04	5.50E-04	6.35E-04	8.48E-04	8.48E-04	-	1.18E-03
			Creep Modulus	2.59E+06	2.38E+06	2.23E+06	2.09E+06	1.96E+06	1.82E+06	1.54E+06	1.54E+06	-	1.24E+06
			Creep Coefficient (computed)	0.47	0.59	0.68	0.79	0.90	1.04	1.38	1.38	-	1.92
			Elastic Modulus at Time of Load: 3.46E+06 psi										
	Computed Elastic Strain at Time of Load: 6.13E-04												
	14-day moist cure	40% (2120 psi)	Total	7.73E-04	8.72E-04	9.63E-04	1.06E-03	1.17E-03	1.26E-03	1.49E-03	1.49E-03	-	1.81E-03
			Shrinkage	5.78E-05	9.58E-05	1.34E-04	1.73E-04	2.06E-04	2.22E-04	2.37E-04	2.37E-04	-	2.45E-04
			Elastic	5.73E-04	5.73E-04	5.73E-04	5.73E-04	5.73E-04	5.73E-04	5.73E-04	5.73E-04	5.73E-04	5.73E-04
			Creep	1.42E-04	2.03E-04	2.55E-04	3.16E-04	3.94E-04	4.61E-04	6.75E-04	6.75E-04	-	9.96E-04
			Creep modulus	2.96E+06	2.73E+06	2.56E+06	2.38E+06	2.19E+06	2.05E+06	1.70E+06	1.70E+06	-	1.35E+06
			Creep Coefficient (computed)	0.23	0.33	0.42	0.52	0.64	0.75	1.10	1.10	-	1.62
			Elastic Modulus at Time of Load: 3.46E+06 psi										
	Computed Elastic Strain at Time of Load: 6.13E-04												

No. of Mix	Curing condition	Load level	Strain	Age of testing (days)									
				3	7	14	28	56	91	180	270	360	
7S (3m) (W/C) =0.41	7-day moist cure	40% (2361 psi)	Total	9.07E-04	1.09E-03	1.26E-03	1.40E-03	1.56E-03	1.66E-03	-	-	-	
			Shrinkage	3.90E-05	8.00E-05	1.26E-04	1.70E-04	2.02E-04	2.23E-04	-	-	-	
			Elastic	5.19E-04	5.19E-04	5.19E-04	5.19E-04	5.19E-04	5.19E-04	-	-	-	
			Creep	3.49E-04	4.95E-04	6.19E-04	7.10E-04	8.40E-04	9.14E-04	-	-	-	
			Creep Modulus	2.66E+06	2.33E+06	2.11E+06	1.92E+06	1.74E+06	1.65E+06	-	-	-	
			Creep Coefficient (computed)	0.57	0.81	1.01	1.16	1.37	1.49	-	-	-	
		Elastic Modulus at Time of Load: 4.52E+06 psi											
		Computed Elastic Strain at Time of Load: 6.13E-04											
		50% (2951 psi)	Total	1.10E-03	1.29E-03	1.49E-03	1.66E-03	1.84E-03	1.94E-03	-	-	-	
			Shrinkage	3.90E-05	8.00E-05	1.26E-04	1.70E-04	2.02E-04	2.23E-04	-	-	-	
			Elastic	6.16E-04	6.16E-04	6.16E-04	6.16E-04	6.16E-04	6.16E-04	-	-	-	
			Creep	4.46E-04	5.89E-04	7.44E-04	8.78E-04	1.02E-03	1.10E-03	-	-	-	
			Creep modulus	2.78E+06	2.45E+06	2.17E+06	1.98E+06	1.81E+06	1.72E+06	-	-	-	
			Creep Coefficient (computed)	0.73	0.96	1.21	1.43	1.66	1.79	-	-	-	
		Elastic Modulus at Time of Load: 4.52E+06 psi											
		Computed Elastic Strain at Time of Load: 6.13E-04											

No. of Mix	Curing condition	Load level	Strain	Age of testing (days)									
				3	7	14	28	56	91	180	270	360	
7S (3m) (W/C) =0.41	14-day moist cure	40% (2587 psi)	Total	9.48E-04	1.08E-03	1.21E-03	1.38E-03	1.56E-03	1.65E-03	-	-	-	
			Shrinkage	3.80E-05	7.30E-05	1.11E-04	1.48E-04	1.83E-04	2.04E-04	-	-	-	
			Elastic	5.46E-04	5.46E-04	5.46E-04	5.46E-04	5.46E-04	5.46E-04	-	-	-	
			Creep	3.64E-04	4.62E-04	5.52E-04	6.90E-04	8.27E-04	9.01E-04	-	-	-	
			Creep modulus	2.84E+06	2.57E+06	2.36E+06	2.09E+06	1.89E+06	1.79E+06	-	-	-	
			Creep Coefficient (computed)	0.65	0.83	0.99	1.24	1.49	1.62	-	-	-	
		Elastic Modulus at Time of Load: 4.60E+06 psi											
		Computed Elastic Strain at Time of Load: 5.56E-04											
		50% (3116 psi)	Total	1.16E-03	1.31E-03	1.47E-03	1.65E-03	1.82E-03	1.92E-03	-	-	-	
			Shrinkage	3.80E-05	7.30E-05	1.11E-04	1.48E-04	1.83E-04	2.04E-04	-	-	-	
			Elastic	6.43E-04	6.43E-04	6.43E-04	6.43E-04	6.43E-04	6.43E-04	-	-	-	
			Creep	4.79E-04	5.92E-04	7.12E-04	8.55E-04	9.95E-04	1.07E-03	-	-	-	
			Creep modulus	2.78E+06	2.52E+06	2.30E+06	2.08E+06	1.90E+06	1.82E+06	-	-	-	
			Creep Coefficient (computed)	0.69	0.85	1.02	1.23	1.43	1.54	-	-	-	
		Elastic Modulus at Time of Load: 4.60E+06 psi											
		Computed Elastic Strain at Time of Load: 6.95E-04											

No. of Mix	Curing condition	Load level	Strain	Age of testing (days)								
				3	7	14	28	56	91	180	270	360
8S (1y) (W/C) =0.44	7-day moist cure	40% (1917 psi)	Total	6.27E-04	7.02E-04	8.28E-04	9.78E-04	1.15E-03	1.30E-03	1.66E-03	-	1.96E-03
			Shrinkage	4.70E-05	8.77E-05	1.41E-04	2.15E-04	3.05E-04	3.68E-04	4.45E-04	-	4.98E-04
			Elastic	5.23E-04	5.23E-04	5.23E-04	5.23E-04	5.23E-04	5.23E-04	5.23E-04	5.23E-04	5.23E-04
			Creep	5.63E-05	9.06E-05	1.64E-04	2.39E-04	3.27E-04	4.10E-04	6.88E-04	-	9.43E-04
			Creep Modulus	3.31E+06	3.12E+06	2.79E+06	2.51E+06	2.26E+06	2.05E+06	1.58E+06	-	1.31E+06
			Creep Coefficient (computed)	0.11	0.18	0.33	0.48	0.66	0.82	1.38	-	1.90
			Elastic Modulus at Time of Load: 3.86E+06 psi									
	Computed Elastic Strain at Time of Load: 4.97E-04											
	14-day moist cure	40% (1917 psi)	Total	8.81E-04	9.42E-04	1.02E-03	1.13E-03	1.30E-03	1.47E-03	1.77E-03	-	2.12E-03
			Shrinkage	3.04E-04	3.35E-04	3.62E-04	3.91E-04	4.22E-04	4.45E-04	4.81E-04	-	5.18E-04
			Elastic	5.48E-04	5.48E-04	5.48E-04	5.48E-04	5.48E-04	5.48E-04	5.48E-04	5.48E-04	5.48E-04
			Creep	2.89E-05	6.00E-05	1.08E-04	1.92E-04	3.32E-04	4.74E-04	7.42E-04	-	1.05E-03
			Creep modulus	3.32E+06	3.15E+06	2.92E+06	2.59E+06	2.18E+06	1.88E+06	1.49E+06	-	1.20E+06
			Creep Coefficient (computed)	0.06	0.12	0.22	0.39	0.67	0.95	1.49	-	2.11
			Elastic Modulus at Time of Load: 3.86E+06 psi									
	Computed Elastic Strain at Time of Load: 4.97E-04											

No. of Mix	Curing condition	Load level	Strain	Age of testing (days)									
				3	7	14	28	56	91	180	270	360	
8S (3m) (W/C) =0.44	7-day moist cure	40% (2712 psi)	Total	1.13E-03	1.26E-03	1.41E-03	1.57E-03	1.76E-03	1.91E-03	-	-	-	
			Shrinkage	7.30E-05	1.23E-04	1.61E-04	1.94E-04	2.28E-04	2.50E-04	-	-	-	
			Elastic	6.14E-04	6.14E-04	6.14E-04	6.14E-04	6.14E-04	6.14E-04	-	-	-	
			Creep	4.43E-04	5.26E-04	6.33E-04	7.61E-04	9.20E-04	1.05E-03	-	-	-	
			Creep Modulus	2.71E+06	2.53E+06	2.34E+06	2.04E+06	1.82E+06	1.68E+06	-	-	-	
			Creep Coefficient (computed)	0.77	0.92	1.10	1.33	1.61	1.83	-	-	-	
		Elastic Modulus at Time of Load: 4.84E+06 psi											
		Computed Elastic Strain at Time of Load: 5.73E-04											
		50% (3320 psi)	Total	1.30E-03	1.44E-03	1.61E-03	1.82E-03	2.05E-03	2.23E-03	-	-	-	
			Shrinkage	7.30E-05	1.23E-04	1.61E-04	1.94E-04	2.28E-04	2.50E-04	-	-	-	
			Elastic	7.22E-04	7.22E-04	7.22E-04	7.22E-04	7.22E-04	7.22E-04	-	-	-	
			Creep	5.00E-04	5.92E-04	7.22E-04	9.04E-04	1.10E-03	1.25E-03	-	-	-	
			Creep modulus	2.56E+06	2.38E+06	2.17E+06	1.97E+04	1.77E+06	1.63E+06	-	-	-	
			Creep Coefficient (computed)	0.70	0.83	1.01	1.26	1.53	1.74	-	-	-	
		Elastic Modulus at Time of Load: 4.84E+06 psi											
		Computed Elastic Strain at Time of Load: 7.17E-04											

No. of Mix	Curing condition	Load level	Strain	Age of testing (days)									
				3	7	14	28	56	91	180	270	360	
8S (3m) (W/C) =0.44	14-day moist cure	40% (2950 psi)	Total	1.14E-03	1.26E-03	1.39E-03	1.55E-03	1.73E-03	1.89E-03	-	-	-	
			Shrinkage	5.00E-05	9.80E-05	1.36E-04	1.69E-04	2.02E-04	2.30E-04	-	-	-	
			Elastic	6.54E-04	6.54E-04	6.54E-04	6.54E-04	6.54E-04	6.54E-04	-	-	-	
			Creep	4.36E-04	5.10E-04	6.04E-04	7.26E-04	8.77E-04	1.00E-03	-	-	-	
			Creep modulus	2.92E+06	2.68E+06	2.51E+06	2.26E+06	2.02E+06	1.87E+06	-	-	-	
			Creep Coefficient (computed)	0.72	0.85	1.00	1.21	1.46	1.66	-	-	-	
		Elastic Modulus at Time of Load: 5.00E+06 psi											
		Computed Elastic Strain at Time of Load: 6.02E-04											
		50% (3863 psi)	Total	1.37E-03	1.52E-03	1.68E-03	1.88E-03	2.12E-03	2.29E-03	-	-	-	
			Shrinkage	5.00E-05	9.80E-05	1.36E-04	1.69E-04	2.02E-04	2.30E-04	-	-	-	
			Elastic	8.31E-04	8.31E-04	8.31E-04	8.31E-04	8.31E-04	8.31E-04	-	-	-	
			Creep	4.93E-04	5.96E-04	7.10E-04	8.81E-04	1.08E-03	1.23E-03	-	-	-	
			Creep modulus	2.71E+06	2.53E+06	2.34E+06	2.14E+06	1.93E+06	1.78E+06	-	-	-	
			Creep Coefficient (computed)	0.65	0.79	0.94	1.17	1.43	1.63	-	-	-	
		Elastic Modulus at Time of Load: 5.00E+06 psi											
		Computed Elastic Strain at Time of Load: 7.53E-04											

No. of Mix	Curing condition	Load level	Strain	Age of testing (days)								
				3	7	14	28	56	91	180	270	360
9LF (1y) (W/C) =0.31	7-day moist cure	40% (2055 psi)	Total	1.12E-03	1.23E-03	1.38E-03	1.53E-03	1.68E-03	1.79E-03	1.95E-03	2.00E-03	2.02E-03
			Shrinkage	4.89E-05	9.56E-05	1.62E-04	2.26E-04	2.88E-04	3.22E-04	3.67E-04	3.78E-04	3.84E-04
			Elastic	6.26E-04	6.26E-04	6.26E-04	6.26E-04	6.26E-04	6.26E-04	6.26E-04	6.26E-04	6.26E-04
			Creep	4.43E-04	5.10E-04	5.92E-04	6.77E-04	7.71E-04	8.44E-04	9.62E-04	9.93E-04	1.01E-03
			Creep Modulus	1.92E+06	1.81E+06	1.69E+06	1.58E+06	1.47E+06	1.40E+06	1.29E+06	1.27E+06	1.26E+06
			Creep Coefficient (computed)	0.67	0.78	0.90	1.03	1.17	1.29	1.46	1.51	1.54
			Elastic Modulus at Time of Load: 3.13E+06 psi									
		Computed Elastic Strain at Time of Load: 6.57E-04										
		50% (2568 psi)	Total	1.34E-03	1.49E-03	1.64E-03	1.81E-03	1.99E-03	2.11E-03	2.29E-03	2.34E-03	2.36E-03
			Shrinkage	4.89E-05	9.56E-05	1.62E-04	2.26E-04	2.88E-04	3.22E-04	3.67E-04	3.78E-04	3.84E-04
			Elastic	7.67E-04	7.67E-04	7.67E-04	7.67E-04	7.67E-04	7.67E-04	7.67E-04	7.67E-04	7.67E-04
			Creep	5.21E-04	6.24E-04	7.13E-04	8.19E-04	9.32E-04	1.02E-03	1.16E-03	1.20E-03	1.21E-03
			Creep modulus	1.99E+06	1.85E+06	1.74E+06	1.62E+06	1.51E+06	1.43E+06	1.34E+06	1.31E+06	1.30E+06
			Creep Coefficient (computed)	0.64	0.76	0.87	1.00	1.14	1.25	1.41	1.46	1.47
	Elastic Modulus at Time of Load: 3.13E+06 psi											
	Computed Elastic Strain at Time of Load: 8.20E-04											

No. of Mix	Curing condition	Load level	Strain	Age of testing (days)									
				3	7	14	28	56	91	180	270	360	
9LF (1y) (W/C) =0.31	14-day moist cure	40% (2481 psi)	Total	1.17E-03	1.27E-03	1.39E-03	1.51E-03	1.63E-03	1.71E-03	1.82E-03	1.86E-03	1.88E-03	
			Shrinkage	4.56E-05	8.11E-05	1.37E-04	1.89E-04	2.39E-04	2.76E-04	3.19E-04	3.31E-04	3.33E-04	
			Elastic	6.77E-04	6.77E-04	6.77E-04	6.77E-04	6.77E-04	6.77E-04	6.77E-04	6.77E-04	6.77E-04	6.77E-04
			Creep	4.47E-04	5.14E-04	5.79E-04	6.41E-04	7.18E-04	7.62E-04	8.29E-04	8.53E-04	8.70E-04	
			Creep modulus	2.21E+06	2.08E+06	1.98E+06	1.88E+06	1.78E+06	1.72E+06	1.65E+06	1.62E+06	1.60E+06	
			Creep Coefficient (computed)	0.59	0.68	0.76	0.84	0.95	1.00	1.09	1.12	1.15	
		Elastic Modulus at Time of Load: 3.27E+06 psi											
		Computed Elastic Strain at Time of Load: 7.59E-04											
		50% (2864 psi)	Total	1.30E-03	1.43E-03	1.56E-03	1.69E-03	1.84E-03	1.94E-03	2.07E-03	2.12E-03	2.14E-03	
			Shrinkage	4.56E-05	8.11E-05	1.37E-04	1.89E-04	2.39E-04	2.76E-04	3.19E-04	3.31E-04	3.33E-04	
			Elastic	7.77E-04	7.77E-04	7.77E-04	7.77E-04	7.77E-04	7.77E-04	7.77E-04	7.77E-04	7.77E-04	7.77E-04
			Creep	4.74E-04	5.76E-04	6.51E-04	7.26E-04	8.20E-04	8.88E-04	9.73E-04	1.01E-03	1.03E-03	
			Creep modulus	2.29E+06	2.12E+06	2.01E+06	1.91E+06	1.79E+06	1.72E+06	1.64E+06	1.60E+06	1.59E+06	
			Creep Coefficient (computed)	0.54	0.66	0.74	0.83	0.94	1.01	1.11	1.15	1.17	
		Elastic Modulus at Time of Load: 3.27E+06 psi											
		Computed Elastic Strain at Time of Load: 8.76E-04											

No. of Mix	Curing condition	Load level	Strain	Age of testing (days)								
				3	7	14	28	56	91	180	270	360
10LS (1y) (W/C) =0.39	7-day moist cure	40% (1175 psi)	Total	1.21E-03	1.31E-03	1.43E-03	1.56E-03	1.69E-03	1.80E-03	1.91E-03	1.95E-03	1.97E-03
			Shrinkage	7.00E-05	1.30E-04	1.98E-04	2.60E-04	3.19E-04	3.60E-04	3.96E-04	4.07E-04	4.10E-04
			Elastic	5.46E-04	5.46E-04	5.46E-04	5.46E-04	5.46E-04	5.46E-04	5.46E-04	5.46E-04	5.46E-04
			Creep	4.90E-04	5.39E-04	5.90E-04	6.53E-04	7.30E-04	7.91E-04	9.68E-04	9.96E-04	1.01E-03
			Creep Modulus	1.03E+06	9.92E+05	9.51E+05	9.05E+05	8.54E+05	8.18E+05	7.76E+05	7.62E+05	7.55E+05
			Creep Coefficient (computed)	0.98	1.08	1.18	1.31	1.47	1.59	1.94	2.00	2.03
			Elastic Modulus at Time of Load: 2.36E+06 psi									
		Computed Elastic Strain at Time of Load: 4.98E-04										
		50% (1468 psi)	Total	1.34E-03	1.47E-03	1.61E-03	1.77E-03	1.92E-03	2.02E-03	2.17E-03	2.20E-03	2.21E-03
			Shrinkage	7.00E-05	1.30E-04	1.98E-04	2.60E-04	3.19E-04	3.60E-04	3.96E-04	4.07E-04	4.10E-04
			Elastic	7.21E-04	7.21E-04	7.21E-04	7.21E-04	7.21E-04	7.21E-04	7.21E-04	7.21E-04	7.21E-04
			Creep	5.23E-04	5.94E-04	6.72E-04	7.63E-04	8.56E-04	9.21E-04	1.05E-03	1.07E-03	1.08E-03
			Creep modulus	1.16E+06	1.10E+06	1.04E+06	9.74E+05	9.18E+05	8.82E+05	8.28E+05	8.18E+05	8.15E+05
			Creep Coefficient (computed)	0.84	0.96	1.08	1.23	1.38	1.48	1.69	1.73	1.74
	Elastic Modulus at Time of Load: 2.36E+06 psi											
	Computed Elastic Strain at Time of Load: 6.22E-04											

No. of Mix	Curing condition	Load level	Strain	Age of testing (days)									
				3	7	14	28	56	91	180	270	360	
10LS (1y) (W/C) =0.39	14-day moist cure	40% (1418 psi)	Total	9.04E-04	1.01E-03	1.15E-03	1.25E-03	1.36E-03	1.48E-03	1.58E-03	1.62E-03	1.95E-03	
			Shrinkage	5.00E-05	1.22E-04	1.82E-04	2.30E-04	2.89E-04	3.33E-04	3.61E-04	3.72E-04	3.84E-04	
			Elastic	7.81E-04	7.81E-04	7.81E-04	7.81E-04	7.81E-04	7.81E-04	7.81E-04	7.81E-04	7.81E-04	
			Creep	2.82E-04	3.34E-04	3.99E-04	4.43E-04	5.03E-04	5.74E-04	4.41E-04	4.68E-04	7.89E-04	
			Creep modulus	1.66E+06	1.60E+06	1.46E+06	1.40E+06	1.32E+06	1.24E+06	1.16E+06	1.14E+06	9.03E+05	
			Creep Coefficient (computed)	0.54	0.63	0.76	0.84	0.96	1.09	0.84	0.89	1.50	
		Elastic Modulus at Time of Load: 2.69E+06 psi											
		Computed Elastic Strain at Time of Load: 5.27E-04											
		50% (1872 psi)	Total	1.16E-03	1.27E-03	1.39E-03	1.53E-03	1.68E-03	1.80E-03	1.94E-03	1.99E-03	2.00E-03	
			Shrinkage	5.00E-05	1.01E-04	1.82E-04	2.30E-04	2.89E-04	3.33E-04	3.61E-04	3.72E-04	3.84E-04	
			Elastic	7.13E-04	7.13E-04	7.13E-04	7.13E-04	7.13E-04	7.13E-04	7.69E-04	7.69E-04	7.69E-04	
			Creep	3.95E-04	4.60E-04	4.99E-04	5.85E-04	6.81E-04	7.55E-04	8.13E-04	8.46E-04	8.49E-04	
			Creep modulus	1.69E+06	1.60E+06	1.54E+06	1.44E+06	1.34E+06	1.28E+06	1.18E+06	1.16E+06	1.16E+06	
			Creep Coefficient (computed)	0.57	0.66	0.72	0.84	0.98	1.08	1.17	1.21	1.22	
		Elastic Modulus at Time of Load: 2.69E+06 psi											
		Computed Elastic Strain at Time of Load: 6.96E-04											

No. of Mix	Curing condition	Load level	Strain	Age of testing (days)								
				3	7	14	28	56	91	180	270	360
1GF (3m) (W/C) =0.24	7-day moist cure	40% (3182 psi)	Total	8.66E-04	9.73E-04	1.07E-03	1.17E-03	1.28E-03	1.35E-03	-	-	-
			Shrinkage	2.34E-05	4.46E-05	7.16E-05	1.06E-04	1.42E-04	1.65E-04	-	-	-
			Elastic	6.89E-04	6.89E-04	6.89E-04	6.89E-04	6.89E-04	6.89E-04	-	-	-
			Creep	1.53E-04	2.39E-04	3.08E-04	3.76E-04	4.46E-04	4.98E-04	-	-	-
			Creep Modulus	4.09E+06	3.72E+06	3.46E+06	3.24E+06	3.04E+06	2.90E+06	-	-	-
			Creep Coefficient (computed)	0.26	0.41	0.53	0.65	0.77	0.86	-	-	-
			Elastic Modulus at Time of Load: 5.50E+06 psi									
	Computed Elastic Strain at Time of Load: 5.78E-04											
	14-day moist cure	40% (3182 psi)	Total	7.47E-04	8.31E-04	9.06E-04	9.86E-04	1.07E-03	1.13E-03	-	-	-
			Shrinkage	2.16E-05	4.24E-05	6.83E-05	1.00E-04	1.32E-04	1.51E-04	-	-	-
			Elastic	6.66E-04	6.66E-04	6.66E-04	6.66E-04	6.66E-04	6.66E-04	-	-	-
			Creep	5.94E-05	1.23E-04	1.72E-04	2.20E-04	2.71E-04	3.09E-04	-	-	-
			Creep modulus	4.75E+06	4.37E+06	4.12E+06	3.89E+06	3.68E+06	3.54E+06	-	-	-
			Creep Coefficient (computed)	0.10	0.21	0.30	0.38	0.47	0.53	-	-	-
			Elastic Modulus at Time of Load: 5.50E+06 psi									
	Computed Elastic Strain at Time of Load: 5.78E-04											

No. of Mix	Curing condition	Load level	Strain	Age of testing (days)									
				3	7	14	28	56	91	180	270	360	
2GF (1y) (W/C) =0.33	14-day moist cure	40% (2588 psi)	Total	1.02E-03	1.17E-03	1.33E-03	1.53E-03	1.75E-03	1.87E-03	2.00E-03	2.06E-03	2.08E-03	
			Shrinkage	3.22E-05	6.11E-05	1.09E-04	1.61E-04	2.04E-04	2.29E-04	2.48E-04	2.54E-04	2.54E-04	
			Elastic	6.01E-04	6.01E-04	6.01E-04	6.01E-04	6.01E-04	6.01E-04	6.01E-04	6.01E-04	6.01E-04	6.01E-04
			Creep	3.90E-04	5.11E-04	6.23E-04	7.69E-04	9.44E-04	1.04E-03	1.15E-03	1.21E-03	1.22E-03	
			Creep modulus	2.61E+06	2.33E+06	2.11E+06	1.89E+06	1.67E+06	1.57E+06	1.66E+06	1.43E+06	1.42E+06	
			Creep Coefficient (computed)	0.75	0.98	1.19	1.47	1.81	2.00	2.20	2.31	2.34	
		Elastic Modulus at Time of Load: 4.96E+06 psi											
		Computed Elastic Strain at Time of Load: 5.22E-04											
		50% (3235 psi)	Total	1.33E-03	1.49E-03	1.82E-03	1.92E-03	2.17E-03	2.32E-03	2.46E-03	2.53E-03	2.55E-03	
			Shrinkage	3.22E-05	6.11E-05	1.09E-04	1.61E-04	2.04E-04	2.29E-04	2.48E-04	2.54E-04	2.54E-04	
			Elastic	7.77E-04	7.77E-04	7.77E-04	7.77E-04	7.77E-04	7.77E-04	7.77E-04	7.77E-04	7.77E-04	
			Creep	2.48E+06	2.26E+06	1.89E+06	1.84E+06	1.64E+06	1.54E+06	1.44E+06	1.50E+06	1.52E+06	
			Creep modulus	2.48E+06	2.26E+06	1.89E+06	1.84E+06	1.64E+06	1.54E+06	1.46E+06	1.42E+06	1.41E+06	
			Creep Coefficient (computed)	0.81	1.01	1.43	1.51	1.83	2.02	2.21	2.30	2.33	
		Elastic Modulus at Time of Load: 4.96E+06 psi											
		Computed Elastic Strain at Time of Load: 6.52E-04											

No. of Mix	Curing condition	Load level	Strain	Age of testing (days)										
				3	7	14	28	56	91	180	270	360		
2GF (3m) (W/C) =0.33	7-day moist cure	40% (2262 psi)	Total	-	-	1.13E-03	1.21E-03	1.32E-03	1.45E-03	1.70E-03	-	-		
			Shrinkage	3.34E-05	6.01E-05	8.34E-05	1.33E-04	2.10E-04	2.28E-04	2.61E-04	-	-		
			Elastic	7.36E-04	7.36E-04	7.36E-04	7.36E-04	7.36E-04	7.36E-04	7.36E-04	-	-		
			Creep	-	-	3.07E-04	3.37E-04	3.78E-04	4.85E-04	7.04E-04	-	-		
			Creep Modulus	-	-	2.17E+06	2.11E+06	2.03E+06	1.85E+06	1.57E+06	-	-		
			Creep Coefficient (computed)	-	-	0.68	0.74	0.84	1.07	1.55	-	-		
			Elastic Modulus at Time of Load: 4.99E+06 psi											
			Computed Elastic Strain at Time of Load: 4.53E-04											
			14-day moist cure	40% (2262 psi)	Total	7.51E-04	8.42E-04	9.24E-04	1.01E-03	1.10E-03	1.17E-03	7.51E-04	-	-
					Shrinkage	3.28E-05	6.91E-05	1.13E-04	1.63E-04	2.08E-04	2.32E-04	3.28E-05	-	-
	Elastic	5.35E-04			5.35E-04	5.35E-04	5.35E-04	5.35E-04	5.35E-04	5.35E-04	-	-		
	Creep	1.83E-04			2.38E-04	2.76E-04	3.13E-04	3.59E-04	3.98E-04	1.83E-04	-	-		
	Creep modulus	3.15E+06			2.93E+06	2.79E+06	2.67E+06	2.53E+06	2.42E+06	3.15E+06	-	-		
	Creep Coefficient (computed)	0.40			0.53	0.61	0.69	0.79	0.88	0.40	-	-		
	Elastic Modulus at Time of Load: 4.99E+06 psi													
	Computed Elastic Strain at Time of Load: 4.53E-04													

No. of Mix	Curing condition	Load level	Strain	Age of testing (days)								
				3	7	14	28	56	91	180	270	360
3GF (1y) (W/C) =0.33	7-day moist cure	40% (2905 psi)	Total	8.11E-04	9.31E-04	1.08E-03	1.24E-03	1.43E-03	1.54E-03	1.64E-03	1.68E-03	1.71E-03
			Shrinkage	2.44E-05	4.67E-05	7.56E-05	1.13E-04	1.57E-04	1.83E-04	2.07E-04	2.12E-04	2.13E-04
			Elastic	5.30E-04	5.30E-04	5.30E-04	5.30E-04	5.30E-04	5.30E-04	5.30E-04	5.30E-04	5.30E-04
			Creep	2.57E-04	3.54E-04	4.79E-04	6.00E-04	7.41E-04	8.28E-04	9.07E-04	9.40E-04	9.62E-04
			Creep Modulus	3.69E+06	3.28E+06	2.88E+06	2.57E+06	2.29E+06	2.14E+06	2.02E+06	1.98E+06	1.95E+06
			Creep Coefficient (computed)	0.51	0.71	0.96	1.20	1.48	1.66	1.81	1.88	1.92
			Elastic Modulus at Time of Load: 5.61E+06 psi									
		Computed Elastic Strain at Time of Load: 5.00E-04										
		50% (3631 psi)	Total	1.04E-03	1.19E-03	1.36E-03	1.55E-03	1.75E-03	1.88E-03	2.00E-03	2.07E-03	2.09E-03
			Shrinkage	2.44E-05	4.67E-05	7.56E-05	1.13E-04	1.57E-04	1.83E-04	2.07E-04	2.12E-04	2.13E-04
			Elastic	6.66E-04	6.66E-04	6.66E-04	6.66E-04	6.66E-04	6.66E-04	6.66E-04	6.66E-04	6.66E-04
			Creep	3.53E-04	4.74E-04	6.21E-04	7.70E-04	9.24E-04	1.03E-03	1.13E-03	1.19E-03	1.22E-03
			Creep modulus	3.56E+06	3.19E+06	2.82E+06	2.53E+06	2.28E+06	2.14E+06	2.02E+06	1.96E+06	1.93E+06
			Creep Coefficient (computed)	0.57	0.76	0.99	1.23	1.48	1.65	1.81	1.90	1.94
	Elastic Modulus at Time of Load: 5.61E+06 psi											
	Computed Elastic Strain at Time of Load: 6.25E-04											

No. of Mix	Curing condition	Load level	Strain	Age of testing (days)									
				3	7	14	28	56	91	180	270	360	
3GF (3m) (W/C) =0.41	7-day moist cure	40% (2299 psi)	Total	6.32E-04	-	9.12E-04	-	-	-	1.29E-03	1.45E-03	-	
			Shrinkage	1.89E-05	1.33E-05	8.01E-05	6.78E-05	-	-	2.21E-04	2.23E-04	-	
			Elastic	4.79E-04	4.79E-04	4.79E-04	4.79E-04	4.79E-04	4.79E-04	4.79E-04	4.79E-04	-	
			Creep	1.34E-04	-	3.53E-04	-	-	-	5.87E-04	7.53E-04	-	
			Creep Modulus	3.75E+06	-	2.76E+06	-	-	-	2.16E+06	1.87E+06	-	
			Creep Coefficient (computed)	0.30	-	0.78	-	-	-	1.30	1.67	-	
			Elastic Modulus at Time of Load: 5.10E+06 psi										
	Computed Elastic Strain at Time of Load: 4.51E-04												
	14-day moist cure	40% (2299 psi)	Total	8.76E-04	9.90E-04	1.09E-03	1.20E-03	1.32E-03	1.40E-03				-
			Shrinkage	2.03E-05	4.04E-05	6.76E-05	1.05E-04	1.48E-04	1.77E-04				-
			Elastic	5.86E-04	5.86E-04	5.86E-04	5.86E-04	5.86E-04	5.86E-04				-
			Creep	2.70E-04	3.64E-04	4.39E-04	5.12E-04	5.84E-04	6.36E-04				-
			Creep modulus	2.69E+06	2.42E+06	2.24E+06	2.09E+06	1.96E+06	1.88E+06				-
			Creep Coefficient (computed)	0.60	0.81	0.97	1.14	1.29	1.41				-
Elastic Modulus at Time of Load: 5.10E+06 psi													
Computed Elastic Strain at Time of Load: 4.51E-04													

No. of Mix	Curing condition	Load level	Strain	Age of testing (days)								
				3	7	14	28	56	91	180	270	360
4GF (3m) (W/C) =0.37	7-day moist cure	40% (2578 psi)	Total	1.14E-03	1.23E-03	1.27E-03	1.33E-03	1.49E-03	1.59E-03	1.83E-03	-	-
			Shrinkage	6.74E-05	1.06E-04	1.36E-04	1.73E-04	2.21E-04	2.23E-04	2.47E-04	-	-
			Elastic	5.99E-04	5.99E-04	5.99E-04	5.99E-04	5.99E-04	5.99E-04	5.99E-04	-	-
			Creep	4.73E-04	5.26E-04	5.39E-04	5.61E-04	6.68E-04	7.70E-04	9.89E-04	-	-
			Creep Modulus	2.32E+06	2.21E+06	2.19E+06	2.14E+06	1.96E+06	1.82E+06	1.57E+06	-	-
			Creep Coefficient (computed)	0.97	1.08	1.10	1.15	1.37	1.58	2.03	-	-
			Elastic Modulus at Time of Load: 5.10E+06 psi									
			Computed Elastic Strain at Time of Load: 4.88E-04									
			14-day moist cure	40% (2578 psi)	Total	-	1.03E-03	1.18E-03	1.26E-03	1.37E-03	1.43E-03	1.46E-03
	Shrinkage	1.13E-04			1.76E-04	2.29E-04	2.98E-04	3.41E-04	3.15E-04	3.29E-04	3.30E-04	-
	Elastic	5.46E-04			5.46E-04	-						
	Creep	-			3.10E-04	4.06E-04	4.17E-04	4.81E-04	5.74E-04	5.81E-04	8.59E-04	-
	Creep modulus	-			2.91E+06	2.62E+06	2.58E+06	2.42E+06	2.22E+06	2.21E+06	1.77E+06	-
	Creep Coefficient (computed)	-			0.64	0.83	0.85	0.99	1.18	1.19	1.76	-
	Elastic Modulus at Time of Load: 5.10E+06 psi											
	Computed Elastic Strain at Time of Load: 4.88E-04											

No. of Mix	Curing condition	Load level	Strain	Age of testing (days)									
				3	7	14	28	56	91	180	270	360	
5GF (1y) (W/C) =0.41	14-day moist cure	40% (2803 psi)	Total	1.01E-03	1.15E-03	1.28E-03	1.43E-03	1.59E-03	1.67E-03	1.78E-03	1.82E-03	1.84E-03	
			Shrinkage	3.89E-05	6.44E-05	1.04E-04	1.40E-04	1.68E-04	1.84E-04	2.13E-04	2.23E-04	2.27E-04	
			Elastic	5.72E-04	5.72E-04	5.72E-04	5.72E-04	5.72E-04	5.72E-04	5.72E-04	5.72E-04	5.72E-04	
			Creep	4.19E-04	5.33E-04	6.16E-04	7.38E-04	8.71E-04	9.26E-04	9.90E-04	1.02E-03	1.04E-03	
			Creep modulus	2.88E+06	2.57E+06	2.39E+06	2.17E+06	1.96E+06	1.89E+06	1.79E+06	1.76E+06	1.74E+06	
			Creep Coefficient (computed)	0.75	0.95	1.10	1.31	1.55	1.65	1.76	1.82	1.85	
		Elastic Modulus at Time of Load: 4.16E+06 psi											
		Computed Elastic Strain at Time of Load: 5.62E-04											
		50% (3504 psi)	Total	1.25E-03	1.42E-03	1.57E-03	1.76E-03	1.96E-03	2.06E-03	2.19E-03	2.25E-03	2.27E-03	
			Shrinkage	3.89E-05	6.44E-05	1.04E-04	1.40E-04	1.68E-04	1.84E-04	2.13E-04	2.23E-04	2.27E-04	
			Elastic	7.03E-04	7.03E-04	7.03E-04	7.03E-04	7.03E-04	7.03E-04	7.03E-04	7.03E-04	7.03E-04	
			Creep	5.09E-04	6.50E-04	7.67E-04	9.20E-04	1.09E-03	1.17E-03	1.27E-03	1.32E-03	1.34E-03	
			Creep modulus	2.89E+06	2.59E+06	2.38E+06	2.16E+06	1.96E+06	1.87E+06	1.78E+06	1.73E+06	1.72E+06	
			Creep Coefficient (computed)	0.72	0.93	1.09	1.31	1.55	1.67	1.81	1.88	1.90	
		Elastic Modulus at Time of Load: 4.16E+06 psi											
		Computed Elastic Strain at Time of Load: 7.02E-04											

No. of Mix	Curing condition	Load level	Strain	Age of testing (days)									
				3	7	14	28	56	91	180	270	360	
5GS (3m) (W/C) =0.33	7-day moist cure	40% (2065 psi)	Total	7.19E-04	7.84E-04	8.68E-04	-	-	-	-	1.43E-03	-	
			Shrinkage	7.90E-05	9.68E-05	1.11E-04	-	-	-	-	2.09E-04	-	
			Elastic	5.81E-04	5.81E-04	5.81E-04	5.81E-04	5.81E-04	5.81E-04	5.81E-04	5.81E-04	5.81E-04	-
			Creep	5.89E-05	1.06E-04	1.76E-04	-	-	-	-	-	6.40E-04	-
			Creep Modulus	3.51E+06	3.27E+06	2.97E+06	-	-	-	-	-	1.69E+06	-
			Creep Coefficient (computed)	0.12	0.21	0.35	-	-	-	-	-	1.29	-
			Elastic Modulus at Time of Load: 4.16E+06 psi										
	Computed Elastic Strain at Time of Load: 4.96E-04												
	14-day moist cure	40% (2065 psi)	Total	7.54E-04	8.40E-04	9.16E-04	9.98E-04	1.08E-03	1.14E-03	7.54E-04	8.40E-04	-	
			Shrinkage	4.27E-05	7.16E-05	1.03E-04	1.39E-04	1.72E-04	1.91E-04	4.27E-05	7.16E-05	-	
			Elastic	5.90E-04	5.90E-04	5.90E-04	5.90E-04	5.90E-04	5.90E-04	5.90E-04	5.90E-04	5.90E-04	-
			Creep	1.22E-04	1.79E-04	2.23E-04	2.69E-04	3.19E-04	3.59E-04	1.22E-04	1.79E-04	-	
			Creep modulus	3.09E+06	2.86E+06	2.71E+06	2.56E+06	2.42E+06	2.32E+06	3.09E+06	2.86E+06	-	
			Creep Coefficient (computed)	0.25	0.36	0.45	0.54	0.64	0.72	0.25	0.36	-	
			Elastic Modulus at Time of Load: 4.16E+06 psi										
	Computed Elastic Strain at Time of Load: 4.96E-04												

No. of Mix	Curing condition	Load level	Strain	Age of testing (days)									
				3	7	14	28	56	91	180	270	360	
6GS (1y) (W/C) =0.36	14-day moist cure	40% (2251 psi)	Total	1.05E-03	-	-	1.38E-03	1.67E-03	1.86E-03	2.16E-03	-	2.46E-03	
			Shrinkage	-	6.16E-05	1.09E-04	1.30E-04	1.45E-04	1.92E-04	2.22E-04	-	2.50E-04	
			Elastic	8.47E-04	8.47E-04	8.47E-04	8.47E-04	8.47E-04	8.47E-04	8.47E-04	8.47E-04	8.47E-04	
			Creep	-	-	-	3.98E-04	6.73E-04	8.22E-04	1.09E-03	-	1.36E-03	
			Creep Modulus	-	-	-	1.81E+06	1.48E+06	1.35E+06	1.16E+06	-	1.02E+06	
			Creep Coefficient (computed)	-	-	-	0.84	1.43	1.75	2.32	-	2.89	
		Elastic Modulus at Time of Load: 4.78E+06 psi											
		Computed Elastic Strain at Time of Load: 4.71E-04											
		50% (2251) psi	Total	7.97E-04	-	-	1.13E-03	1.32E-03	1.51E-03	1.72E-03	-	2.07E-03	
			Shrinkage	3.01E-05	-	1.09E-04	1.42E-04	2.01E-04	2.59E-04	2.64E-04	-	2.88E-04	
			Elastic	7.02E-04	7.02E-04	7.02E-04	7.02E-04	7.02E-04	7.02E-04	7.02E-04	7.02E-04	7.02E-04	
			Creep	6.46E-05	-	-	2.86E-04	4.19E-04	5.46E-04	7.50E-04	-	1.08E-03	
			Creep modulus	2.94E+06	-	-	2.28E+06	2.01E+06	1.80E+06	1.55E+06	-	1.26E+06	
			Creep Coefficient (computed)	0.14	-	-	0.61	0.89	1.16	1.59	-	2.30	
		Elastic Modulus at Time of Load: 4.78E+06 psi											
		Computed Elastic Strain at Time of Load: 4.71E-04											

No. of Mix	Curing condition	Load level	Strain	Age of testing (days)								
				3	7	14	28	56	91	180	270	360
6GS (3m) (W/C) =0.36	7-day moist cure	40% (2780 psi)	Total	8.68E-04	9.65E-04	1.05E-03	1.14E-03	1.23E-03	1.30E-03	-	-	-
			Shrinkage	2.05E-05	3.70E-05	5.69E-05	8.10E-05	1.05E-04	1.20E-04	-	-	-
			Elastic	6.08E-04	6.08E-04	6.08E-04	6.08E-04	6.08E-04	6.08E-04	-	-	-
			Creep	2.39E-04	3.19E-04	3.85E-04	4.52E-04	5.21E-04	5.72E-04	-	-	-
			Creep Modulus	3.20E+06	2.92E+06	2.73E+06	2.56E+06	2.40E+06	2.30E+06	-	-	-
			Creep Coefficient (computed)	0.46	0.62	0.75	0.88	1.01	1.11	-	-	-
			Elastic Modulus at Time of Load: 5.41E+06 psi									
			Computed Elastic Strain at Time of Load: 5.14E-04									
	14-day moist cure	40% (2780 psi)	Total	7.61E-04	8.61E-04	9.51E-04	1.05E-03	1.15E-03	1.22E-03	-	-	-
			Shrinkage	6.95E-05	8.69E-05	1.04E-04	1.25E-04	1.51E-04	1.71E-04	-	-	-
			Elastic	6.48E-04	6.48E-04	6.48E-04	6.48E-04	6.48E-04	6.48E-04	-	-	-
			Creep	4.36E-05	1.26E-04	1.99E-04	2.76E-04	3.53E-04	4.04E-04	-	-	-
			Creep modulus	3.92E+06	3.50E+06	3.20E+06	2.94E+06	2.71E+06	2.58E+06	-	-	-
			Creep Coefficient (computed)	0.08	0.25	0.39	0.54	0.69	0.79	-	-	-
			Elastic Modulus at Time of Load: 5.41E+06 psi									
			Computed Elastic Strain at Time of Load: 5.14E-04									

No. of Mix	Curing condition	Load level	Strain	Age of testing (days)									
				3	7	14	28	56	91	180	270	360	
7GS (1y) (W/C) =0.41	14-day moist cure	40% (2645 psi)	Total	9.53E-04	1.08E-03	1.21E-03	1.38E-03	1.55E-03	1.63E-03	1.73E-03	1.78E-03	1.77E-03	
			Shrinkage	4.33E-05	7.44E-05	1.00E-04	1.31E-04	1.62E-04	1.81E-04	2.01E-04	2.09E-04	2.12E-04	
			Elastic	5.17E-04	5.17E-04	5.17E-04	5.17E-04	5.17E-04	5.17E-04	5.17E-04	5.17E-04	5.17E-04	
			Creep	3.93E-04	4.87E-04	5.97E-04	7.36E-04	8.72E-04	9.29E-04	1.01E-03	1.05E-03	1.04E-03	
			Creep Modulus	2.91E+06	2.64E+06	2.38E+06	2.11E+06	1.90E+06	1.83E+06	1.73E+06	1.68E+06	1.69E+06	
			Creep Coefficient (computed)	0.78	0.97	1.18	1.46	1.73	1.84	2.01	2.09	2.07	
		Elastic Modulus at Time of Load: 5.25E+06 psi											
		Computed Elastic Strain at Time of Load: 5.04E-04											
		50% (3306) psi	Total	1.21E-03	1.36E-03	1.52E-03	1.71E-03	1.90E-03	1.98E-03	2.09E-03	2.14E-03	2.16E-03	
			Shrinkage	4.33E-05	7.44E-05	1.00E-04	1.31E-04	1.62E-04	1.81E-04	2.01E-04	2.09E-04	2.12E-04	
			Elastic	6.52E-04	6.52E-04	6.52E-04	6.52E-04	6.52E-04	6.52E-04	6.52E-04	6.52E-04	6.52E-04	
			Creep	5.12E-04	6.34E-04	7.64E-04	9.24E-04	1.08E-03	1.14E-03	1.24E-03	1.28E-03	1.30E-03	
			Creep modulus	2.84E+06	2.57E+06	2.33E+06	2.10E+06	1.90E+06	1.84E+06	1.75E+06	1.71E+06	1.70E+06	
			Creep Coefficient (computed)	0.81	1.01	1.21	1.47	1.72	1.81	1.97	2.03	2.06	
		Elastic Modulus at Time of Load: 5.25E+06 psi											
		Computed Elastic Strain at Time of Load: 6.30E-04											

No. of Mix	Curing condition	Load level	Strain	Age of testing (days)								
				3	7	14	28	56	91	180	270	360
7GS (3m) (W/C) =0.41	7-day moist cure	40% (2035 psi)	Total	9.21E-04	-	-	-	-	1.54E-03	1.54E-03	1.65E-03	-
			Shrinkage	-	9.01E-05	1.10E-04	1.25E-04	-	3.08E-04	3.34E-04	3.38E-04	-
			Elastic	8.03E-04	8.03E-04	8.03E-04	8.03E-04	8.03E-04	8.03E-04	8.03E-04	8.03E-04	-
			Creep	-	-	-	-	-	4.26E-04	4.01E-04	5.13E-04	-
			Creep Modulus	-	-	-	-	-	1.66E+06	1.69E+06	1.55E+06	-
			Creep Coefficient (computed)	-	-	-	-	-	0.93	0.88	1.12	-
			Elastic Modulus at Time of Load: 4.46E+06 psi									
	Computed Elastic Strain at Time of Load: 4.56E-04											
	14-day moist cure	40% (2035 psi)	Total	7.43E-04	8.56E-04	9.58E-04	1.07E-03	1.19E-03	1.27E-03	-	-	-
			Shrinkage	4.78E-05	7.07E-05	9.56E-05	1.26E-04	1.58E-04	1.80E-04	-	-	-
			Elastic	5.84E-04	5.84E-04	5.84E-04	5.84E-04	5.84E-04	5.84E-04	-	-	-
			Creep	1.11E-04	2.01E-04	2.79E-04	3.61E-04	4.47E-04	5.10E-04	-	-	-
			Creep modulus	2.93E+06	2.59E+06	2.36E+06	2.15E+06	1.97E+06	1.86E+06	-	-	-
			Creep Coefficient (computed)	0.24	0.44	0.61	0.79	0.98	1.12	-	-	-
			Elastic Modulus at Time of Load: 4.46E+06 psi									
	Computed Elastic Strain at Time of Load: 4.56E-04											

No. of Mix	Curing condition	Load level	Strain	Age of testing (days)										
				3	7	14	28	56	91	180	270	360		
8GS (1y) (W/C) =0.44	7-day moist cure	40% (1998 psi)	Total	1.20E-03	5.24E-03	5.24E-03	1.57E-03	1.94E-03	2.23E-03	2.52E-03	2.69E-03	3.07E-03		
			Shrinkage	7.54E-05	-	-	1.63E-04	1.91E-04	2.10E-04	2.22E-04	2.27E-04	2.34E-04		
			Elastic	9.76E-04	9.76E-04	9.76E-04	9.76E-04	9.76E-04	9.76E-04	9.76E-04	9.76E-04	9.76E-04		
			Creep	1.52E-04	-	-	4.31E-04	7.70E-04	1.05E-03	1.32E-03	1.48E-03	1.86E-03		
			Creep Modulus	1.77E+06	-	-	1.42E+06	1.14E+06	9.87E+05	8.69E+05	8.13E+05	7.03E+05		
			Creep Coefficient (computed)	0.32	-	-	0.90	1.60	2.18	2.75	3.08	3.87		
			Elastic Modulus at Time of Load: 4.15E+06 psi											
			Computed Elastic Strain at Time of Load: 4.81E-04											
			14-day moist cure	40% (1998 psi)	Total	1.01E-03	-	-	1.56E-03	1.53E-03	2.04E-03	2.48E-03	2.49E-03	2.92E-03
					Shrinkage	-	3.14E-05	6.40E-05	-	1.47E-04	1.53E-04	1.60E-04	1.67E-04	1.78E-04
	Elastic	7.93E-04			7.93E-04	7.93E-04	7.93E-04	7.93E-04	7.93E-04	7.93E-04	7.93E-04	7.93E-04		
	Creep	1.90E-04			4.68E-03	4.67E-03	2.76E-04	5.89E-04	1.09E-03	1.53E-03	1.53E-03	1.95E-03		
	Creep modulus	-			-	-	-	1.45E+06	1.06E+06	8.62E+05	8.61E+05	7.30E+05		
	Creep Coefficient (computed)	-			-	-	-	1.22	2.27	3.17	3.18	4.04		
	Elastic Modulus at Time of Load: 4.15E+06 psi													
	Computed Elastic Strain at Time of Load: 4.81E-04													

No. of Mix	Curing condition	Load level	Strain	Age of testing (days)								
				3	7	14	28	56	91	180	270	360
8GS (3m) (W/C) =0.44	7-day moist cure	40% (1916 psi)	Total	-	-	1.31E-03	1.60E-03	1.94E-03	2.20E-03	-	-	-
			Shrinkage	-	-	1.24E-04	1.59E-04	1.88E-04	2.03E-04	-	-	-
			Elastic	-	-	9.76E-04	9.76E-04	9.76E-04	9.76E-04	-	-	-
			Creep	-	-	2.05E-04	4.62E-04	7.72E-04	1.02E-03	-	-	-
			Creep Modulus	-	-	1.83E+06	1.50E+06	1.23E+06	1.08E+06	-	-	-
			Creep Coefficient (computed)	-	-	0.52	1.18	1.96	2.60	-	-	-
			Elastic Modulus at Time of Load: 4.88E+06 psi									
	Computed Elastic Strain at Time of Load: 3.93E-04											
	14-day moist cure	40% (1916 psi)	Total	1.05E-03	1.24E-03	1.42E-03	1.62E-03	1.83E-03	1.98E-03	-	-	-
			Shrinkage	2.39E-05	4.57E-05	7.26E-05	1.06E-04	1.40E-04	1.60E-04	-	-	-
			Elastic	7.93E-04	7.93E-04	7.93E-04	7.93E-04	7.93E-04	7.93E-04	-	-	-
			Creep	2.35E-04	4.03E-04	5.54E-04	7.18E-04	8.98E-04	1.03E-03	-	-	-
			Creep modulus	2.10E+06	1.80E+06	1.60E+06	1.43E+06	1.28E+06	1.18E+06	-	-	-
			Creep Coefficient (computed)	0.60	1.03	1.41	1.83	2.28	2.62	-	-	-
			Elastic Modulus at Time of Load: 4.88E+06 psi									
	Computed Elastic Strain at Time of Load: 3.93E-04											